BEHAVIOR OF BELLOWS

CHARLES BECHT


CENTRE FOR NFLD. STUDIES
MEMORIAL UNIVERSITY
OF NEWFOUNDLAND

INFORMATION TO USERS

This manuscript has been reproduced from the microfilm master. UMI films the text directly from the original or copy submitted. Thus, some thesis and dissertation copies are in typewriter face, while others may be from any type of computer printer.

The quality of this reproduction is dependent upon the quality of the copy submitted. Broken or indistinct print, colored or poor quality illustrations and photographs, print bleedthrough, substandard margins, and improper alignment can adversely affect reproduction.

In the unlikely event that the author did not send UMI a complete manuscript and there are missing pages, these will be noted. Also, if unauthorized copyright material had to be removed, a note will indicate the deletion.

Oversize materials (e.g., maps, drawings, charts) are reproduced by sectioning the original, beginning at the upper left-hand corner and continuing from left to right in equal sections with small overlaps.

Photographs included in the original manuscript have been reproduced xerographically in this copy. Higher quality 6" x 9" black and white photographic prints are available for any photographs or illustrations appearing in this copy for an additional charge. Contact UMI directly to order.

Bell & Howell Information and Learning
300 North Zeeb Road, Ann Arbor, MI 48106-1346 USA
800-521-0600

BEHAVIOR OF BELLOWS

By

Charles Becht, IV

A DISSERTATION

SUBMITTED TO THE SCHOOL OF GRADUATE STUDIES

IN PARTIAL FULFILLMENT OF THE REQUIREMENTS

FOR THE DEGREE OF

DOCTOR OF PHILOSOPHY

FACULTY OF ENGINEERING AND APPLIED SCIENCE

MEMORIAL UNIVERSITY OF NEWFOUNDLAND

St. John's, Newfoundland, Canada

May 2000

Abstract

While analysis of bellows, and in particular unreinforced bellows, has been investigated over the course of the last several decades, there remain a significant number of unanswered questions with respect to their behavior. The present research addresses their behavior under cyclic displacement loading; in particular, strain due to displacement. Prediction of strain range due to displacement is important in the fatigue design of bellows. In addition, a number of other areas are clarified by ancillary research.

Design of bellows for cyclic displacement loading primarily relies on data obtained from bellows fatigue tests. Further, fatigue data on bellows fabricated from one material is not considered a reliable indication of the fatigue performance of bellows fabricated from another material. This is because there has not been a good correlation between the fatigue performance of bellows based on calculated stress versus cycles to failure with that for the material of construction, as represented by polished bar fatigue curves.

This research shows that the differences in fatigue behavior of reinforced and unreinforced bellows, and the differences between bellows fatigue data and polished bar fatigue data is due to plastic strain concentration that occurs in bellows.

The existing, widely used charts and equations for evaluation of unreinforced bellows were found in this research to have sufficient accuracy for calculation of the significant stresses in the elastic regime for most bellows geometries. Some specific observations for further improvement are made. However, it was found that the elastic prediction of stresses in unreinforced bellows is not sufficient to accurately evaluate the displacement strains in bellows. Significant plastic strain concentration due to displacement loading occurs in the highly stressed regions of bellows. Regimes of behavior, depending on geometry parameters, were found. Prediction of fatigue performance of bellows is significantly improved by proper consideration of the effect of convolution geometry on plastic strain concentration.

Consideration of strain concentration effects eliminated the apparent disparity between the fatigue behavior of reinforced and unreinforced bellows. Further, it was found that polished bar fatigue data could be used to predict bellows fatigue life for a range of geometries.

Acknowledgments

I would like to acknowledge the help and support of a number of people.

My wife, Mary and children, for their patience and understanding while I undertook this research.

Dr. Seshadri, my thesis advisor, for his encouragement and advice, without which I would not have undertaken this PhD program. Dr. Haddara and Dr. Monahan for their advice and guidance.

Alan Connell, Bonnie Winkler and Mickey Smajda of Becht Engineering for their assistance. Alan ran many of the parametric analyses and created most of the plots of the data. Bonnie and Mickey assembled and formatted my dissertation into an attractive document.

Ken Jacquay, who started the Department of Energy funded bellows research program at Rockwell International that I took over in 1979. Without this start, I perhaps never would have developed my interest in bellows.

The Welding Research Council for their financial support of this research.

Contents

List of Figures

List of Tables

Nomenclature

A	Material constant in fatigue equation.
A_A	Area of bar A.
A_B	Area of bar B.
A_c	= (0.571q+2w). Cross sectional metal area of one bellows convolution.
A_r	Cross sectional metal area of one reinforcing member (ring).
B	Material constant in fatigue equation.
C_d	Correction factor for meridional stress due to deflection, per EJMA Standards.
C_f	Correction factor for bellows stiffness, per EJMA Standards.
C_p	Correction factor for bellows meridional bending stress due to pressure, per EJMA Standards.
C_r	Convolution height factor for reinforced bellows, per the following equation:

$$C_r = 0.3 - \left(\frac{100}{0.6\ P^{1.5} + 320}\right)^2$$

with P in psi.

D_b	Inside diameter of cylindrical tangent and bellows convolutions.
D_m	$=D_b + w + 2nt$. Mean diameter of bellows convolutions.
e	Total equivalent axial movement per convolution.
E	Modulus of elasticity at temperature for material. Subscripts "b," "c," "f," and "r" denote the bellows, collar fastener and reinforcing member material, respectively.
E_A	Elastic modulus of bar A.
E_B	Elastic modulus of bar B.
f_{ir}	Reinforced bellows theoretical axial stiffness.
H	$= PD_mq$. Resultant total internal pressure load acting on the bellows and reinforcement.
K_A	Axial stiffness of bar A.
K_B	Axial stiffness of bar B.
L_A	Length of bar A.
L_B	Length of bar B.
l_f	Length of one fastener.
n	Number of bellows material plies of thickness "t."
N	Total number of convolutions in one bellows.
N_c	Number of cycles to failure.
P	Internal pressure.
P_s	Limiting pressure based on column instability (column squirm).
QW	= q/2w. Nondimensional parameter in solution of shell equation for toroid.

QDT = $q/(2.2(D_m\ t_p)^{1/2})$. Nondimensional parameter in solution of shell equation for toroid.

q Bellows pitch.

r Meridional radius of toroid.

R' Circumferential radius of bellows.

R Ratio of the internal pressure resisted by the bellows convolution to the internal pressure resisted by the reinforcement.

S_1 Collar circumferential membrane stress due to internal pressure.

S_2 Bellows circumferential membrane stress due to internal pressure.

S_2' Reinforcing member circumferential stress due to internal pressure.

S_3 Bellows meridional membrane stress due to internal pressure.

S_4 Bellows meridional bending stress due to internal pressure.

S_5 Bellows meridional membrane stress due to deflection.

S_6 Bellows meridional bending stress due to deflection.

S_T Stress range.

t Nominal thickness of one ply.

t_c Collar thickness.

t_p $= t\ (D_b\ /D_m)^{1/2}$. Bellows material thickness factor for one ply, to correct for thinning during forming.

v Poisson's ratio.

w Convolution depth.

Δ Total deflection imposed on bar A and B.

Δ_A Deflection calculated to be absorbed by bar A by elastic analysis.

Δ_B Deflection calculated to be absorbed by bar B by elastic analysis.

$\Delta^{e\text{-}p}{}_A$ actual displacement absorbed by A, elastic plastic case.

$\Delta^{e\text{-}p}{}_B$ actual displacement absorbed by B, elastic plastic case.

μ Geometric parameter.

Chapter 1

Introduction

Design equations using charts with factors that were developed from parametric shell analysis have become the accepted method for bellows analysis, worldwide. The equations and charts in the Standards of the Expansion Joint Manufacturers Association (EJMA Standards), originally developed by Anderson (1964a and 1964b), are, for example, being adopted by the European Union for their expansion joint rules that are being incorporated into the European Pressure Vessel Standard. A comprehensive review of European and U.S. standards devoted to expansion joints has been provided by Osweiller (1995).

The analytical work on bellows through the mid-1960's was focused on developing analytical solutions. The complicating factor for bellows is the toroidal sections that form the roots and crowns of the convolutions. The shell equations for the toroid can not be directly solved; approximate solutions were developed. Anderson incorporated correction factors to compensate for inaccuracies in the approximate solution to develop design equations that have been successfully used for the past 30 years. Since that time, nearly all of the analytical work in bellows research has used numerical methods because of the greater accuracy, and because the advent and improvements to digital computers provided a means to perform such numerical analysis

(e.g. finite element method). However, the charts and equations developed by Anderson remain in use for bellows design.

The primary focus of this research was the response of bellows to displacement loading. This relates to the design of bellows for fatigue. Bellows are typically subjected to cyclic displacement loading that can cause fatigue failure. The approach that has been taken to fatigue design of bellows is the use of empirical fatigue curves, based on bellows fatigue tests. Correlation of bellows fatigue performance with basic material property data, polished bar fatigue data, has not been successfully performed. The design fatigue curves for reinforced and unreinforced bellows that are in use, today, provide an indication that the phenomena of bellows fatigue under displacement loading is not fully understood.

An obvious discrepancy is the difference between the fatigue design curves for reinforced and unreinforced bellows. Figure 1-1 shows the design fatigue curve from the Process Piping Code, ASME B31.3, the development of which is described in Becht (1989a,1995). The fatigue curve for reinforced bellows is higher than that of unreinforced bellows, yet the material used to manufacture the bellows is the same; there is no fundamental reason to expect improved fatigue strength of reinforced bellows material. If the stresses are properly calculated for both reinforced and unreinforced bellows, they should theoretically correlate with the same fatigue curve. If the calculation of

stress properly considers the effect of geometry and type of construction, the fatigue curve would simply be a material property. The difference in these fatigue curves was what originally prompted this research.

Because of uncertainties relative to the difference between bellows fatigue data and polished bar fatigue data, current industry practice, as reflected in Process Piping Code, ASME B31.3, requires actual bellows fatigue testing for each material and does not permit analogies between materials with similar polished bar fatigue characteristics. Further, separate fatigue tests are required for reinforced and unreinforced bellows, since each presently has a different fatigue curve.

If sufficient understanding is developed to permit prediction of bellows fatigue life directly from polished bar fatigue data (i.e. basic material property data), using the current or similar stress equations, it would substantially benefit industry. It could significantly reduce the number of bellows fatigue tests currently considered to be necessary to develop fatigue design curves for various materials, and for reinforced and unreinforced bellows.

The scope of the research covered a number of areas. An initial evaluation of the existing equations for calculating stress in bellows that are based on elastic shell theory and equilibrium principles was made. While the more significant, bending stresses were found to be accurately calculated, the

lesser, membrane stress solutions were found to significantly underpredict the maximum membrane stresses in bellows for some bellows geometries. This was investigated, and the source of the deviation was found.

For ring reinforced bellows, the interaction of the bellows convolutions and the reinforcing rings, and the effect of internal pressure on this interaction was investigated. This is a nonlinear large displacement gap problem; however, the effect of plasticity was found to, in fact, simplify the evaluation of the reinforced bellows strain range due to displacement.

The effect of plasticity on the strain range of both unreinforced and reinforced bellows was investigated. Significant, geometry dependent, plastic strain concentration effects were found. The effect of geometry on strain concentration was investigated, and the fundamental reasons why certain bellows are subject to significant plastic strain concentration and others are not, was discovered.

Existing bellows fatigue data was re-evaluated with this understanding of plastic strain concentration, and also compared to raw polished bar fatigue data for the material. It is found in the present work that the differences in bellows response is due to plastic strain concentration. With an improved understanding of plastic strain concentration in bellows, the fatigue behavior of reinforced and unreinforced bellows is unified, and both can be compared to polished bar fatigue data.

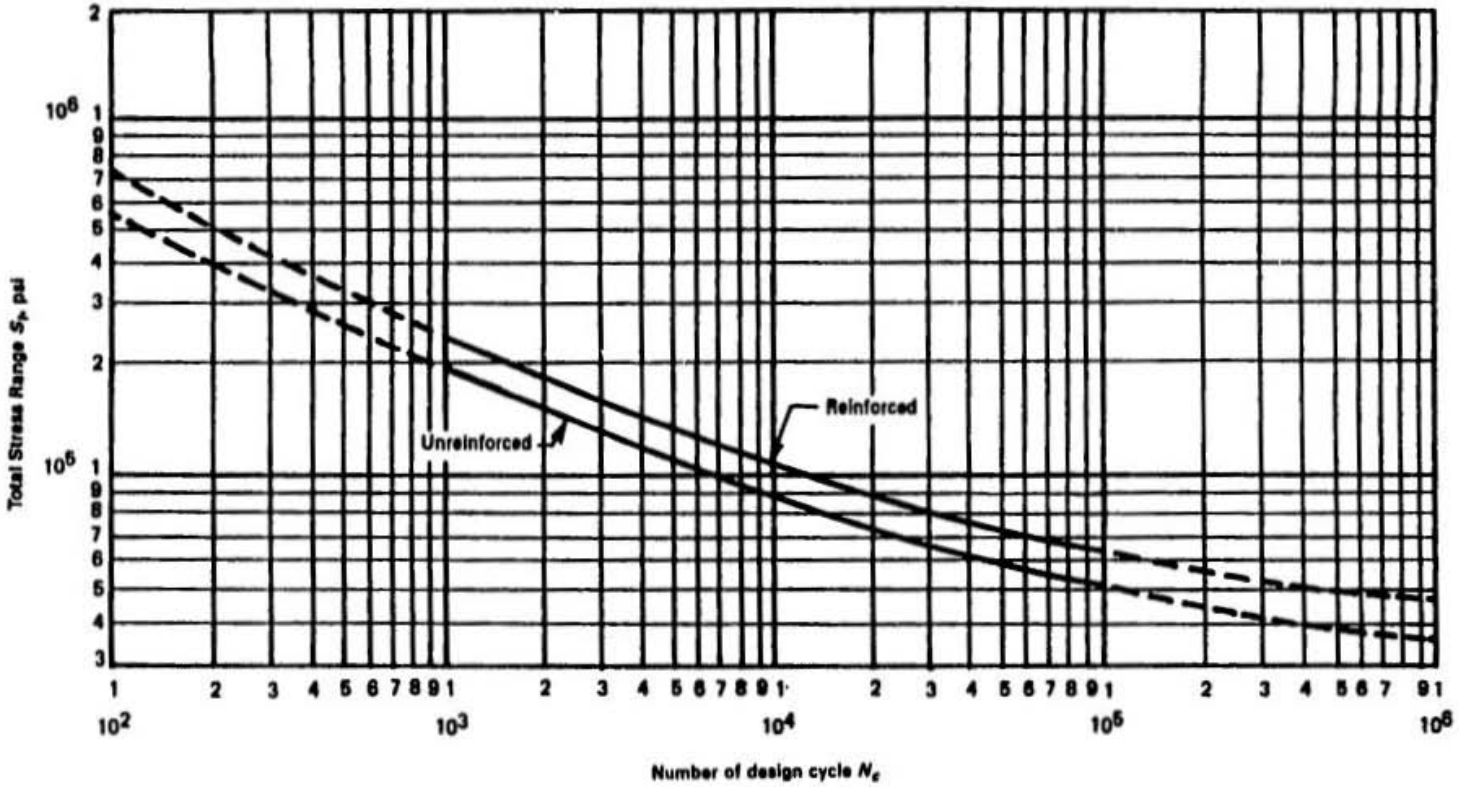

$$N_c = \left(\frac{A}{S_t - B}\right)^2$$

$$S_t = 0.7\,(S_3 + S_4) + S_5 + S_6$$

Bellows	Cycles	A	B
Unreinforced	≤ 40,000	5.2×10^6	38,300
	> 40,000	6.7×10^6	30,600
Reinforced	≤ 40,000	6.6×10^6	48,500
	> 40,000	8.5×10^6	38,800

GENERAL NOTES:

(a) These curves are intended to evaluate the design fatigue life at ambient temperature for austenitic stainless steel bellows which have not been heat treated. They are considered valid primarily in the range of 10^3 cycles to 10^6 cycles, due to the limited data available for the very low and very high cyclic ranges.

(b) The equations are of the form provided in "Design of Pressure Vessels for Low Cycle Fatigue" by B.F. Langer, ASME paper 61-WA-18. The constants were modified to reflect actual bellows test data reduced to a design curve in accordance with the rules of the BPV Code, Section VIII, Division 2, Appendix 6. The calculations of S_5 and S_6 shall be based on a modulus of elasticity equal to 28.3×10^6 psi.

(c) For nomenclature, refer to EJMA Standards.

(d) Factors have been included in these design fatigue curves to account for the normal effects of size, surface finish, and scatter of the data. Therefore, the design cycle life should realistically represent the estimated number of operating cycles. An overly conservative estimate of cycles can result in an increased number of convolutions and a joint more prone to instability.

Figure 1-1, Bellows Design Fatigue Curves (ASME B31.3)

Chapter 2

Literature Review and Theoretical Background

2.1 Overview of Bellows Behavior

Bellows Geometry

A bellows is a convoluted shell consisting of a series of toroidal shells, usually connected with annular plates that are the called sidewalls. The shape and terms used are shown in Figure 2.1-1. A bellows with no sidewalls is a special case, and is called a semitoroidal bellows. Various types of bellows and convolution shapes used in practice are illustrated in Figure 2.1-2.

Bellows are used to provide additional flexibility in shell structures such as piping and heat exchanger shells. They must withstand internal pressure, while at the same time providing the required flexibility (i.e. the ability to absorb movement). These deflections are typically in the form of axial deflection and bending rotation, and in some cases lateral displacement of the ends.

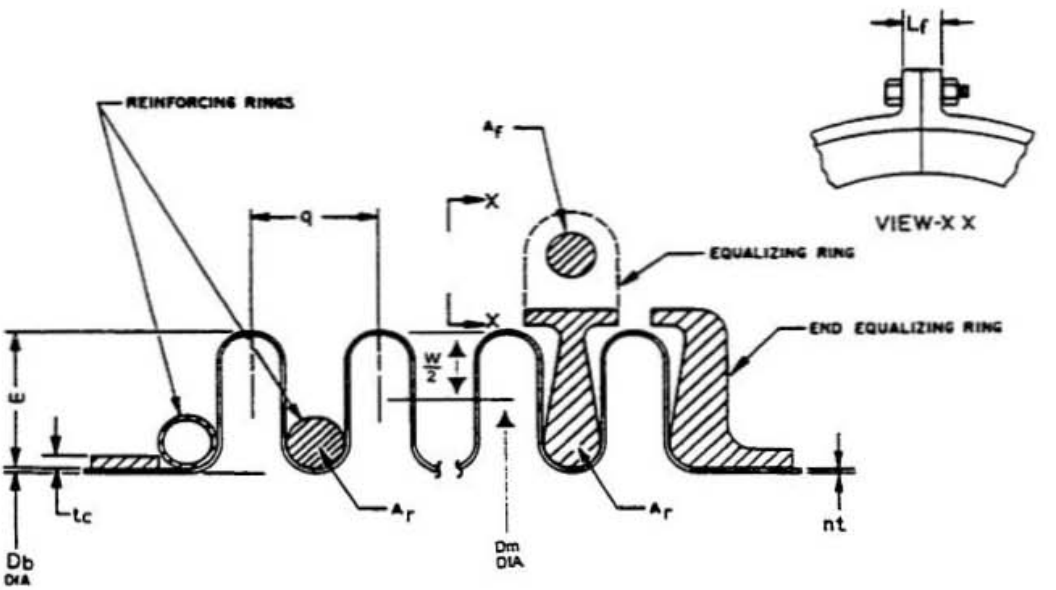

Figure 2.1-1, Bellows Geometry (EJMA, 1993)

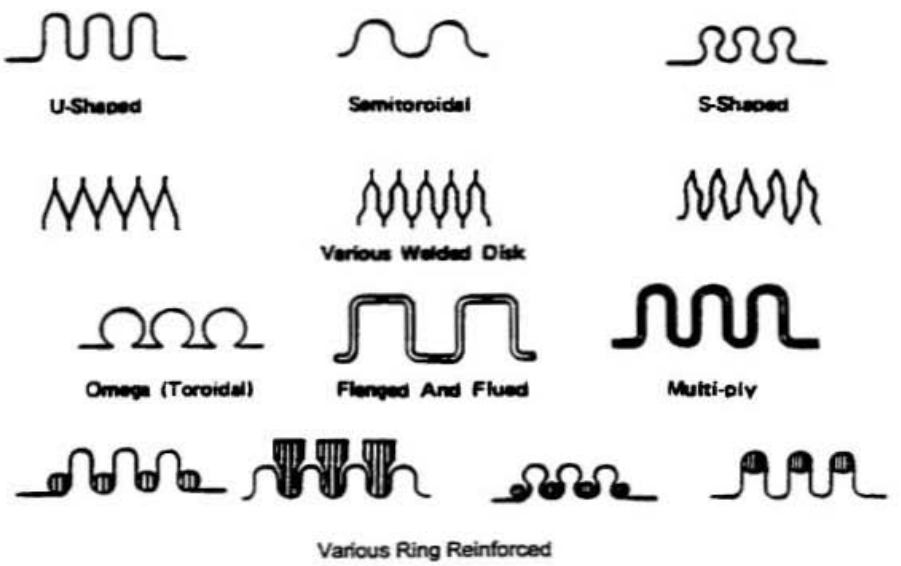

Figure 2.1-2, Convolution Shapes for Various Types of Bellows

Bellows are generally manufactured with a much thinner wall than the cylindrical shells to which they are attached (required to provide the necessary flexibility). However, they are provided with sufficient metal area to resist the circumferential force due to pressure by forming the wall into convolutions. Where this does not provide sufficient metal wall area, reinforcing rings are added, usually on the outside of the bellows in the root locations, in order to provide additional resistance to pressure induced rupture (burst failure).

Bellows are subject to circumferential and meridional membrane and bending stresses due to internal (or external) pressure and imposed displacement. The direction of these stresses is illustrated in Figure 2.1-3.

Response to Internal Pressure

An unreinforced bellows under internal pressure load is subject to circumferential and meridional stresses. The circumferential membrane strain distribution can be fairly uniform, as shown by Becht (1981) by analysis and strain gage results. The average circumferential stress is readily predicted using equilibrium principles, as shown in section 3.1. This is a primary membrane stress.

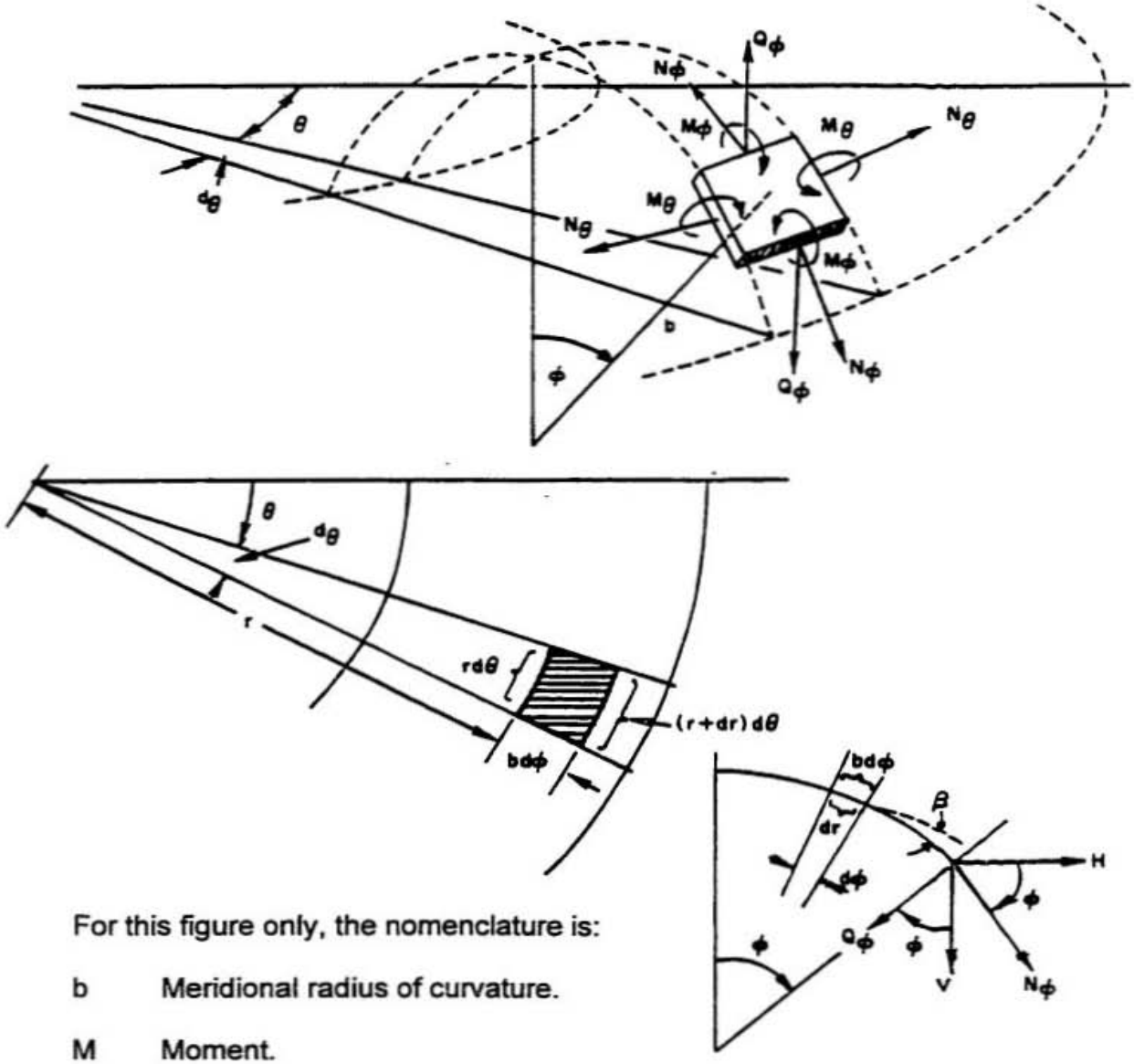

For this figure only, the nomenclature is:

b Meridional radius of curvature.

M Moment.

N Normal force.

Q Transverse force.

r Circumferential radius of curvature.

θ Circumferential angle or, as subscript, circumferential force or moment.

φ Meridional angle or, as subscript, meridional force or moment.

Figure 2.1-3, Circumferential and Meridional Stresses in Bellows (Anderson, 1964b)

Primary stress is a term used to describe stresses that are load controlled, that satisfy equilibrium. It is differentiated in the ASME Boiler and Pressure Vessel Code, Section VIII, Div 2 from secondary stresses which are deformation or strain controlled. Section 2.4 on plastic strain concentration describes deformation controlled stresses in greater detail. Primary stresses are typically limited by material strength properties such as yield stress and tensile strength. Secondary stresses are typically limited by material properties such as fatigue strength.

The bellows convolutions have planar symmetry, with the planes, normal to the bellows axis, cutting through the root and crown apexes. Because of this symmetry, the roots and crowns can be visualized as points of fixed meridional bending restraint and the bellows toroidal and sidewall portions, between, can be envisioned as a curved beam with fixed ends. See Figure 2.1-4. In fact, earlier evaluations of bellows were based on these concepts. Via this analogy, one can visualize that there will be a meridional bending stress distribution, with maximum bending stress in the root, crown, and sidewall of the bellows, as illustrated in Figure 2.1-5. The end tangent and half of the first convolution are shown.

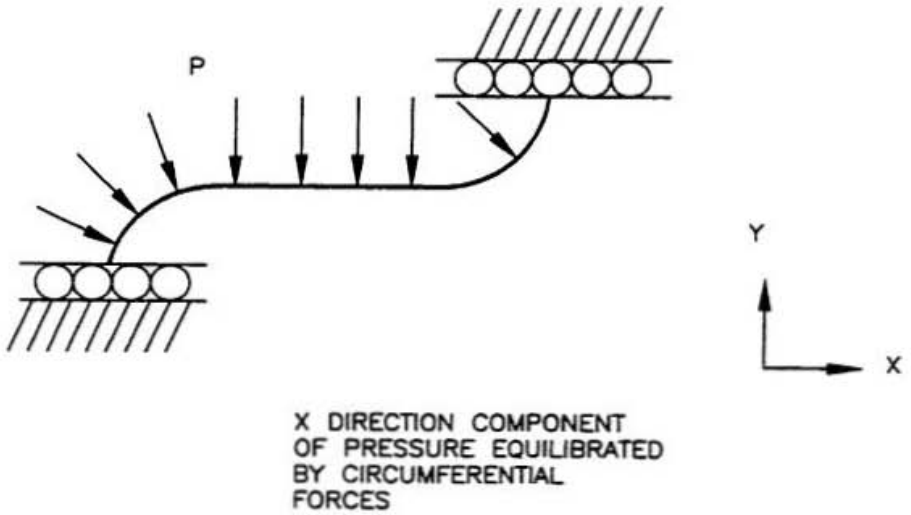

Figure 2.1-4, Curved Beam Representation of Bellows

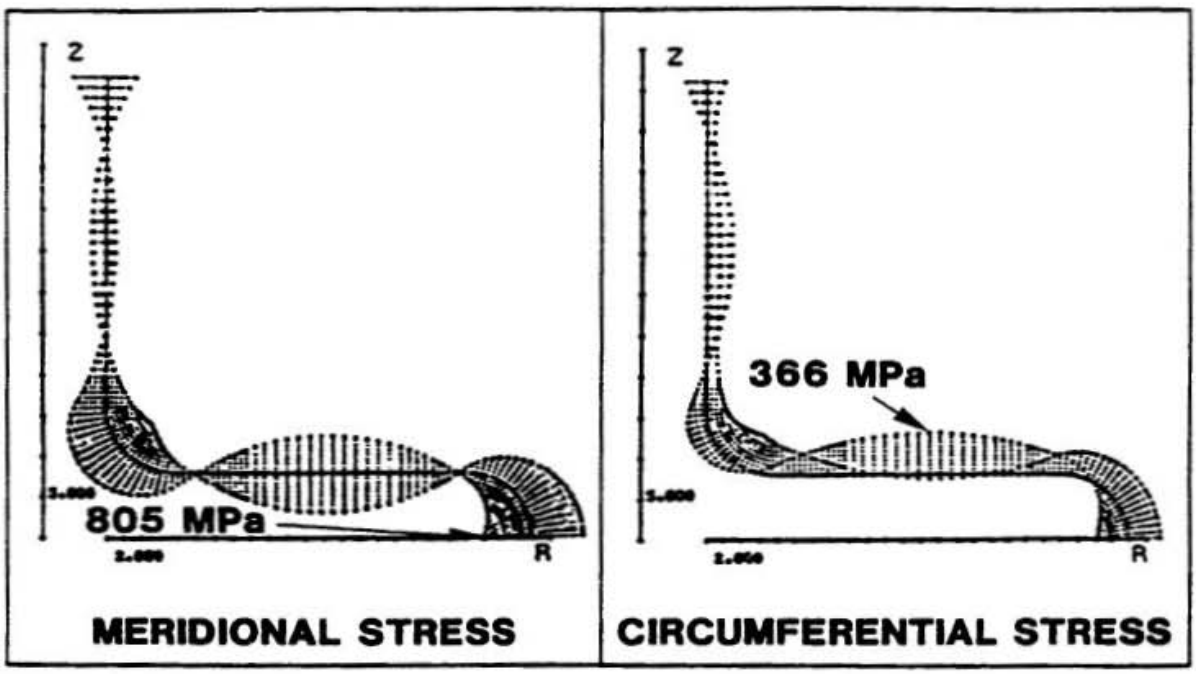

Figure 2.1-5, Bellows Stresses Due to Internal Pressure
(Osweiller, 1989)

Circumferential bending stresses result from Poisson effects and small meridional membrane stresses also exist. Because of circumferential constraint, the circumferential bending stress is equal to Poisson's ratio times the meridional bending stress. The meridional membrane stress is small compared to the meridional bending stress. The bending stress is higher by about a factor of w/t (convolution height divided by convolution thickness), as described in section 3.1, which is typically a large factor for bellows, which are typically thin walled.

There are three primary types of failure that are of concern with respect to internal pressure loads. The first is simply burst failure due to excessive circumferential membrane stress. This is the failure mode for which reinforcing rings are used. It results when the circumferential membrane stress exceeds the tensile strength of the material.

The second type of failure is a limit load type of failure resulting from the formation of plastic hinges in the roots, sidewalls and crowns of the bellows. This failure mode, called in-plane squirm by the industry, was demonstrated by Becht (1980) to be a limit load type of failure. Prior to this research performed by Becht, this failure mode was not understood by industry to be dependent on yield strength; at the time, these findings were the source of considerable controversy. However, the above described mechanism of this failure mode is now generally accepted and the EJMA Standards have been

revised accordingly, as described later herein. Whereas the aforementioned burst failure is caused by circumferential membrane stress, this failure is caused by meridional bending stress.

After the limit load is reached, the in-plane squirm failure can be observed in several fashions. These include collapse of the convolutions, root bulge where a bellows root moves laterally relative to the bellows centerline, and bulges out on one side, and simply cocking of one convolution relative to another (which typically precedes root bulge). A photograph of a bellows that had undergone root bulge is shown in Figure 2.1-6.

The third type of failure is called column squirm. It is a buckling failure of the bellows due to internal pressure. This failure mode is described in the section on instability.

The criteria for design of bellows under internal pressure has changed in the EJMA Standards as a result of the findings of Becht on the mechanism of in-plane squirm. It was shown by Becht (1980) that the design rules in the 5th edition of the EJMA Standards for internal pressure were in some cases unconservative. In fact, it was possible to design a bellows that would fail at a pressure lower than the design pressure. As a result, both ASME Section VIII, Div 1 and ASME B31.3 contain an allowable stress basis that differs from the EJMA Standards, 5th edition.

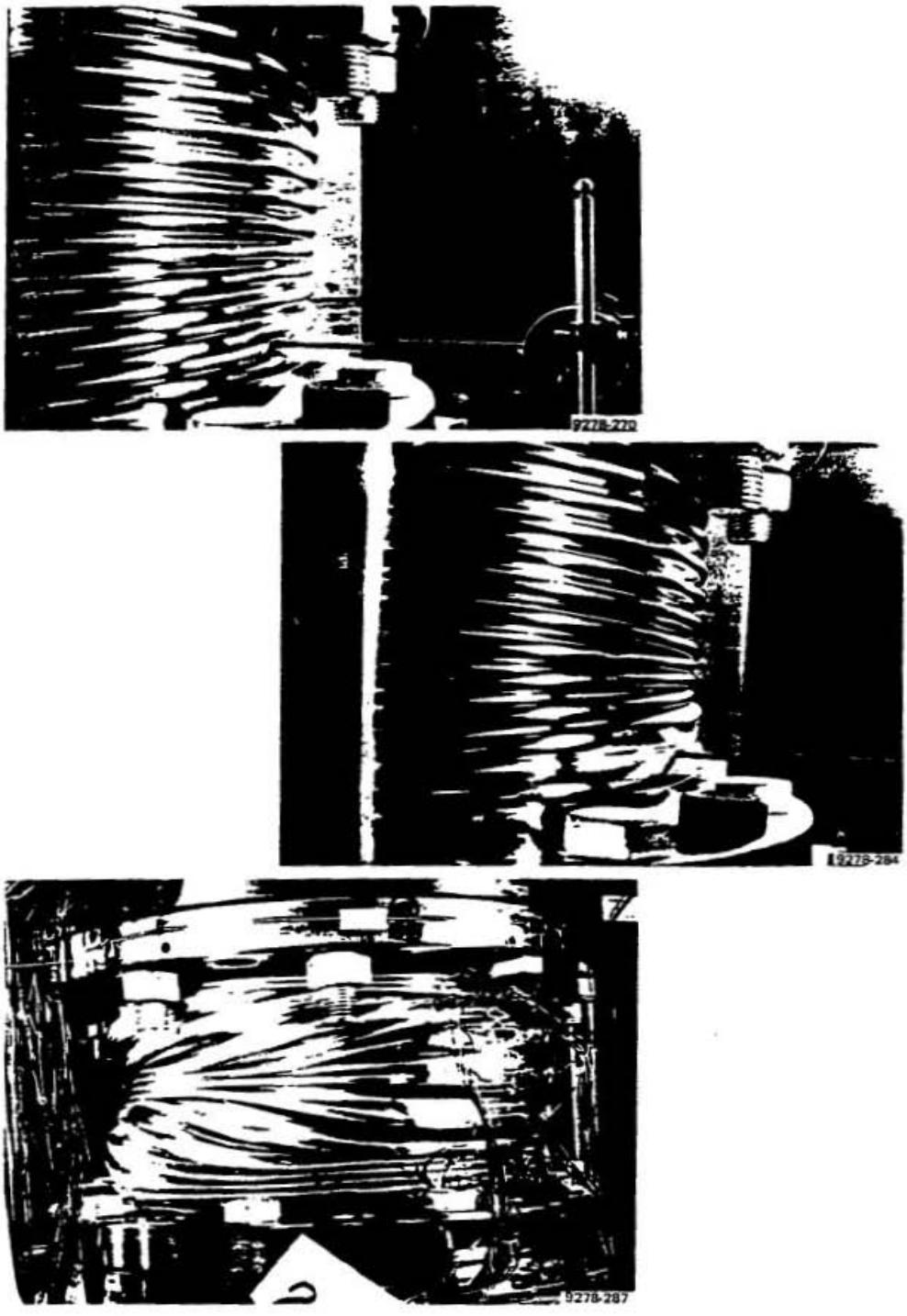

Figure 2.1-6, Bellows with Root Bulge Failure
(Becht and Skopp, 1981a)

The source of the nonconservatism was an inconsistency between the allowable stress basis and empirical test data. Based on test data, the EJMA Standards included a design approach that permitted a pressure induced meridional bending stress which was significantly greater than the specified minimum yield strength of the material. It permitted a stress as high as 2.86 times the Section VIII, Div 1 allowable stress in tension which could be as high as 1.9 times the minimum yield strength (or 2.6 times for austenitic stainless steel). This would imply that these meridional bending stresses are not primary stresses which could result in limit load failures, although this is not the case. As stated above, they are primary stresses that can result in limit load failure.

The reason that bellows generally do not fail at this high level of stress is that the material, in the as-formed condition, is cold worked and therefore has a yield strength two or more times higher than the specified minimum yield strength that the Code allowable stress is based on. The bellows that were tested in developing the pressure stress limits in the EJMA Standards were all in the as-formed condition and had the benefit of a higher than specified minimum yield strength. Thus, a high multiple of the Code allowable stress, which was based on specified minimum yield strength values, was found to be an acceptable level of stress. Thus, the 2.86 factor.

If the bellows is annealed after forming, as is sometimes required for corrosive or high temperature service, the benefit of the cold work in terms of increased yield strength is no longer available, and the EJMA pressure design equations became unconservative. Figure 2.1-7 illustrates how the root in a test bellows bulged outward to failure when the meridional stress due to internal pressure exceeded 1.5 times the actual yield strength in an annealed bellows (Becht and Skopp, 1981a). The plot contains the root radial displacement, as measured with a dial gage; the arrangement with the dial gage is shown in Figure 2.1-6.

New design equations have been developed by Broyles (1994) for unreinforced bellows that address this non-conservatism; these equations were incorporated in the 6th edition of the EJMA Standards. The equations essentially treat the meridional bending stress due to internal pressure as a primary bending stress with a yield strength based stress limit. It is left to the bellows designer to select the yield strength, so a high yield strength value can be used when designing a bellows that will not be annealed after forming, and a low yield strength value (e.g. specified minimum) can be used with a bellows that has been annealed after forming.

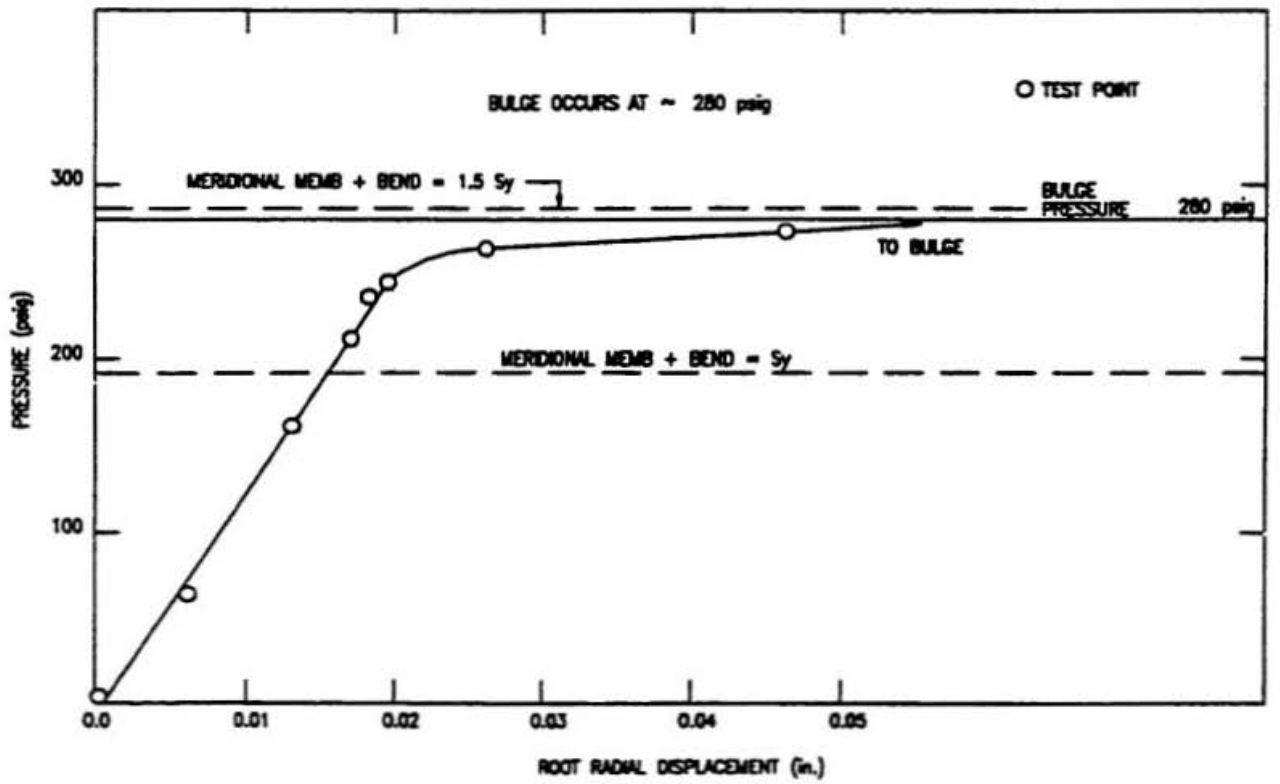

Figure 2.1-7, Root Radial Displacement During Pressurization

(Becht and Skopp, 1981a)

Koves (1995) has evaluated the effect of circumferential stress on this failure mode, in-plane squirm (limit load due to meridional bending stress). Considering Von Mises or Tresca yield theory, tensile circumferential membrane stress effectively reduces the meridional compressive stress at which yield will occur. This points out the effect of the biaxial stress state in a bellows.

Updike and Kalnins (1995) performed elastic-plastic buckling analysis demonstrating that bifurcation buckling occurs in the bellows following the formation of plastic hinges at the roots, crests and sidewalls, an axisymmetric limit state. This work investigates the post-limit state deformations which result in nonsymmetric deformation such as in-plane squirm and root bulge.

Response to Deflection Loading

Deflection of the bellows can be envisioned as an axial displacement of the crown relative to the root of the bellows. This creates a bending distribution, with maximum bending stresses in the root and the crown. These are illustrated in Figure 2.1-8. In this figure, the end tangent and half of the first convolution are shown. Poisson effect circumferential bending stresses also exist, as well as circumferential membrane stress due to radial displacement of the root and crown.

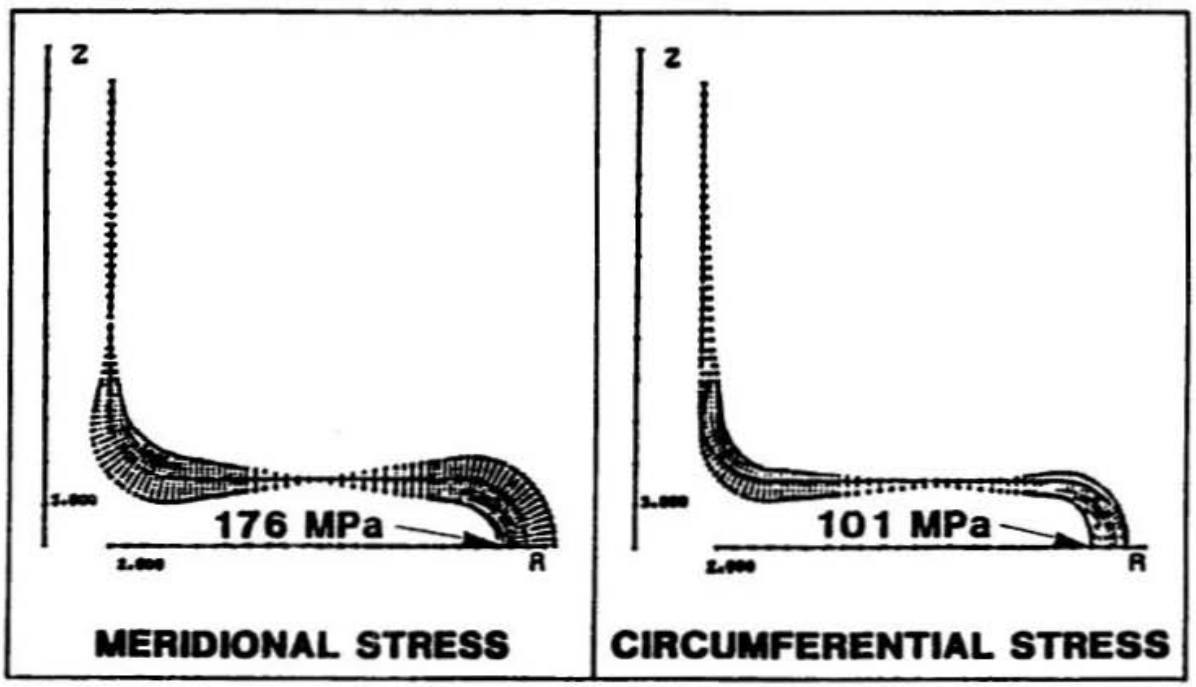

Figure 2.1-8, Bellows Stresses Due to Deflection
(Osweiller, 1984)

Strain concentration occurs as bellows are deflected in the plastic regime. Tanaka (1974) found that strain concentration occurs at the high stress zones after yielding occurs under axial displacement loading; the degree of strain concentration was found to depend upon the geometry. A maximum strain concentration of two was found. The effect of strain concentration is shown very distinctly in bellows test data developed by Kobatake et al. (1986) and shown in Figure 2.1-9.

Plastic strain concentration could be eliminated by incorporating a sufficient number of convolutions, or greater convolution depths, or reduced wall thickness, to keep the deflection stresses within the elastic range. However, in general, this is not practical in a bellows. Incorporation of more convolutions makes the bellows more susceptible to column squirm failure due to internal pressure. Greater convolution depths and reduced wall thickness makes the bellows more susceptible to in-plane squirm due to internal pressure as well as column squirm. Bellows design requires a balance between the need for flexibility, ability to accommodate cyclic deformation, and resistance to pressure. Bellows can function satisfactorily, cycling in the plastic regime, so that it would not be appropriate to reduce the design margin with respect to pressure loads to design a bellows to remain elastic, to avoid plastic strain concentration.

The approach that has been taken in industry for design of bellows with respect to deflection is to use empirical fatigue curves based on bellows testing.

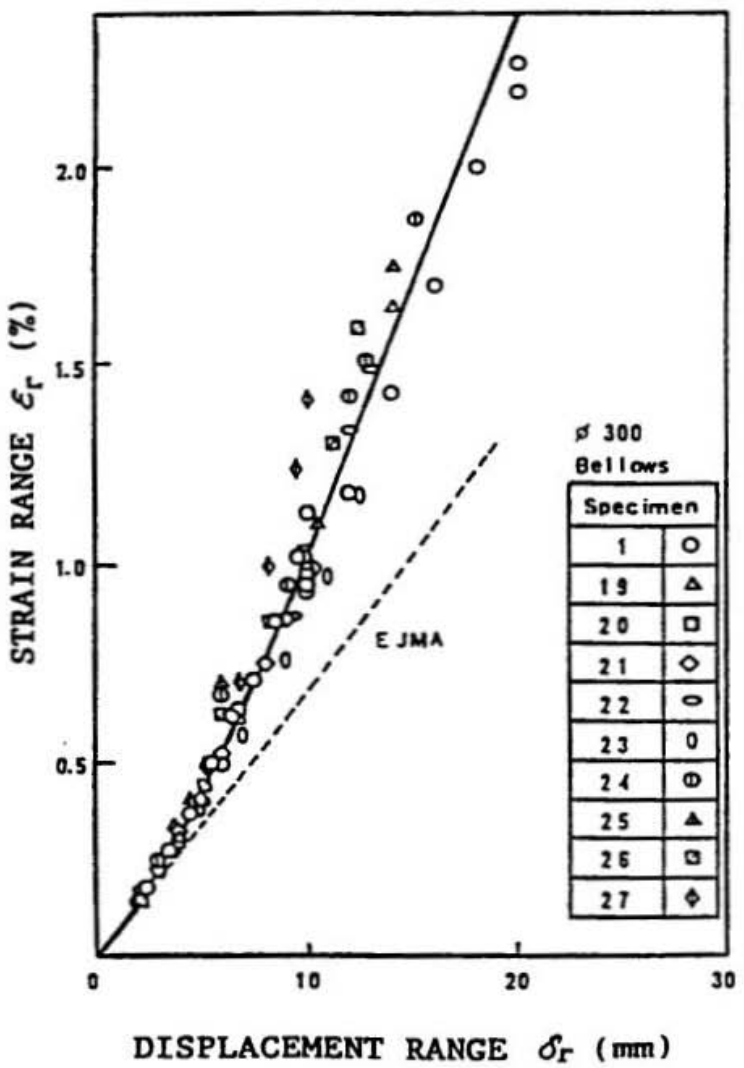

Figure 2.1-9, Strain Concentration Under Deflection Loading

(Kobatake, 1986)

Bellows Fatigue Design Curves

Empirical design fatigue curves are used for bellows. The advantage of empirical fatigue curves such as those included in the EJMA Standards is that they were based on component testing. Effects such as plastic strain concentration are inherently included in empirical fatigue curves, and need not be determined analytically. This simplifies the consideration of a number of complex phenomena. Further, the correlation of the fatigue data with stresses calculated using elastic theory permits design of bellows by elastic analysis.

Unreinforced Bellows Fatigue Curve Development. Investigation (Becht, 1989a and 1995) of available bellows fatigue data revealed that the slope of the EJMA fatigue curve did not represent the fatigue data well. The slope of the curve appeared shallow relative to the data. A slope where stress range (actually strain range times elastic modulus) is a function of $N_c^{-1/2}$, per the Manson-Coffin relation between plastic strain range and cycles to failure, appeared to follow the data better. This slope is the basis for the fatigue curves in ASME Section VIII, Div 2 and was the final slope adopted for bellows in ASME Section VIII, Div 1, Appendix 26, and is widely accepted.

A collection of bellows fatigue data that was provided by the EJMA was evaluated by Becht (1989a, 1995) to develop a new design fatigue curve. The bellows had been deflection cycled, with varying amounts of constant internal pressure. Only the deflection induced stress was included in the development of the fatigue curve because the pressure was held constant (non-cyclic). The steady state pressure should not significantly impact the fatigue life, because the strain range in the tested bellows was generally sufficiently into the plastic regime to eliminate mean stress effects on fatigue. If the pressure stress was added to the cyclic deflection stress in development of the fatigue curve, the fatigue curve would have been unconservatively high. Note that this is a departure from what was done in development of the fatigue curve in the EJMA standards, which included the pressure stress in development of the fatigue curve.

Some of the test bellows contained significantly more pressure than is permitted by the EJMA Standards. This high internal pressure can cause ratchet and other problems, and was considered to distort the fatigue test results. Ratchet in bellows, discussed later, is progressive strain accumulation caused by the combination of cyclic deflection induced stress combined with sufficiently high steady state pressure induced stress. Therefore, from this data, bellows tests where the stress due to internal pressure was more than 50% greater than the allowable stress were eliminated. This eliminated a

number of low data points that were not representative of bellows that would be designed in accordance with the code rules.

A best fit curve for that fatigue test data using an equation of the form:

$S_T=AN_C^{-0.5}+B$, or, as presented in the ASME B31.3 Code

$$N_C = \left(\frac{A}{S_T - B} \right)^2 \qquad (2.1)$$

where N_C is number of cycles to failure, S_T is the calculated bellows stress range and A and B are material constants, was developed. This equation is of the form proposed by Langer (1961), which is based on the Manson-Coffin equation, but adapted for use with elastically calculated stress instead of plastic strain. The curve was then adjusted down in stress until it lower bounded the data. Finally, the maximum of a factor of 1.25 on stress or 2.6 on cycles was applied to develop a design curve.

The factors of 1.25 on stress and 2.6 on cycles were based on ASME Section VIII, Div 2, Appendix 6, Experimental Stress Analysis, and reflected a number of tests greater than 5. While factors of 2 and 20 are applied to polished bar fatigue data in ASME Pressure Vessel Code fatigue design curves, these lesser factors (1.25 and 2.6 in this case) are applied to fatigue data from component testing, that inherently includes effects which impact fatigue life,

such as surface finish and size. The factor of 2.6 on cycles governed below 40,000 cycles and the factor of 1.25 on stress governed above 40,000 cycles. Thus, the equation changes at 40,000 cycles.

Figure 2.1-10 shows the fatigue test data, the lower bound curve, and the resulting design curve, including the safety margins, for unreinforced, as-formed, austenitic stainless steel bellows.

The manner in which temperature is considered to affect the fatigue strength was considered in the same fashion as in ASME Section VIII, Div 2. The basic philosophy is that the strain range versus cycles to failure is independent of temperature up to about 400°C. However, in typical code practice, elastically calculated stress is used rather than strain. The elastically calculated stress is the strain times the elastic modulus. While the strain range for a given number of cycles to failure is temperature independent, the elastic modulus is not, so there would be different elastic stress range versus cycles to failure curves for each temperature. However, rather than provide a different fatigue curve for each temperature, a single temperature independent fatigue curve based on stress is provided based on the ambient temperature elastic modulus. If the stress is calculated using an elastic modulus other than the ambient temperature elastic modulus, the stress must be corrected by the ratio of elastic moduli (the elastic modulus at ambient temperature divided by the elastic modulus used in the calculation) to arrive at a consistent strain basis.

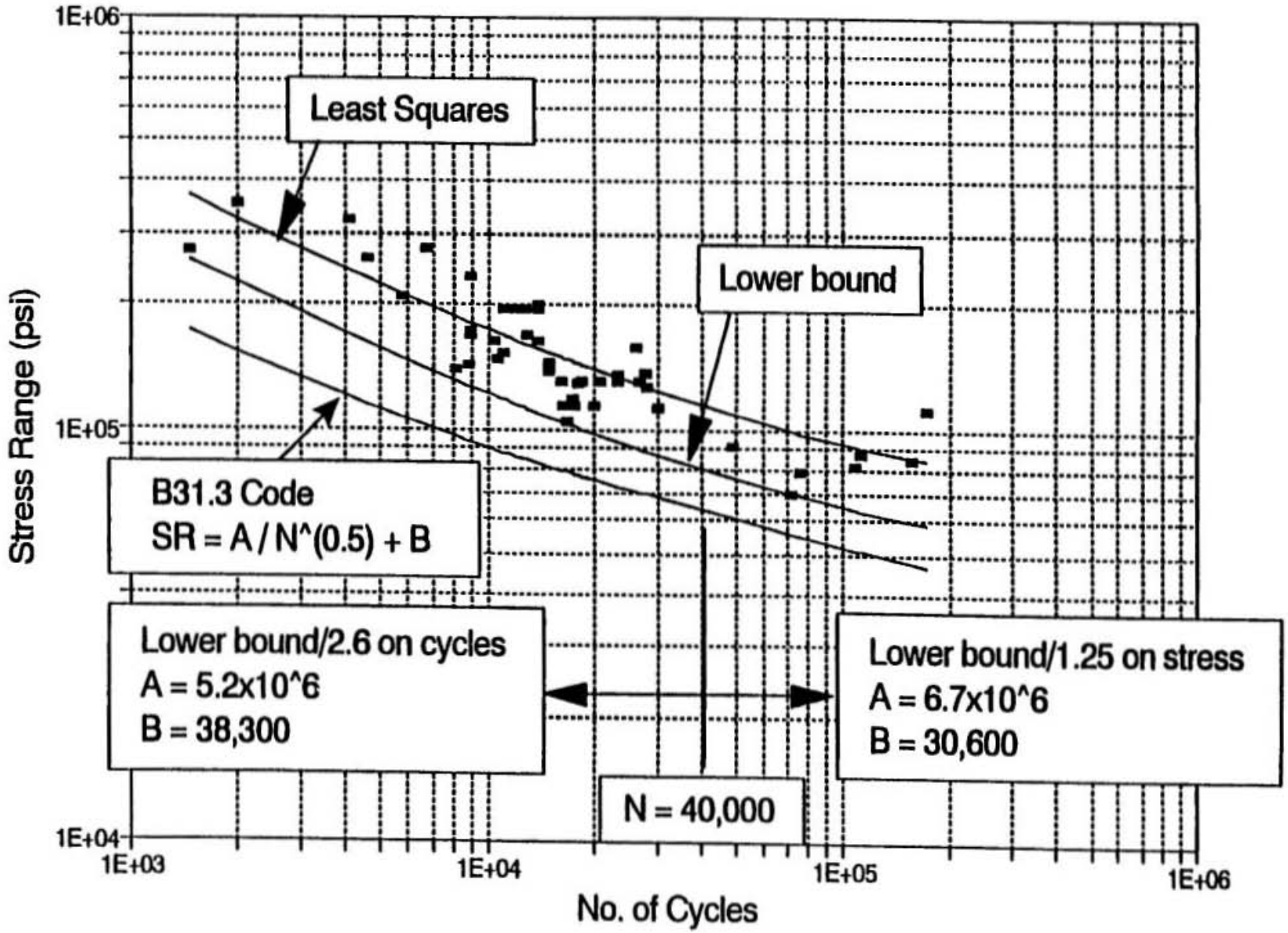

Figure 2.1-10, Fatigue Curve Development for Unreinforced Bellows
(Becht, 1995)

The correction factor for temperature is the ratio of the elastic modulus for the fatigue test condition (typically ambient temperature) to that used in calculating the stresses. This was simplified in ASME B31.3 by requiring that the calculation of stresses be done with the elastic modulus at ambient temperature (the fatigue test condition). By that means, no correction factor is required.

Reinforced Bellows Fatigue Curve Development. The deflection induced stress equations for reinforced bellows include an adjustment to account for the effect of internal pressure. Internal pressure is considered to reduce the effective convolution height by causing a greater interaction between the bellows sidewalls and the reinforcing ring. The basis for this adjustment is not documented.

A best fit fatigue curve was also developed for reinforced bellows fatigue data, but did not represent the data well. One possible cause was that the high cycle data tended to have low internal pressure whereas the low cycle data tended to have high internal pressure. Therefore, any inaccuracy in how internal pressure influences stress due to deflection (reduction in effective convolution height) would distort the fatigue data. For example, if internal pressure was calculated to cause a greater increase in deflection induced stress than actually occurs, the calculated cyclic stress in the low cycle region with tests at a higher internal pressure would be shifted up relative to those tested at lower internal pressure in the higher cycle region.

Considering the apparent poor representation of the data, the same curve as was developed for unreinforced bellows was used for reinforced bellows, except that it was shifted by a factor on stress until it lower bounded the reinforced bellows fatigue test data. The same factors as were applied to the unreinforced curve to develop a design curve were then applied to the reinforced curve.

Figure 2.1-11 shows the fatigue test data, the lower bound curve, and the resulting design fatigue curve for reinforced, as-formed, austenitic stainless steel bellows.

Instability

In addition to normally expected buckling failures under external pressure, bellows are subject to a beam-column type of buckling called "column squirm" that is caused by internal pressure. Failures can be catastrophic as in the Flixborough disaster (Newland, 1976; Warner and Newland, 1975). Stability evaluations have been limited to unreinforced U-shaped bellows and, therefore, discussion is limited to that type. However, the general principles are common to all bellows, including ring reinforced. Column squirm occurs because a lateral load develops as the bellows (or cylinder) bows since the surface area decreases on one side and increases on the other side of the bellows. This is illustrated in Figure 2.1-12. A lateral load proportional to bellows curvature results.

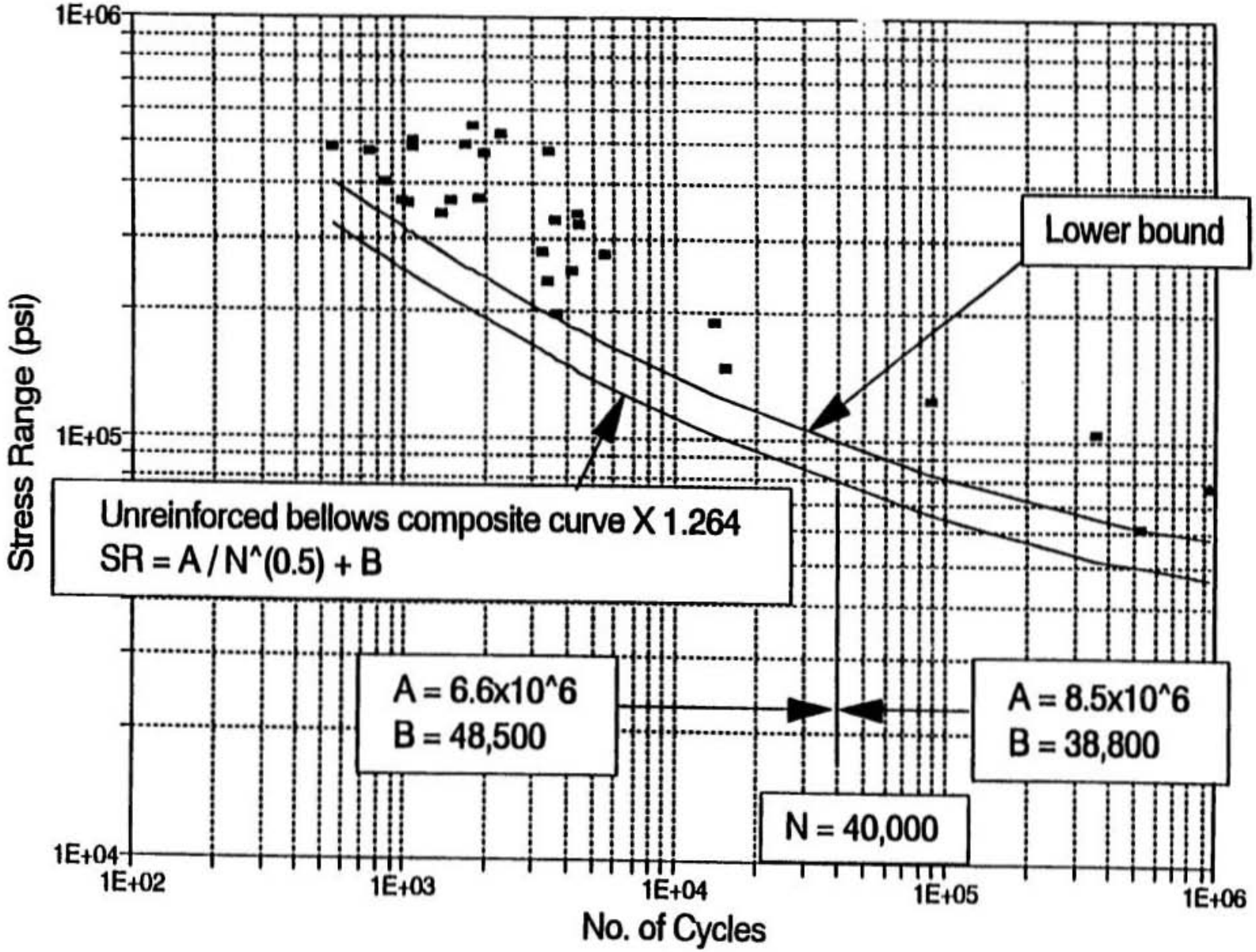

Figure 2.1-11, Fatigue Curve Development for Reinforced Bellows
(Becht, 1995)

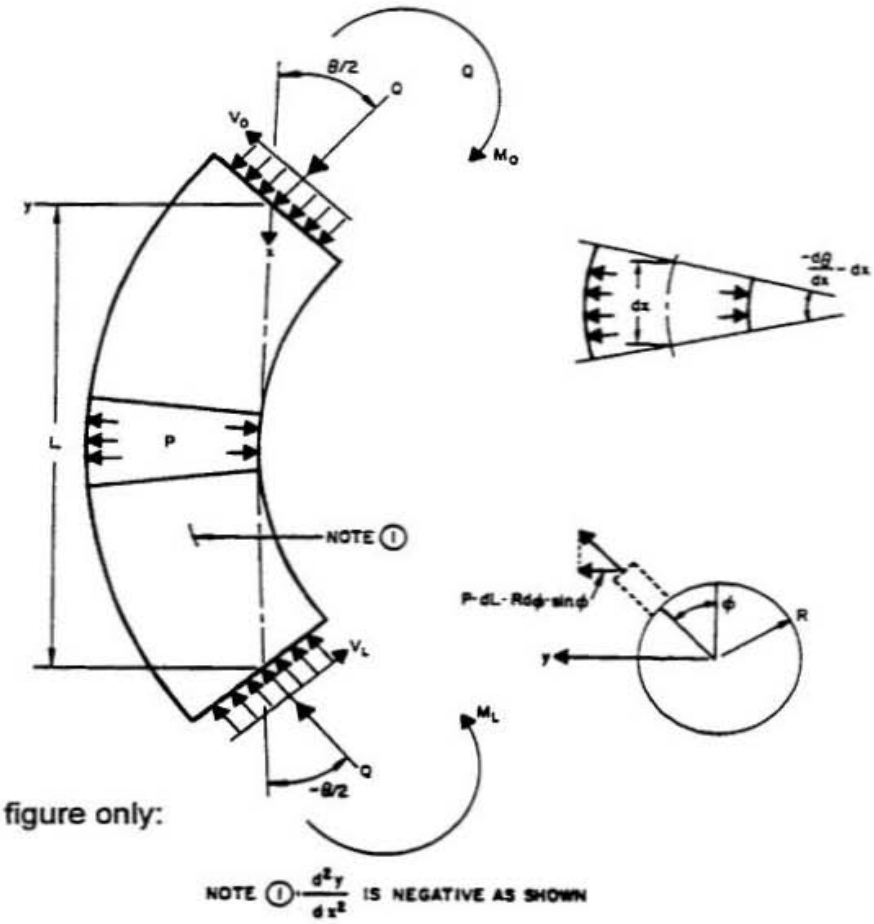

Nomenclature for this figure only:

L Length.

M End Moment.

P Pressure.

Q End force on fluid column.

R Radius.

V End shear.

θ Curvature of cylinder (bellows).

φ Circumferential angle.

Figure 2.1-12, Column Squirm of Bellows (Anderson, 1964a)

Buckling occurs when, for an incremental increase in deflection, the additional lateral force exceeds the additional restoring force due to bellows stiffness. The squirm buckling mode is also possible for cylinders under internal pressure. However, it is not common since the tensile axial force resulting when the ends are closed is sufficient to prevent the buckling due to radial pressure forces. This axial force tends to pull the cylinder straight. Such an axial force is not present in a bellows and thus they are susceptible to column squirm.

As shown by Haringx for an internally pressurized cylinder (1952a) and a bellows (1952b), the differential equation describing deflection and thus, the instability solution, is the same as that for column buckling; that is, Euler buckling with axial load replaced by pressure times the bellows mean cross-sectional area. Because of the similarity in solutions, bellows instability under internal pressure is generally evaluated using an equivalent axial load, even though the bellows is not really buckling due to axial load. It is buckling due to the lateral load caused by internal pressure. Using the equivalent axial load approach, Newland (1964) evaluated the effect of bracing struts on squirm of a universal expansion joint.

Siede (1960) evaluated the relationship between internal and external pressure, bellows angulation, and bellows stiffness for hinged bellows. He found that internal pressure effectively reduces rotational stiffness. In one evaluation of stability, he found that small, fixed-end rotations did not have a

significant effect on squirm pressure. However, deflection due to constant-end moments acted similar to an imperfection in column buckling.

Newell (1962) provides a complete discussion of stability and deflection of bellows under internal pressure, axial deflection, and angulation. He noted that initial curvature of a bellows has the same effect as a distributed lateral load in beam-column behavior. He also developed a solution for buckling under torsional loading.

Numerical methods can be used to evaluate bellows stability. For external pressure, Listvinsky (1979) used KSHELL2 to evaluate buckling of a U-shaped bellows and Becht (1984) used BOSOR4 to evaluate buckling of an Omega bellows. Ooka et al. (1989, 1994) evaluated the effect of the duration of pressure pulses on buckling response of bellows and predicted in-plane and column squirm response in the dynamic problem numerically. This investigation was prompted by concerns regarding the bellows performance in the event of a sodium-water reaction in a liquid metal fast breeder reactor. As should be expected, bellows can withstand higher pressures for shorter durations.

Campbell et al. (1981a) examined possible methods for predicting creep buckling (squirm) of bellows. This paper includes a literature search, evaluation of programs, and possible simplified methods. Included is the derivation of an equivalent cylinder to simulate a bellows.

Significant study has been undertaken recently to improve prediction of buckling for short bellows by simplified closed form solutions. These bellows are in an elastic-plastic buckling regime. This includes work by Broyles (1989) and Tsukimori et al. (1989b). The effect of plasticity reduces the buckling pressure to less than the elastically predicted value with shorter bellows. Revised column squirm buckling equations based on the work of Broyles have been incorporated into the 6th edition of the EJMA Standards (Broyles, 1994).

Ratchet

Ratchet is progressive strain accumulation with the accumulation of deflection cycles of a bellows. It is caused by cyclic deflection induced meridional bending stresses in combination with steady, pressure induced meridional membrane and bending stress. The phenomena is described by Bree (1967). While not a failure mode per se, it can lead to accumulation of excessive deformation and affect fatigue performance of the bellows. However, it is not considered in general practice. The only studies of this phenomena were for liquid metal fast breeder reactor applications (Porowski and O'Donnell, 1977; Becht et al., 1981c; Yamashita et al., 1989). While it does occur in bellows, as confirmed in tests reported by Becht et al. (1981c), it is not considered in general practice.

Elevated Temperature Considerations

ASME B31.3, ASME Section VIII, Div 1, the EJMA Standards prior to the 7th edition and most other codes and standards today do not address design of bellows in the creep range of the material of construction. This can often be avoided in piping by designing the expansion joint such that the bellows element operates at a significantly lower temperature than the process temperature. Where this is not possible, additional design considerations are required.

Because of concerns regarding issues such as heat-to-heat variability and the effect of tolerances, ASME Section III, Div 1, Code Case N290 for Class 1 nuclear bellows at elevated temperature, requires accelerated life testing at elevated temperatures. As discussed by Campbell and Kipp (1981b), this is a complex, not to mention costly process.

Anderson (1964a) advocated use of the American National Standards Institute Piping Code (presently ASME B31 Codes) stress limits for deflection induced stresses in bellows design based on evaluation of bellows tests at 650°C. Kobatake et al. (1981) showed good correlation between the Coffin-Manson law and elevated temperature bellows creep-fatigue tests. They also showed the inelastic rules of ASME Section III, Div 1, Subsection NH, which they interpreted for Hastelloy-X at 750 and 900°C, were conservative with respect

to test data. Becht (1984) used an elevated temperature shakedown concept (Becht, 1983) similar to the piping code allowable stress for deflection in design of high-temperature bellows. Welded bellows with stresses limited to the hot yield stress by Feely and Goryl (1950), and mentioned by Kleppe (1955), operated satisfactorily for many years in 480°C to 590°C environments, whereas bellows in the same service designed to much higher stresses had failed in less than two years.

Hold times are critical in creep fatigue because creep strain (and damage) accumulates with time. For example, a one hour hold time each cycle for Type 304 SS at 550°C was shown to reduce cyclic life by as much as a factor of four, when compared to zero hold time data (Yamamoto et al. (1986); Kobatake et al. (1986)). Significantly greater factors have been shown in polished bar tests at higher temperatures. Some guidance for elevated temperature design of metallic bellows expansion joints is provided by Becht (1989a) and Broyles (1995). Criteria developed in the Japanese Liquid Metal Fast Breeder Reactor Program are described by Tsukimori et al. (1989a).

The 7th edition of the EJMA Standards incorporates Appendix G on design of elevated temperature bellows, based on the work of Broyles (1995). It provides a method for conservatively lower bounding the cyclic life at elevated temperature based on limited elevated temperature fatigue testing.

There remains substantial room for development of design methods for bellows at elevated temperature. The proven method of using empirical fatigue curves at low temperatures is complicated by the addition of other factors such as time. The present work is limited to behavior at temperatures below the creep regime.

Effect of Reinforcing Rings

Reinforcing rings come in two basic types. These are simple rings and equalizing rings. The simple rings can be simply round bar. Equalizing rings, as shown in Figure 2.1-1, have a tear drop shape that the bellows conforms to as it is compressed and/or pressurized. They are termed equalizing rings because they are intended to assure that each of the convolutions takes an equal proportion of the total deformation.

All reinforcing rings are intended to add metal to withstand the circumferential forces due to internal pressure. This reduces the circumferential membrane stress in the bellows wall. They are also considered to reduce the effective height of the convolution. This simple analogy makes it readily apparent that adding reinforcing rings will increase the stress due to deflection (because the effective convolution height is reduced) and reduces the bending stress due to internal pressure (for the same reason). Internal pressure is considered to increase the effect of the reinforcing ring on the convolution (increasing the

reduction in effective convolution height). The pressure tends to bulge out the convolution sidewalls, increasing interaction between the sidewalls and reinforcing ring. Compressive deflection of the bellows also increases interaction between the sidewalls and reinforcing ring.

2.2 Development of Analytical Methods

Theoretical Methods

The general theory of elastic shells, as first proposed by Love, has been reduced to two formulations for axisymmetric shells, the Love-Meissner and the E. Reissner formulations. Both result in two coupled second-order differential equations with two variables. Solutions were developed for specific types of shells with constant curvature (e.g., cones) which could be combined at the junctions using conditions of continuity to synthesize a general shell. The case of a toroidal shell (this shape is present in most formed bellows) has not been evaluated exactly without a computer. However, approximate solutions were developed for the toroid which permitted analysis of bellows.

Advances in analysis techniques for piping elbows led to two techniques which were used for evaluating the toroidal elements of formed bellows. These were: 1) expressing one of the variables (e.g., meridional bending

deformation) in terms of a Fourier series, truncating the series and solving for the coefficients of the remaining terms by minimizing potential or complementary energy by setting the derivatives with respect to the unknown coefficients equal to zero; and 2) solving the second-order differential equations for general shells of revolution by asymptotic integration. Because of the assumptions and approximations in both methods, neither is accurate over the full range of toroid geometries; however, they are complementary. The series solutions are valid for small values of $\mu=[12(1-\nu^2)]^{1/2}r^2/R't$, where r is the meridional radius of the toroid, R' is the mean circumferential radius of the bellows, and t is the wall thickness) whereas the asymptotic solution is valid for large values of μ. Dahl (1953) compared a four-term series solution to the asymptotic solution for an Omega bellows and found them to overlap for values of μ between approximately 5 and 40. Note that the range of μ for which the series solution is accurate is dependent on the number of included terms.

The most accurate evaluation of bellows using analytical solutions was by Anderson (1964a, 1964b), who used the asymptotic solution for the toroid. He included correction factors to compensate for the errors introduced by approximations. This work was the basis for the stress equations provided in the EJMA Standards. Since the inaccuracies caused by approximations in the analytical solutions are avoided by numerical analysis using digital computers, essentially all research on bellows stresses since the work of Anderson has been done using numerical methods.

Numerical Methods

Numerical methods of solution reached wide application with the advent of the digital computer. These methods are the finite difference, numerical integration, and finite element method. The first two methods solve the shell equations using approximate, numerical techniques. The third method relies on partitioning a shell into a number of finite elements, in which displacement polynomials in terms of undetermined coefficients are assumed.

Finite Difference. In the finite difference method (Penny, 1961; Radkowski, 1962; Sepetoski, 1962; Budiansky, 1963), the second-order differential equations are replaced by a set of linear algebraic difference equations. The derivatives are written over a finite length instead of an infinitesimal length. The accuracy increases as the finite difference length approaches zero (i.e., the shell is divided into a greater number of parts) and the difference approaches the exact differential. To check accuracy (convergence on exact solution), the problem should be run with two different mesh densities.

The finite difference energy method (Kraus, 1965; Bushnell, 1973; Bushnell, 1971; Bathe, 1982), an improvement on the finite difference method, uses the principle of minimum potential energy. Rather than express the shell equations in finite difference form, the total potential energy is approximated by finite differences and minimized with respect to nodal point displacements

to solve for the displacements. This method is very similar to the finite element method; however, it often provides a more efficient formulation for shell analysis, as shown by Bushnell (1973) for a particular case.

Numerical Integration. In numerical integration, the second-order differential equations are converted to first-order differential equations by finite difference approximation, initial values are assumed for the unknown boundary conditions at the leading edge, and the equations are integrated (e.g., by the Runge-Kutta method) across the shell. The solution is found by assuming different boundary conditions at the leading edge and interpolating to get a solution that satisfies the known boundary conditions at the far end of the shell. Yet, since edge effects are localized in a shell, the solution at the final edge can become insensitive to the assumed initial values at the leading edge as the shell length is increased. As a result, significant round-off errors can occur with long shells.

Kalnins (1964) developed a segmental approach to numerical integration that solved the round-off problem. The shell is divided into segments, each of which is small enough that the final edge is sensitive to the leading edge. A series of simultaneous equations are generated from continuity conditions for the variables at the segment junctions and boundary conditions at the ends of the shell. This numerical integration method has the advantage that accuracy is predetermined by maintaining the segment length below some

critical length for the shell; there is no need to vary mesh density to check accuracy.

Finite Element. The finite element method uses elemental stiffnesses to form an overall stiffness matrix. The shell is approximated by a number of finite elements with known displacement polynomials or "shape functions." The stiffness of each element is determined via energy methods with either closed form solutions or, more generally, by numerical integration over the finite element.

With isoparametric elements, the solution converges on the exact solution as the mesh is made finer. As in the finite difference solution, one must run the problem with different mesh densities to check convergence. It may be of interest to note, as shown by Lestingi and Brown (1973), that the equations generated by multisegment numerical integration can be converted to stiffnesses on a segment-by-segment basis.

The finite element method was used in the present research.

2.3 Application of Analytical Methods

Single-Ply Unreinforced Bellows

Methods of predicting stress/strain in single-ply unreinforced bellows have progressed through several stages. These have been: 1) use of simple-beam or beam and cylinder approximations, 2) use of shell theory with approximations, 3) use of design charts and formulas based on approximate shell theory, 4) elastic numerical analysis, and 5) nonlinear numerical analysis. Most bellows design today is by design charts and formulas based on approximate shell theory. These are the equations and charts in the EJMA Standards, described in Chapter 3 herein. There is some design and/or design verification using linear numerical analysis and, more rarely, by nonlinear numerical analysis. However, the nonlinear analyses have improved understanding of some significant complexities in bellows response.

While the simplified analysis equations developed by Anderson (1964a, 1964b), which are in the EJMA Standards and are described in Chapter 3, have been used for design of most bellows over the past 30 years, detailed analysis has been via numerical methods. Most of the recent work has used finite element analysis. This is because direct analytical solution of the shell equations for the toroid is not possible. Exact solution by numerical methods avoids the errors introduced by approximations necessary for analytical solution of the toroid shell equations.

Although subsequent paragraphs primarily discuss evaluations of axial displacement of bellows, they are also relevant for bending. Gross bending displacement of the bellows is generally treated as an equivalent axial displacement for both stress and stiffness calculations such as in the EJMA Standards. Such an approach was used by Donnell (1932) for corrugated pipes. Turner (1959) used this approach for bellows and verified it with test data. Trainer, et al. (1968) measured axial and bending stiffnesses and found the bending stiffness to differ from that predicted based on axial stiffness by as much as 30 percent. However, bending stiffnesses were calculated with fairly good accuracy by computer analysis (using Fourier series approach to nonsymmetry). The difference may have resulted from a size effect; all the tested bellows were five inches or less in diameter. This candidate has found very good correlation, using the equivalent displacement approach, of strain gage data taken from a 450 mm (18 in.) diameter bellows that was first displaced axially and then in bending. The strains in the convolution crowns, which are the farthest point from the neutral axis, were slightly higher than predicted and the strains in the roots were slightly lower.

Early Developments. The earliest stress/deflection analyses of bellows and corrugated pipe relied on simple beam (Chandler, 1941) or beam and cylinder (Salzman, 1946) approximations. Except in specific cases, these gave qualitative but not quantitative assessments of bellows stress and deflection. For the specific case of a welded disk bellows evaluated by Feely and Goryl

(1950), the predictions based on beam approximations correlated well with test data.

Analytical solutions were developed based on energy (truncated series) methods and asymptotic integration, discussed previously. These solutions were predominantly for axial loading, although pressure loading was sometimes evaluated as noted in the subsequent paragraphs. A discussion of the developments in Russia, not covered herein, is provided by Trainer et al. (1968).

The response of bellows to axial force/deflection was evaluated by a number of investigators using energy methods. Pressure stresses were also evaluated as noted. Salzman (1946) evaluated a U-shaped bellows using a three-term series to represent the meridional bending deformation. Dahl (1953) used a four-term series for a Omega bellows. Turner and Ford (1956), used a five-term series to represent circumferential stress and evaluate semi-toroidal bellows (including S-types). Turner (1959) extended the work to include U-shaped bellows. He also evaluated pressure loading by approximating the bellows with beam theory, using curved beams for the toroids. Palmer (1960) extended the work of Salzman to include corrugated pipe with any included angle. Laupa and Weil (1962) evaluated U-shaped and semi-toroidal bellows using a five-term series to express the bending deformation of the toroid and circular plate to represent the convolution sidewalls. They also evaluated pressure stresses with shell theory. In

evaluations using energy methods, the lengths of the series were limited because as more terms are included, the matrices that must be manipulated became larger.

Clark (1950) developed solutions for axial deflection of Omega bellows and corrugated pipe using asymptotic integration. He also developed a solution for pressure loading by combining an approximate particular solution for the pressure loading with the approximate complementary solution developed for axial loads. Clark and Reissner (1953) extended the solution of Clark (1950) to large deflection problems. Clark (1958) extended the solution for Omega bellows to include generalized geometry (e.g., noncircular Omega). Hetenyi and Timms (1960) used asymptotic integration for welded curved-disk bellows. Corrections were incorporated into the solution of Clark to permit large values of r/R' (e.g., greater than one), where r is the meridional radius of curvature and R' is the circumferential radius of curvature.

Anderson (1964a, 1964b) used the asymptotic solution of Clark to develop solutions for deflection stresses in U-shaped bellows and introduced corrections to compensate for the approximations by Clark. Thus, solutions were developed that were applicable over the full range of toroid geometry. Pressure stresses were also evaluated similarly to Clark (1950), but extended to include U-shaped bellows. Anderson performed parametric analyses of bellows geometries using these equations to develop design charts. These charts were for nondimensionalized meridional bending stress due to

pressure, stiffness and meridional bending stress due to displacement. This work is the basis for the stress equations for unreinforced bellows in the EJMA Standards, and is more fully described in Chapter 3.

Hamada et al. (Hamada and Takenzono, 1965a; Hamada and Takenzono, 1965b; Hamada and Takenzono, 1965c; Hamada, et al., 1970) also developed design equations and charts for U-shaped bellows under axial load and internal pressure. These were developed using the shell theory of Ota et al. (Ota and Hamada, 1963; Ota, Hamada, and Furukawa, 1963) for the toroid and plate theory for the sidewalls.

Evaluations by Numerical Methods. Design charts have also been prepared from parametric numerical analysis. These charts can be used similarly to the ones developed by Anderson (1964a, 1964b) and Hamada et al. (Hamada and Takenzono, 1965a; Hamada and Takenzono, 1965b; Hamada and Takenzono, 1965c; Hamada, et al., 1970). Hamada, et al. (1971) developed charts for bellows stress and stiffness under applied bending moment using the Fourier series approach with the finite difference method of Budiansky and Radkowski (1963). Hamada et al. (1976) developed charts and equations, therefor, giving maximum stress range for U-shaped bellows under internal pressure and axial displacement. These were based on parametric finite difference solutions using the method of Sepetoski, et al. (1962). Janzen (1979) evaluated pressure and deflection stresses in U-shaped bellows using statistical analysis in conjunction with parametric finite element solution.

Trainer, et al. (1968) evaluated U-shaped and welded disc bellows using NON-LIN, a multisegment numerical integration computer program by Lestingi (elastic, large displacement). The theoretical calculations were based on measured bellows dimensions. In general, there was fairly good correlation of strains due to pressure and deflection. It is worth noting that satisfactory fatigue life correlations could not be made with welded bellows because of considerable variation in fatigue life and failure location for nominally identical bellows subjected to the same deflection loading. This is presumably because of variability in welding.

Lestingi and Hulbert (1972) used NON-LIN to evaluate pressure and deflection of U-shaped and welded bellows and showed fairly good correlation with test data. Listvinsky used KSHELL1, a multisegment numerical integration program by Kalnins, to evaluate a U-shaped bellows design. Becht and Skopp (1981b) used finite element analysis (MARC computer program) to evaluate elastic-plastic response of a U-shaped bellows under separate and combined axial deflection and internal pressure. The calculations were made with measured bellows dimensions; very good correlation with strain gage data was found. Osweiller (1989) found similar results in comparison of elastic finite element results to the stress predictions per the EJMA Standards, leading to the incorporation of the equations from the EJMA Standards into the French Pressure Vessel Code, CODAP.

Plasticity complicates bellows response, even under deflection loading. Tanaka (1974), following Hamada and Tanaka (1978, 1974), found that strain concentration occurs at the high-stress zones after yielding under axial displacement loading. They developed elastic-plastic solutions using the finite difference method and correlated predicted cyclic lives with bellows fatigue data in order to develop factors that could be applied to elastic analysis results to account for strain concentration. Strain concentration was found to depend upon a parameter, μ (here, μ=r /tR'). A maximum fatigue life reduction of 4 was found for values of μ greater than 1.5, which corresponds to a strain concentration of about 2. That implies that elastic analysis should not be linearly extrapolated even for displacement-induced strain.

Kobatake, et al. (Kobatake, et al., 1975; Kobatake, et al., 1981) evaluated high-temperature cyclic loading with creep using finite element analysis. They found that both calculated inelastic strain range and creep damage (calculated using linear time fraction summation) correlated well with cycles to failure data from bellows creep-fatigue tests (Kobatake, et al., 1981).

Remarks. At present, design equations and charts, such as can be found in the EJMA Standard, provide ready means for calculating bellows stress and stiffness. They have achieved international acceptance, and are the basis used in Codes and Standards throughout the world.

Inelastic analyses such as those to evaluate strain concentration have provided useful insights into bellows response. Where the material and load histogram are well characterized, such as in Becht (1981b), good correlations between analysis and test have been found.

Multi-Ply Bellows

A multi-ply bellows is a bellows in which the convolution wall is composed of more than one layer of material. Behavior of multi-ply bellows is complicated by the fact that the plies may or may not act independently. If there is sufficient internal pressure, the plies may lock together by frictional forces and act monolithically. Although an "exact" analysis is possible using present-day nonlinear analysis programs, rigorous analysis has been very limited. Note that even exact solutions of ideal geometries may fall short because residual stresses and gaps between plies resulting from fabrication can have a significant effect. Nonlinear numerical analysis can presently provide qualitative answers to questions regarding ply interaction; further experience/correlations with data are required before such analysis can be considered to provide a reliable, quantitative assessment.

The equations by Anderson (1964a, 1964b) for U-shaped, reinforced, and Omega bellows include multi-ply construction. Although there is no discussion of the rationale, it is clear from the equations that the plies are assumed to always act independently. The same assumption is carried into the EJMA Standards.

Trainer, et al. (1980) tried to use an equivalent bellows model to represent two-ply bellows. The elastic modulus was adjusted to represent different degrees of ply interaction. Evaluation of test data indicated that the problem was too complex to evaluate satisfactorily with the simple model. Gaps between plies resulting from fabrication were found to have a significant effect on measured bellows strains.

Vrillon, et al. (1975) used finite element analysis to investigate a two-ply ring-reinforced bellows. They assumed no friction and no disengagement between plies and found good correlation with a natural frequency test of an unpressurized bellows. With internal pressure, frequencies increased 13 to 20 percent, which shows there is an interaction between plies and/or with the rings caused by pressure. Note that complete locking of the plies together would be expected to about double the frequency.

The evaluations contained herein are limited to single ply bellows.

Ring-Reinforced Bellows

Ring-reinforced bellows are complicated by the nonlinear interaction between shell and ring. The contact between the ring and shell is a function of pressure and deflection load. The bellows tends to wrap around the ring as pressure is increased.

The EJMA Standards are based on the work of Anderson, at least for the development of the equations for stress in unreinforced bellows. However, for reinforced bellows, Anderson (1964a, 1964b) developed lower bound solutions for stress. These were used to calculate lower bound stresses at failure of test bellows and, thereby, lower bound allowable stresses. These lower bound equations are not used in the EJMA Standards.

Malkmus developed empirical equations for reinforced bellows which are contained in the EJMA Standards. These equations use a reduced convolution height in conjunction with the equations for unreinforced bellows. The development of these equations is not presently documented in the open literature.

Miyazaki et al. (1993) performed elastic-plastic finite element analysis of a single geometry ring reinforced bellows with the loading conditions varied parametrically. The rings were equalizing rings. He found that friction

between the ring and ply did not affect the results. He found little effect of the equalizing rings at lower levels of compressive deflection, but significant effects at high levels. Evaluation of the results indicates that this was due to over-compression of the bellows, beyond reasonable values that may be used in practice. The bellows was compressed to the point where the sidewalls were completely in contact with the equalizing rings, so that any additional compressive deflection had to be absorbed by the convolution crown toroid, alone. Thus, the significant effects found in this study are not relevant to normal bellows applications.

2.4 Plastic Strain Concentration

Plastic strain concentration (also termed elastic follow-up) is shown in this research to be an important consideration with respect to the response of bellows to cyclic deflection loading. This section provides theoretical background information with respect to this phenomena.

Component evaluations, including bellows, are generally performed by elastic analysis, even when the components may be loaded beyond yield. Secondary stresses are typically allowed to exceed yield strength. Secondary stresses are deflection or strain controlled, not equilibrium controlled. When the imposed strain exceeds the strain at which the material yields, an elastic calculation will result in a stress in excess of yield. This is not a true stress,

but is simply the strain times the elastic modulus. This calculated stress value is used in design as a measure of the strain. Thus, for example, fatigue curves showing stress versus number of cycles to failure show stress values well in excess of materials' yield strengths.

The elastically calculated stress is assumed to be proportional to the strain, and is typically used in the fatigue analysis of a component. Errors are introduced when plastic strain concentration (more generally termed elastic follow-up) occurs. In the event of plastic strain concentration, the actual strain in local, highly stressed regions of a component exceeds the elastically calculated strain.

Consider a component with a local region in which plastic strain concentration is occurring and a remainder of the component. Plastic strain concentration requires that the stress in the local region be higher relative to the yield strength of the material than the remainder. Plastic strain concentration also becomes more severe, the more flexible the remainder is, relative to the local region. This is because there is then more strain, that was elastically calculated to be absorbed in the remainder of the component that has the potential to be shifted to the local region by action of plasticity.

As an example, consider a cantilevered pipe subject to lateral deflection of the free end, with a portion adjacent to the fixed end constructed with a reduced diameter

or thickness pipe or lower yield strength material. The elastic analysis assumes that strains will be distributed in the system in accordance with the relative elastic stiffnesses. However, consider what happens when the locally weak section yields. As the material yields, a greater proportion of additional strain due to displacement occurs in the local region because its effective stiffness has been reduced by yielding of the material. Thus, there is plastic strain concentration in the local region.

An example of a two bar system under axial tension or compression provides an illustration of plastic strain concentration. The problem is illustrated in Figure 2.4-1. The elastic distribution of the total displacement, Δ, between bar A and bar B is as follows

$$\Delta_A = \frac{K_B}{K_A + K_B}\Delta \tag{2.2}$$

$$\Delta_B = \frac{K_A}{K_A + K_B}\Delta \tag{2.3}$$

where:

A_A = area of bar A

E_A = elastic modulus of bar A

K_A = A_AE_A/L_A, elastic axial stiffness of bar A

K_B = A_BE_B/L_B, elastic axial stiffness of bar B

A_B = area of bar B

E_B = elastic modulus of bar B

L_A = length of bar A

L_B = length of bar B

Δ = total axial displacement imposed on two bars

Δ_A = displacement absorbed by bar A

Δ_B = displacement absorbed by bar B

Assuming elastic, perfectly plastic behavior of the material, with a yield stress, σ_y, the stress in bar B cannot exceed yield, so the load in bar A cannot exceed $\sigma_y A_B$. Therefore, after bar B starts to yield, the displacement in each bar is as follows.

$$\Delta_A^{e-p} = \frac{\sigma_y A_B}{K_A} \tag{2.4}$$

$$\Delta_B^{e-p} = \Delta - \Delta_A^{e-p} \tag{2.5}$$

where

$\Delta^{e-p}{}_A$ = actual displacement absorbed by A, elastic plastic case

$\Delta^{e-p}{}_B$ = actual displacement absorbed by B, elastic plastic case

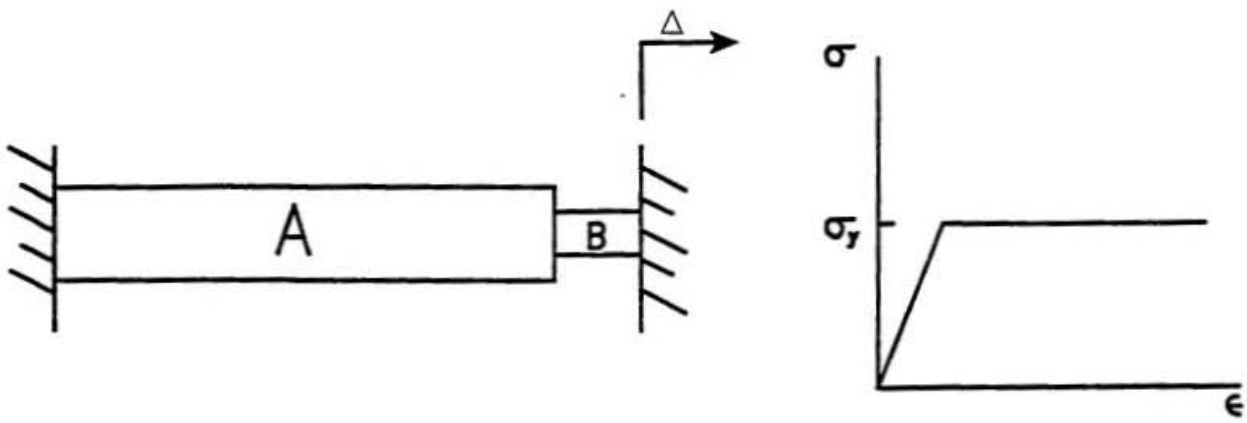

Figure 2.4-1, Two-Bar Plastic Strain Concentration Model

The strain concentration is the actual strain in bar B, considering elastic plastic behavior, divided by the elastically calculated strain in bar B. Since strain is displacement divided by length, the strain concentration is as follows.

$$strain\,concentration = \frac{\Delta_B^{e-p} / L_B}{\Delta_B / L_B} = \frac{\left(\Delta - \frac{\sigma_y A_B}{K_A}\right) / L_B}{\left(\frac{K_A}{K_A + K_B}\Delta\right) / L_B} \tag{2.6}$$

This can be rearranged as follows.

$$strain\,concentration = \left(1 + \frac{K_B}{K_A}\right)\left(1 - \frac{\sigma_y A_B}{\Delta K_A}\right) \tag{2.7}$$

If we consider a general region under lower stress or in a stronger condition coupled with a local region under higher stress or with weaker material (e.g. lower σ_y), the more flexible the general region (stiffer the local region) is, the more severe the elastic follow-up. This can be observed looking at equation 2.7. As the stiffness of bar B increases relative to bar A, the more severe the plastic strain concentration.

In bellows, strain concentration due to displacement loading occurs in the roots and crowns of the bellows, the location of highest bending stress. The root and crown can be considered the local region and the sidewall the remainder. The greater the

convolution height, the more flexible the remainder is, and the larger the potential for plastic strain concentration. While a larger convolution height may make it less likely for the bellows to yield when subject to displacement loading, because the bellows is more flexible and subject to lower stresses for a given displacement load, once the bellows does yield, the strain concentration should be worse. This is because there was more strain, elastically calculated to be absorbed by sidewall deflection, that is, instead, shifted to the local yielded region.

Chapter 3

EJMA Equations for Bellows

3.1 EJMA Stress Equations for Unreinforced Bellows

Most bellows today are designed using the equations provided in the Standards of the Expansion Joint Manufacturers Association. These equations and the charts used with them are based on the work of Anderson (1964a, 1964b), and are based on shell theory and equilibrium considerations. The equations for unreinforced bellows that are presently in the EJMA Standards, 7th edition, are as follows. Dimensions are illustrated in Figure 2.1-1 and defined in the nomenclature.

The bellows circumferential stress due to internal pressure, S_2, is:

$$S_2 = \frac{P\,D_m}{2\,n\,t_p}\left(\frac{1}{0.571 + 2w/q}\right) \qquad \textbf{(3.1)}$$

Equation 3.1 is based on equilibrium considerations, as shown in Figure 3.1-1. It is the pressure times the mean bellows diameter divided by the metal area of the convolutions. This is a primary membrane stress.

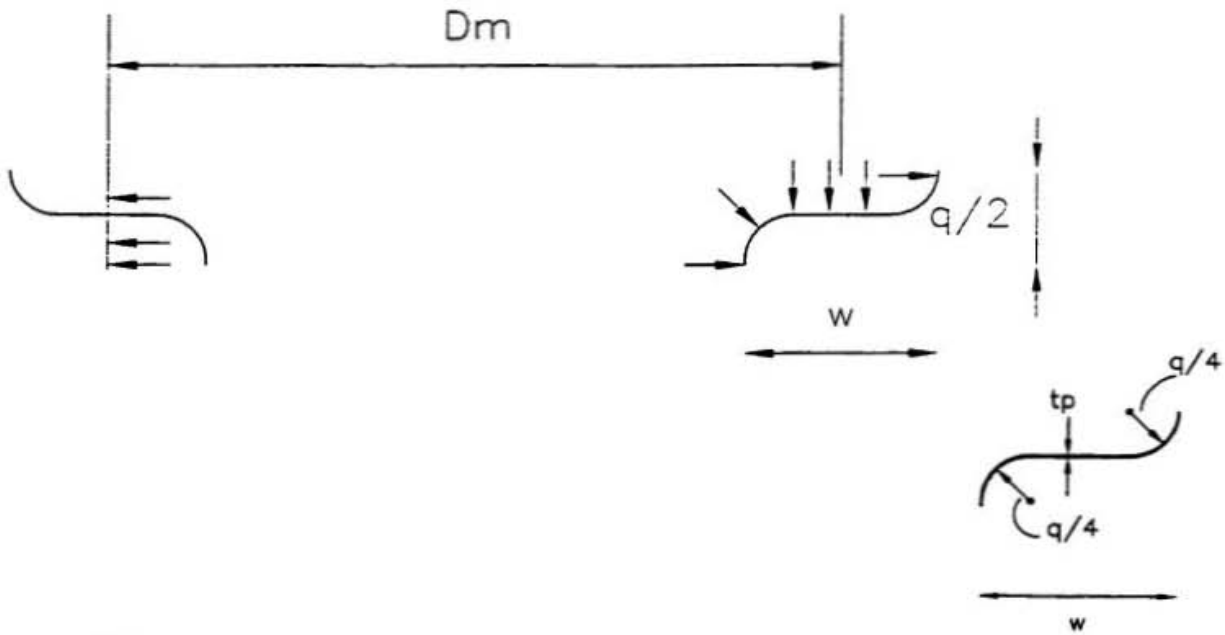

$$S_2 = \frac{PD_m q}{2A_c}$$

Both sides of bellows:

$$S_2 = \frac{PD_m q}{2t_p}\left(\frac{1}{.571q + 2w}\right)$$

$$A_c = 2\left[\left(\pi 2\frac{q}{4}t_p\right)\frac{2}{4} + \left(w - \frac{2q}{4}\right)t_p\right]$$

$$S_2 = \frac{PD_m}{2t_p}\left(\frac{1}{.571 + 2w/q}\right)$$

$$A_c = t_p(.571q + 2w)$$

Solution for Single Ply.

For Multi-Ply Substitute nt_p for t_p.

Figure 3.1-1, Pressure-Induced Circumferential Membrane Stress

A primary stress is a load controlled stress, versus a secondary stress, which is deformation controlled. These terms are used in the ASME Boiler and Pressure Vessel Code, Section VIII, Div 2 to describe different types of stress for which different design criteria are used.

The bellows meridional membrane stress due to internal pressure, S_3, is:

$$S_3 = \frac{P\ w}{2\ n\ t_p} \qquad \textbf{(3.2)}$$

Equation 3.2 is based on equilibrium considerations, as shown in Figure 3.1-2. It is the pressure acting on the sidewalls, divided by the metal area of the root and crown. This equation simply treats the convolution as a curved beam. This is a primary membrane stress.

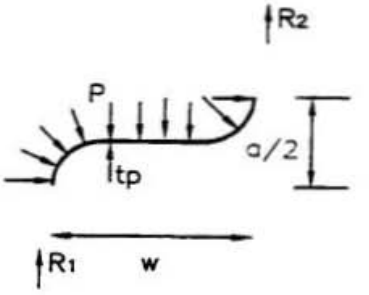

Assume $R_1 = R_2 = t_p S_3$

From Equilibrium

$$2t_p S_3 = R_1 + R_2 = Pw$$

$$S_3 = \frac{Pw}{2t_p}$$

Solution for Single Ply.

For Multi-Ply, Substitute nt_p for t_p.

Figure 3.1-2, Pressure-Induced Meridional Membrane Stress

The following equations, 3.3 through 3.5, are based on shell theory. Anderson developed an approximate general solution, from shell theory, for the toroid that included four unknown constants. The shell equation was nondimensionalized using the two parameters, $QDT=q/(2.2(D_m t_p)^{1/2})$ and $QW=q/(2w)$. The convolution sidewall was then represented as a strip of uniform width and four assumed boundary conditions were used to develop four simultaneous equations to solve for the four unknown constants. The parametric solution of these nondimensional equations yielded the factors C_p, C_f, and C_d, which are used to calculate S_4, S_5 and S_6, below. The charts providing these factors, developed by Anderson, are provided in the EJMA Standards and are provided herein as Figures 3.1-3, 3.1-4 and 3.1-5.

The bellows meridional bending stress due to internal pressure, S_4, is:

$$S_4 = \frac{P}{2\,n}\left(\frac{w}{t_p}\right)^2 C_p \qquad \textbf{(3.3)}$$

The distribution of meridional bending stress in a convolution is illustrated in Figure 2.1-5. There was controversy as to whether this was a primary or secondary bending stress. As discussed in *Resistance to Internal Pressure* in Section 2.1, these were shown by Becht (1980) to be primary bending stress since the formation of plastic hinges in the convolution results in a limit load failure.

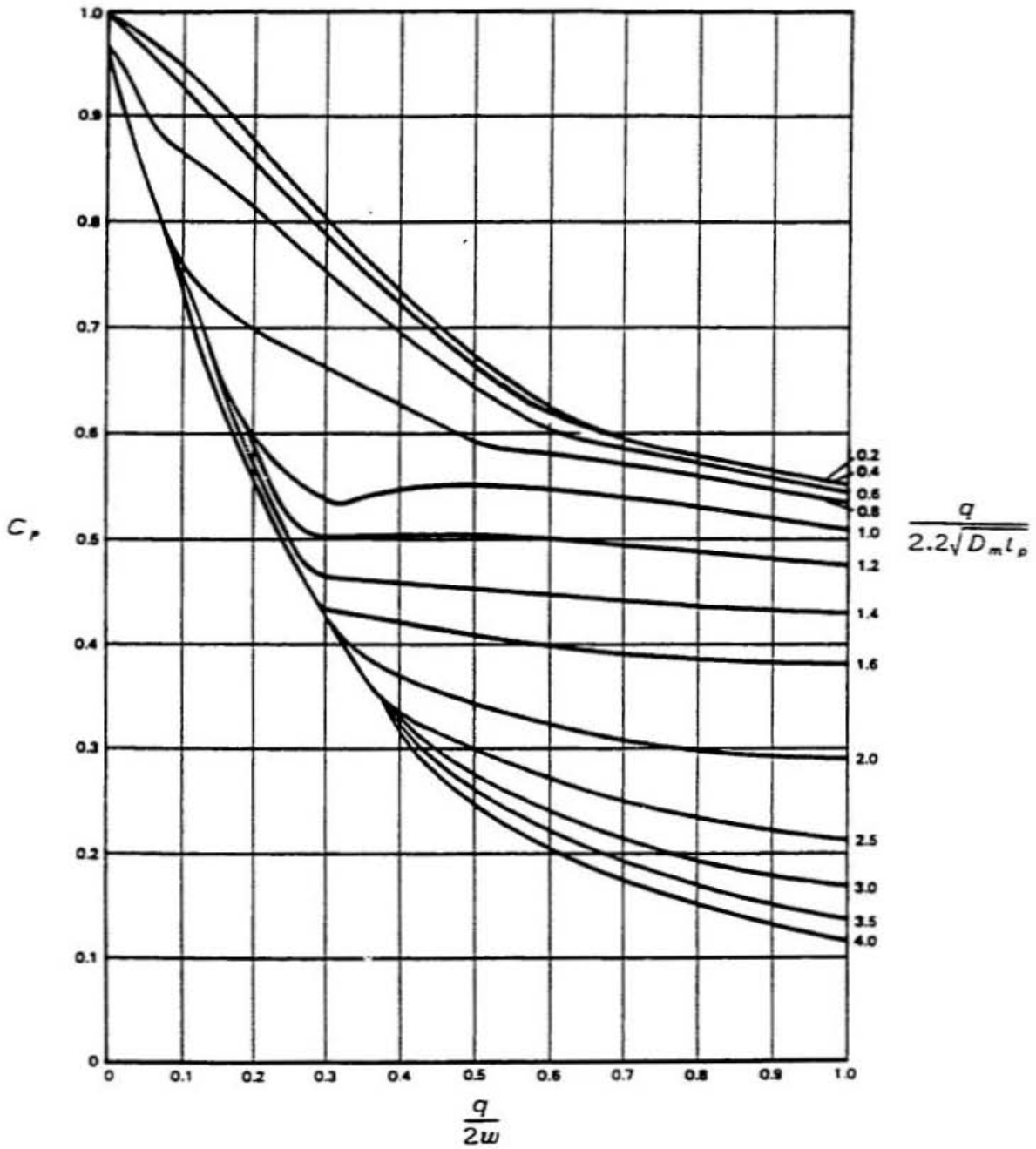

Figure 3.1-3, Chart for C_p (EJMA, 1993)

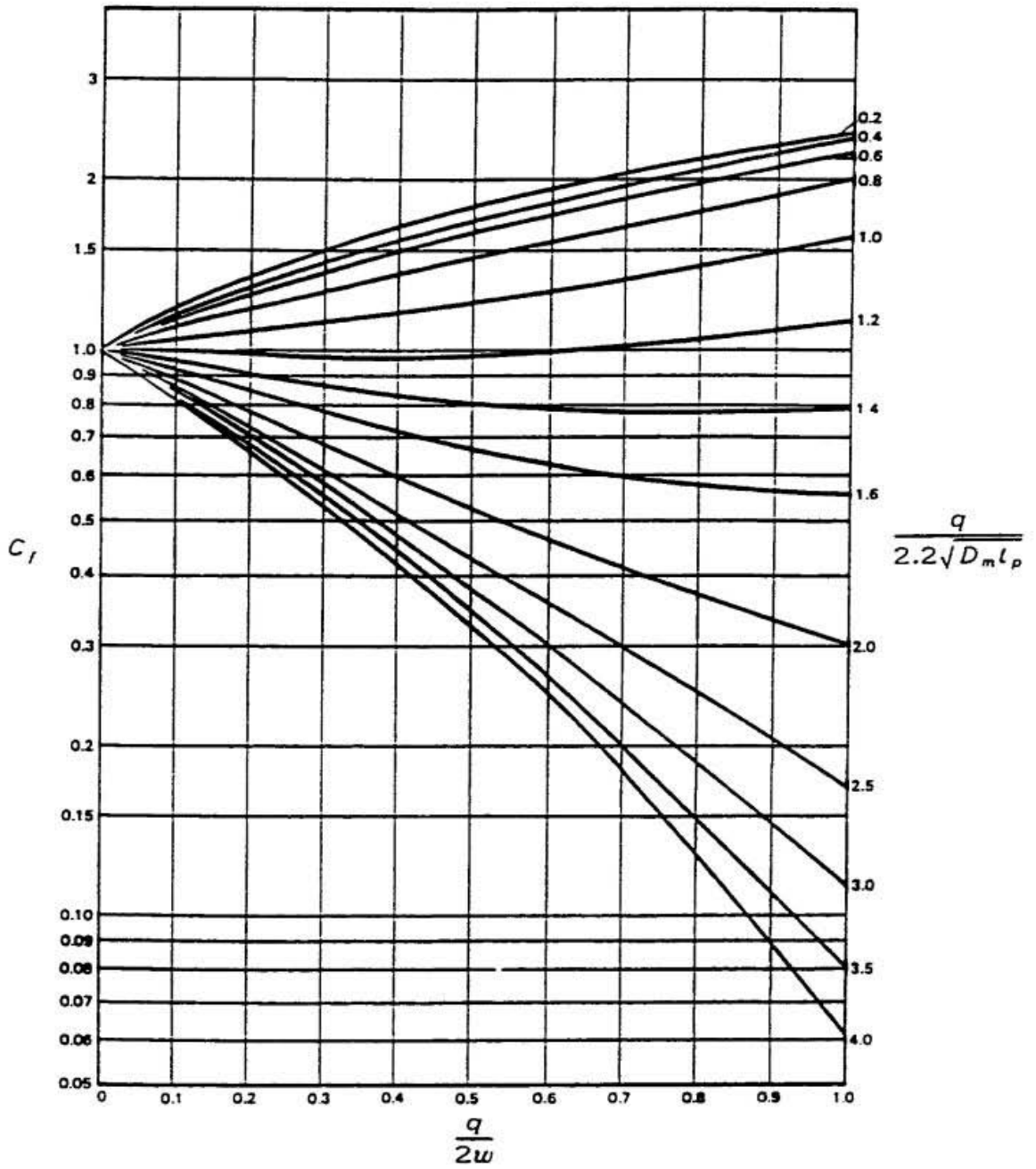

Figure 3.1-4, Chart for C_f (EJMA, 1993)

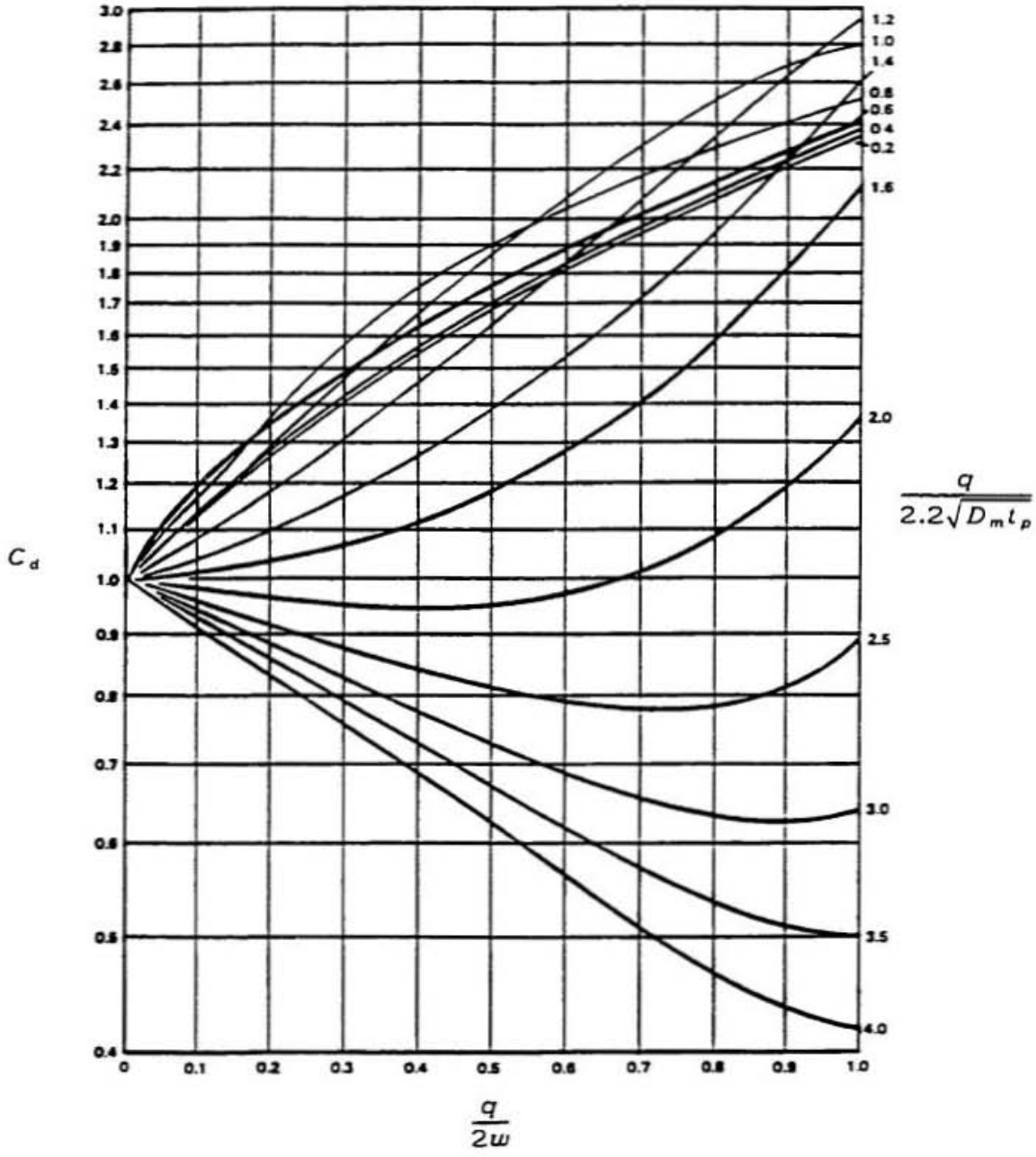

Figure 3.1-5, Chart for C_d (EJMA, 1993)

The bellows meridional membrane stress due to deflection, S_5, is:

$$S_5 = \frac{E_b\, t_p^2\, e}{2\, w^3\, C_f} \qquad \textbf{(3.4)}$$

The meridional membrane stress due to deflection is the force required to deflect the bellows, per equation 3.6, divided by the metal area based on the mean diameter and wall thickness of the bellows, as shown in Figure 3.1-6. Because this stress is due to displacement, it would typically be considered to be a secondary stress. However, it is not self limiting because the spring of the bellows will maintain the load, even if meridional membrane yielding occurs. Thus, considering elastic follow-up, the meridional membrane stress due to deflection could be considered to behave as a primary stress. However, this is not of any real consequence in the design of typical bellows since the meridional membrane stress due to deflection is generally a relatively low stress. Further, since bellows are typically cycled well into the plastic regime, an elastic calculation of bellows stiffness does not accurately represent the meridional membrane stress in any case.

The bellows meridional bending stress due to deflection, S_6, is:

$$S_6 = \frac{5\, E_b\, t_p\, e}{3\, w^2\, C_d} \qquad \textbf{(3.5)}$$

$$\frac{F}{e} = f_{iu}$$

(f_{ir} for reinforced bellows)

where F is the axial force to deflect a convolution a distance, e.

$$F = \frac{1.7 D_m E_b t_p^3 ne}{w^3 C_f}$$

Calculate S_5 based on mean diameter

$$S_5 = \frac{F}{\pi D_m t_p}$$

$$S_5 = \frac{1.7}{\pi} \frac{E_b t_p^2 ne}{w^3 C_f} \approx \frac{E_b t_p^2 ne}{2 w^3 C_f}$$

Figure 3.1-6, Deflection-Induced Meridional Membrane Stress

The distribution of meridional stress due to displacement is illustrated in Figure 2.1-8. Since the meridional bending stress due to displacement is displacement controlled and generally self limiting, it is considered to be a secondary stress. The work in Chapter 4, though, demonstrates that plastic strain concentration occurs under certain conditions of geometry. Under that condition, the strain range is greater than would be expected based on S_6.

The bellows theoretical elastic axial stiffness per convolution, f_{iu}, is:

$$f_{iu} = 1.7\frac{D_m E_b t_p^3 n}{w^3 C_f} \tag{3.6}$$

The limiting design pressure based on elastic column squirm, assuming a single bellows with both ends rigidly supported and a sufficiently long bellows for elastic buckling, is:

$$P_{sc} = \frac{0.34 \pi f_{iu}}{N^2 q} \tag{3.7}$$

This equation includes a factor of safety of 2.25 relative to the expected squirm pressure and includes an empirical correlation (Broyles, 1994).

The work of Anderson and these resulting equations are the definitive treatment of the calculation of the stresses in unreinforced bellows by direct solution of the equation of shells. It has been shown to be sufficiently accurate for design in prior comparisons with elastic finite element analysis results (Becht and Skopp, 1981b; Osweiller, 1989) and, in a more comprehensive manner, in Chapter 4.

It has been shown that the bending stresses, S_4 and S_6 are calculated accurately over a wide range of bellows geometries. However, it is shown in the present work, as discussed in Chapter 4, that the meridional membrane stress due to pressure differs from that calculated using equation 3.2.

The meridional membrane stress due to deflection, calculated per equation 3.4, is also shown in Chapter 4 to differ from the actual maximum stresses. The reason for this is described in Chapter 4. However, as discussed elsewhere herein, this is of little consequence to bellows design. It should be noted that Anderson did not develop equations for meridional membrane stress; thus, equations 3.2 and 3.4 from the EJMA Standards are not from his work.

While the elastic shell equations developed by Anderson have sufficient accuracy for calculating the elastic bending stress due to pressure and displacement, the present work shows that the elastic analysis of unreinforced bellows is not sufficient to characterize the response to displacement loading. Rather, strain concentration effects that occur as the bellows is deflection cycled in the plastic regime significantly affect the cycle life of bellows.

3.2 EJMA Stress Equations for Reinforced Bellows

The equations for reinforced bellows that are presently in the EJMA Standards, 7th edition, are as follows. Dimensions are illustrated in Figure 2.1-1 and defined in the nomenclature.

The bellows circumferential stress due to internal pressure, S_2, is:

$$S_2 = \frac{P\, D_m\, q}{2\, A_c} \left(\frac{R}{R + 1}\right) \tag{3.8}$$

where, for integral reinforcing members:

$$R = \frac{A_c\, E_b}{A_r\, E_r} \tag{3.9}$$

and, for reinforcing members joined by fasteners:

$$R = \frac{A_c\, E_b}{D_m}\left(\frac{I_f}{A_f\, E\, f} + \frac{D_m}{A_r\, E_r}\right) \tag{3.10}$$

The reinforcing member circumferential stress due to internal pressure, S_2', is:

$$S_2' = \frac{P\, D_m\, q}{2\, A_r} \left(\frac{1}{R + 1}\right) \tag{3.11}$$

Using the equation for R given in (3.9) yields stress in the ring. Using the equation for R given in (3.10) yields the stress in the fastener.

Note that while H, which equals PD_mq, is used in the equations shown in the EJMA Standards; PD_mq is used herein to make the origin of the equations more recognizable.

Equations 3.8 and 3.11 are from equilibrium, derived similarly to equation 3.1. The only difference is that the metal area of the ring is included. Further, for rings that include fasteners, the effective hoop stiffness of the ring, considering the combination of ring and fastener stiffness, is used. As in the case of unreinforced bellows, these circumferential membrane stresses are primary.

The following equations for S_3, S_4, S_5 and S_6 are the same as the equations for unreinforced bellows, except that an effective, reduced convolution height is used, and a factor of 0.85 is included for the pressure equations. The convolution height is reduced by the dimension C_rq, so that $(w-C_rq)$ is substituted for the convolution height, w. The equation for C_r, which is a function of internal pressure, is shown in the Nomenclature.

The bellows meridional membrane stress due to internal pressure, S_3, is:

$$S_3 = \frac{0.85\ P\ (w - C_r\ q)}{2\ n\ t_p} \qquad \textbf{(3.12)}$$

This is a primary membrane stress. Considering that equation 3.12 is based on simple equilibrium principles, the only rationale for reduction of this stress with the inclusion of reinforcing rings is that some portion of this pressure force acting in the direction of the bellows axis is passed through the reinforcing ring since the convolution bears on it.

The bellows meridional bending stress due to internal pressure, S_4, is:

$$S_4 = \frac{0.85\ P}{2\ n}\left(\frac{w - C_r\ q}{t_p}\right)^2 C_p \qquad \textbf{(3.13)}$$

The reduction in effective convolution height due to the reinforcing ring reduces the meridional bending stress. This stress is presently considered to be a secondary stress, since the reinforcing rings are considered to hold the bellows together to some extent, even with the formation of plastic hinges in the convolution walls. However, this remains a debatable point, and a subject for future research.

The bellows meridional membrane stress due to deflection, S_5, is:

$$S_5 = \frac{E_b\, t_p^2\, e}{2\,(w - C_r\, q)^3\, C_f} \qquad \textbf{(3.14)}$$

The reduction in effective convolution height increases the stiffness of the bellows and therefore increases the meridional membrane stress due to deflection. The same as in the case of unreinforced bellows, this is considered to be a secondary stress, but is subject to elastic follow-up.

The bellows meridional bending stress due to deflection, S_6, is:

$$S_6 = \frac{5\, E_b\, t_p\, e}{3\,(w - C_r\, q)^2\, C_d} \qquad \textbf{(3.15)}$$

The reduction in effective convolution height increases the meridional bending stress due to deflection. This stress is a secondary stress. As in unreinforced bellows, plastic strain concentration is a concern.

The bellows theoretical elastic axial stiffness per convolution, f_{ir}, is:

$$f_{ir} = 1.7\frac{D_m\, E_b\, t_p^3\, n}{(w - C_r\, q)^3\, C_f} \qquad \textbf{(3.16)}$$

The bellows stiffness is increased by the reduction in effective convolution height.

The limiting design pressure based on elastic column squirm, assuming a single bellows with reinforcing rings (not equalizing rings) and with both ends rigidly supported is:

$$P_{sc} = \frac{0.34\ \pi\ f_{ir}}{N^2\ q} \qquad \textbf{(3.17)}$$

This equation includes a factor of safety of 2.25 relative to the expected squirm pressure and an empirical correlation (Broyles, 1994). Since the addition of reinforcement makes the bellows stiffer, it is more resistant to column squirm.

The basis for the reinforced bellows equations (essentially the use of a reduced, effective convolution height) is not documented in the literature, and there are significant nonlinear complications, such as the interaction between the convolution shell and the reinforcing rings, which is a nonlinear, large displacement gap problem. While such complications preclude direct solution, it was found, as discussed in Chapter 4, that the present equations, with possibly some small modifications, are sufficiently accurate for displacement loading. A significant finding is that the effect of plasticity and resulting strain concentration which is very significant to unreinforced bellows response is not as significant for most reinforced bellows.

Chapter 4

Bellows Evaluation

4.1 Scope of Research and Overview of Evaluation Approach

This research is focused on developing better understanding of bellows behavior. This understanding can lead to improvement of bellows analysis and design methods. These methods are based on equations and charts that were developed from parametric elastic shell analysis. They have been proven to be generally sufficient, and are used worldwide in the design of bellows.

The current method requires fatigue testing of bellows to develop empirical fatigue curves. Separate testing is required for reinforced and unreinforced bellows and for each material of construction. While very costly, this is necessary because prior work has not developed sufficient understanding of bellows response to deflection loading, and determined how bellows fatigue behavior can be directly compared to polished bar fatigue data for the material. The present research is aimed at developing that understanding, which would have a substantial impact on design rules for bellows, used worldwide. It is shown herein that the key consideration is the effect of plasticity in deflection.

This research includes the following specific areas of investigation.

A series of elastic finite element analyses of unreinforced bellows was performed to evaluate the accuracy, in greater detail than has been done before, of the charts and equations presently used in the design of bellows.

While the elastic prediction of displacement stress in bellows using existing equations was generally found to have good accuracy for the stresses that are significant in design, the effect of plasticity was further investigated. The effect of plastic strain concentration on the response of unreinforced bellows to displacement loading was evaluated using the results from elastic-plastic finite element analyses. A new understanding of the effect of bellows geometry, reinforcing rings, and plasticity on displacement strains, and specifically plastic strain concentration, in bellows is presented herein.

This new understanding was tested by re-evaluating bellows fatigue data that was previously used to develop bellows fatigue curves. It was found that proper consideration of plastic strain concentration effects unifies the reinforced and unreinforced fatigue data, and in fact correlates bellows fatigue data with polished bar fatigue data.

For reinforced bellows, the interaction between the convolutions and the reinforcing rings was also investigated with a series of nonlinear elastic finite element analyses. Some of the key areas that were addressed included:

- the effect of the reinforcing ring on stresses;
- effect of pressure on displacement response of bellows (pressure has been considered to increase displacement stresses by causing greater interaction between the convoluted shell and the reinforcing ring); and
- nonlinear interaction between the convoluted shell and the reinforcing ring due to displacement loading.

One of the findings of the elastic analyses of reinforced bellows was that the displacement stresses were significantly affected by whether the displacement tended to open or close the bellows convolutions. The effect of plasticity on this behavior was investigated using elastic-plastic (with large displacement theory) finite element analyses; it is shown that the differences between bellows opening and closing displacement are washed out by the effects of plasticity.

These evaluations were carried out by using finite element analysis. Direct solution by shell theory, using some approximations to enable solution, had been done by

Anderson. Elastic finite element analyses confirmed that this prior work is generally sufficiently accurate. Inelastic finite element analyses have shown that the elastic stress analysis is not sufficient to fully characterize the response of bellows to displacement loading.

The analyses were performed using the COSMOS/M finite element analysis program. Both axisymmetric and three dimensional shell analyses were performed. Axisymmetric analyses were performed for elastic analysis of unreinforced bellows and a three dimensional wedge was used for inelastic analyses of unreinforced bellows. Elastic analyses were also performed using the three dimensional shell elements for a few cases to confirm that a one element wide wedge of the bellows provided accurate results, as compared to the axisymmetric shell analysis. For reinforced bellows, the preferred gap elements required the use of thin shell elements (e.g. four node quadrilateral shell elements). Therefore, the reinforced bellows analyses were performed using three dimensional shell analysis.

The primary focus of the evaluations is meridional bending stress, since this is significantly greater than the meridional membrane stress. This is readily demonstrated by evaluating equations 3.2 verses 3.3 and 3.4 versus 3.5. The ratio of the bending to membrane stress is approximately proportional to the ratio of bellows convolution height, w, to thickness, t. Because metallic bellows of interest are thin walled shells, this ratio is relatively large, making the meridional bending

stress much larger than the meridional membrane stress. Since the stress criteria are relative to the sum of these two components, meridional membrane stress is generally relatively insignificant in bellows design.

The effect of plasticity is relevant because bellows are deflection cycled well into the plastic regime, often to elastically calculated stress ranges greater than two times the yield strength of the material. Design of bellows is a compromise between pressure capacity, for which thicker walls and deeper convolutions are desired, and capacity to accept numerous deflection cycles without fatigue failure, for which thinner walls and shallower convolutions are desired. The most common design range for deflection stresses is from greater than 690 MPa (100,000 psi) to greater than 2,000 MPa (300,000 psi). The higher permissible deflection stress permits thicker walls and shallower convolutions, that are necessary to provide the required pressure capacity. Note that simply adding more convolutions to increase flexibility and decrease stress for a given deflection does not solve the problem, since that increases the potential for column squirm, another pressure induced failure mode.

4.2 Elastic Parametric Evaluations of Unreinforced Bellows

Unreinforced bellows geometries were evaluated using parametric elastic finite element analysis. The purpose of these evaluations was to 1) evaluate the accuracy and range of applicability of the existing equations for unreinforced bellows, 2) establish the validity of the finite element models based on the generally better understood elastic behavior of unreinforced bellows, and 3) to provide unreinforced bellows calculations for comparison with reinforced bellows calculations.

Parametric analyses were conducted using linear axisymmetric shell elements with the COSMOS/M finite element analysis program. These shell elements are two node conical shell elements.

A full convolution was modeled. While a half convolution model is sufficient because of planar symmetry at the convolution root and crown, the model was quick to run and the full model provided a better illustration of the displacement. The model was divided into six segments, consisting of the two sidewalls and four halves of the root and crown toroidal segments. These segments were each provided the same number of elements, a number which was varied to check for convergence. As 50 elements per segment and 100 elements per segment provided essentially the same results, the parametric analysis was performed using 50 elements per segment.

The results were also compared to calculations performed using three dimensional shell elements to analyze a slim (one element wide) wedge of the bellows. Boundary conditions for the three dimensional shell analyses were defined in the cylindrical coordinate system to provide symmetric boundary conditions that represent an axisymmetric shell. Results generally compared within 1% for meridional stress and about 2% for circumferential stress, providing verification of the two models.

Stress equations provided in Section 3.1 for prediction of meridional membrane stress due to pressure, S_3, meridional bending stress due to pressure, S_4, meridional membrane stress due to deflection, S_5, and meridional bending stress due to deflection, S_6, were evaluated.

The EJMA equation for S_3 is simply based on equilibrium; pressure acting in the axial direction on the wall of the convolutions must be carried as a meridional membrane stress across the root and crown.

The equations for S_4, S_5, and S_6 are based on shell theory. The shell effects are introduced via charts for factors C_p, C_f, and C_d which are based on nondimensionalized parametric shell analysis. C_p is nondimensionalized meridional bending stress due to pressure. C_f is the nondimensionalized inverse of bellows stiffness. C_d is the nondimensionalized inverse of meridional bending stress due to deflection. The nondimensional parameters are q/2w, (termed QW herein) and $q/2.2(D_m t_p)^{½}$ (termed QDT herein), where q is bellows pitch, w is convolution height, t_p is bellows thickness considering thinning due to forming, and D_m is the mean bellows diameter.

Figure 4.2-1 illustrates the effect of parameters QW and QDT on the geometry of bellows.

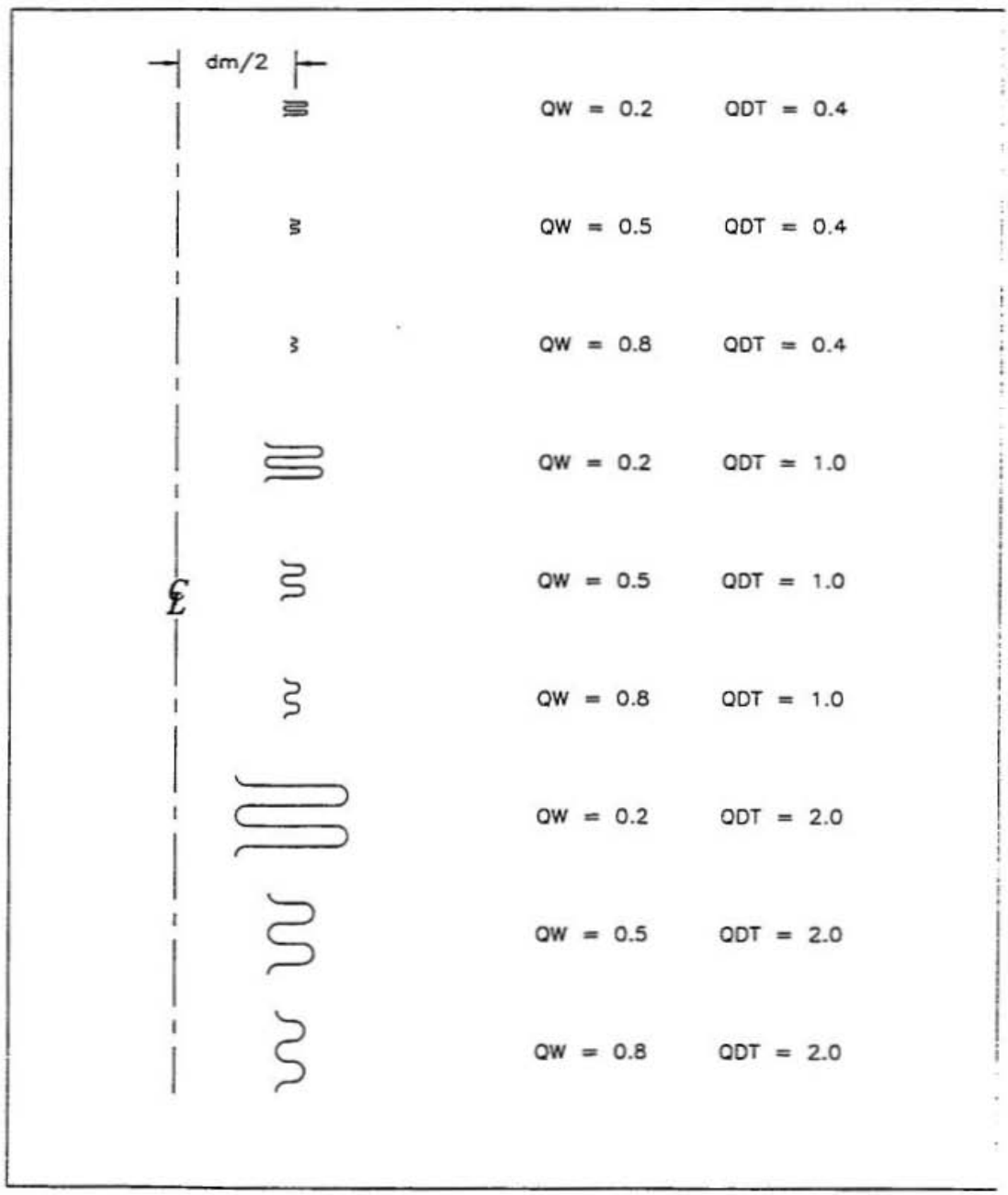

Figure 4.2-1, Bellows Geometries

Parametric analyses were run. For each case, D_m and t_p were assumed and the other bellows dimensions were calculated based on varying the two parameters QW and QDT. Most of the analyses were performed using D_m=610 mm (24 inch) and t_p=0.51 mm (0.02 inch). Cases with other diameters and thicknesses were also run to confirm the diameter and thickness independence of the results. For all cases, the following material properties and loads were assumed: E=207,000 MPa ($30x10^6$ psi), v=0.3, P=690 kPa (100 psi) for cases with internal pressure and e=2.5 mm (0.1 inch) for cases with axial deflection.

Maximum stresses were calculated for each case, and are provided in Table I. Based on the stresses calculated with the finite element analyses, factors C_p, C_f, and C_d were calculated that would make the EJMA equations, documented in Section 3.1, match the finite element results. These factors are also contained in Table I.

Figure 4.2-2 shows the calculated values of the factors, given QW=0.5 and QDT=1.0 for various diameters. Figure 4.2-3 shows the calculated values of the factors, given QW=0.5 and QDT=1.0 for various thicknesses. These two charts demonstrate that the parameters QW and QDT make the charts independent of thickness and diameter. These figures confirm that these parameters adequately capture the thickness and diameter dependence of factors C_p, C_f, and C_d.

TABLE I

Summary of Elastic Analysis Results for Unreinforced Bellows

Dm	tp	QDT	QW	q	w	Stresses Calculated Based on Elastic Finite Element Analysis						Parameters for EJMA Equations To Match FEA Results			S3
						Due to 100 psi			Due to 0.1 inch Displacement						
						Clr Mem	S3	S4	Clr Mem	S5	S6	Cp	Cf	Cd	EJMA/FEA
						E_b=30,000,000 psi									
In.	In.			In.	In.	psi	psi	psi	psi	psi	psi				
24	0.02	0.4	0.2	0.610	1.524	14835	3931	252369	3425	151	32781	0.869	1.122	1.313	0.969
24	0.02	0.4	0.3	0.610	1.016	17714	2591	102547				0.795			0.980
24	0.02	0.4	0.5	0.610	0.610	24391	1538	30997	14853	1723	151912	0.667	1.537	1.771	0.991
24	0.02	0.4	0.8	0.610	0.381	33395	961	10667	29925	5774	319849	0.588	1.878	2.153	0.991
24	0.02	0.6	0.2	0.915	2.286	96779	6008	530637	3357	69.7	13817	0.812	0.720	1.385	0.951
24	0.02	0.6	0.5	0.915	0.915	27543	2323	67885	14478	548	65145	0.649	1.431	1.835	0.984
24	0.02	0.6	0.8	0.915	0.572	34496	1430	23717	21297	1850	139373	0.581	1.737	2.196	0.999
24	0.02	0.8	0.5	1.219	1.219	35069	3122	109788	13693	369.2	33628	0.591	0.896	2.000	0.976
24	0.02	1	0.2	1.524	3.811	552820	18999	1110000	2362	74.5	5737	0.612	0.146	1.200	0.501
24	0.02	1	0.3	1.524	2.540	199400	6372	434060	4911	147	10918	0.538	0.249	1.419	0.759
24	0.02	1	0.5	1.524	1.524	47958	3940	158994	12158	364	23197	0.548	0.466	1.856	0.967
24	0.02	1	0.8	1.524	0.953	42421	2404	60337	26973	880	44459	0.532	0.769	2.479	0.991
24	0.06	2	0.2	5.280	13.200	489973	81213	1890000	599	92	2529	0.781	0.026	0.681	0.135
24	0.02	1.5	0.5	2.286	2.286	114845	7520	276910	6331	330.8	16118	0.424	0.152	1.187	0.760
12	0.02	2	0.2	2.156	5.389	680731	85831	2654000	1090.5	127.9	4688	0.731	0.030	0.735	0.157
24	0.02	2	0.2	3.048	7.621	1255000	103574	4920000	488	38	2143	0.676	0.036	0.803	0.184
48	0.02	2	0.2	4.311	10.778	2403000	133212	9379000	227	11.83	1010	0.646	0.041	0.852	0.202
24	0.02	2	0.3	3.048	5.081		38408	1570000		80	4522	0.487	0.057	0.857	0.331
24	0.02	2	0.4	3.048	3.811	230349	19821	667469	2070	149	7838	0.368	0.073	0.879	0.481
24	0.02	2	0.5	3.048	3.048	133488	12229	399513	3494	251	12060	0.344	0.084	0.892	0.623
24	0.02	2	0.8	3.048	1.905	85139	5207	133382	11747	859	28440	0.294	0.101	0.969	0.915
48	0.02	2	0.8	4.311	2.694	169515	7287	266723	5844	301	14111	0.294	0.102	0.976	0.924
6	0.02	1	0.5	0.762	0.762	12387	2045	39696	50858	3128	95520	0.547	0.433	1.803	0.932
24	0.02	1	0.5	1.078	1.078	24305	2827	79466	24773	1060	46948	0.547	0.452	1.834	0.953
	0.02	1	0.5	1.524	1.524	47958	3940	158994	12158	364	23197	0.548	0.466	1.856	0.967
48	0.02	1	0.5	2.156	2.156	95015	5518	318040	5999	126	11503	0.548	0.475	1.871	0.977
96	0.02	1	0.5	3.048	3.048	188800	7753	636110	2972	43.88	5718	0.548	0.483	1.882	0.983
24	0.005	1	0.5	0.762	0.762	188800	7753	636110	11887	176	22873	0.548	0.481	1.882	0.983
24	0.01	1	0.5	1.078	1.078	95015	5518	318040	12000	252	23006	0.548	0.475	1.871	0.977
24	0.02	1	0.5	1.524	1.524	47958	3940	158994	12158	364	23197	0.548	0.466	1.856	0.967
24	0.04	1	0.5	2.156	2.156	24305	2827	79466	12386	530	23474	0.547	0.452	1.834	0.953
24	0.06	1	0.5	2.640	2.640	16372	2335	52953	12564	664	23692	0.547	0.442	1.817	0.942
6	0.01	2	0.5	1.078	1.078		6771	257429		686	33804	0.443	0 175	1.273	0.796

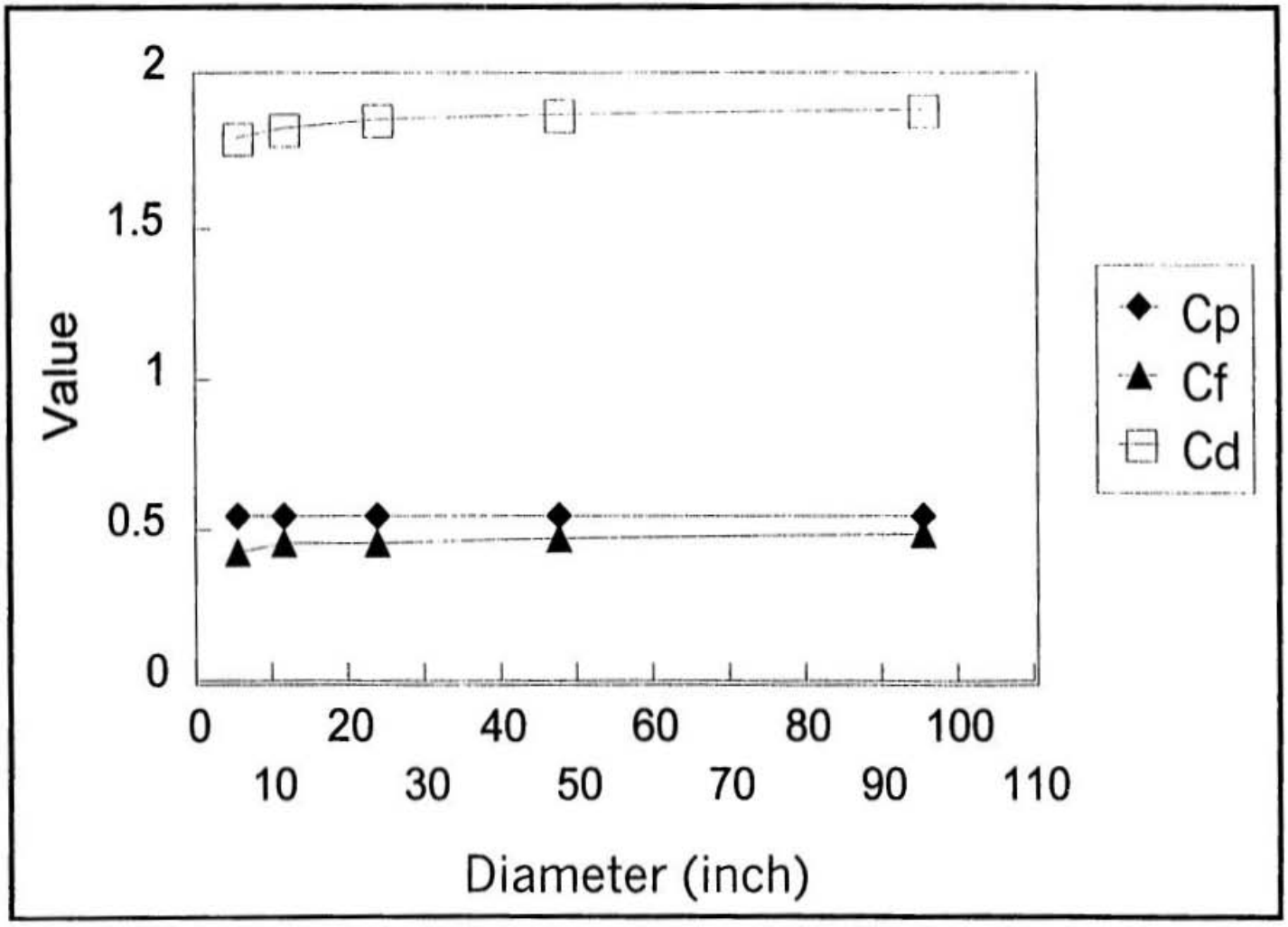

Figure 4.2-2, Diameter Dependence of EJMA Factors

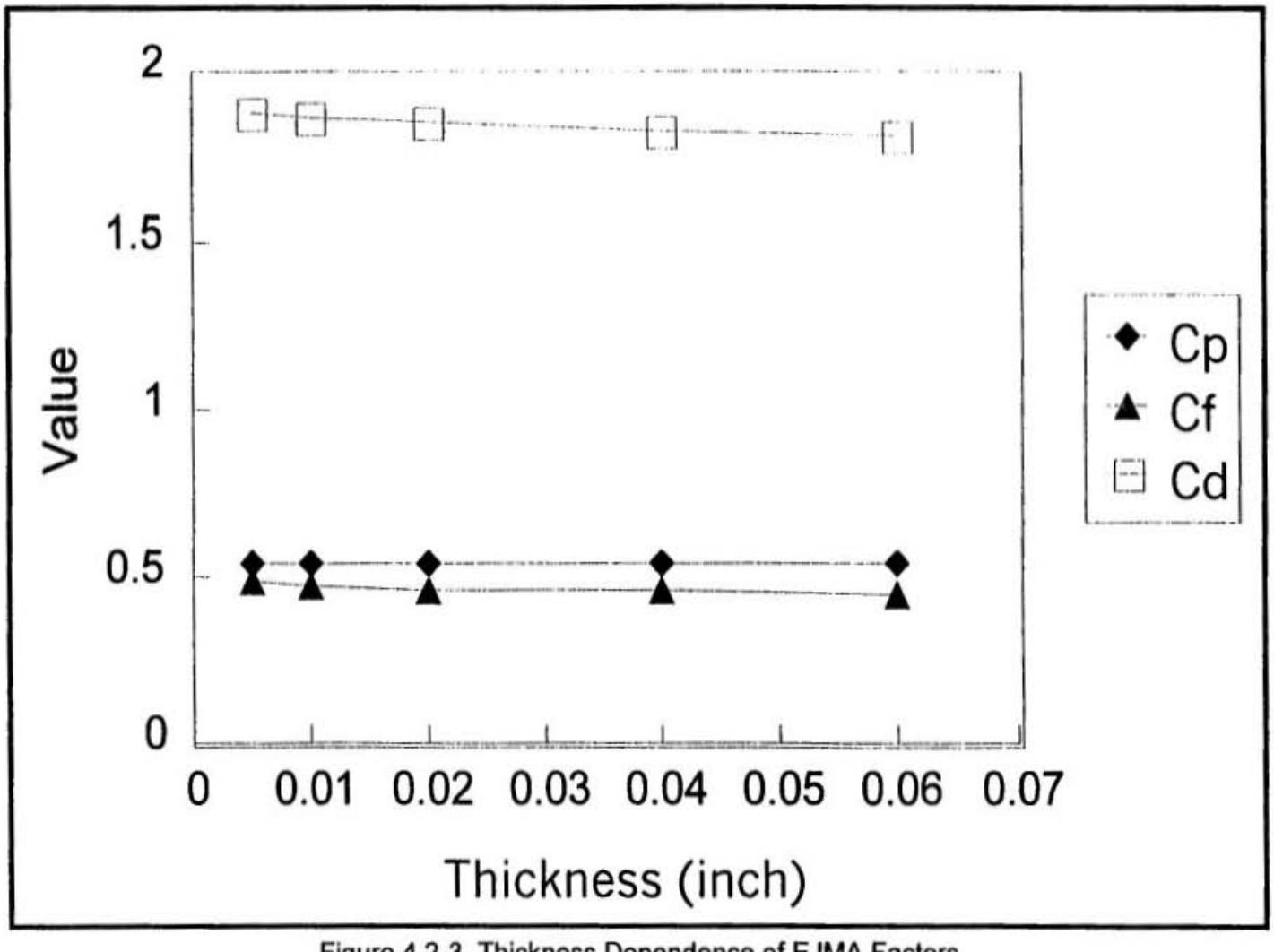

Figure 4.2-3, Thickness Dependence of EJMA Factors

This confirms what should be expected if the equations of Anderson are accurate, since these parameters were used to nondimensionalize the shell analysis of the toroidal portions of the bellows.

The calculated factors C_p, C_f, and C_d that would make the EJMA equations match the finite element results for the 610 mm (24 inch) size are plotted, in Figures 4.2-4 through 4.2-6, on the charts provided in the EJMA Standards. A plot of the ratio of the calculated meridional membrane stress due to pressure to S_3, per the EJMA equation, is provided in Figure 4.2-7.

The results generally confirm earlier findings that were based on much more limited studies. The calculation of maximum bending stress due to pressure and deflection, as shown by comparison of the factors calculated by finite element analysis and those provided in the EJMA charts (see Figure 4.2-4 and 4.2-6) is sufficiently accurate except for very deep convolution bellows (low values of QW). As discussed previously, these are the meridional stresses that are generally of concern in bellows design. Since the focus of this work is fatigue design, it is specifically the equation for S_6, meridional bending stress due to displacement, that is of primary concern herein.

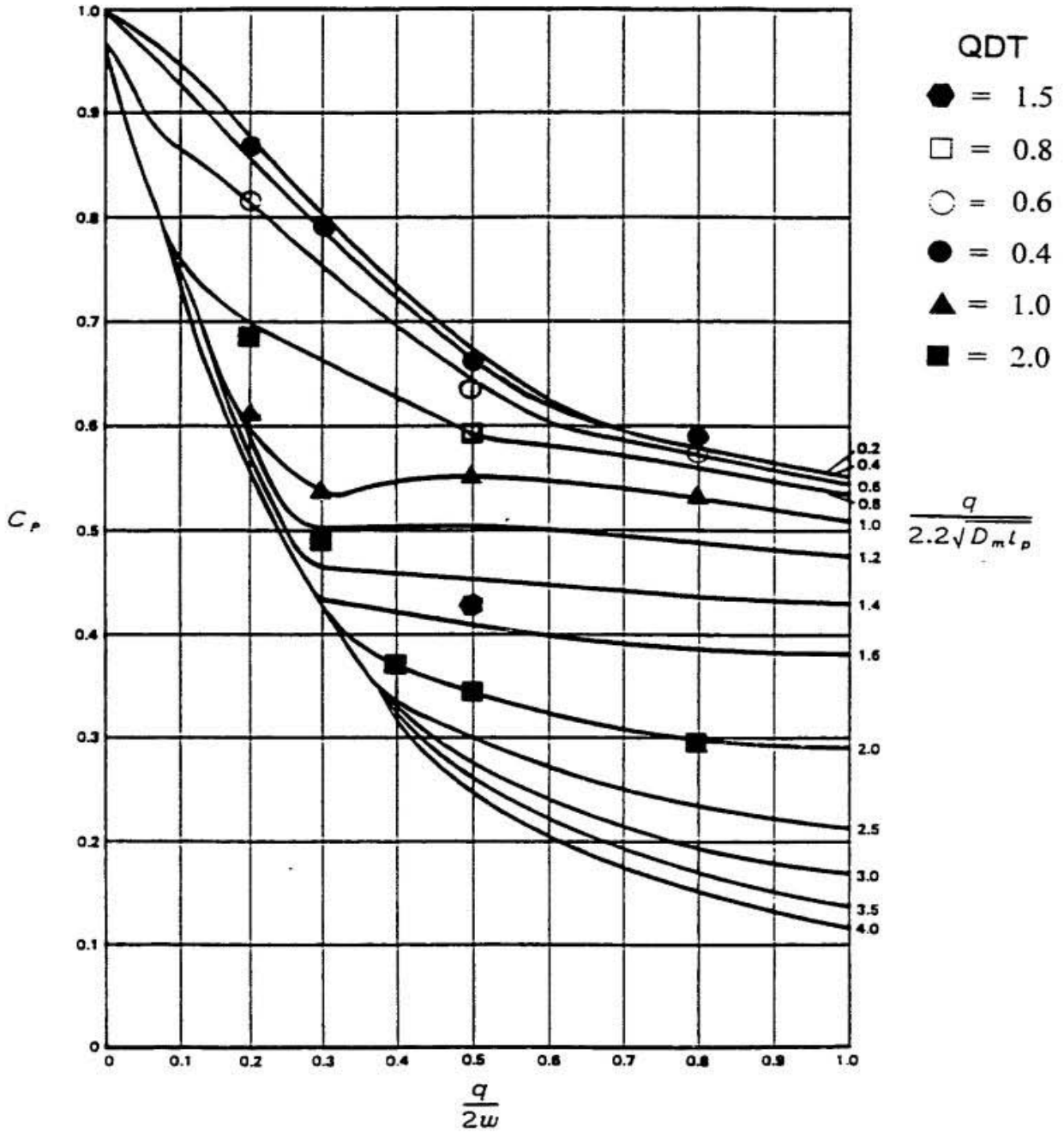

Figure 4.2-4, Comparison of Calculated C_p Versus EJMA Chart

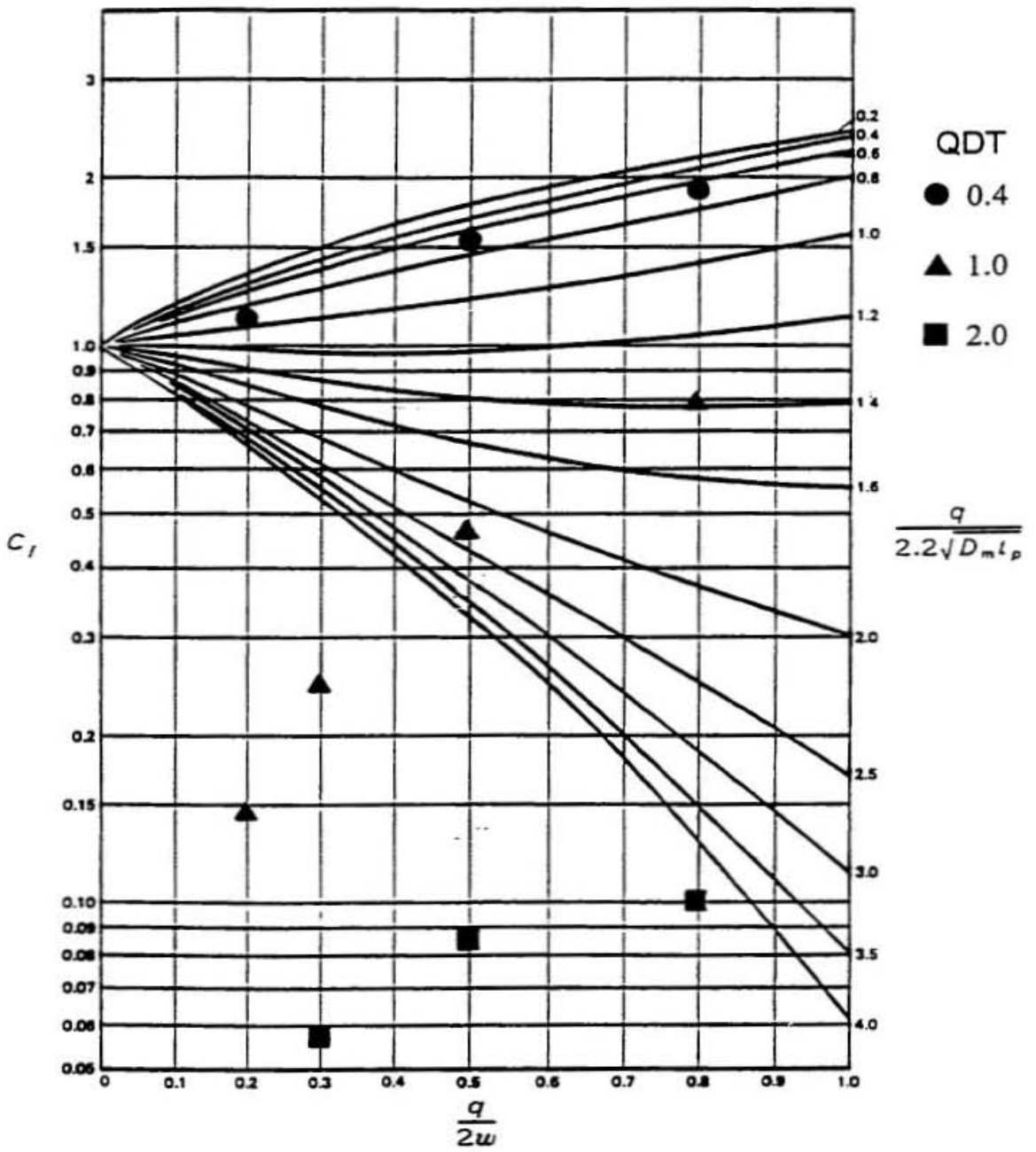

Figure 4.2-5, Comparison of Calculated C_f Versus EJMA Chart

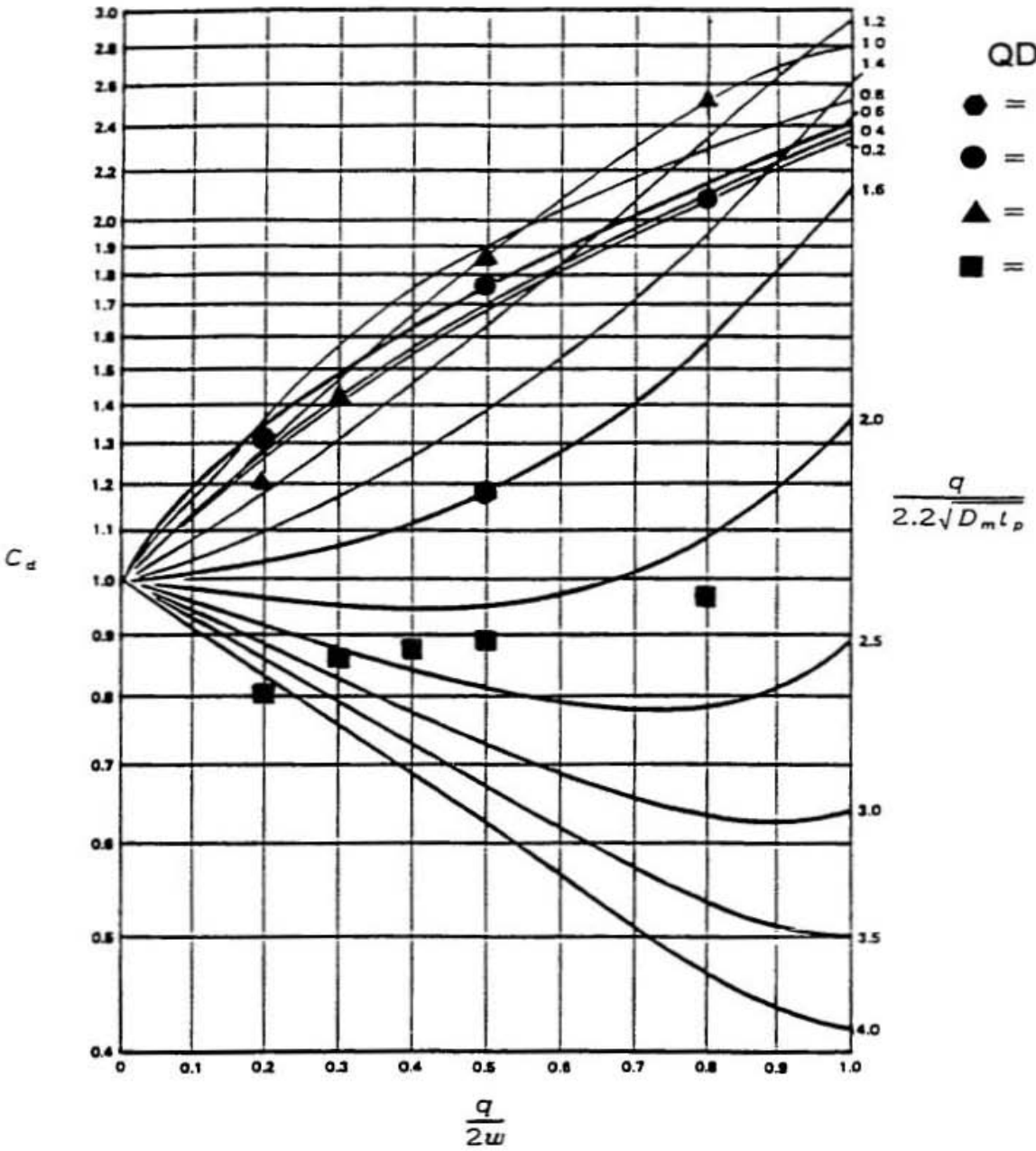

Figure 4.2-6, Comparison of Calculated C_d Versus EJMA Chart

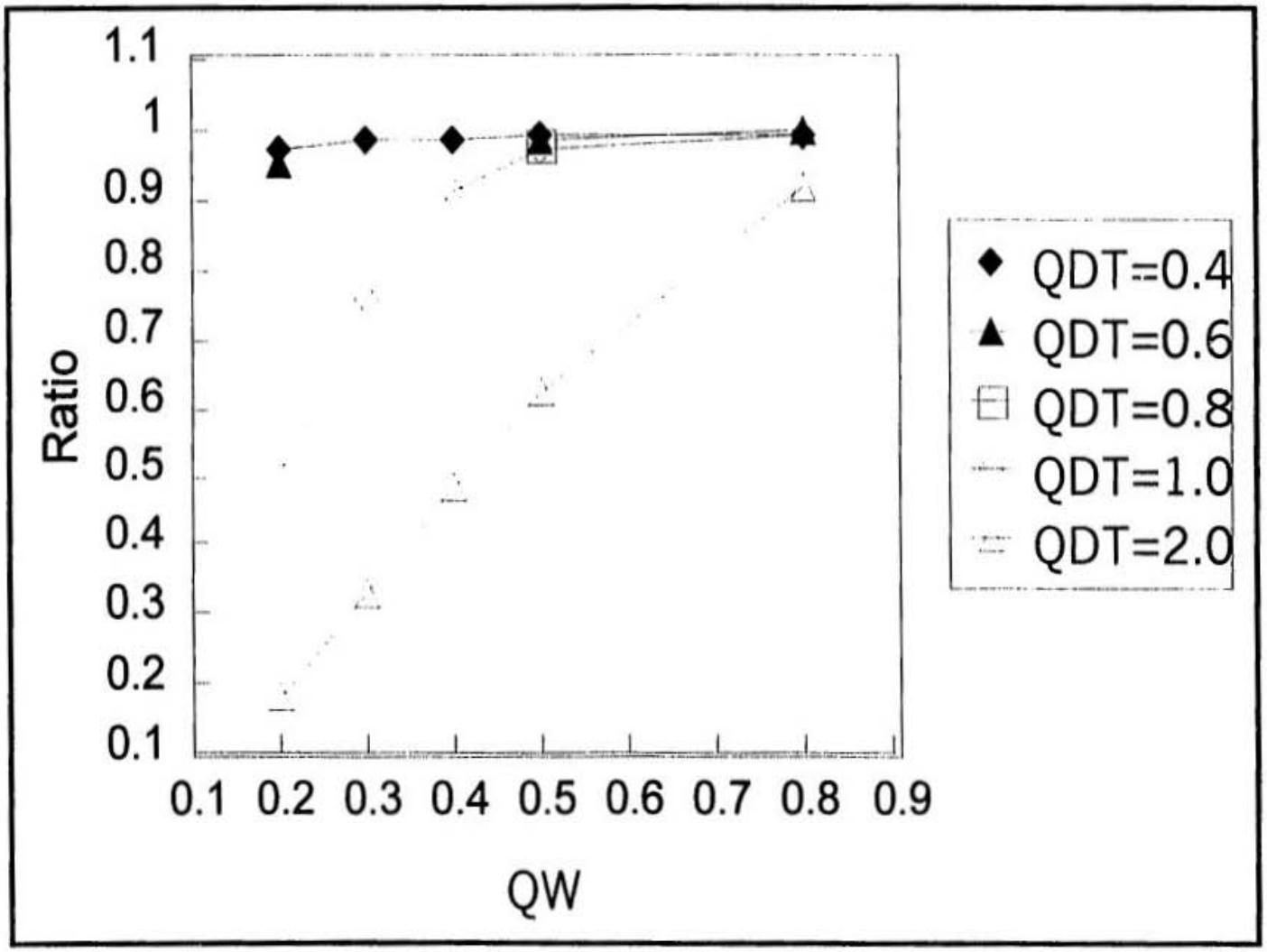

Figure 4.2-7, S3 (EJMA) / Meridional Membrane due to Pressure (FEA)

As discussed in Section 3.1, the meridional membrane stress due to pressure, S3, that is calculated in the equation is based on equilibrium and, in fact, must be the stress at the location considered. The difference between the maximum meridional membrane stress calculated by finite element analysis and that calculated using the EJMA equation for S3, as shown in Figure 4.2-7, is due to the fact that the maximum meridional membrane stress for deep convolution, and relative to pitch, smaller diameter and thinner walled bellows does not occur at the location considered in the EJMA equation. It generally occurs, in these bellows, in the toroidal portions of the bellows, but closer to the sidewalls.

Plots of stress for various bellows geometries due to internal pressure are provided in Figures 4.2-8 through 4.2-11. In these plots, the apex of the crown is element 1, the apex of the root is element 150, and the apex of the next crown is element 300. The transitions between the toroidal portions and the sidewalls are delineated by dashed vertical lines at elements 50, 100, 200 and 250. The middle of the sidewall are at elements 75 and 225.

In deep convolution (low QW) and thin walled (high QDT) bellows, deformation of the sidewalls in bending due to pressure draws in the root and crown. The meridional membrane stresses in the sidewall that are high draw the root and crown in (towards the center of the convolution), and induce high circumferential stress in the bellows root and crown toroidal sections. Also note that it is the occurrence of

these circumferential stresses that causes the maximum circumferential membrane stress predicted by finite element analysis to deviate from the average circumferential membrane stress calculated using the equation for S_2, although the average circumferential stress must equal S_2 due to equilibrium.

The calculation of membrane stress due to deflection, as shown in Figure 4.2-5, exhibits a substantial difference between the values of C_f in the EJMA Chart and those calculated in the present work. It is particularly in error for deep convolution thin walled bellows (low QW and high QDT). This comes from a consideration that was apparently missed in development of the EJMA Standards.

The chart of C_f was developed by Anderson to provide bellows stiffness. The force resulting from this stiffness was divided by the cross-sectional area of the bellows to calculate the meridional membrane stress in the EJMA Standards. While this does relatively accurately predict the stress in the bellows root and crown, these are not the location of highest meridional membrane stress. Figure 4.2-12 shows values of C_f, predicted based on finite element analysis, that would yield the stress at the outermost portion of the crown. They match the curves provided in the EJMA Standards for C_f fairly well. However, this is not always the location of highest meridional membrane stress due to displacement.

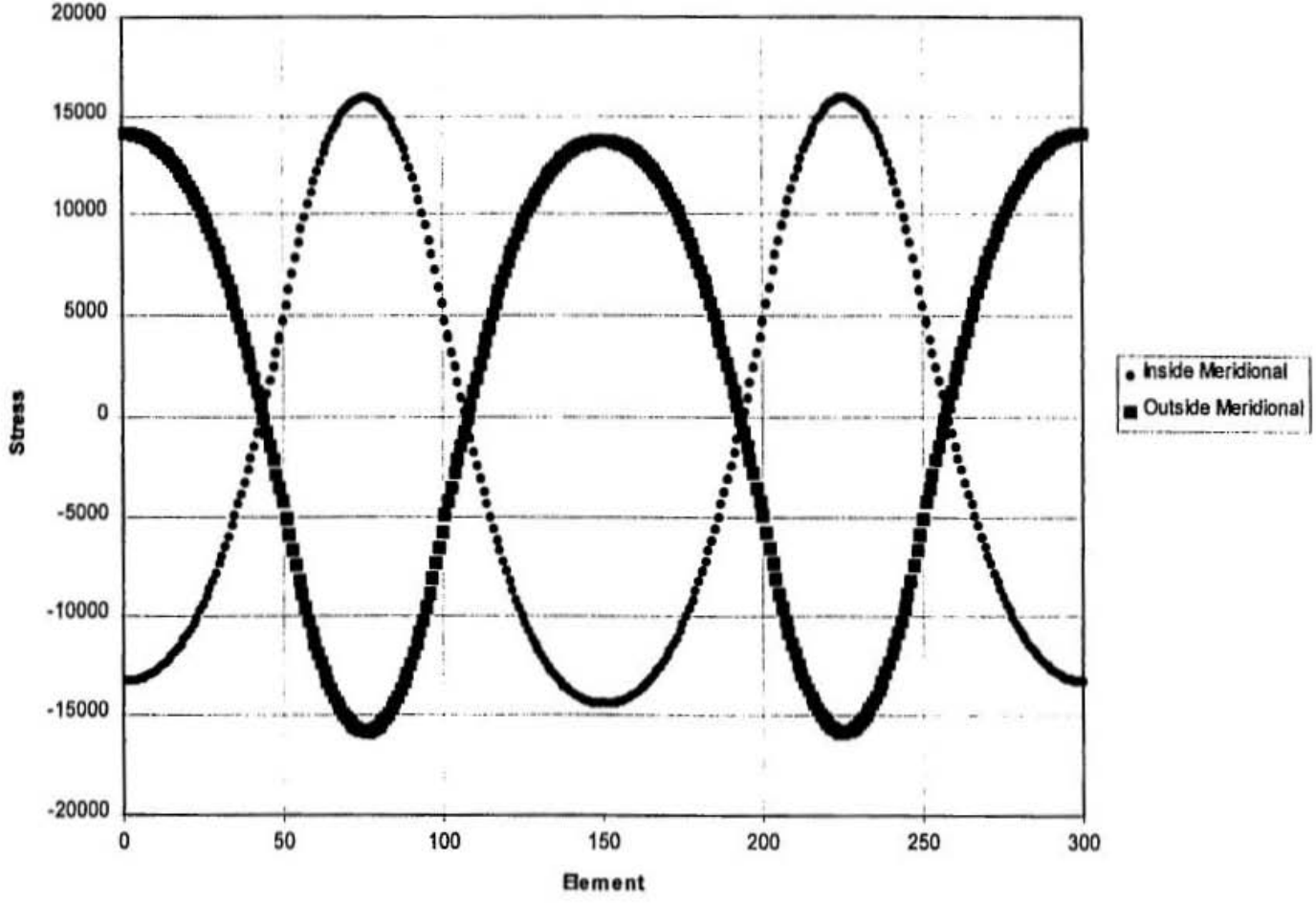

Figure 4.2-8, Pressure Stress in Bellows (QW=0.5, QDT=1.0)

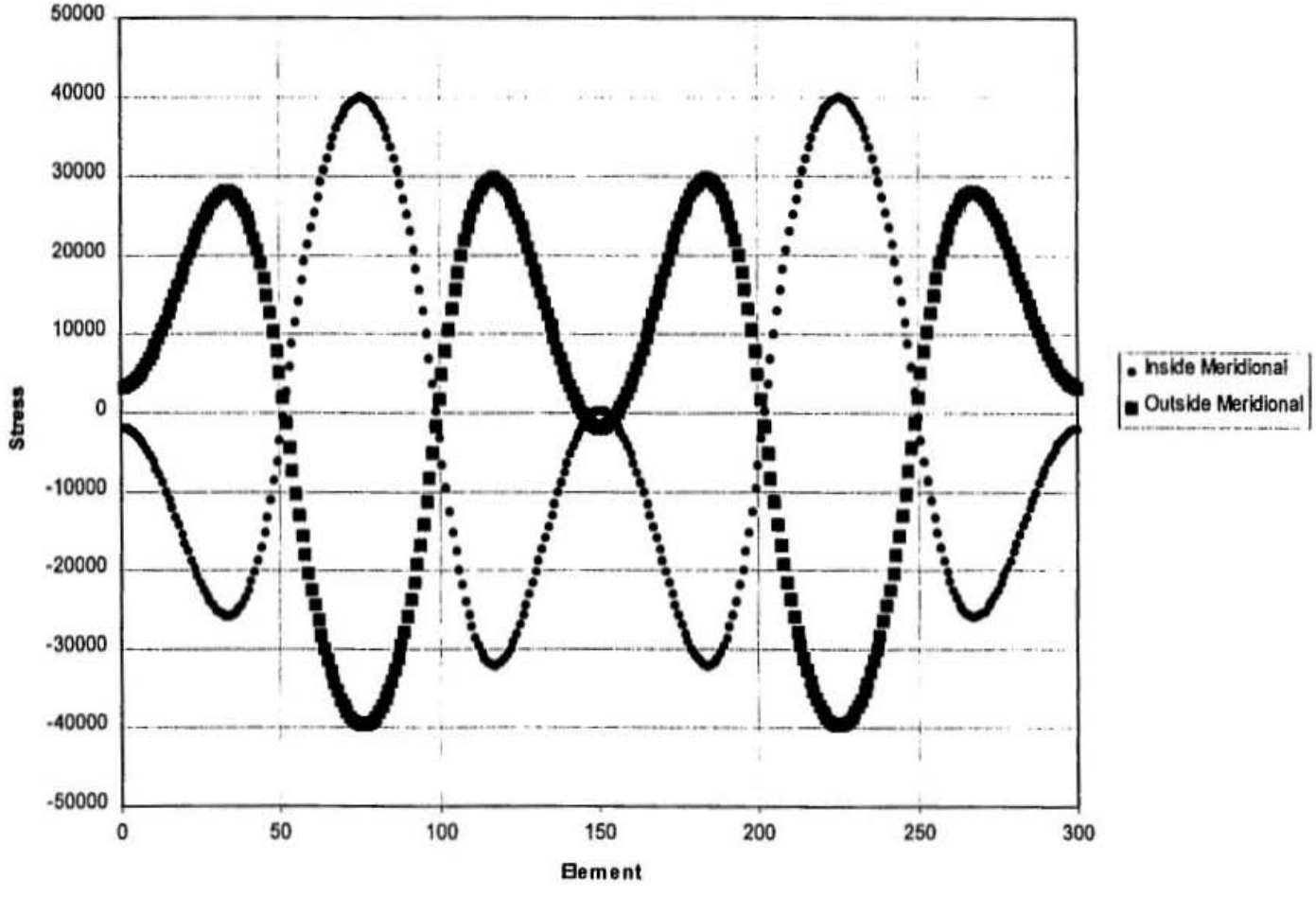

Figure 4.2-9, Pressure Stress in Bellows (QW=0.5, QDT=2.0)

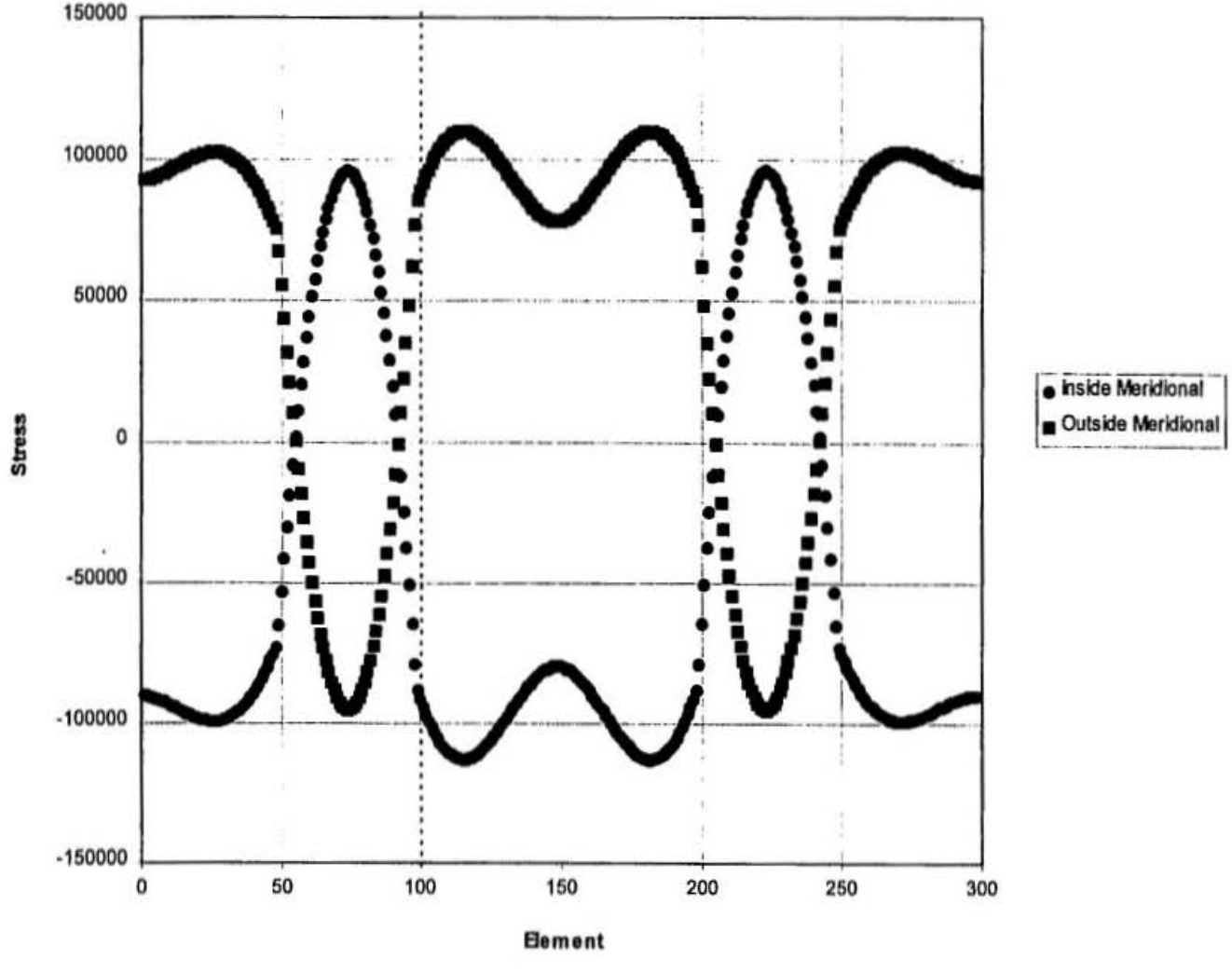

Figure 4.2-10, Pressure Stress in Bellows (QW=0.2, QDT=1.0)

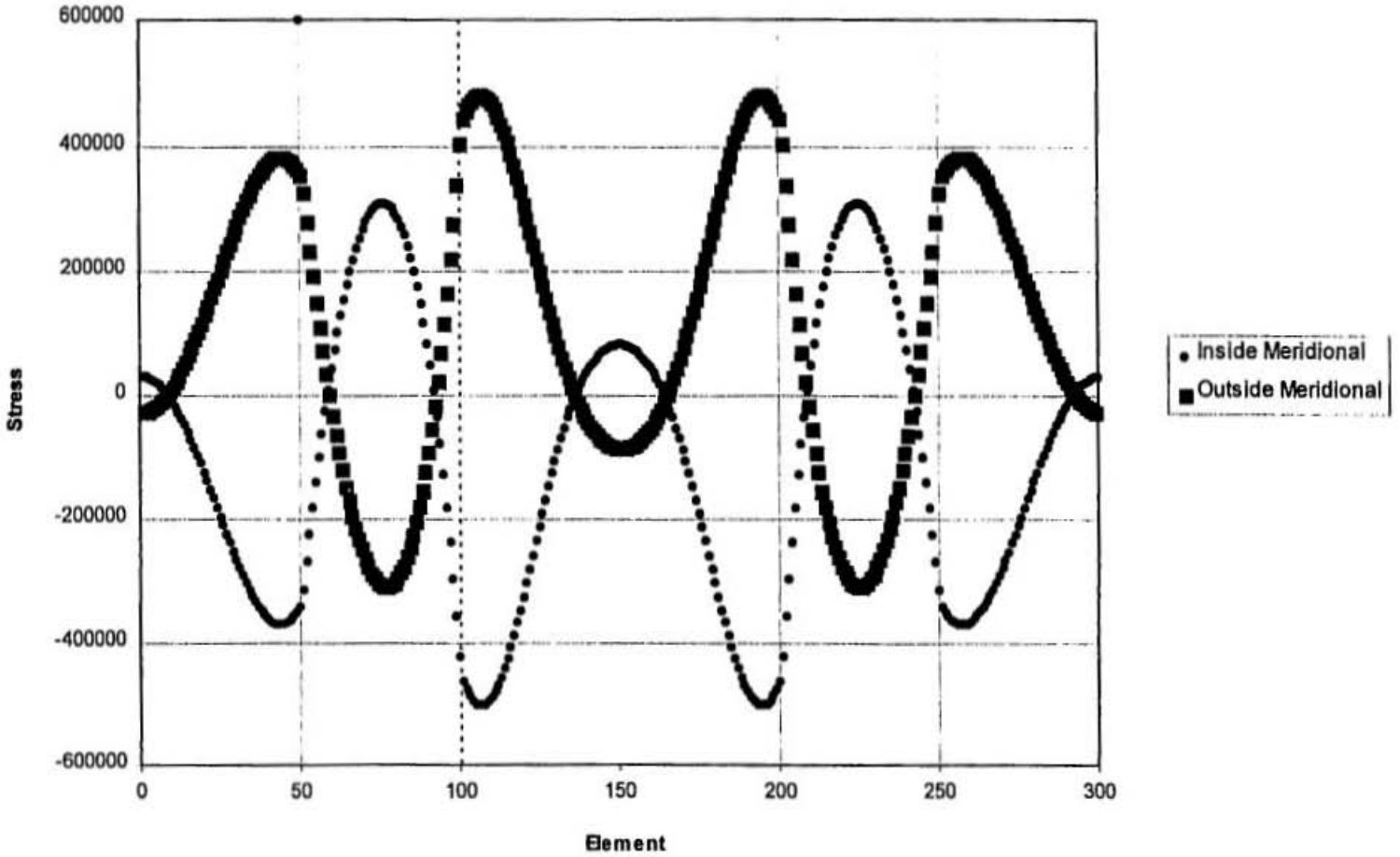

Figure 4.2-11, Pressure Stress in Bellows (QW=0.2, QDT=2.0)

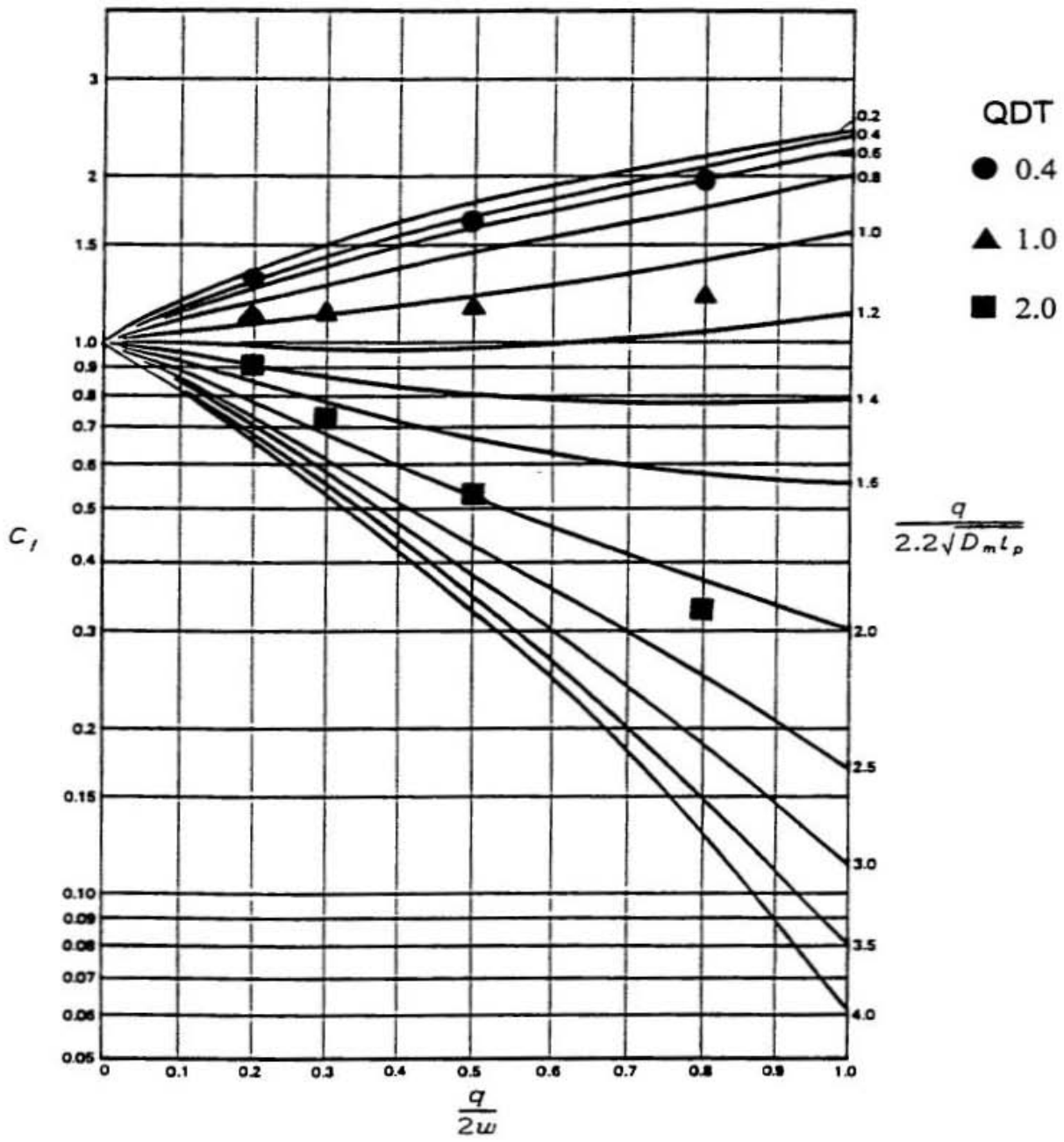

Figure 4.2-12, Calculated C_f at Bellows Crown Versus EJMA Chart

The location of highest meridional stress in deep convolution bellows can occur in the toroidal portions of the bellows, near the junction with the sidewalls. In these deep convolution bellows, the bellows root toroid is pulled out and the bellows crown toroid is pulled in by extension (and the reverse for compression). The result is high circumferential membrane stress in these locations.

For this to occur requires a sufficiently high meridional membrane stress transfer through the bellows sidewall to equilibrate these two opposing actions. Thus, for deep convolution (low QW) and thin walled (high QDT) bellows, the maximum meridional membrane stress is higher than the stress predicted by the EJMA equations. Further, with both deep convolution bellows and thin walled bellows, the bellows has greater flexibility. Thus, the meridional membrane stress at the location for which the stress is calculated in the EJMA Standards becomes low, to the extent that it is not the location of highest meridional membrane stress due to displacement.

The accuracy of the prediction of highest meridional membrane stress could be improved by parametric shell analysis, or by returning to the equations of Anderson and evaluating the meridional membrane stress at other locations. However, the error in calculation of meridional membrane stress due to deflection has very little practical significance in bellows design, and is not the subject of the present research. If the chart were to be revised today, it would be via accurate parametric numerical analysis rather than approximate parametric shell analysis.

The circumferential membrane stress due to displacement is not calculated in the EJMA equations, although it can be quite significant in magnitude. While development of equations to predict this stress is not within the scope of the present research, it was observed that there was a reasonable correlation between the ratio of the meridional bending stress due to deflection to this circumferential membrane stress and the parameter QDT, as shown in Figure 4.2-13. No appearance of correlation existed between this ratio and QW, D_m, or t_p. Development of an equation to calculate this stress is not the subject of the present research. Note that it is not presently necessary to know the value of this stress since bellows are designed using normal stress, not stress intensity.

The EJMA calculation of elastic bending stresses due to pressure and deflection in unreinforced bellows were found to be reasonably accurate within the range of typical geometries that are used. Maximum meridional membrane stresses do not appear to be accurately calculated; however, as previously discussed, they are not generally significant in bellows design because they are very low relative to the bending stresses, and are not the focus of this research. The reason for the deviation has been found in this research, and the prediction of membrane stress can be improved by solving for the membrane stress at the location of highest membrane stress.

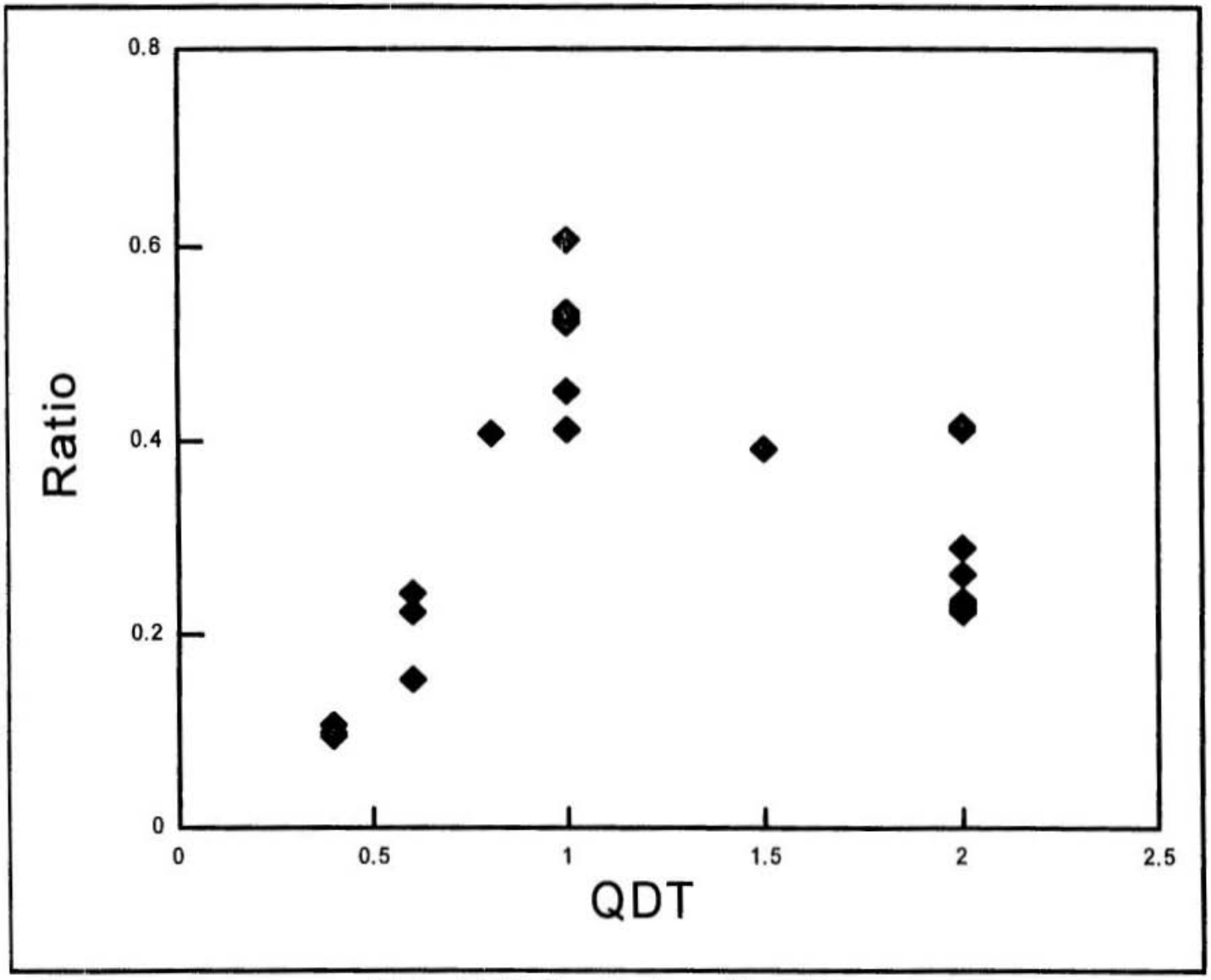

Figure 4.2-13, Circ. Membrane Stress / S_6

The finding that the parameters QW and QDT effectively remove thickness and diameter from any significant influence on the charts of C_p, C_f, and C_d means that the accuracy of the charts can be improved through simple parametric analysis of a large number of bellows geometries. The existing curves can simply be adjusted based on the results of parametric finite element calculations. Note that this is also a reflection of the accuracy of Anderson's approximate shell analysis, as these parameters were used to nondimensionalize the solution for the toroidal sections.

4.3 Inelastic Analysis of Unreinforced Bellows

A number of elastic-plastic large displacement analyses of unreinforced bellows were performed to evaluate the strain range due to displacement loading. This was to improve the understanding of plasticity effects on the response of bellows to displacement loading. These plasticity effects are one of the primary reasons why current design practice, as reflected in industry codes and standards, requires actual bellows fatigue testing for fatigue design of bellows. Unlike many other components, designers are not permitted to use basic material data from polished bar fatigue tests to evaluate the cycle life of the component.

Tanaka (1974) has observed, on the basis of elastic-plastic shell calculations, that unreinforced bellows had a plastic strain concentration at their root and crown due to displacement load. The strain concentration was shown to depend on a

parameter μ, described in Section 2.3, and reached a maximum of two when the parameter reached a value of 1.5.

The parameter used by Tanaka is essentially QDT times a constant. However, consideration of plastic strain concentration, as discussed in Section 2.4, would indicate that the convolution height should have a significant effect on strain concentration. The greater the convolution height, the greater the potential strain concentration.

For the inelastic analyses, the model used a single element wide wedge of one half of a convolution, as shown in Figure 4.3-1. All models used a mean bellows diameter of 610 mm (24 inch) and thickness of 0.51 mm (0.02 inch). A bilinear stress-strain curve was assumed, with a yield strength of 207 MPa (30,000 psi). The slope beyond yield strength was assumed to be 10% of the elastic slope and kinematic hardening was assumed. The analyses included the effects of large displacement.

The model was validated against some available bellows strain gage results provided by Kobatake, et al. (1986) for an austenitic stainless steel bellows. Bellows dimensions and material properties, from Kobatake and Yamamoto, et al. (1986), are provided in Table II. The predicted response, using the model with the

properties from Table II, is compared with the measured response in Figure 4.3-2. The comparison is good, providing validation of the bellows model using test data.

Table II

Data on Kobatake (1986) Bellows

thickness, t	1.4 mm
ID	300 mm
convolution height, w	18 mm
pitch, q	16 mm
Elastic Modulus	153,770 Mpa
Montonic Yield Strength	142.1 Mpa
Hardening Coefficient	3.182 Mpa
Poisson's Ratio	0.306

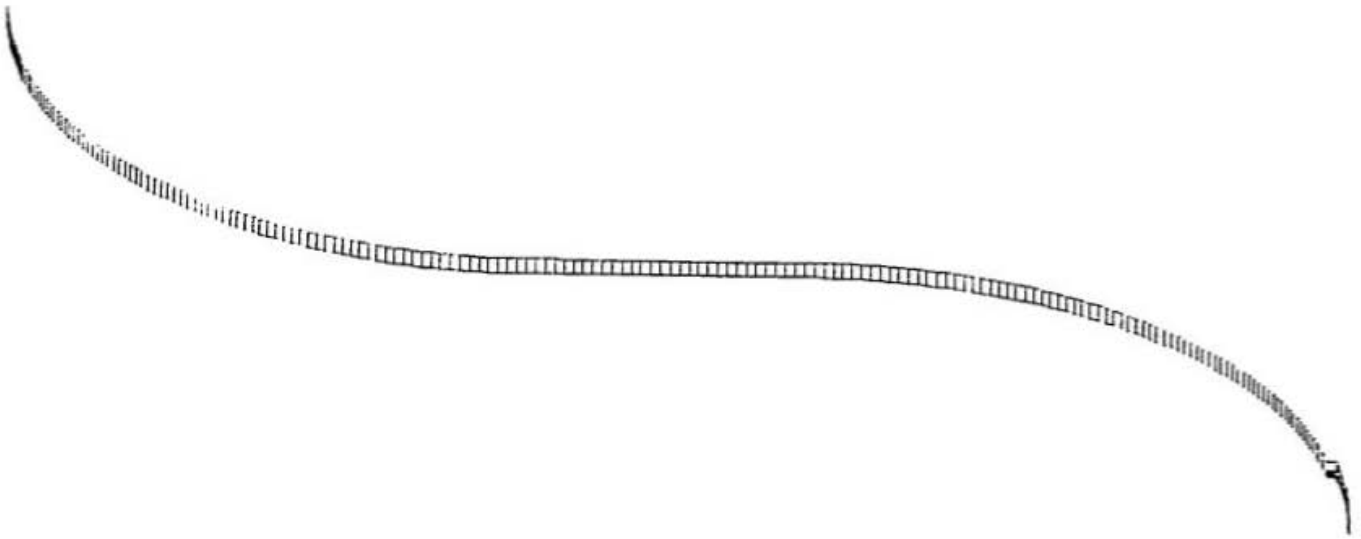

Figure 4.3-1, Wedge Model Used for Elastic-Plastic Analysis

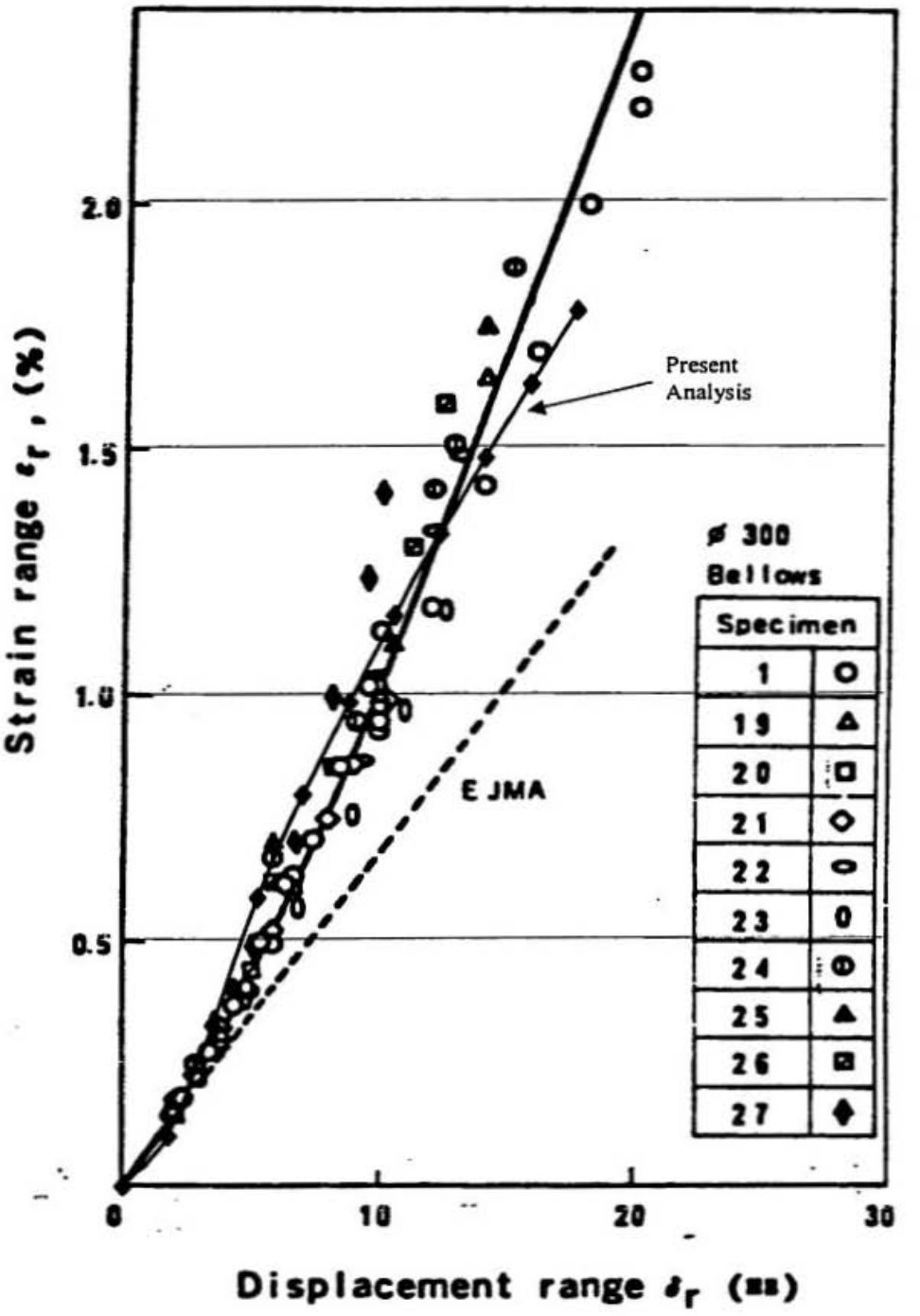

Figure 4.3-2, Comparison of Finite Element Prediction with Kobatake (1986) Data

The models were subject to 1½ cycles of compressive displacement. This provides for the shifting of the yield surface that occurs on the initial displacement which self springs the bellows. Because of this self-springing, subsequent cycles will have lower plastic strain ranges than the first ½ cycle. The third half cycle is representative of subsequent cycles. Typical charts showing strain-displacement behavior are provided in Figures 4.3-3 through 4.3-6. The strain range was taken from the last half cycle of analysis.

Plastic strain concentration was found to depend on a number of factors. First, the greater the displacement, the greater the strain concentration. The higher the convolution height, reflected in a low value of QW, the greater the strain concentration.

To permit comparison of the effects of the parameters, QW and QDT, independent of the degree of plasticity, analyses were run with different bending stress levels. They were run at ½, 3, 6 and 12 times the displacement that would result in an elastic meridional bending stress equal to the yield strength of the material.

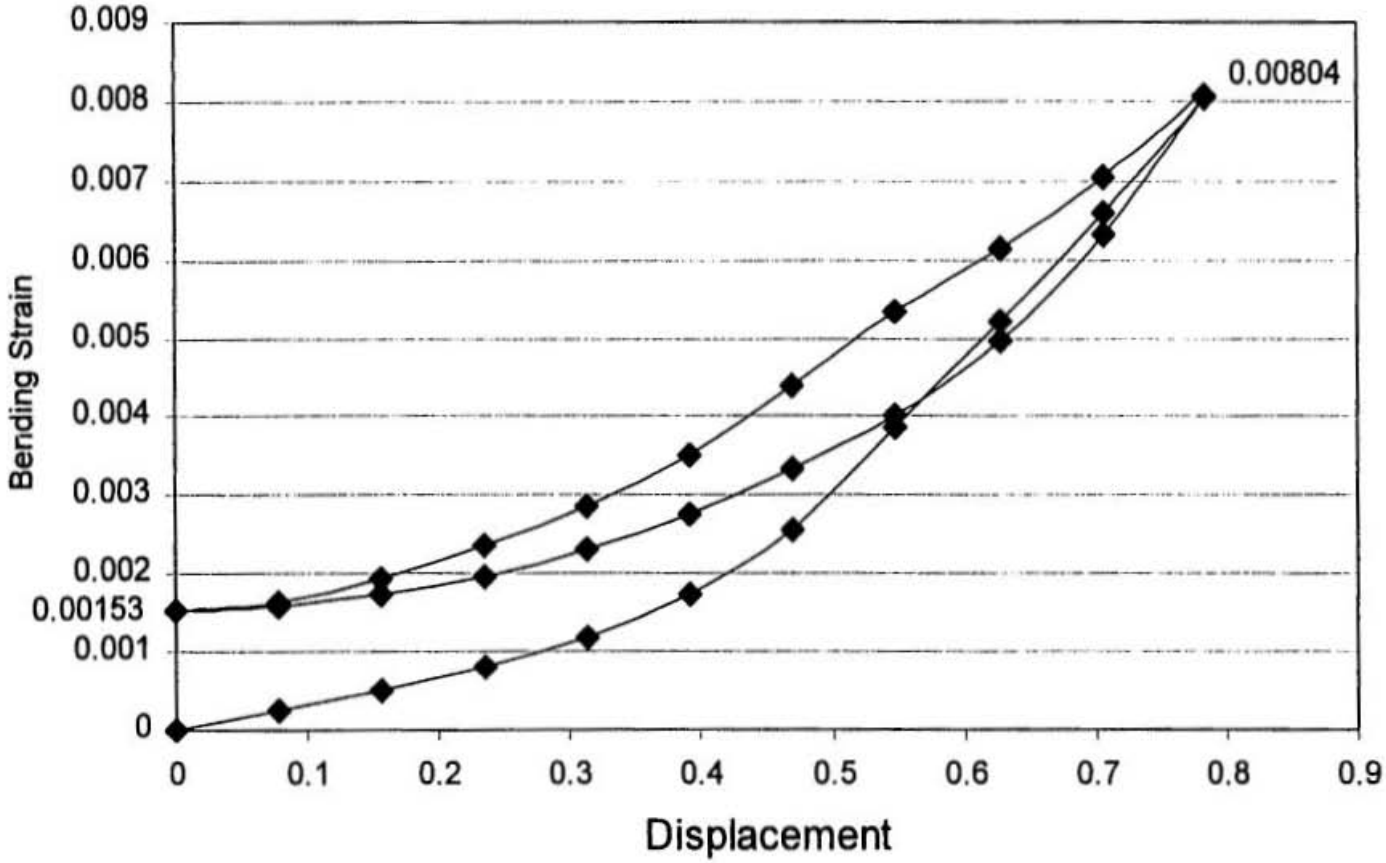

Figure 4.3-3, Strain-Deflection Relation for Unreinforced Bellows (QW=0.2, QDT=1.0)

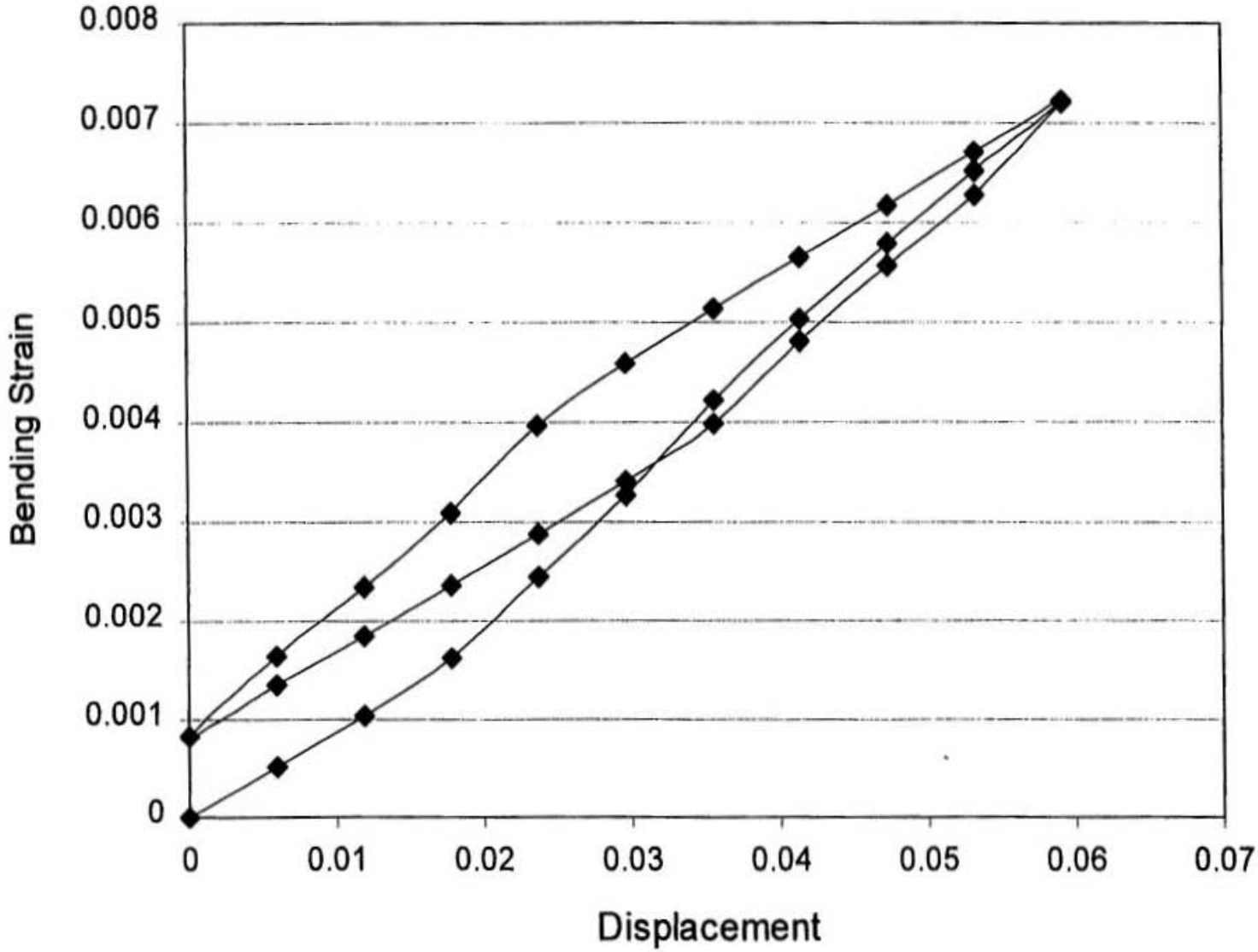

Figure 4.3-4, Strain-Deflection Relation for Unreinforced Bellows (QW=0.5, QDT=0.4)

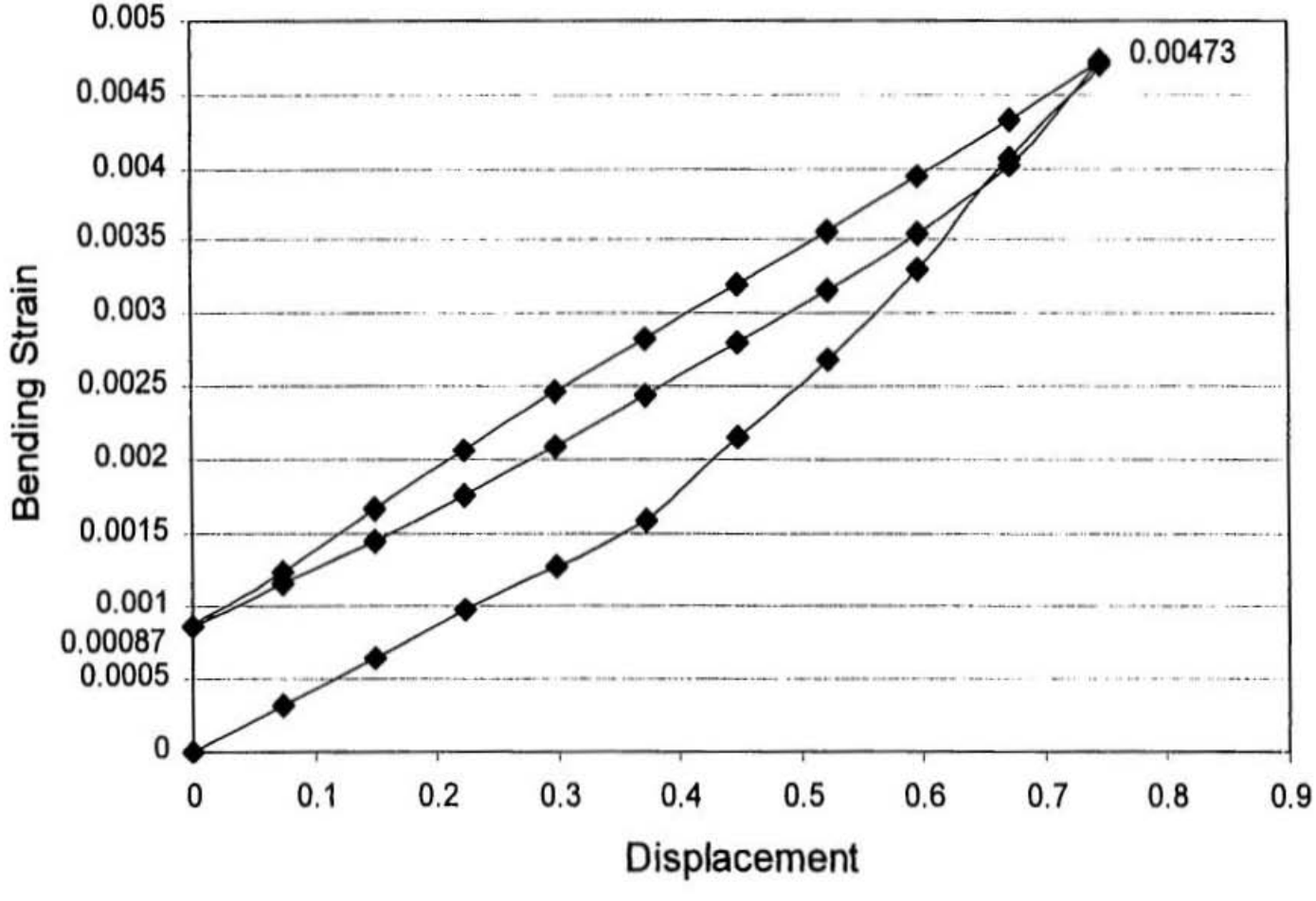

Figure 4.3-5, Strain-Deflection Relation for Unreinforced Bellows (QW=0.5, QDT=2.0)

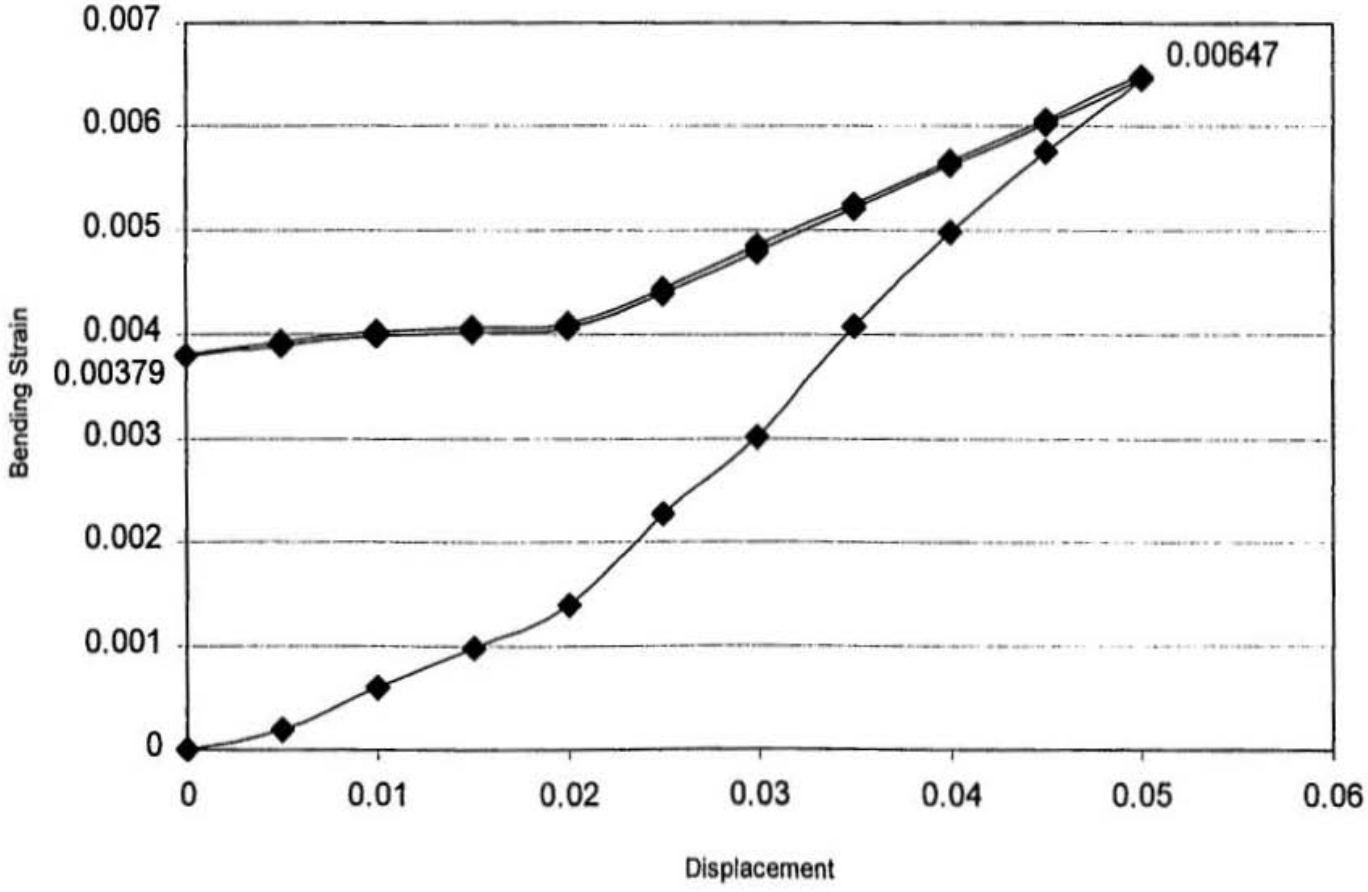

Figure 4.3-6, Strain-Deflection Relation for Unreinforced Bellows (QW=0.8, QDT=1.0)

Figures 4.3-7 through 4.3-9 illustrate the effects of the various factors on strain concentration. Some of the data from which these charts were prepared are in Table III. Strain concentration is taken as the ratio of the elastic plus plastic meridional bending strain from the inelastic analysis to the elastic meridional bending strain that was predicted for the same displacement from an elastic analysis. The elastic strain was determined from an elastic analysis using the same model as was used in the inelastic analysis, for each case.

Figures 4.3-7 through 4.3-9 show the strain concentration for various values of QW and QDT as a function of the multiple of the elastic displacement. The fact that calculated strain concentration is greater with greater displacement loadings should be no surprise since this simply reflects the greater dominance of plasticity. The charts also indicate trends with respect to the effect of the parameters QW and QDT on strain concentration, which was explored in greater detail, as described in the following paragraphs.

Figures 4.3-7 through 4.3-9 show the high dependence of strain concentration on the convolution profile, which is controlled by the parameter QW. An increase in QW increases the convolution height, w. Note, however, that convolution height for the bellows included in Figures 4.3-7 through 4.3-9 is also related to QDT since the bellows pitch increases with the parameter QDT and the convolution height is related to the pitch by the parameter QW.

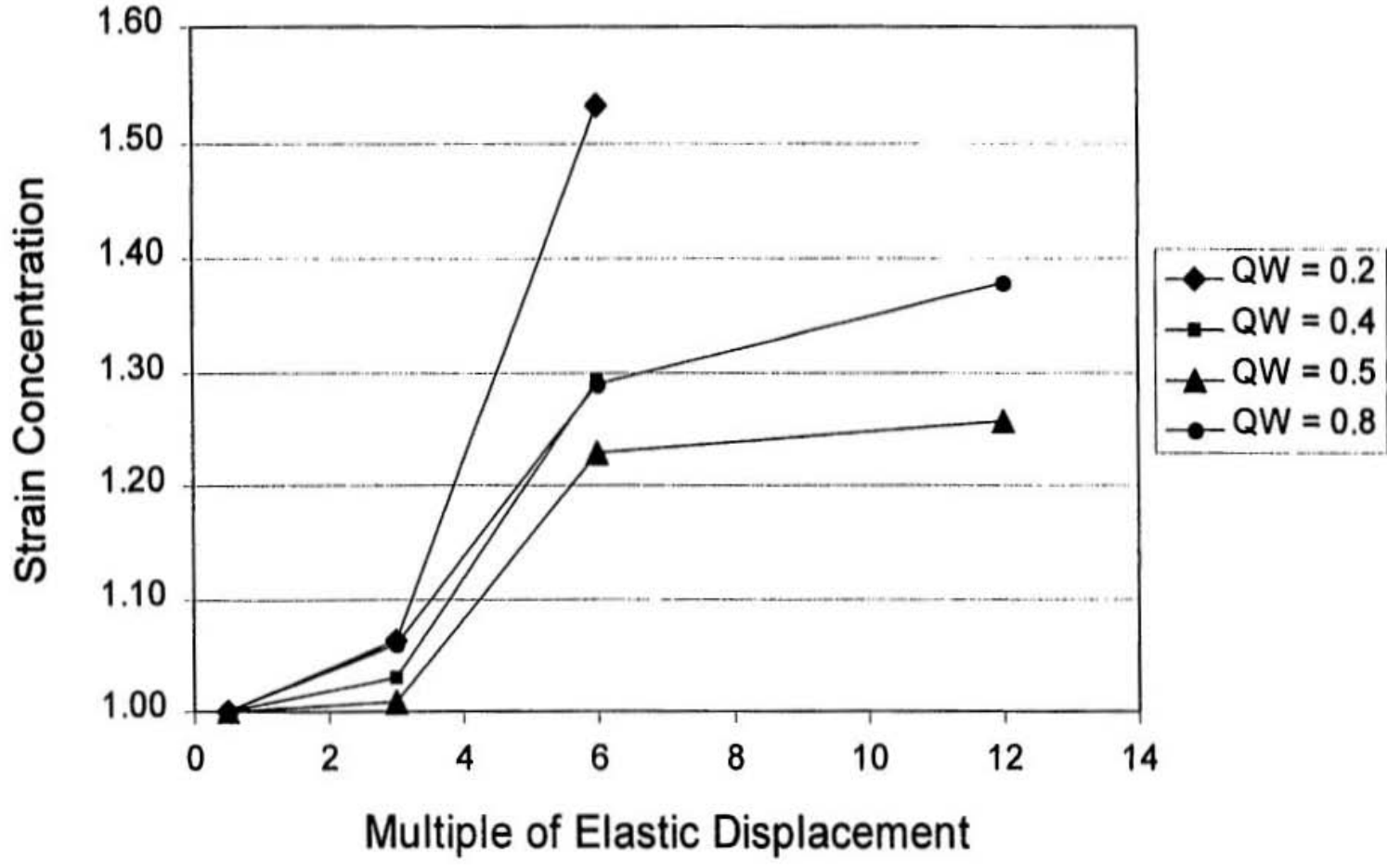

Figure 4.3-7, Strain Concentration vs. Multiple of Elastic Displacement and QW (QDT=0.4)

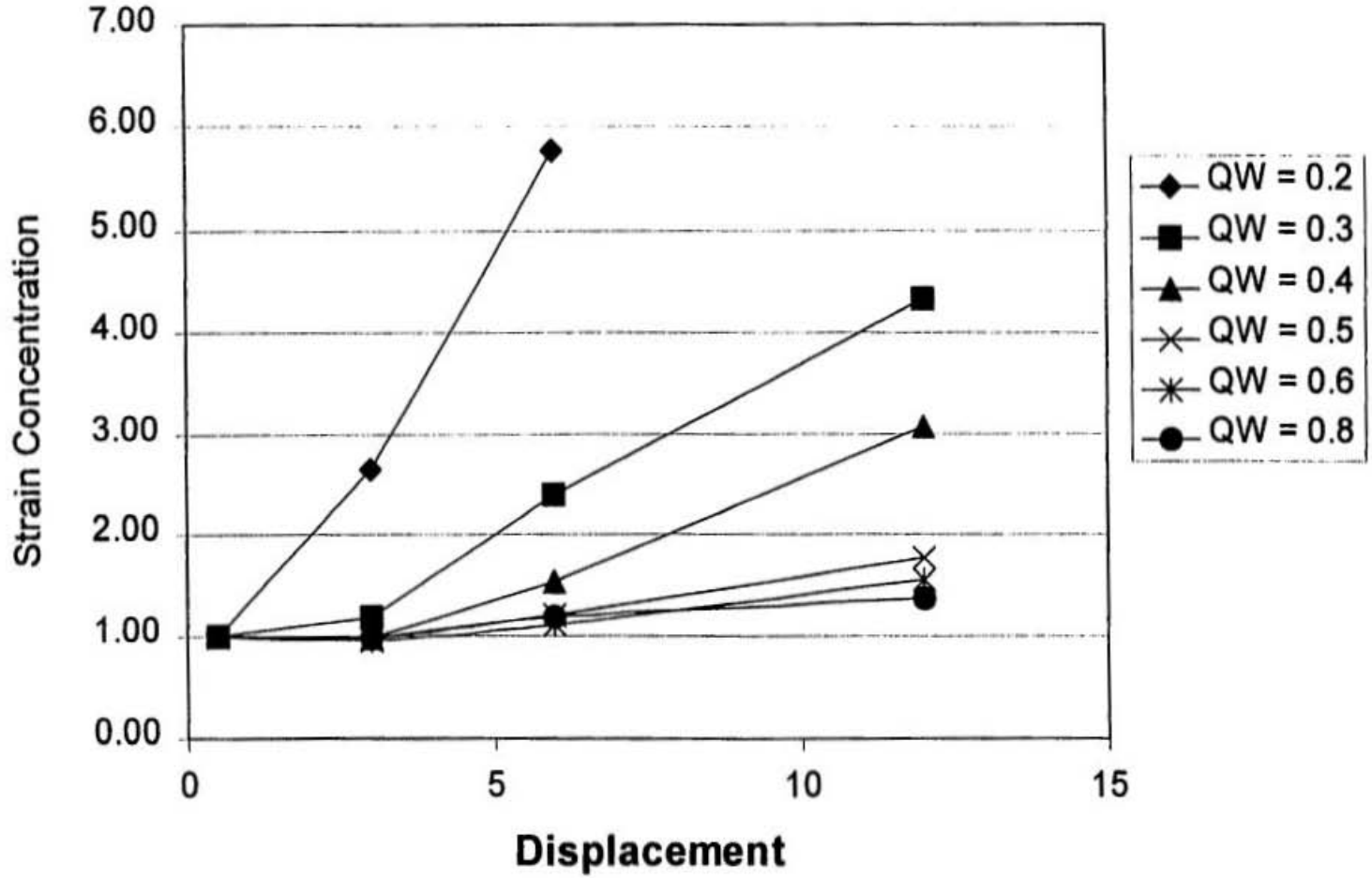

Figure 4.3-8, Strain Concentration vs. Multiple of Elastic Displacement and QW (QDT=1.0)

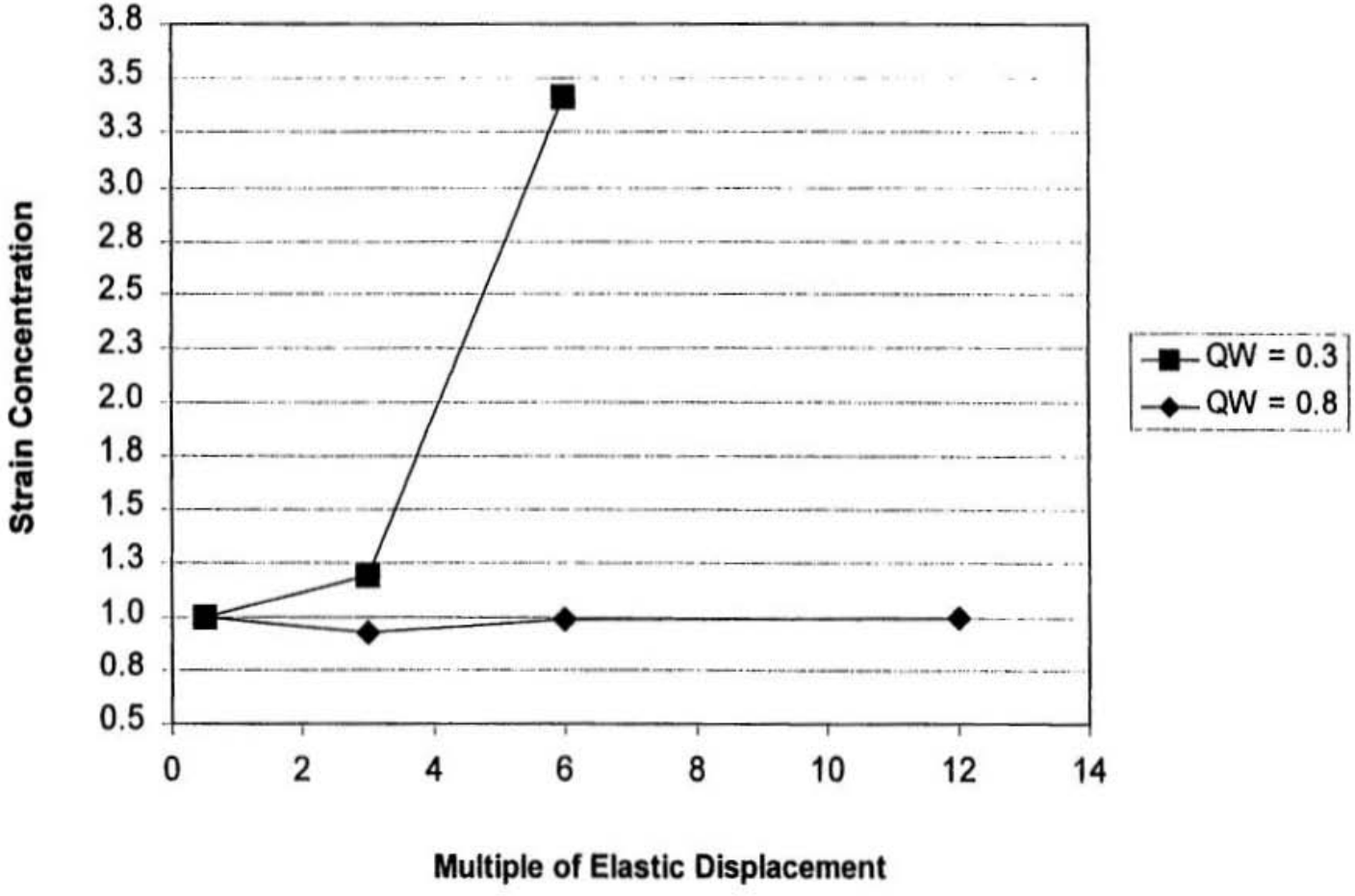

Figure 4.3-9, Strain Concentration vs. Multiple of Elastic Displacement and QW (QDT=2.0)

TABLE III

Strain Concentration for Unreinforced Bellows
Data for 6x Elastic Displacement

D_m = 610 mm (24 in) t_p=0.51 mm (0.02 in)

		Elastic Analysis			Elastic Plastic Analysis		
QW	QDT	Disp (2) inch	S6 (1) psi	6x Max Elastic Displacement (3) inch	Low Strain	High Strain	SCF (4)
0.2	0.4	0.01	2378.1	0.27455	0.00055	0.00842	1.525194
0.2	0.6	0.1	13817.2	0.65136	0.00053	0.01300	2.36250
0.2	1	0.1	5737.1	1.56874	0.00054	0.02971	5.92886
0.2	1.2	0.1	4484.6	2.0068	-0.00159	0.03780	8.20625
0.225	1	0.1	6937.3	1.2973	0.00002	0.02267	4.60366
0.3	1	0.1	10917.8	0.82434	0.00042	0.01221	2.39634
0.3	1.2	0.1	8774.5	1.02570	0.00081	0.01254	2.44375
0.3	2	0.1	4521.9	1.99034	0.00260	0.01230	3.411000
0.4	0.4	0.1	105673.0	0.08517	0.00068	0.00735	1.29264
0.4	0.6	0.1	44979.7	0.20009	0.00045	0.00751	1.36822
0.4	1	0.1	16845.1	0.53428	0.00037	0.00800	1.52113
0.4	1.2	0.1	13827.7	0.65087	0.00086	0.00676	1.19919
0.4	2	0.1	7838.1	1.14824	0.00074	0.00728	1.26667
0.5	0.4	0.01	15191.2	0.05924	0.00083	0.00721	1.23643
0.5	1	0.1	23196.9	0.38798	0.00062	0.00685	1.20698
0.5	2	0.1	12059.9	0.74627	0.00091	0.00535	0.92500
0.6	0.6	0.1	87759.3	0.10255	0.00053	0.00698	1.25878
0.6	1	0.1	29851.2	0.30150	0.00048	0.00615	1.11537
0.6	1.2	0.1	24755.3	0.36356	0.00000	0.00458	0.90873
0.8	0.4	0.1	15992.4	0.02814	0.00070	0.00700	1.31250
0.8	0.6	0.1	139373.0	0.06457	0.00054	0.00683	1.21616
0.8	1	0.005	2223.0	0.20243	0.00027	0.00630	1.16860
0.8	1.2	0.1	35383.0	0.25436	0.00000	0.00495	0.95930
0.8	2	0.1	28440.0	0.31646	0.00152	0.00653	0.98700

(1) meridional bending stress due to displacement
(2) displacement per convolution
(3) six times elastic displacement per 1/2 convolution = 1/2 Disp(30,000/S6)
(4) SCF=strain concentration factor

Figure 4.3-10 shows the effect of convolution height, w, on strain concentration, for cases where the displacement would produce an elastic bending stress range equal to six times the yield strength. It is clear that, as should be expected, an increase in convolution height results in an increase in strain concentration. Further, the effect of QDT is also clearly shown. For a given convolution height, an increase in QDT reduces the strain concentration. However, an increase in QDT with convolution height held constant also results in an increase in QW. As described in the subsequent paragraphs, the effect of the convolution profile, as reflected by QW, is very significant.

Figure 4.3-11 shows the effect of the parameter QW. A decrease in QW (deeper convolutions) results in an increase in strain concentration. The convolution profile is shown to have a very significant effect, with relatively small strain concentration for QW $\geq$0.45. For QW<0.45, the strain concentration becomes much greater and greatly dependent on QDT. Note that bellows with high QDT exhibit lower strain concentration for higher values of QW (shallower convolutions), albeit all bellows in this regime exhibit relatively low strain concentration. However, for bellows with deep convolutions, higher values of QDT results in substantially increased degrees of strain concentration.

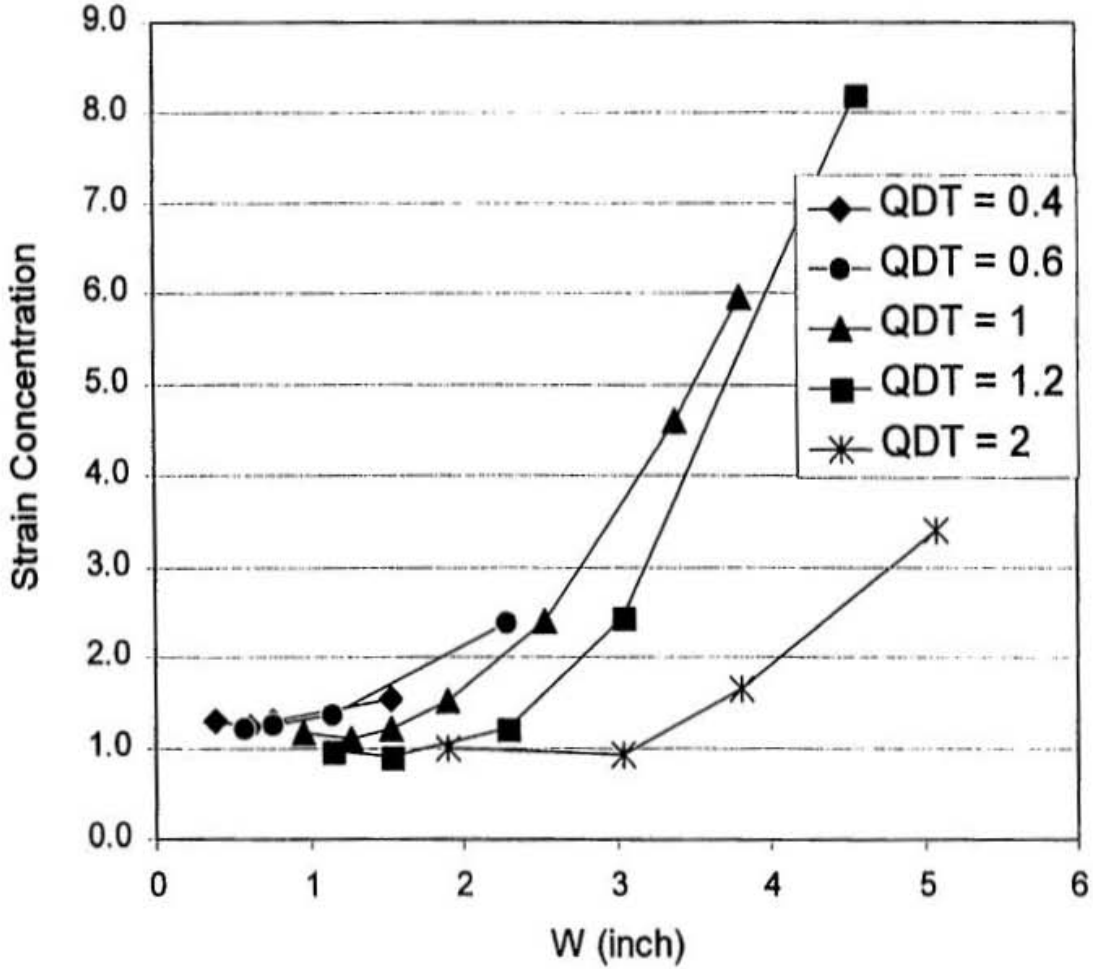

Figure 4.3-10, Strain Concentration vs. Convolution Height

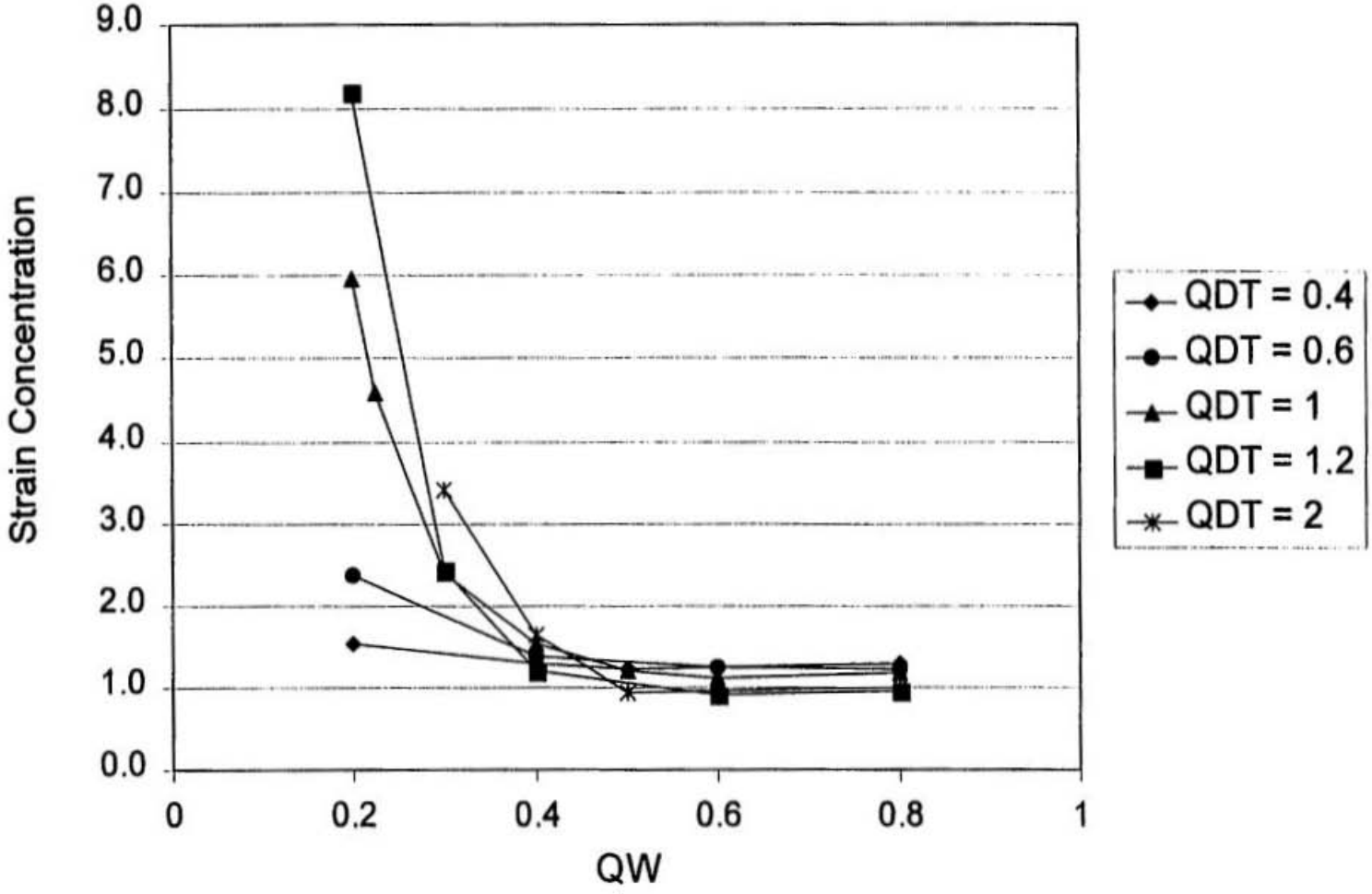

Figure 4.3-11, Strain Concentration vs. QW (All Data)

A series of analyses were run to evaluate the effect of the parameter QW, independent of the convolution height. All of the analyses were for the same convolution height and for QDT=1.0. The pitch was varied with QW and the thickness was varied to hold QDT constant. All were for a displacement that would produce an elastic displacement bending stress range equal to six times the yield strength. The calculated strain concentration as a function of QW is shown in Figure 4.3-12. Again, strain concentration is shown to depend significantly on QW, with relatively small strain concentration for $QW \geq 0.45$.

Because the prior work of Tanaka had indicated a relation with μ, which is directly proportional to QDT, the strain concentration data was evaluated versus QDT, as shown in Figure 4.3-13. Again, these are all for cases where the displacement would produce an elastic bending stress range equal to six times the yield strength. The effect of QDT is shown to be significant for deep convolution bellows (low QW).

To isolate the effects of the variation of QDT from its impact on convolution height, cases were run where the convolution height was held constant but QDT varied by changing the bellows thickness. Cases were run with QW equal to 0.3, 0.4, 0.5 and 0.8. The pitch was held at 38.7 mm (1.52 inch). While different convolution heights were run for each value of QW, the convolution height for all cases with a given value of QW were the same. The results of these evaluations are presented in Figure 4.3-14. It is shown that, with the broad range of geometries included in this

evaluation, QDT is not a good parameter for evaluating strain concentration. The same behavior as is exhibited in Figure 4.3-11 is exhibited, with the effect of QDT dependent on QW. The effect of QDT is more complex than indicated in prior findings of Tanaka.

All of these findings can be understood based on evaluation of the stress distributions that are present in bellows, while considering the basic principles of plastic strain concentration described in Section 2.4. Figures 4.3-15 through 4.3-22 show stress distributions due to compressive displacement for a range of bellows geometries. The dashed lines in the figures indicate the junction between the toroidal sections (root and crown) and the sidewall. The plots start from the outermost part of the convolution crown (on the left end) and go to the innermost part of the convolution root (on the right end). All of the elements have the same meridional length, so the plots are in scale. It is apparent that with high values of QDT (thin walls), the bellows exhibits greater shell (membrane) behavior, while for low values of QDT (thick walls), the bellows exhibits greater beam (bending) behavior.

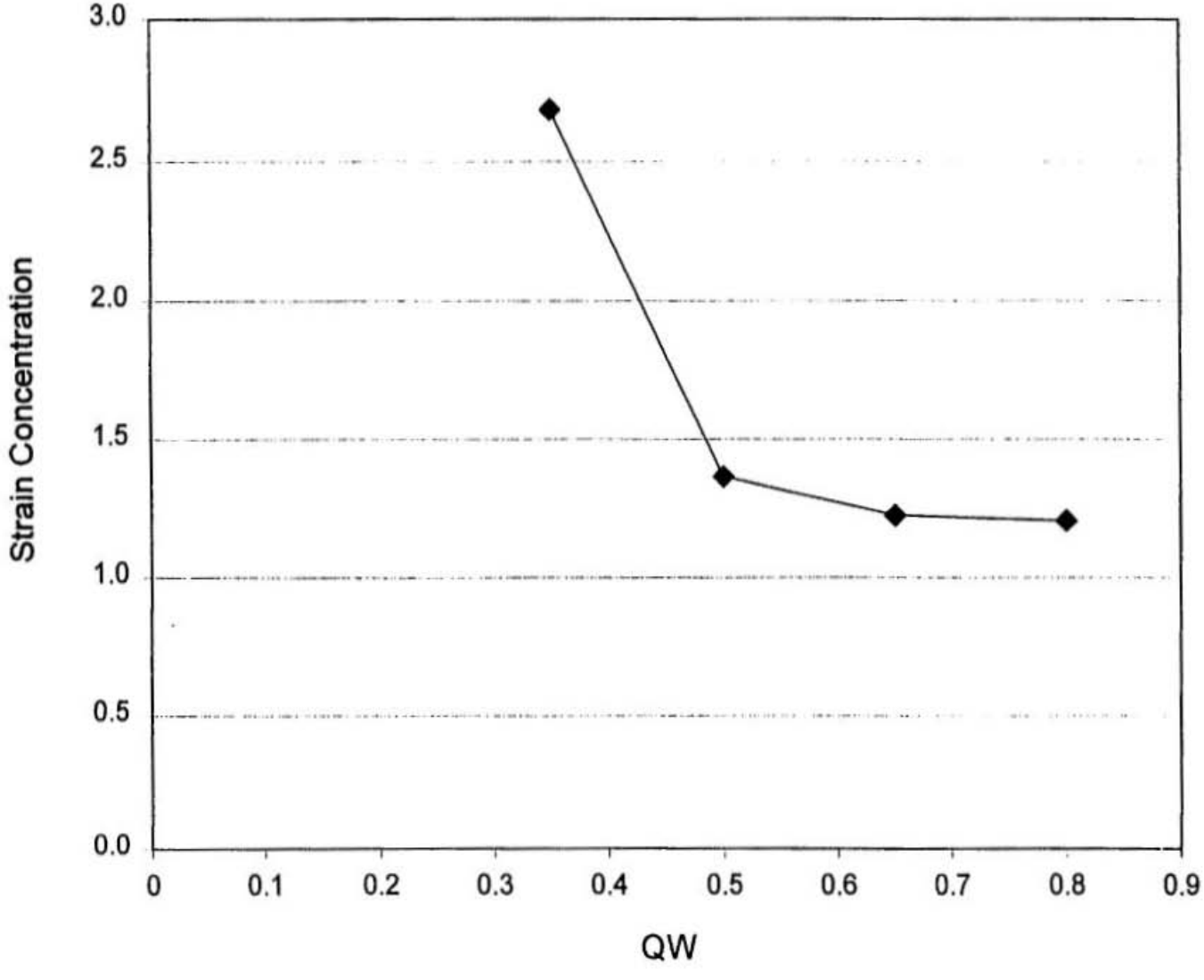

Figure 4.3-12, Strain Concentration vs. QW (w=constant, QDT=1.0)

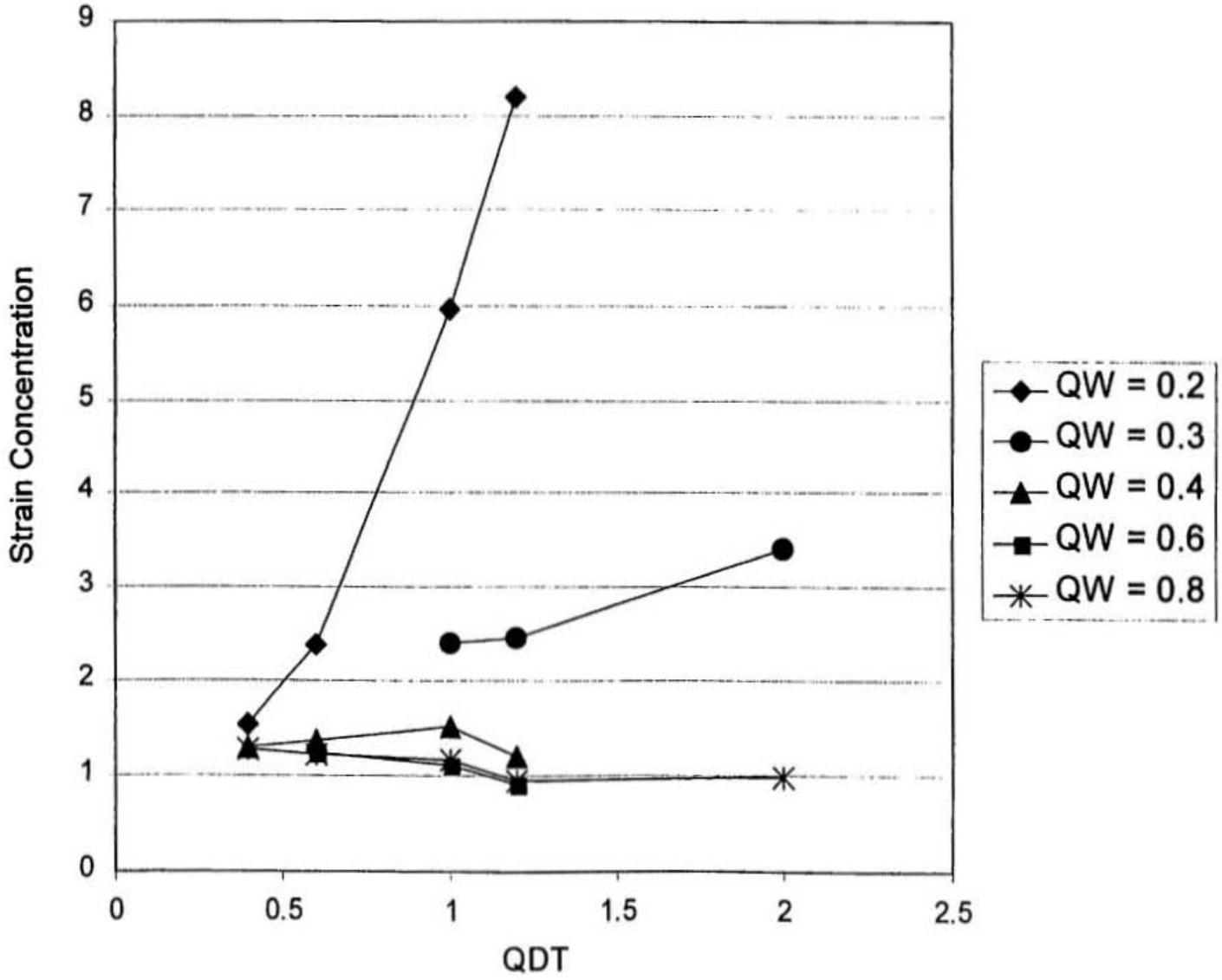

Figure 4.3-13, Strain Concentration vs. QDT (All Data)

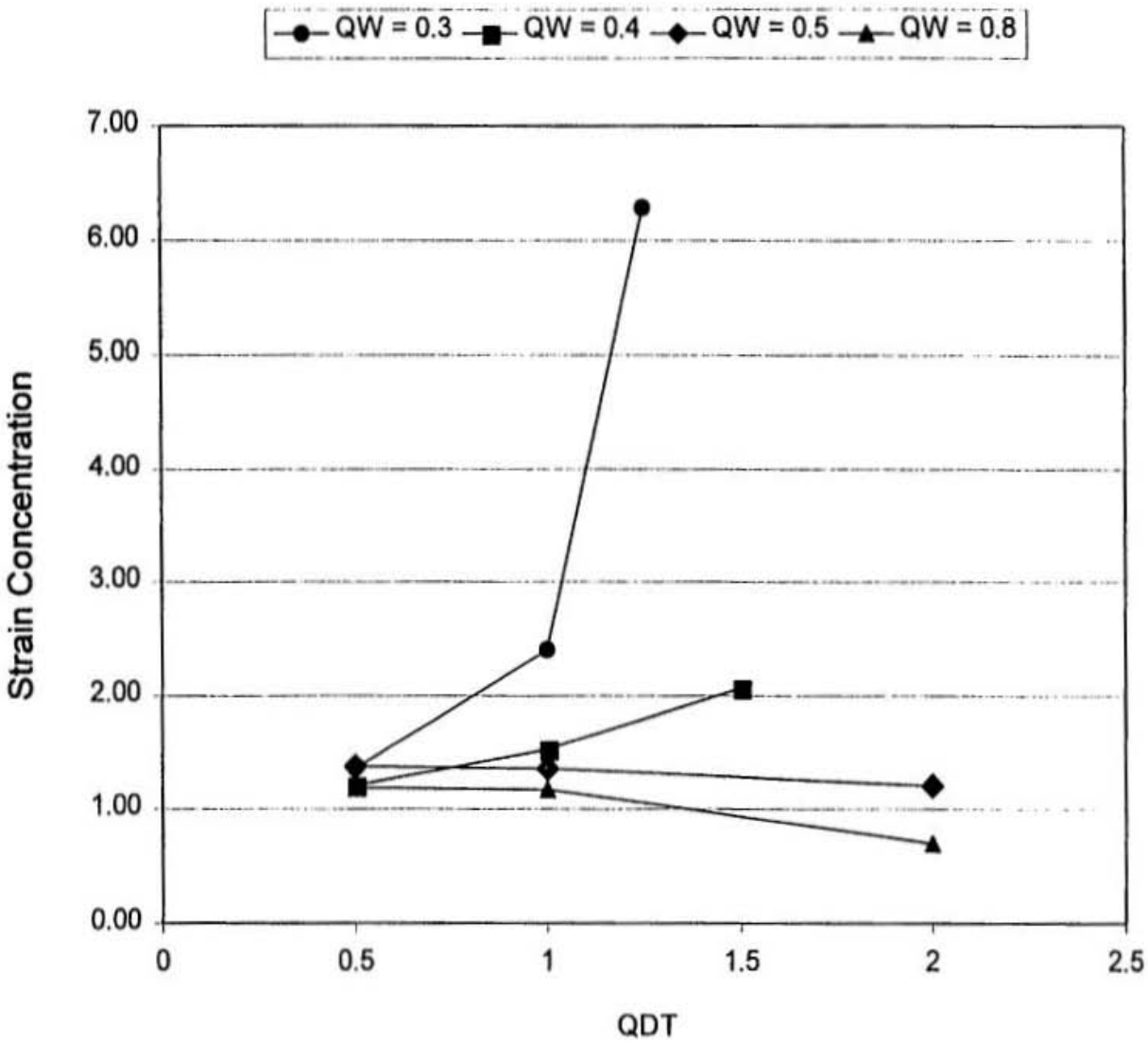

Figure 4.3-14, Strain Concentration vs. QDT (w=constant)

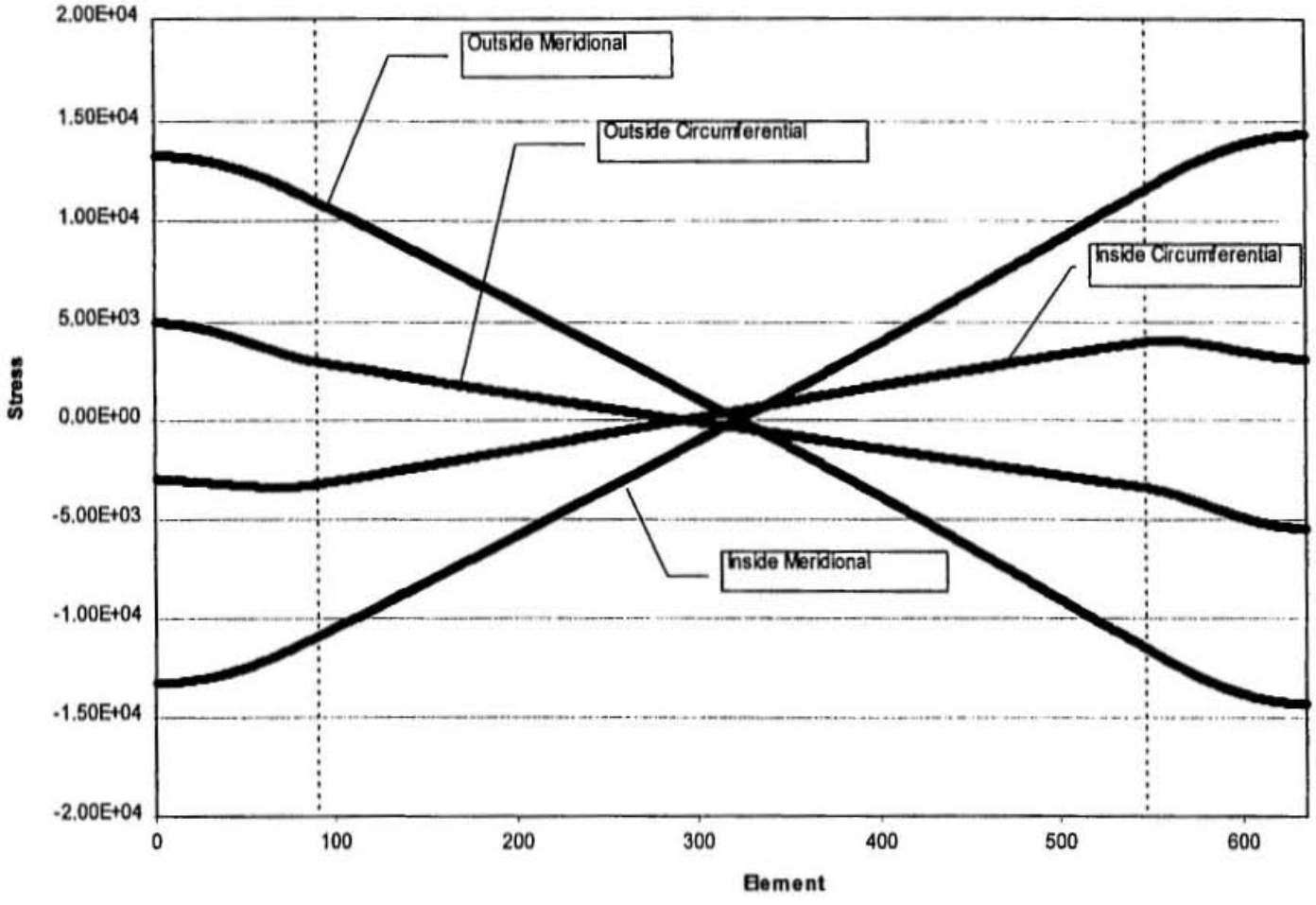

Figure 4.3-15, Surface Stress Due to Displacement (QW=0.2, QDT=0.4)

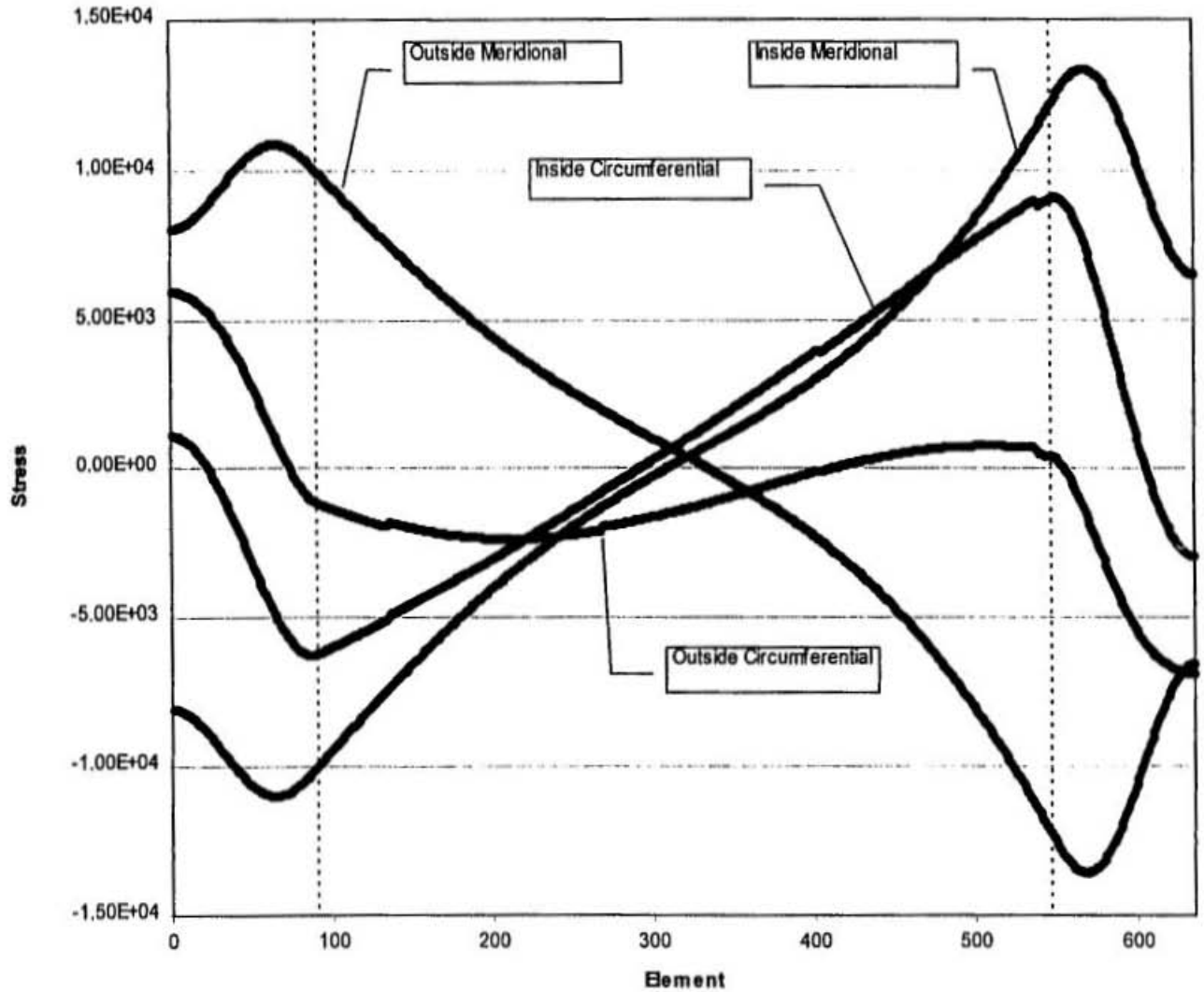

Figure 4.3-16, Surface Stress Due to Displacement (QW=0.2, QDT=1.2)

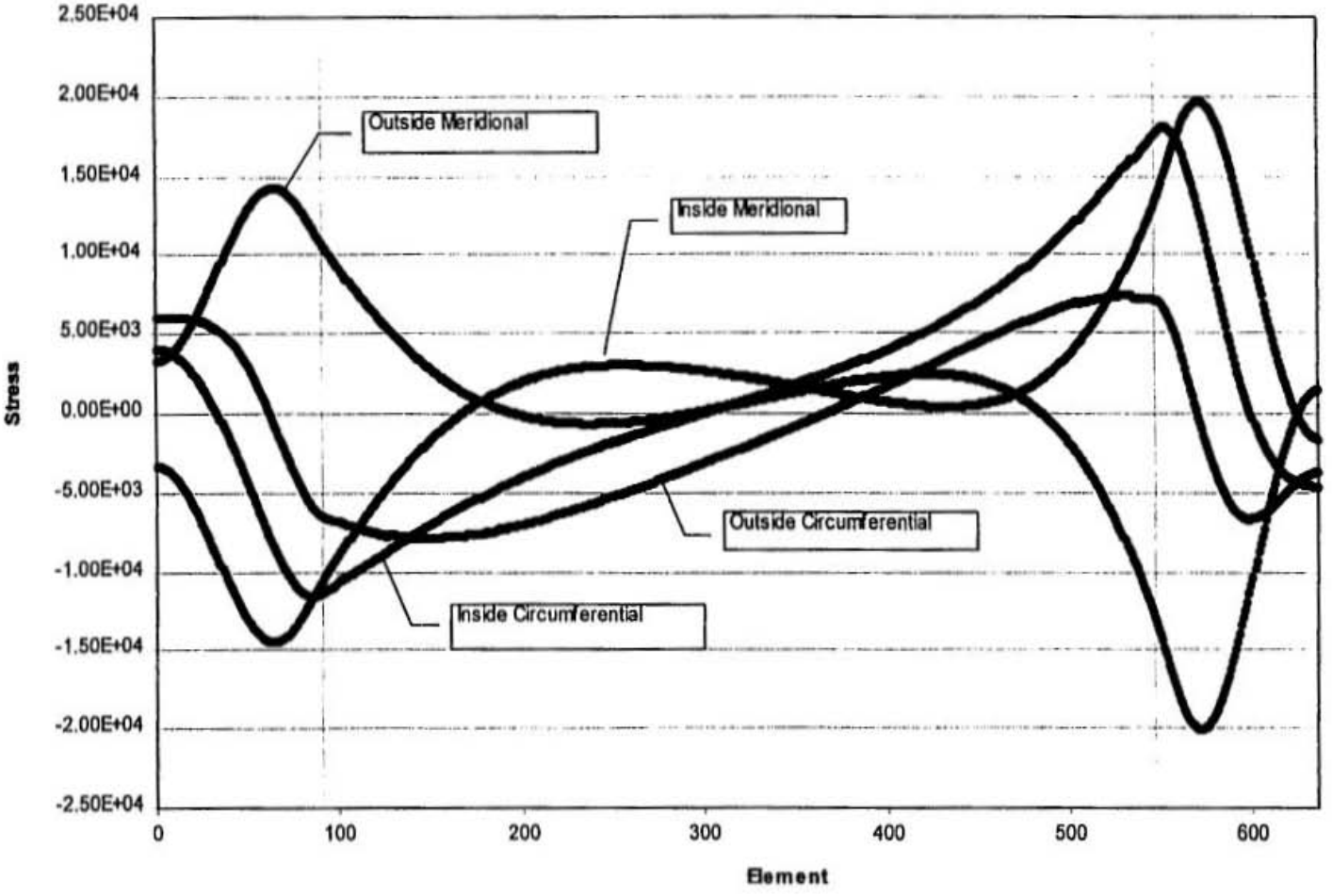

Figure 4.3-17, Surface Stress Due to Displacement (QW=0.2, QDT=2.0)

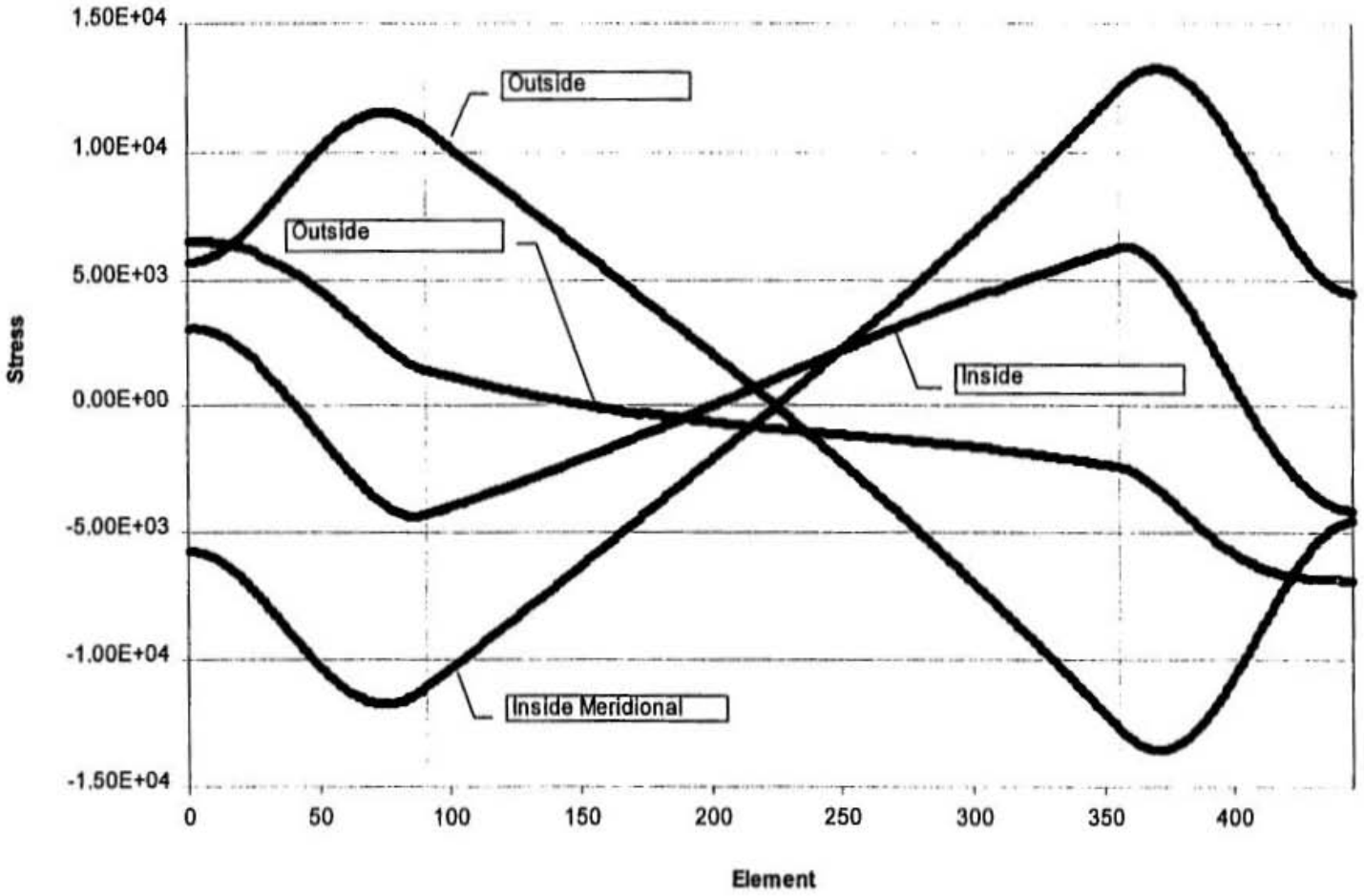

Figure 4.3-18, Surface Stress Due to Displacement (QW=0.3, QDT=1.2)

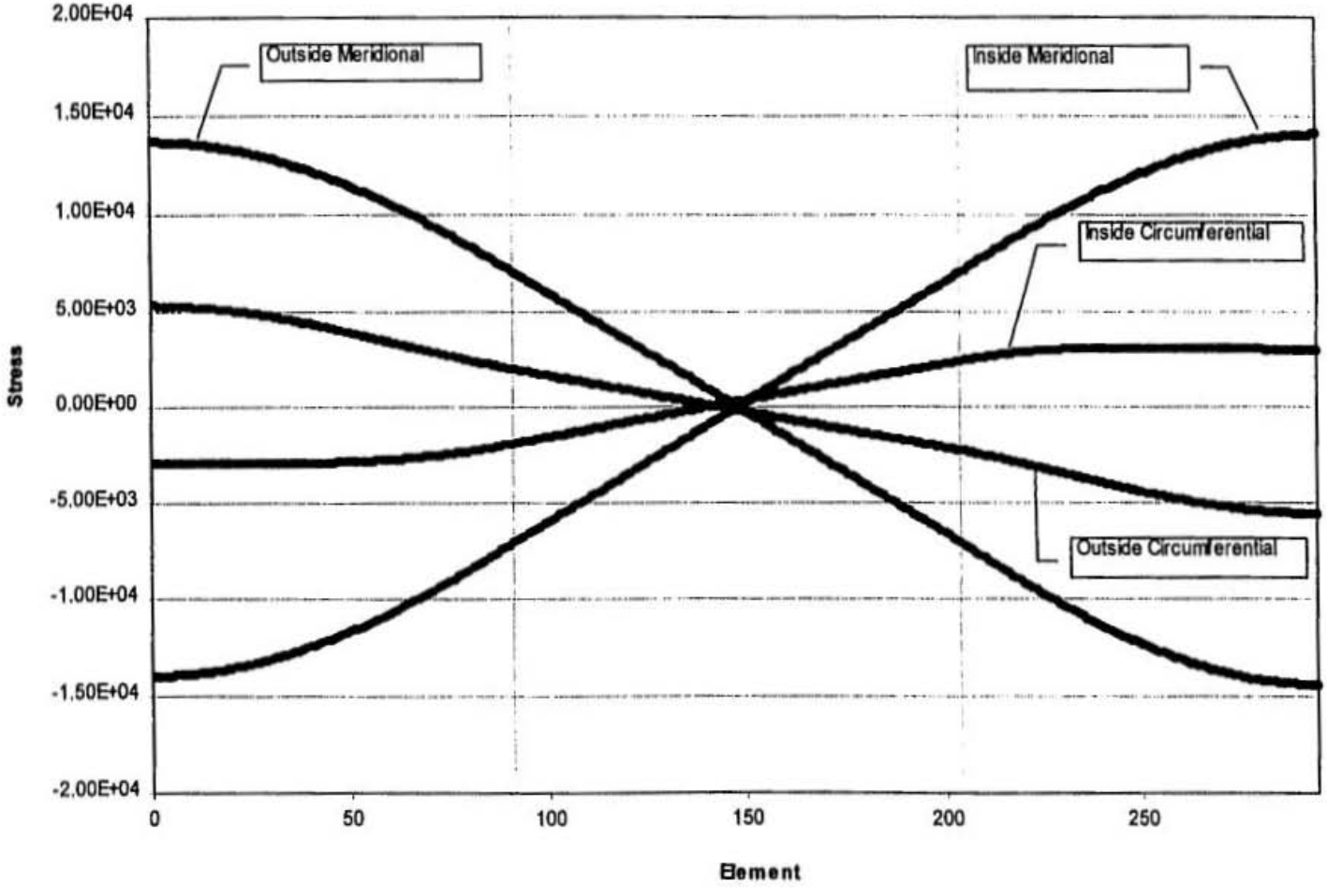

Figure 4.3-19, Surface Stress Due to Displacement (QW=0.5, QDT=0.4)

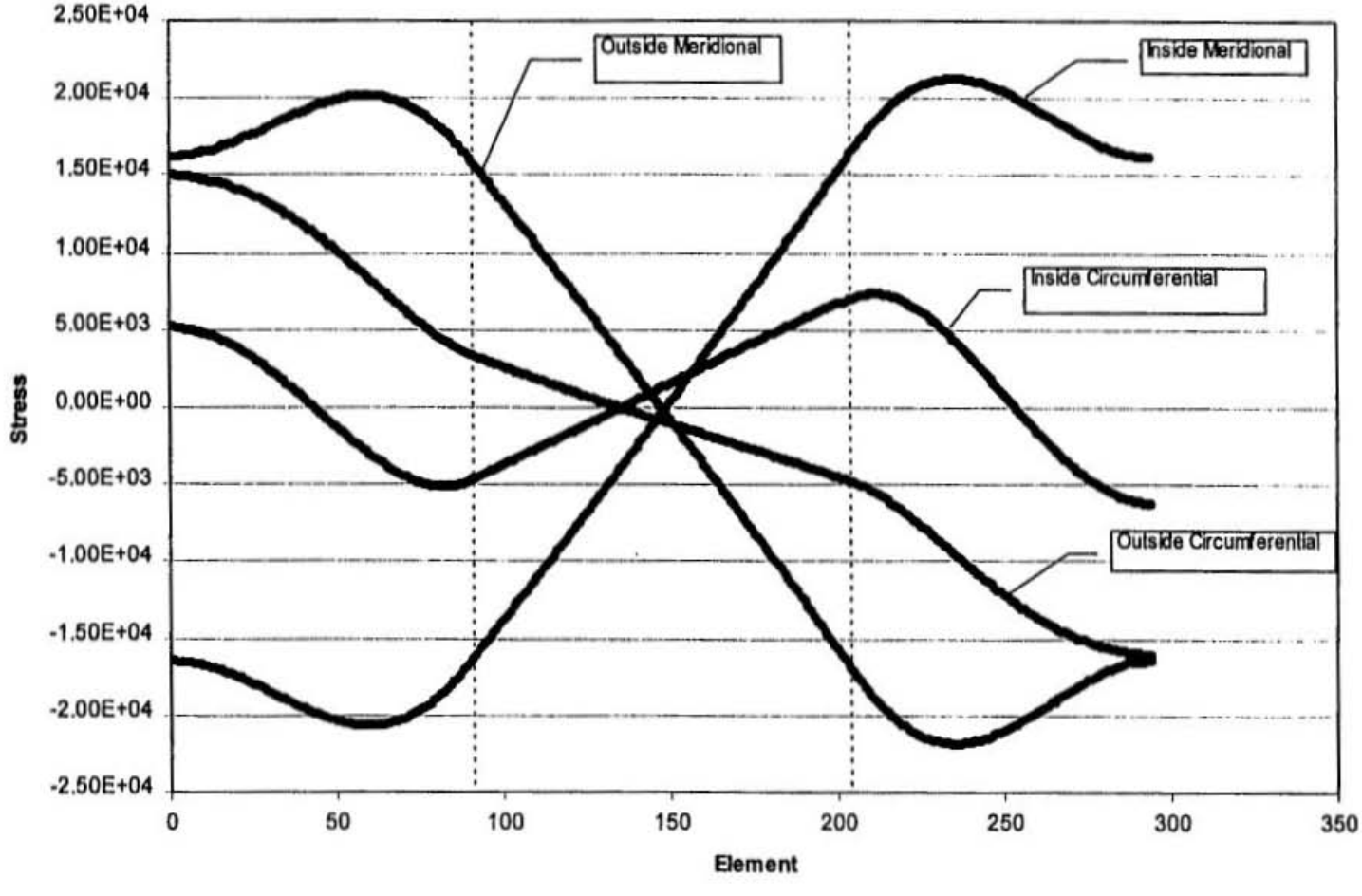

Figure 4.3-20, Surface Stress Due to Displacement (QW=0.5, QDT=1.0)

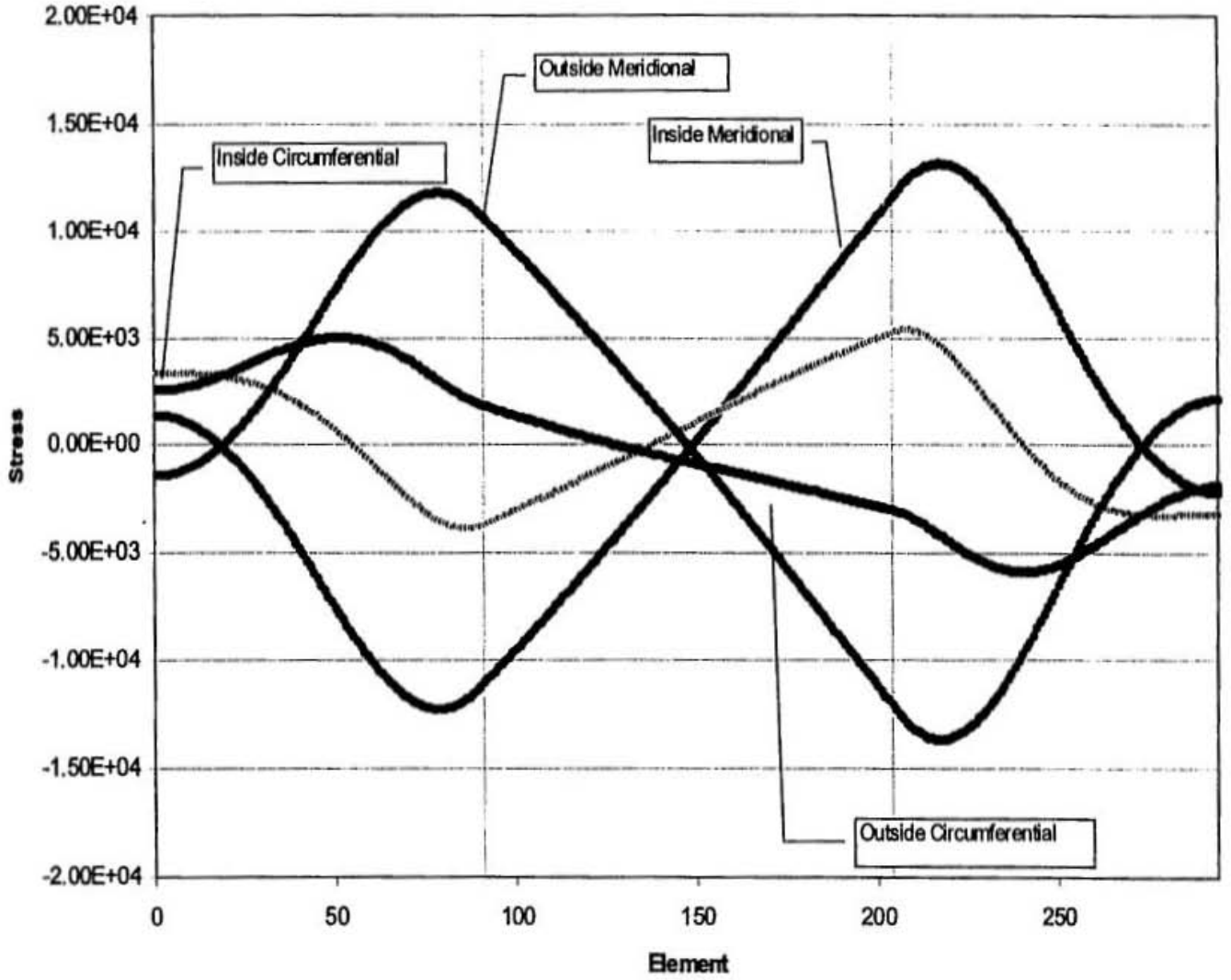

Figure 4.3-21, Surface Stress Due to Displacement (QW=0.5, QDT=2.0)

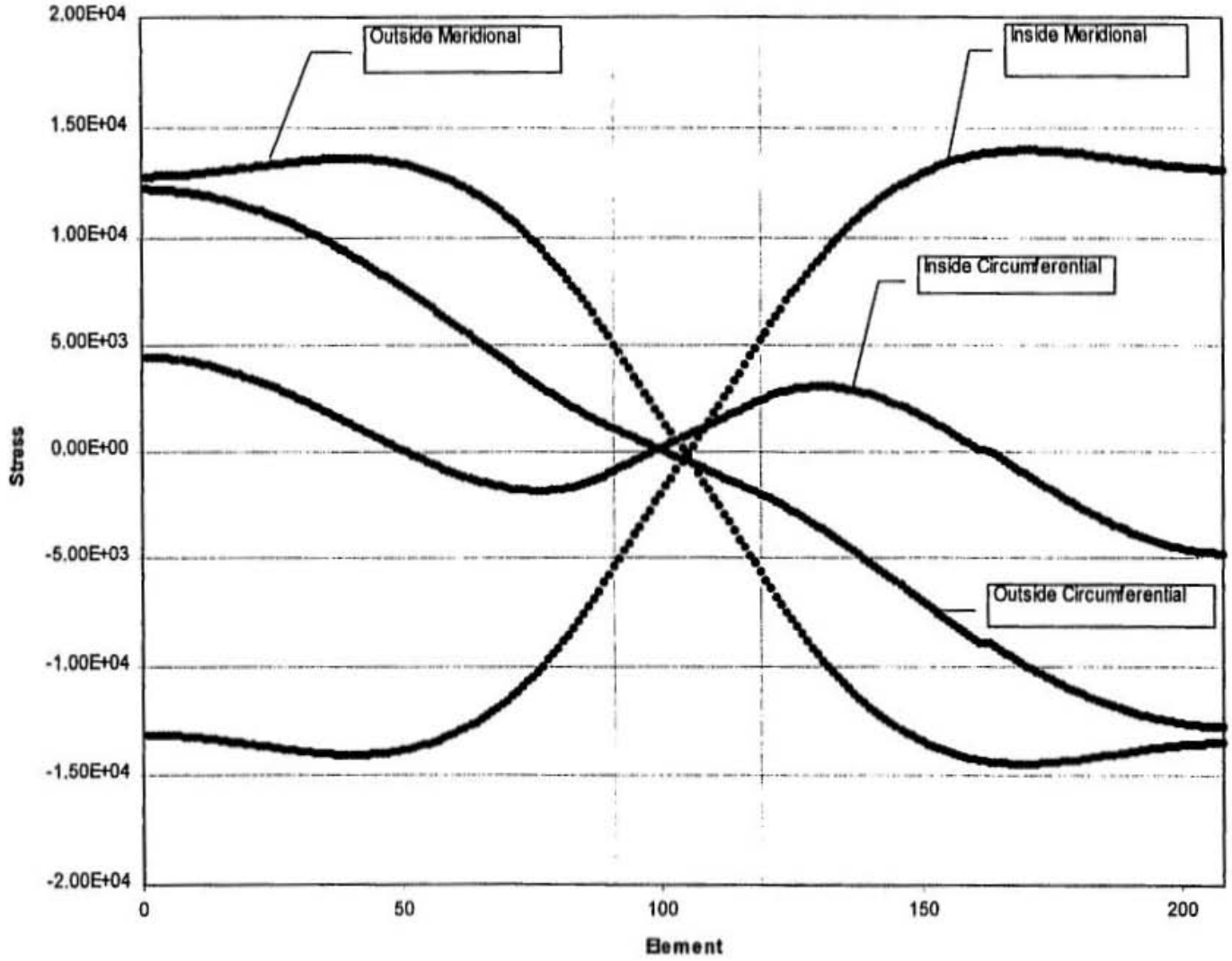

Figure 4.3-22, Surface Stress Due to Displacement (QW=0.8, QDT=1.0)

Review of the stress distributions reveal the following. For deep convolution bellows, the peak of the meridional bending stress is broad for low values of QDT (bellow with thicker walls and/or larger diameter relative to pitch) while there are distinct, sharp peaks of meridional bending stress for high values of QDT. Deep convolution bellows with high values of QDT are subject to significant strain concentration because the local area that is yielded is much smaller (stiffer) than the remainder. Deep convolution bellows with low values of QDT have lower degrees of strain concentration because the plasticity is distributed over a larger region.

An example is provided by comparison of Figures 4.3-16 and 4.3-18. Both are for a value of QDT=1.2. From Figure 4.3-11, it is apparent that the bellows of Figure 4.3-16 is subject to greater plastic strain concentration. Comparison of the stress distributions reveals that the high meridional bending stress is more localized in Figure 4.3-16. Thus, greater plastic strain concentration is to be expected.

Shallow convolution bellows are not as subject to plastic strain concentration because their region of highest meridional bending stress is larger in relation to the remainder of the bellows. For shallow convolution bellows (high QW) with high values of QDT, the plastic strain concentration is reduced (relative to low values of QDT) because the length of the sidewall is reduced for the same value of QW. This is because, while the convolution height is the same, the radii of the toroids are larger so less of the convolution height is composed of the sidewall. This effect is

relatively small as plastic strain concentration in shallow convolutions is relatively insignificant.

While not specifically addressed herein, it is obvious that material properties also play a significant effect on strain concentration. The higher the yield strength, the greater the elastic portion of the strain range and the lower the degree of plasticity and consequent strain concentration. Also, the lower the plastic modulus, the greater the plastic strain concentration. These are mitigated to some extent by cyclic hardening that occurs in austenitic stainless steel, a commonly used material for bellows.

Strain concentration in bellows was found to be highly sensitive to the convolution profile. While the elastic stress prediction is a relatively good indicator of strain range for values of QW greater than about 0.45, it becomes much less so for deeper convolution profiles, QW less than about 0.45.

Deep convolution bellows are subject to plastic strain concentration because of the greater flexibility of the portion of the bellows that shifts strain to the local region of strain concentration. Bellows with thinner walls and/or smaller diameter relative to their pitch (high QDT) are subject to greater plastic strain concentration when the bellows are in the regime of significant plastic strain concentration (QW<0.45)

because the region of high meridional bending stress is more localized. In terms of Section 2.4, the local region that is subject to strain concentration is stiffer.

4.4 Evaluation of Fatigue Data

The impact of strain concentration can be significant on fatigue life. As shown in the prior section, significant and widely varied strain concentration was found in analyses of bellows with QW<0.45, but much less so for bellows with higher values of QW. The bellows fatigue data that was provided by the Expansion Joint Manufacturer's Association for the development of the design rules for bellows in ASME Section VIII, Div 1 and ASME B31.3 were separated into these two regimes of QW, below 0.45 and above 0.45. The data is listed in Table IV. Figure 4.4-1 shows the distribution of the data with respect to QW and QDT.

The deflection stress ranges were calculated in accordance with the Standards of the Expansion Joint Manufacturer's Association, multiplied by a factor of 1.4, and plotted on Figures 4.4-2 and 4.4-3. The 1.4 factor comes from an evaluation of the fatigue data provided herein, and can be considered to reflect effects such as the degree of strain concentration that occurs in shallower convolution profiles, surface finish, etc. It is essentially equal to the factor of 1.43 cited in WRC Bulletin 398 (Stamaugh, et al., 1995) for the difference in the fatigue strength of polished bar versus plate material, and therefore may be largely due to surface finish effects.

The bellows fatigue data for QW>0.45 (see Figure 4.4-2), with the inclusion of the 1.4 factor, follows the polished bar fatigue curve with very little scatter. The bellows fatigue data for QW<0.45 (see Figure 4.4-3) shows greater scatter and appears to fall somewhat below the polished bar fatigue curve, even with the inclusion of the 1.4 factor. This should be expected because the elastic stress prediction is not a good measure of the strain range, considering plasticity, for bellows with QW<0.45.

The bellows fatigue data are compared to the raw (no design margin) polished bar fatigue curve for austenitic stainless steel that was used in the development of Section VIII, Div 2, as provided in the Criteria Document (1972). The polished bar fatigue curve is shown as a curve in both Figures 4.4-2 and 4.4-3. In the development of the ASME B31.3 bellows fatigue curve (Becht, 1995), all of the fatigue data was lower bounded and then additional design margins were applied to the lower bound curve. It is clear from this research that the deep convolution bellows (QW<0.45) controlled the design fatigue curve. This can now be attributed to their greater potential for plastic strain concentration. If the data were separated, a significantly higher fatigue curve would be developed for bellows with QW>0.45.

TABLE IV
Unreinforced Bellows Fatigue Data

ID #	S3+S4	S5+S6	Inside Diameter	Con Height, w	Thickness, t	Pitch, q	# Cons, N	Axial Disp	Pressure	Cycles to Failure
	psi	psi	inch	inch	inch	inch		inch	psi	
3-8	23437	88010	10.75	1	0.036	0.675	5	0.4375	70	111988
3-4	48054	37355	12.75	0.98	0.02	0.911	8	0.625	60	63600
3-6	46353	118465	12.75	1	0.026	0.674	10	1.625	75	17322
3-5	32652	69687	6.625	0.6875	0.019	0.462	10	0.625	59	71512
3-1	14277	272843	8.625	0.8125	0.04	0.442	5	0.75	73	1470
4-8	14956	196516	3.45	1.26	0.038	1.5	5	1.25	50	11280
4-7	14956	196516	3.45	1.26	0.038	1.5	5	1.25	50	12750
4-10	14956	196516	3.45	1.26	0.038	1.5	5	2.5	50	11450
4-9	14956	196516	3.45	1.26	0.038	1.5	5	2.5	50	13869
1-2	14956	196586	3.45	1.26	0.038	1.5	10	2.5	50	10988
1-1	14956	196568	3.45	1.26	0.038	1.5	5	1.25	50	12035
5-1	19681	154043	3.47	1.27	0.0375	1.125	5	1.25	50	11000
5-2	23166	129626	4.11	1.4	0.0375	1.25	5	1.25	50	17865
4-6	26935	162900	4.14	1.39	0.038	1.62	5	1.25	75	13860
1-4	17957	81450	4.14	1.39	0.038	1.62	5	0.625	50	108620
1-3	17957	162900	4.14	1.39	0.039	1.62	5	1.25	50	10400
7-2	25946	149612	4.428	1.44	0.036	1.27	6	0.312	51	10608
7-1	25773	91880	4.432	1.43	0.034	1.24	10	0.200	46	99181
4-5	25481	131168	6.14	2.14	0.05	2.12	5	1.875	50	20500
4-4	25841	131168	6.14	2.14	0.05	2.12	5	1.875	50	26779
1-5	25841	131146	6.14	2.14	0.05	2.12	5	1.875	50	26786
1-6	25841	131146	6.14	2.14	0.05	2.12	5	1.875	50	23200
5-3	31710	112779	6.15	2.17	0.05	1.75	5	1.875	50	30365
7-3	51631	135594	6.577	2.04	0.034	1.27	3	0.500	50.5	23294
7-4	49018	144460	6.577	2.4	0.034	1.94	3	0.500	51.5	8844
2-1	0	210220	6.66	0.485	0.018	0.358	13	1.3	0	5800
6-1	597	352917	6.725	0.575	0.05	0.7	10	0.5	12	1997
5-4	30098	145334	8.156	2.29	0.05	2.25	5	2.5	50	14859
1-8	24859	169484	8.22	2.19	0.05	2.5	5	2.5	50	8900
1-9	24859	84742	8.22	2.19	0.05	2.5	5	1.25	50	155700
1-7	24859	169484	8.22	2.19	0.05	2.5	5	2.5	50	12848
7-6	34938	130556	8.525	2.43	0.05	2.28	8	0.499	51.5	18331
7-5	34599	173204	8.525	2.43	0.05	2.27	8	0.622	51	8942
2-2	37660	130487	8.66	0.485	0.018	0.348	20	1.2	1.25	16000
2-4	0	126551	10.81	0.598	0.018	0.401	15	1.4	0	28000
6-3	3396	158094	10.814	0.968	0.032	0.864	8	0.75	10	26173
6-7	2256	201488	10.83	0.96	0.04	0.88	8	0.75	10	13832
6-2	1413	261110	10.85	0.95	0.05	0.9	8	0.75	10	4586
1-10	35820	138116	12.19	2.52	0.05	2.5	5	3.125	50	14850
6-6	6912	234093	12.814	1.093	0.032	0.864	6	1	15	8919
2-3	0	111870	14.035	1.039	0.025	0.787	10	1.8	0	171000
3-3	19644	140701	16	1.34	0.036	0.763	5	1.1875	32	8068
3-2	45500	132047	16	1.39	0.024	0.872	6	2.3125	33	3617
4-2	41698	114394	19.55	2.57	0.05	2.5	5	3.125	50	17500
4-3	41698	114394	19.55	2.57	0.05	2.5	5	3.125	50	16360
4-1	41698	114394	19.55	2.57	0.05	2.5	5	3.125	50	19950
7-7	47589	105000	19.888	2.83	0.056	2.29	3	0.461	49.5	76545
7-8	41020	78426	19.896	2.82	0.052	2.31	3	0.660	50	16575
3-7	10657	137173	20	1.375	0.049	0.803	5	0.875	30	27649
6-4	2381	324198	20.1	1.2	0.05	0.9	6	1	10	4086
6-5	2958	274752	30.1	1.325	0.05	0.9	6	1	10	6711

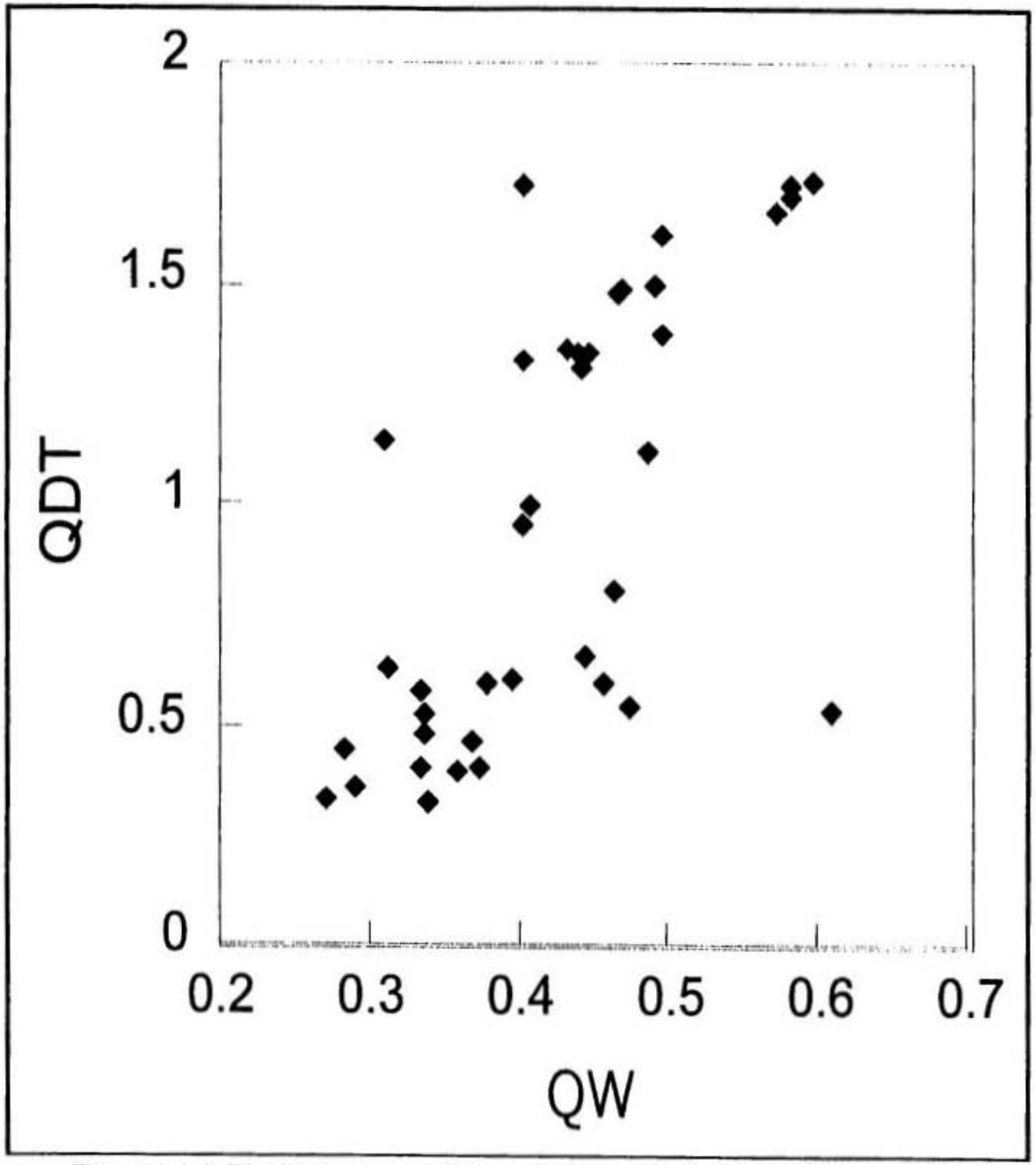

Figure 4.4-1, Distribution of Unreinforced Bellows Fatigue Tested Geometries

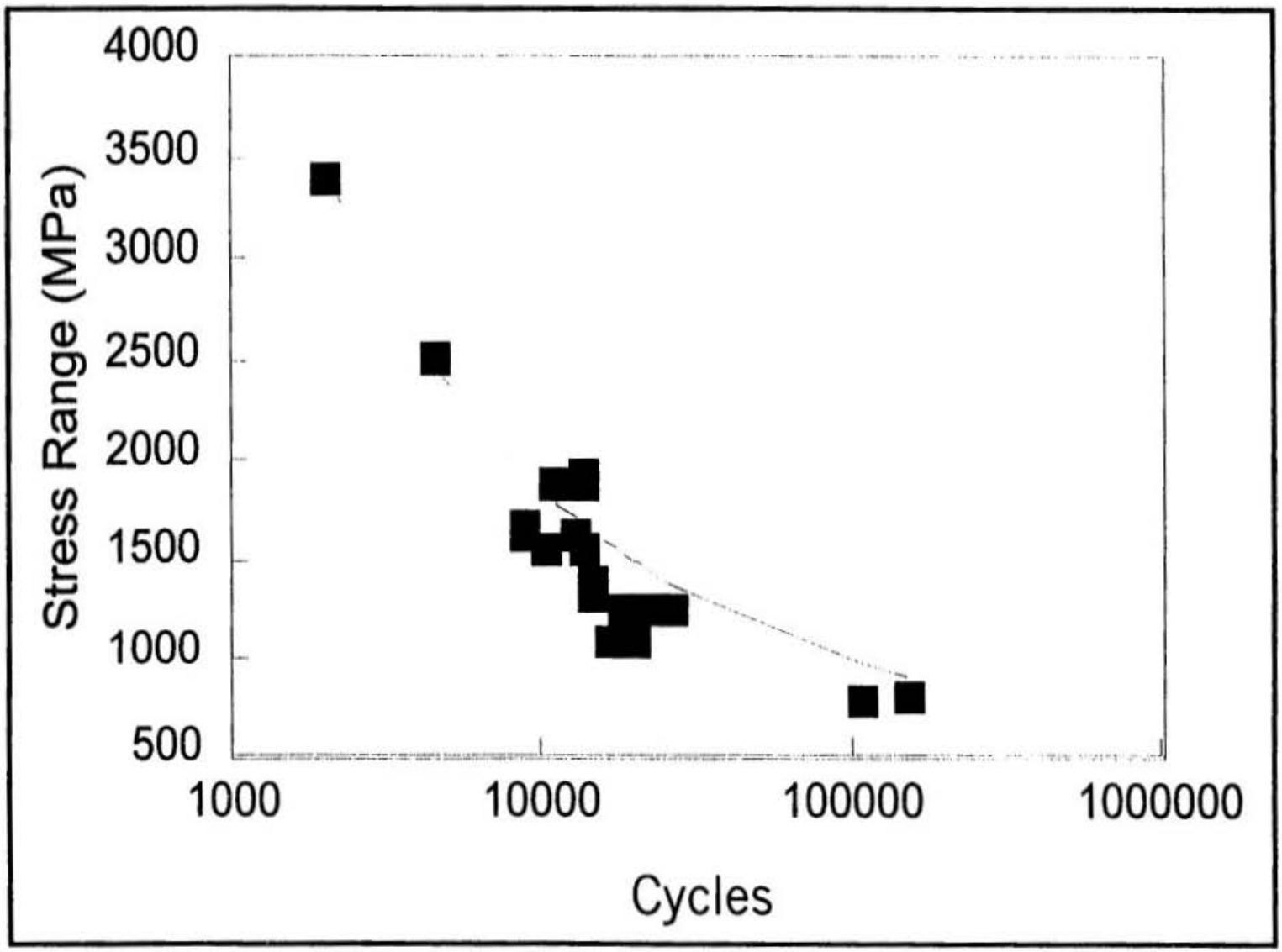

Figure 4.4-2, Unreinforced Fatigue Data (QW>0.45)

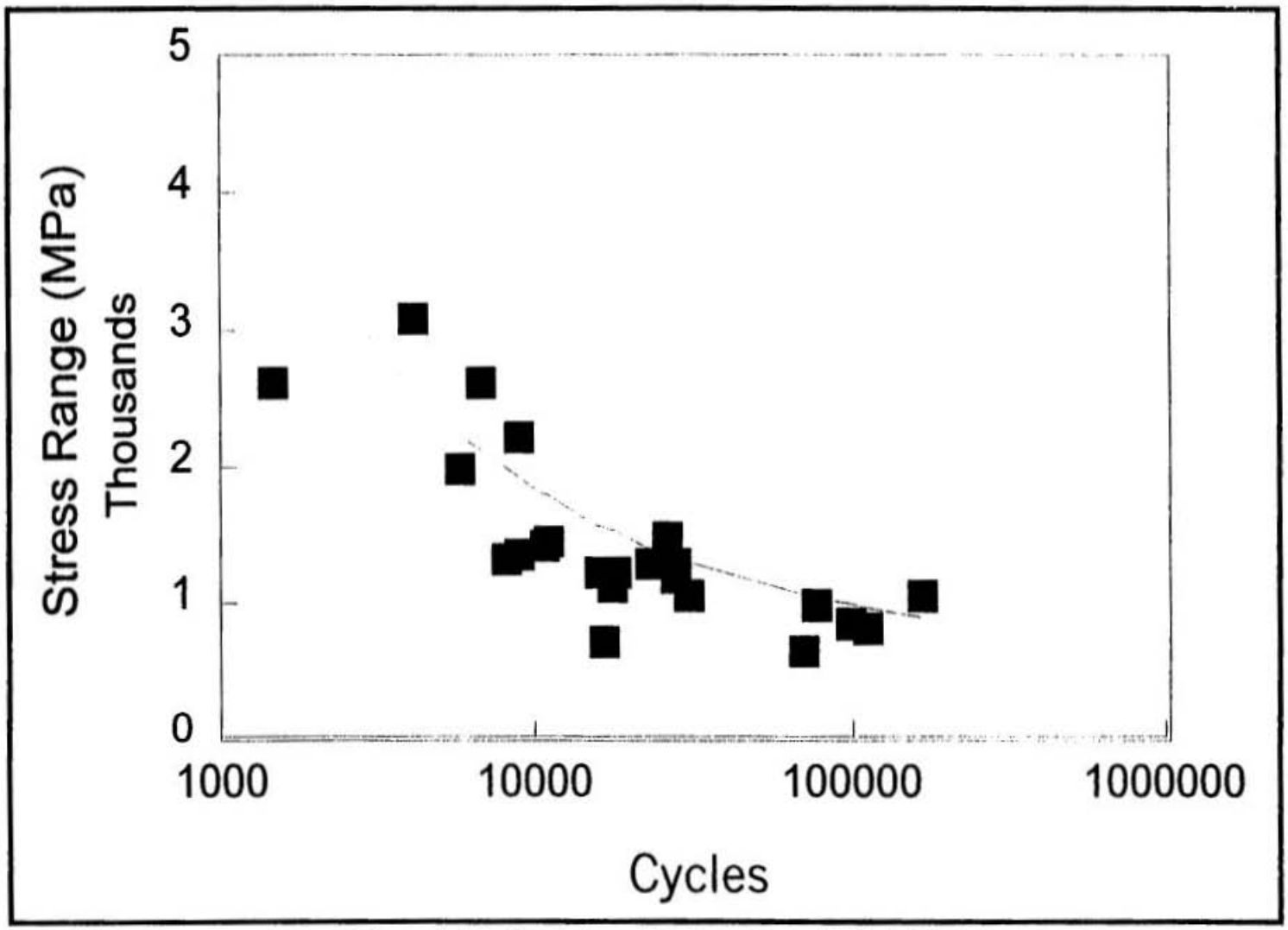

Figure 4.4-3, Unreinforced Fatigue Data (QW<0.45)

For QW>0.45, the fatigue data can be characterized by the polished bar fatigue curve. The factor of 1.4 is well within typical differences between component fatigue tests and polished bar fatigue tests and, more importantly, is consistent among all the bellows fatigue tests. In this regime, the fatigue behavior is now well understood. This will permit codes to make analogies between materials based on the polished bar fatigue curves for bellows with QW>0.45.

Since all bellows geometries are presently treated equally with respect to development of fatigue curves, it is clear that one could develop a higher fatigue curve by testing bellows with smaller convolution heights, higher values of QW, and by performing higher cycle fatigue testing (lower strain range so less strain concentration). This new knowledge of the effect of these factors on strain concentration and fatigue life should be used to critically evaluate future fatigue tests.

Development of bellows fatigue design methods and evaluation of bellows for fatigue should consider the impact of the convolution geometry on the difference between elastically calculated stress and actual strain range, considering plastic strain concentration.

4.5 Reinforced Bellows Model

A parametric finite element model of a reinforced bellows was prepared and run using the COSMOS/M finite element analysis program. The model was of a wedge section of the bellows with one element in the circumferential direction. The one element wedge was used rather than a two dimensional axisymmetric shell because the gap elements that were preferred to model the interface between the reinforcing ring and bellows convolution required use of the three dimensional model. These gap elements permit the nodes of the bellows to contact anywhere on a target surface, the reinforcing ring. While the model is a three dimensional wedge, the boundary conditions force the model to behave as an axisymmetric shell.

Both elastic and elastic-plastic analyses were run. Aside from plasticity, the nonlinear features that were included were gap elements to model the interaction between the bellows sidewalls and the reinforcing ring, and large displacement theory. Cases with elastic plastic material properties with kinematic hardening were run to investigate post-yield behavior and its effect on the nonlinear interaction between the convolutions and the reinforcing rings, and to evaluate plastic strain concentration.

Only one half of a convolution was modeled, considering symmetry, because of the greater demands of the nonlinear analysis on computer resources. The ring was

modeled using eight node solid elements and the convolution was modeled using four node shell elements. A wedge section, one element wide was modeled, with symmetry boundary conditions on all sides of the model, as illustrated in Figure 4.5-1.

The convolution was partitioned, in the general case, into four segments for modeling purposes. These included one half of the root; a portion of the sidewall equal to about 3/4 the toroid meridional radius or the full length of the sidewall, whichever was less; the remainder of the sidewall (if any); and one half of the crown of the convolution. The model was constructed so that the meridional length of the sidewall elements were the same as in the toroidal segments.

The ring was partitioned into six sections, each of which was meshed in an array with solid elements. Eight node and twenty node solid elements were evaluated.

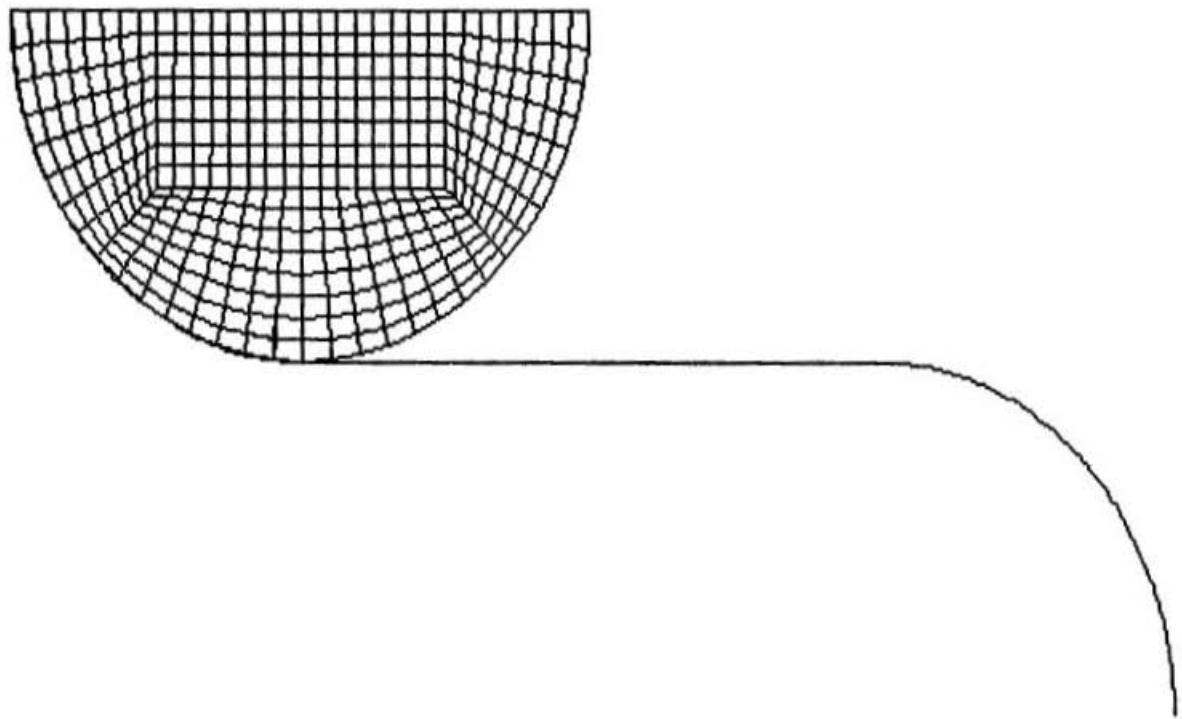

Figure 4.5-1, Reinforced Bellows Model

Gap elements were included between the root toroid and the inner section of the sidewall, and the ring. The gaps were located at the nodes of the bellows and the ring was specified as the target surface. The convolution could therefore contact any portion of the reinforcing ring perimeter. An initial gap of 0.025 mm (0.001 inch) was assumed between the convolution and the reinforcing ring to keep the shell and solid nodes separate.

To model the shell, the SHELL4 (except for elastic-plastic in which SHELL4T was used) element was used, which is a four-noded quadrilateral shell element with six degrees of freedom per node. Shear deformation is neglected for SHELL4, which is a thin shell element. Eight noded isoparametric solid elements (SOLID) were used to model the ring. Single node gap elements (GAP), without friction, were used to model the interaction between the shell and the reinforcing rings. The gap elements were applied to the bellows nodes and the reinforcing ring was specified as the target surface.

Figure 4.5-2 illustrates the various meshes considered with the reinforcing rings. Figure 4.5-3 compares analyses of bellows extension and compression with different mesh densities. Figure 4.5-4 compares analyses of a bellows subjected to internal pressure with different mesh densities.

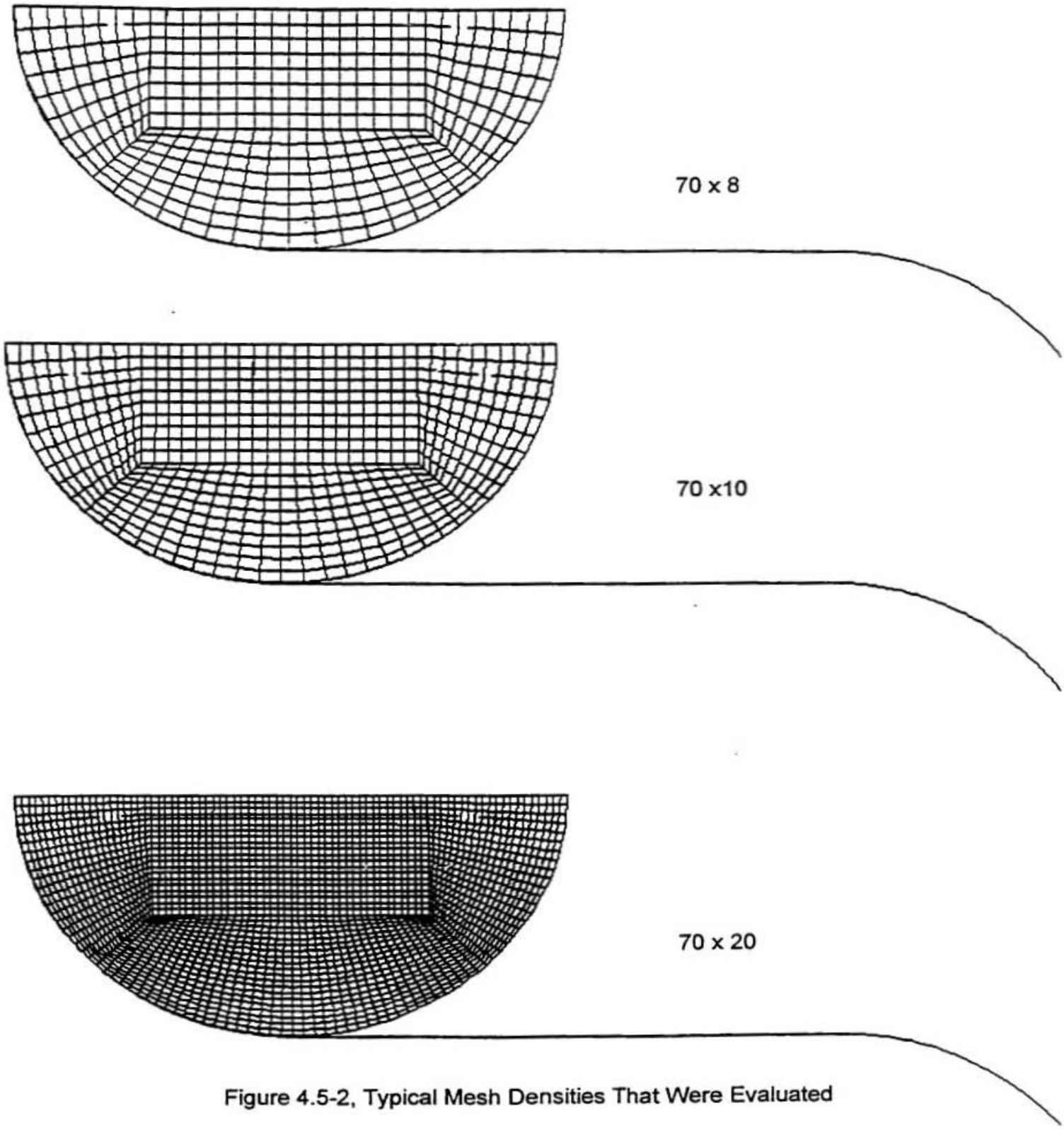

Figure 4.5-2, Typical Mesh Densities That Were Evaluated

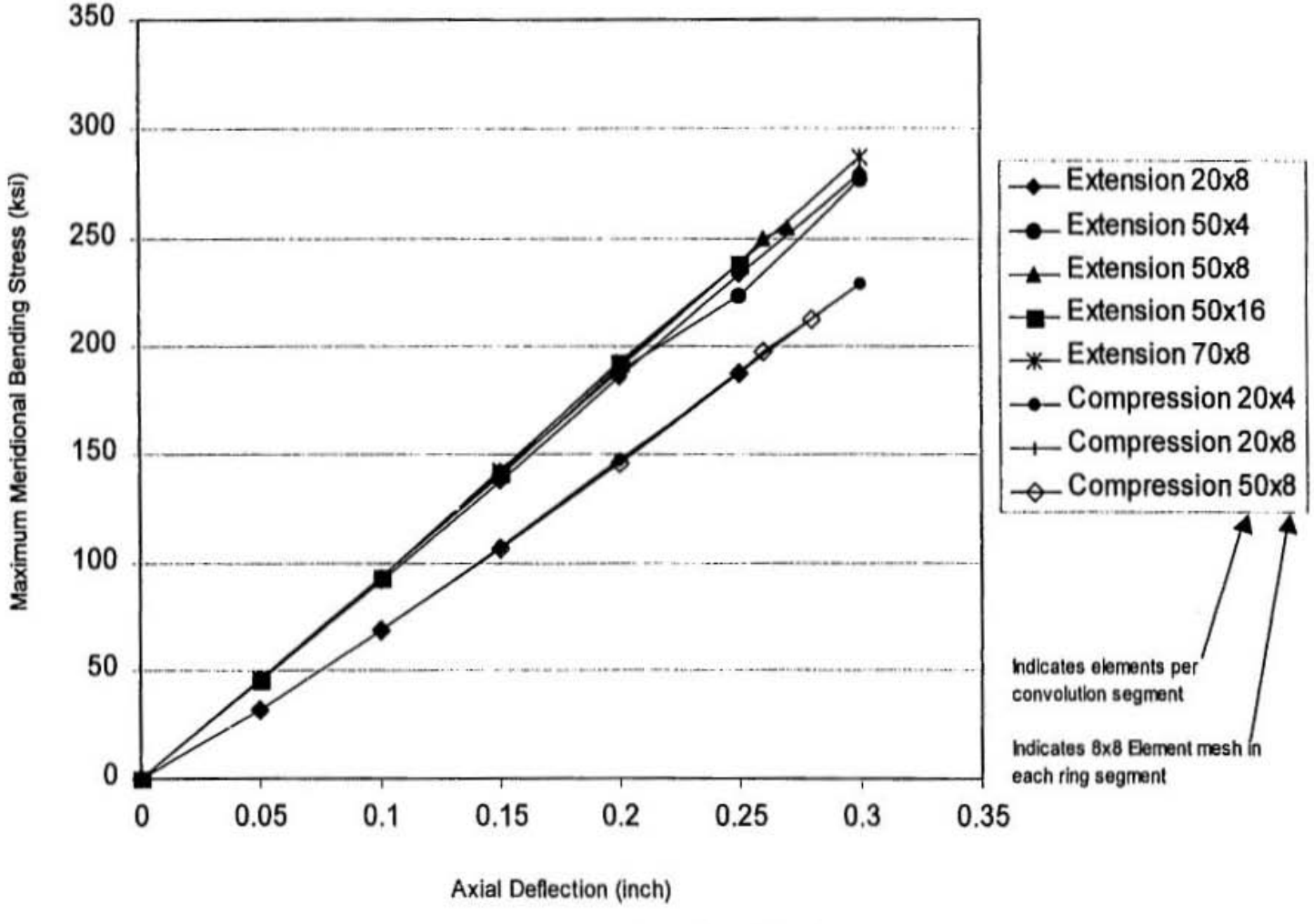

Figure 4.5-3, Convergence Check for Displacement Loading

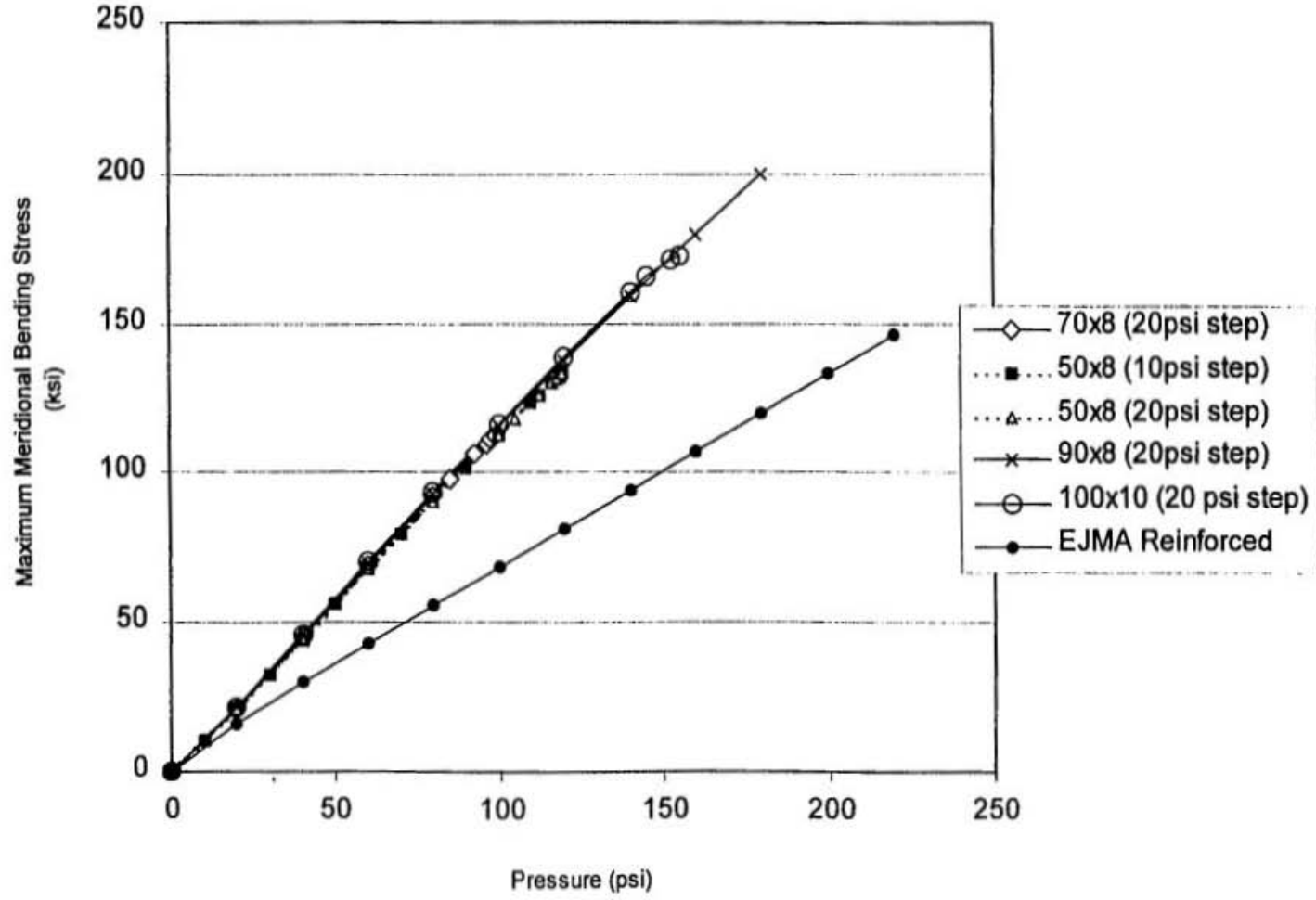

Figure 4.5-4, Convergence Check for Pressure Loading

Based on these results, 90 shell elements per half toroid and the 8x8 solid element mesh using eight node solids (for each section of the ring) were selected for further analysis.

4.6 Elastic Analysis of Reinforced Bellows

Some salient points of behavior are illustrated by a detailed elastic (large displacement with gap elements) investigation of reinforced bellows. The application of reinforced bellows tends to be for a narrower range of geometries than for unreinforced bellows. This is because higher values of QW (shallower convolutions) would be very stiff with reinforcing rings. Further, since reinforced bellows are used for high pressure, deep convolutions, low values of QW, are not appropriate.

Cases with internal pressure were evaluated for various values of QW and QDT. For these analysis, D_m and t_p where held constant at 610 mm (24 inch) and 0.51mm (0.02 inch), respectively. The reinforcing ring is considered to reduce the meridional bending stress relative to unreinforced bellows because it reduces the effective convolution height. Meridional bending stress due to pressure is plotted versus pressure in Figures 4.6-1 through 4.6-5. They are compared to the EJMA predictions of meridional bending stress in unreinforced bellows and reinforced bellows. These figures show that the pressure-stress relationship is nonlinear. This is because the convolution wraps around the ring, changing the outermost contact

point. This decreases the ratio of meridional bending stress to pressure as the pressure is increased.

The stress calculated via finite element analysis is generally bounded by the EJMA equations for reinforced and unreinforced bellows. At higher pressures, the finite element results tend to approach the stresses predicted by the EJMA equation for reinforced bellows. This generally indicates that the EJMA equation tends to under predict the pressure induced meridional bending stresses in reinforced bellows. Note, however, that the calculated stress for QW=0.5, which is in the range of typical reinforced bellows geometries, that the prediction of the EJMA equation is in good agreement with the finite element analysis results.

Prior to initiating substantive work on improving the prediction of meridional bending stress due to pressure, a better understanding of the mechanism of failure of reinforced bellows due to pressure should be developed, as was done for unreinforced bellows by Becht (1980, 1981a). This is an appropriate area for future research, and not the subject of the present research.

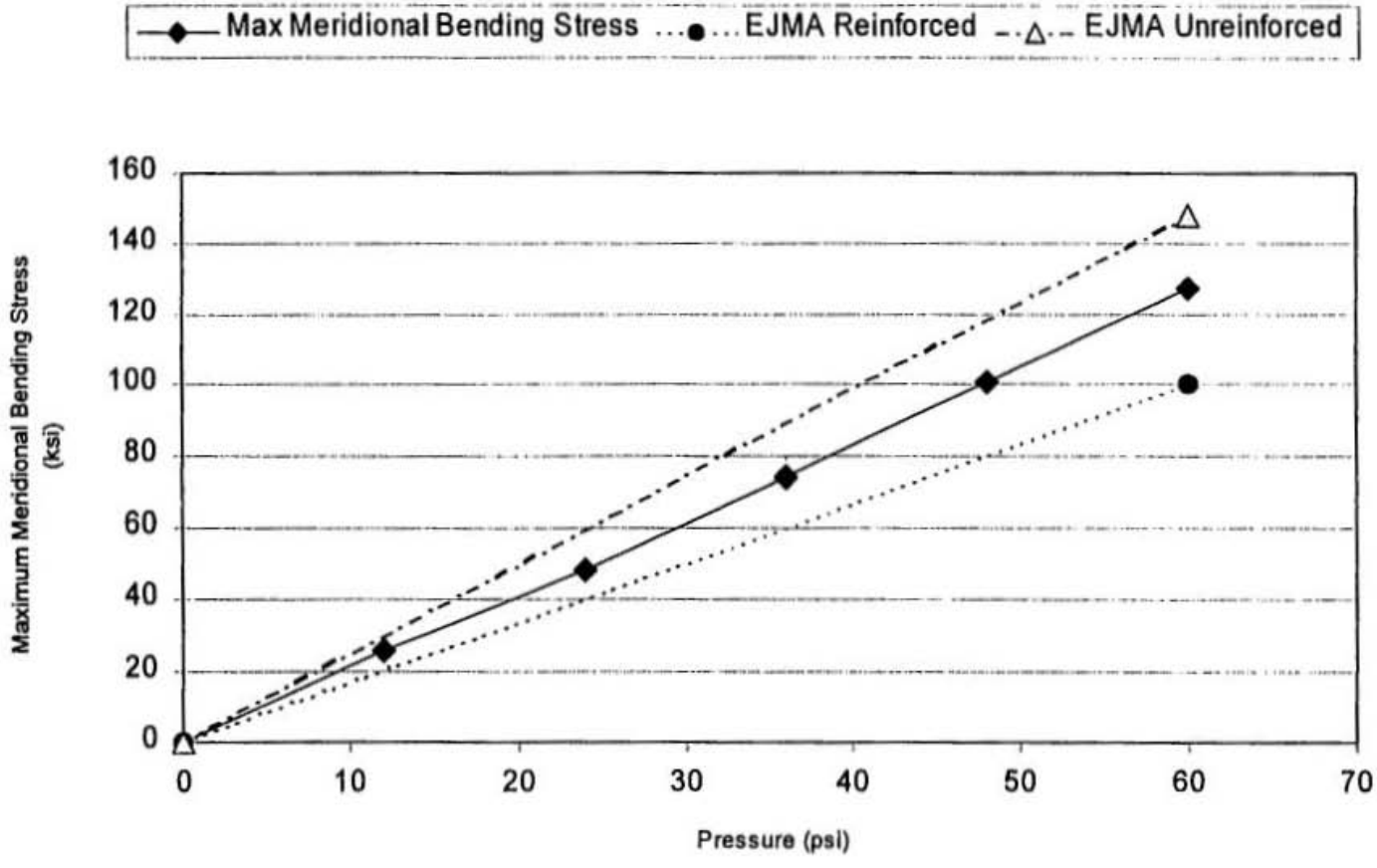

Figure 4.6-1, Meridional Bending Stress vs. Pressure (QW=0.2, QDT=0.4)

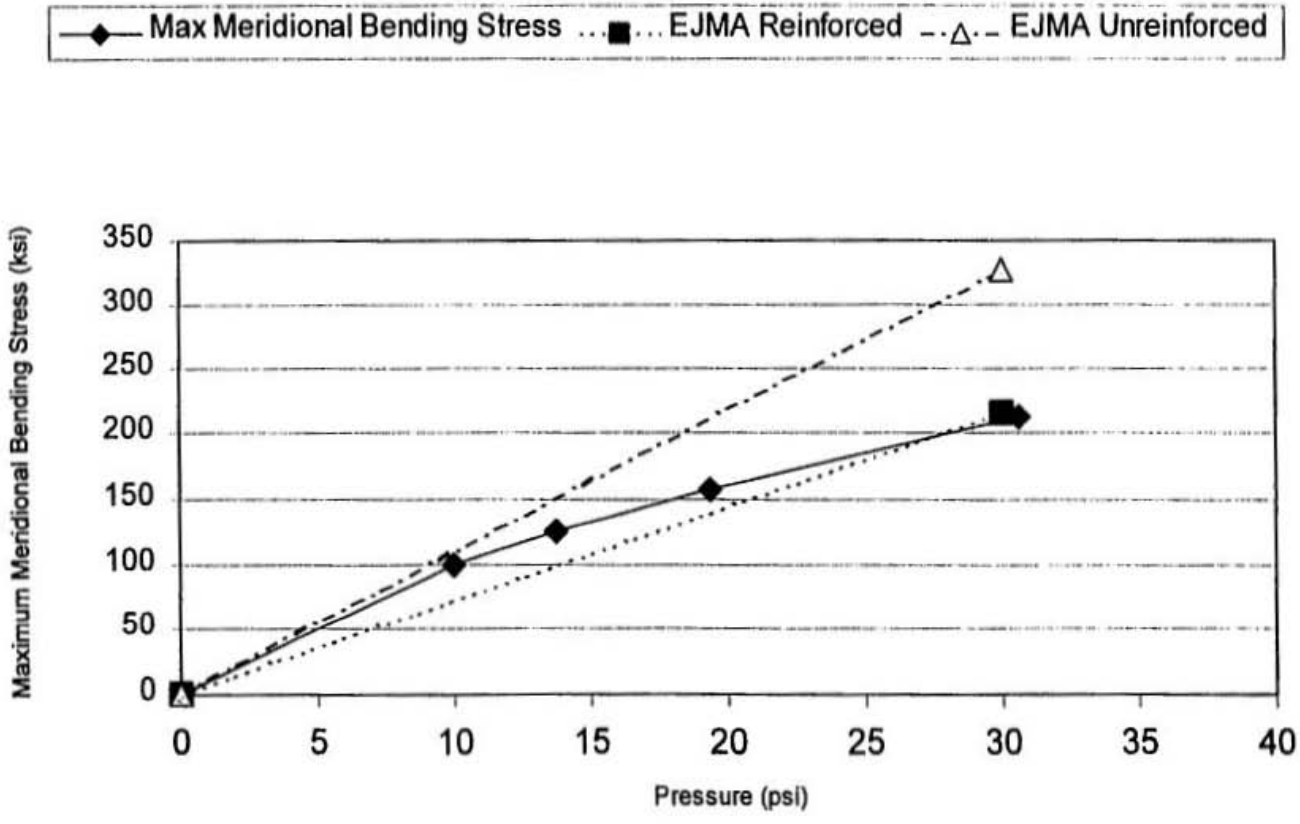

Figure 4.6-2, Meridional Bending Stress vs. Pressure (QW=0.2, QDT=1.0)

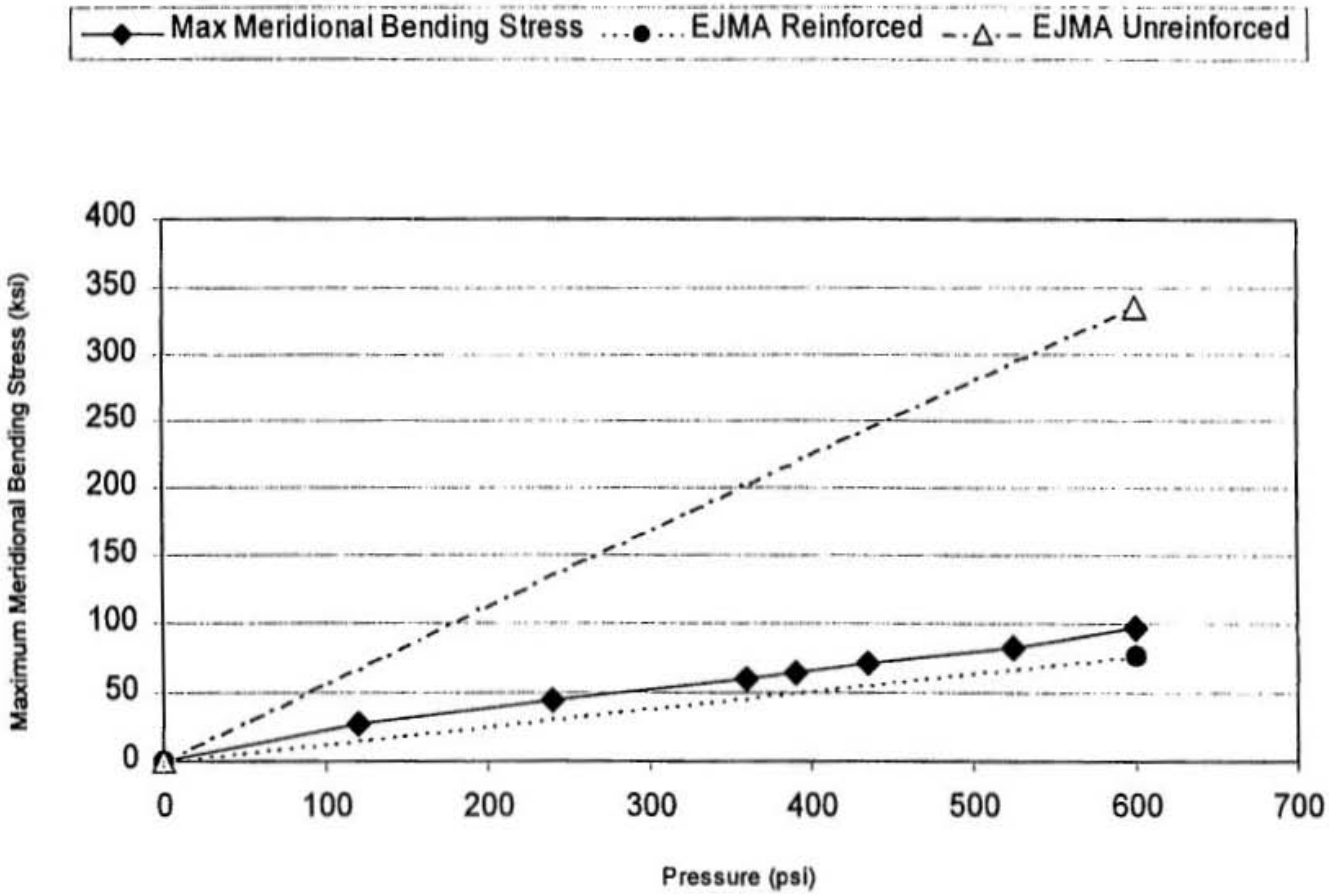

Figure 4.6-3, Meridional Bending Stress vs. Pressure (QW=0.5, QDT=0.4)

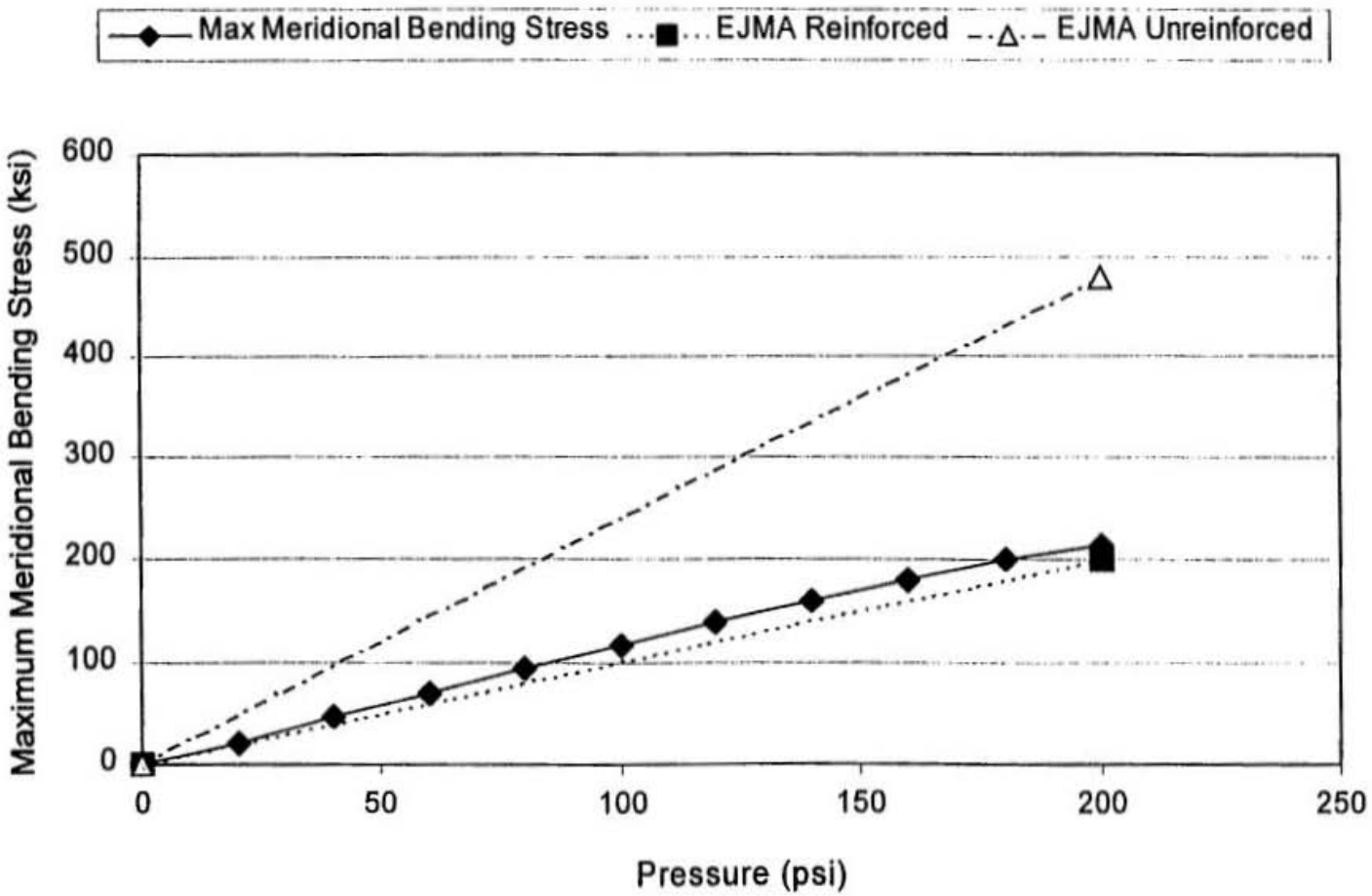

Figure 4.6-4, Meridional Bending Stress vs. Pressure (QW=0.5, QDT=1.0)

157

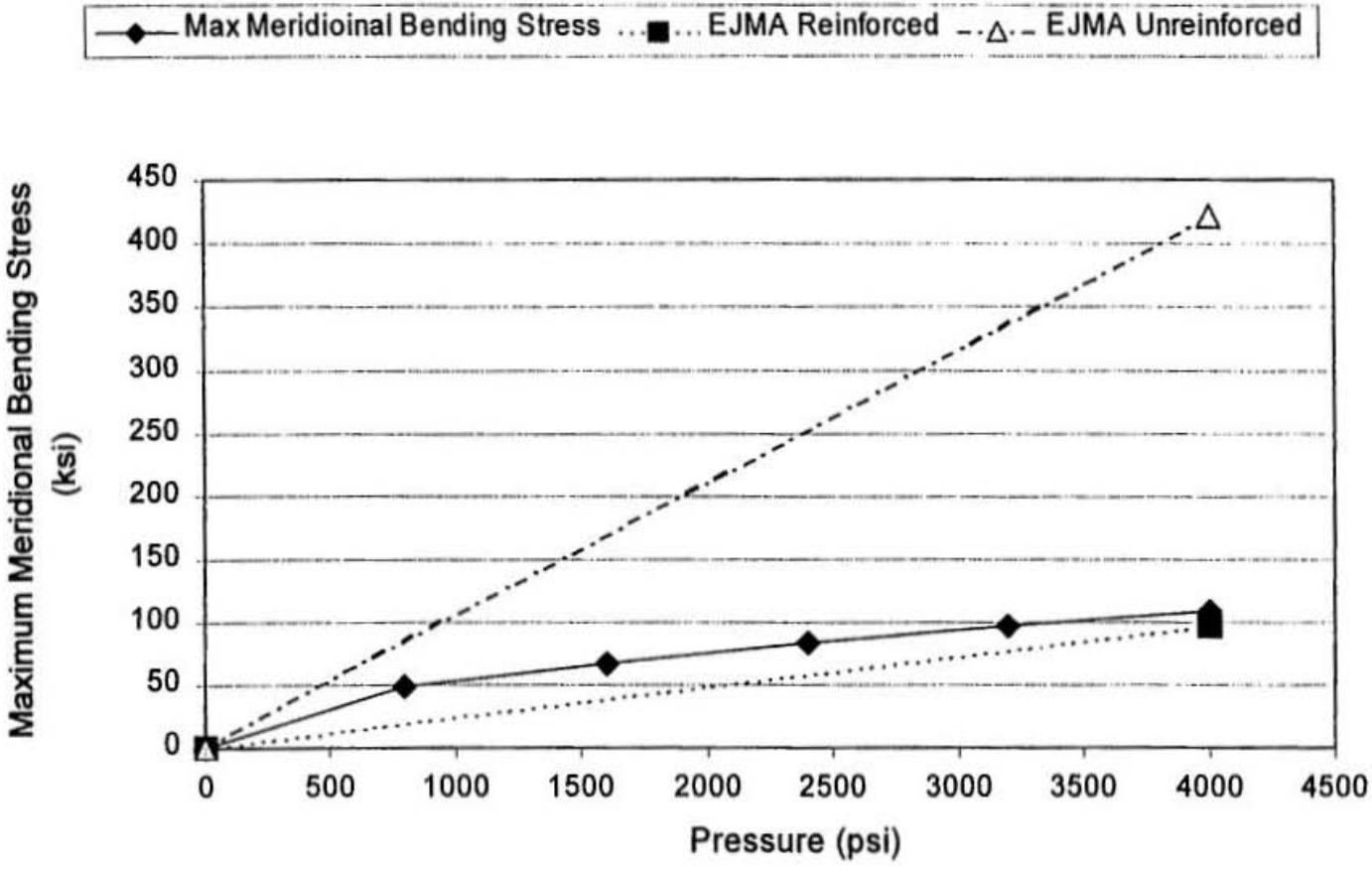

Figure 4.6-5, Meridional Bending Stress vs. Pressure (QW=0.8, QDT=0.4)

With respect to displacement, a significant consideration is that the elastically calculated meridional bending stress in a reinforced bellows significantly differs between when the bellows is compressed and when it is stretched. The reinforcing ring enhances the stress more in the compression mode due to the greater interference between the ring and the bellows convolution. Figure 4.6-6 shows the meridional bending stress for the bellows illustrated in Figure 4.5-1 with the bellows compressed and extended. Also plotted, for comparison purposes, are the stresses predicted in accordance with the EJMA equations for reinforced and unreinforced bellows.

Another item of note is the relative linearity of the stress-displacement curve. While the location of highest stress shifts slightly as the contact point between the bellows convolution and the reinforcing ring moves, the maximum stress versus displacement remains relatively linear.

A further point to explore is the effect of internal pressure on stress due to deflection. Internal pressure is considered in the EJMA equations to increase the stress due to deflection. It is considered to increase the interaction between the convolution and the reinforcing ring.

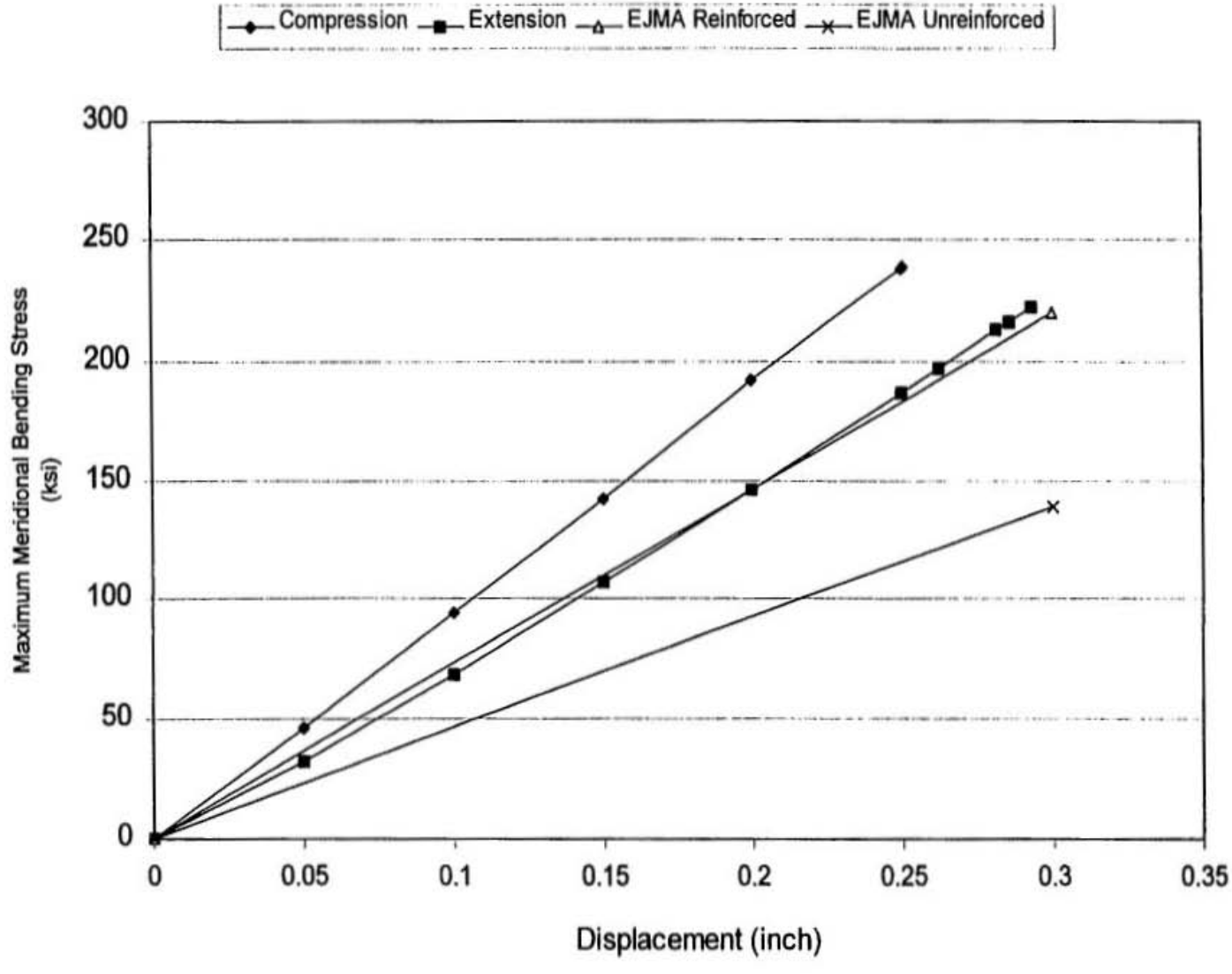

Figure 4.6-6, Meridional Bending Stress vs. Displacement (QW=0.5, QDT=1.0)

Finite element analyses with both pressure and deflection were run for a bellows with QW=0.5 and QDT=1.0. In these cases, the internal pressure was first applied, and then the deflection. When the bellows is compressed, there was very little effect of internal pressure on the deflection stress. This is shown in Figure 4.6-7, which plots stress versus compressive deflection (per half convolution) for four different internal pressures, 0 kPa, 345 kPa, 690 kPa and 1000 kPa (0 psi, 50 psi, 100 psi and 150 psi). The lines are parallel, indicating that there is negligible effect of internal pressure on deflection stress due to compression. Note that this is consistent with the linearity of the stress displacement analysis. The slight movement of the contact point due to internal pressure does not significantly affect the bending stress due to displacement. This conclusion is also valid for deeper convolution bellows, QW<0.5, because the effect of the reinforcing ring on deflection stress decreases with increasing convolution depth. Reinforced bellows are not generally manufactured with QW>0.5, so that case need not be considered. Note that for the case of compression with this bellows geometry, the meridional bending stress due to internal pressure is additive to the deflection stress at the location of highest deflection stress, the outer contact point between the convolution and the reinforcing ring.

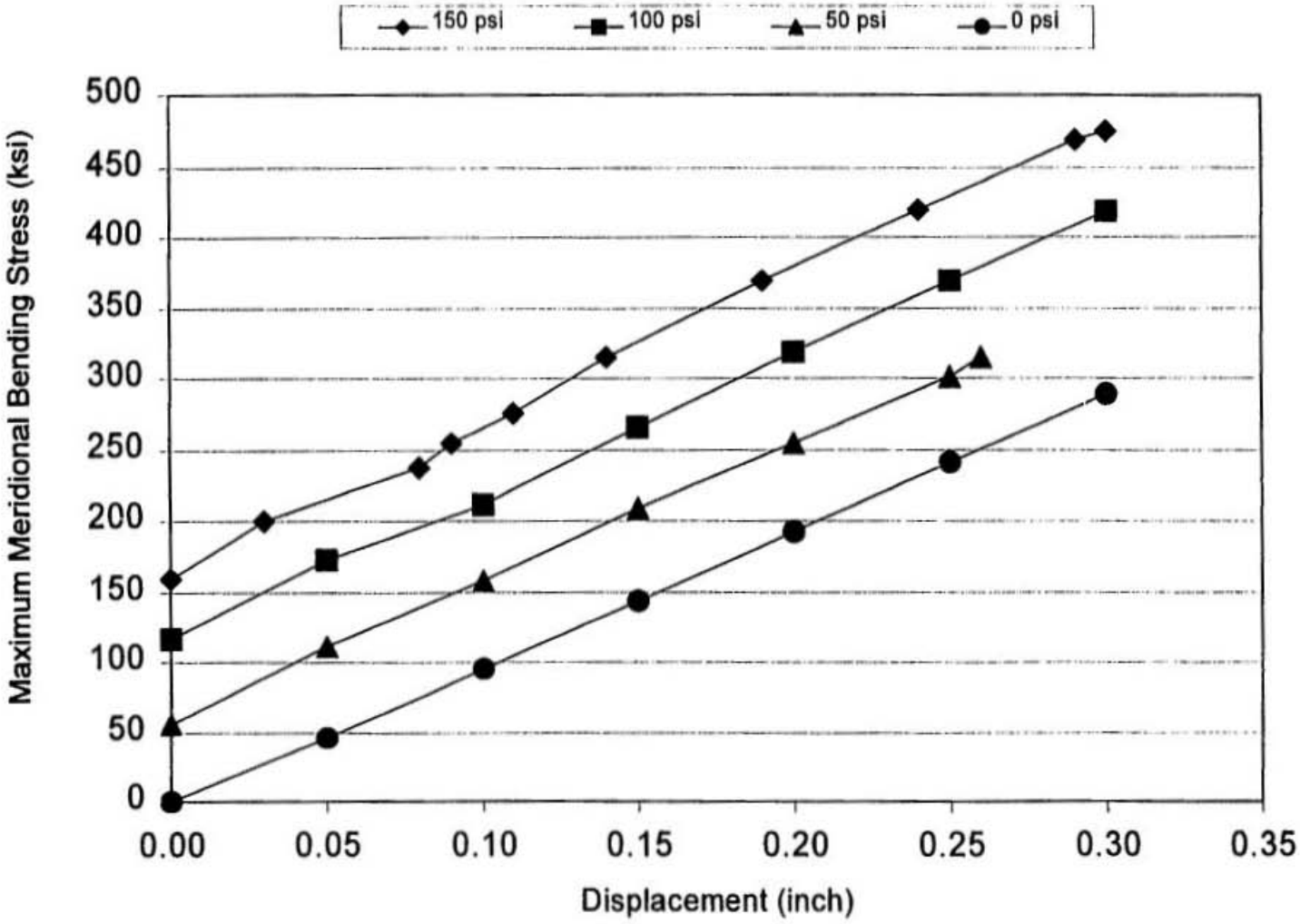

Figure 4.6-7, Meridional Bending Stress for Pressure + Compressive Displacement

The case of bellows extension differs. The pressure stress and deflection stress are of opposite sign at the location of greatest deflection stress. Therefore, application of deflection causes an initial reduction in the maximum value of meridional bending stress in the convolution, until such time as the stress in the crown (at which the pressure and deflection meridional bending stresses are additive) becomes the largest value. Therefore, as shown in Figure 4.6-8, the maximum meridional bending stress decreases with the application of bellows extension, and then increases.

These charts indicate that the presence of pressure in a bellows does not significantly increase the meridional bending stress due to displacement. In Section 4.8, the effect of removing the pressure term from the EJMA equation for displacement stress when evaluating bellows fatigue data is shown.

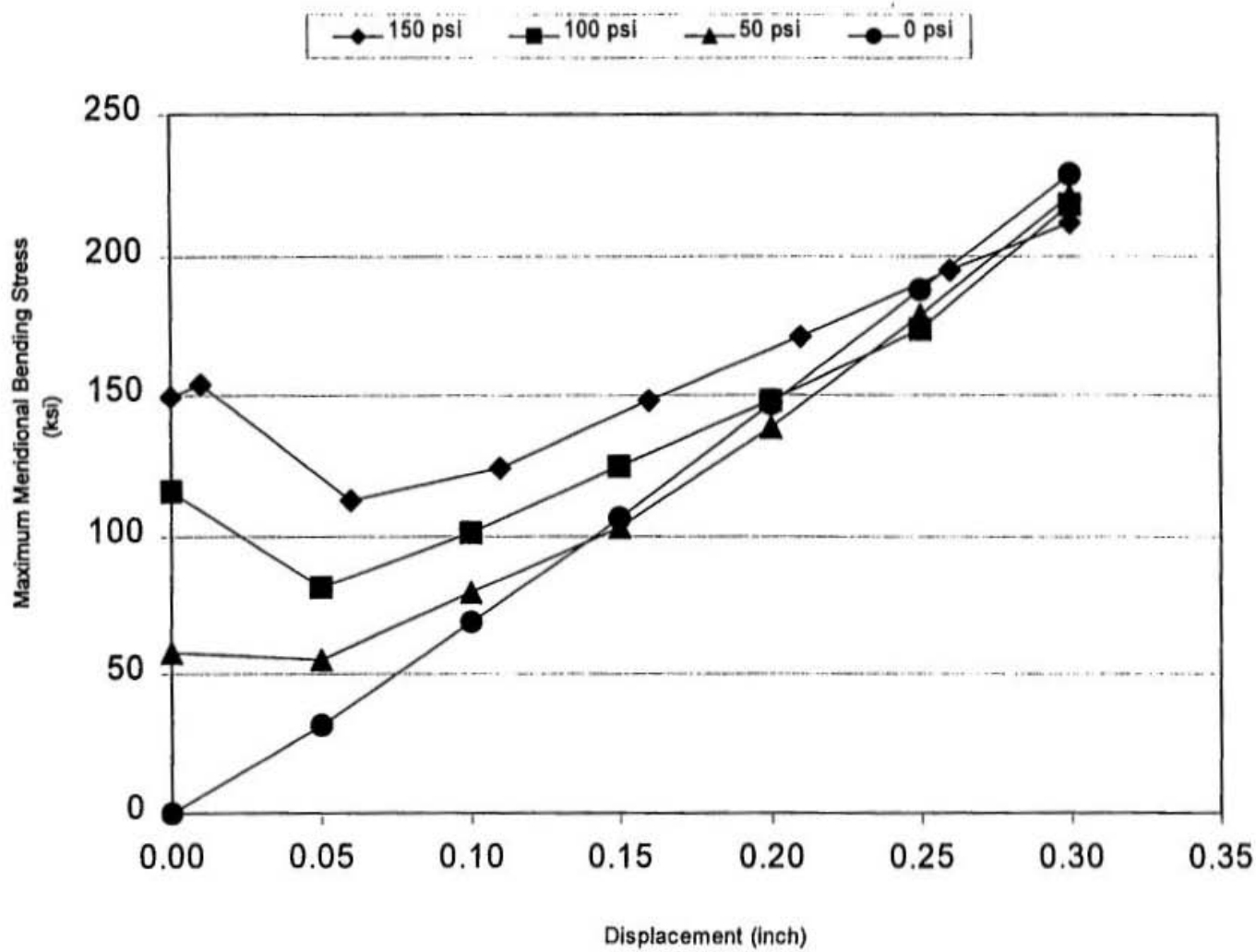

Figure 4.6-8, Meridional Bending Stress for Pressure + Tensile Displacement

Stress distributions based on elastic analysis for displacement loads are shown in Figures 4.6-9 through 4.6-14, for both opening and closing displacements. The stresses are plotted versus the meridional dimension of the bellows, starting at the crown at the origin and moving towards the root, to the right along the axis. The junction between the root and crown toroids and the sidewalls are shown as dashed lines. It can be observed that based on elastic analysis, a sharp peak of the meridional bending stress occurs at the outermost contact point between the convolution and ring when the bellows is subject to closing displacement. When the bellows is subject to opening displacement, a peak also occurs near the junction between the toroidal portion and sidewall at the ring, but is more gradual.

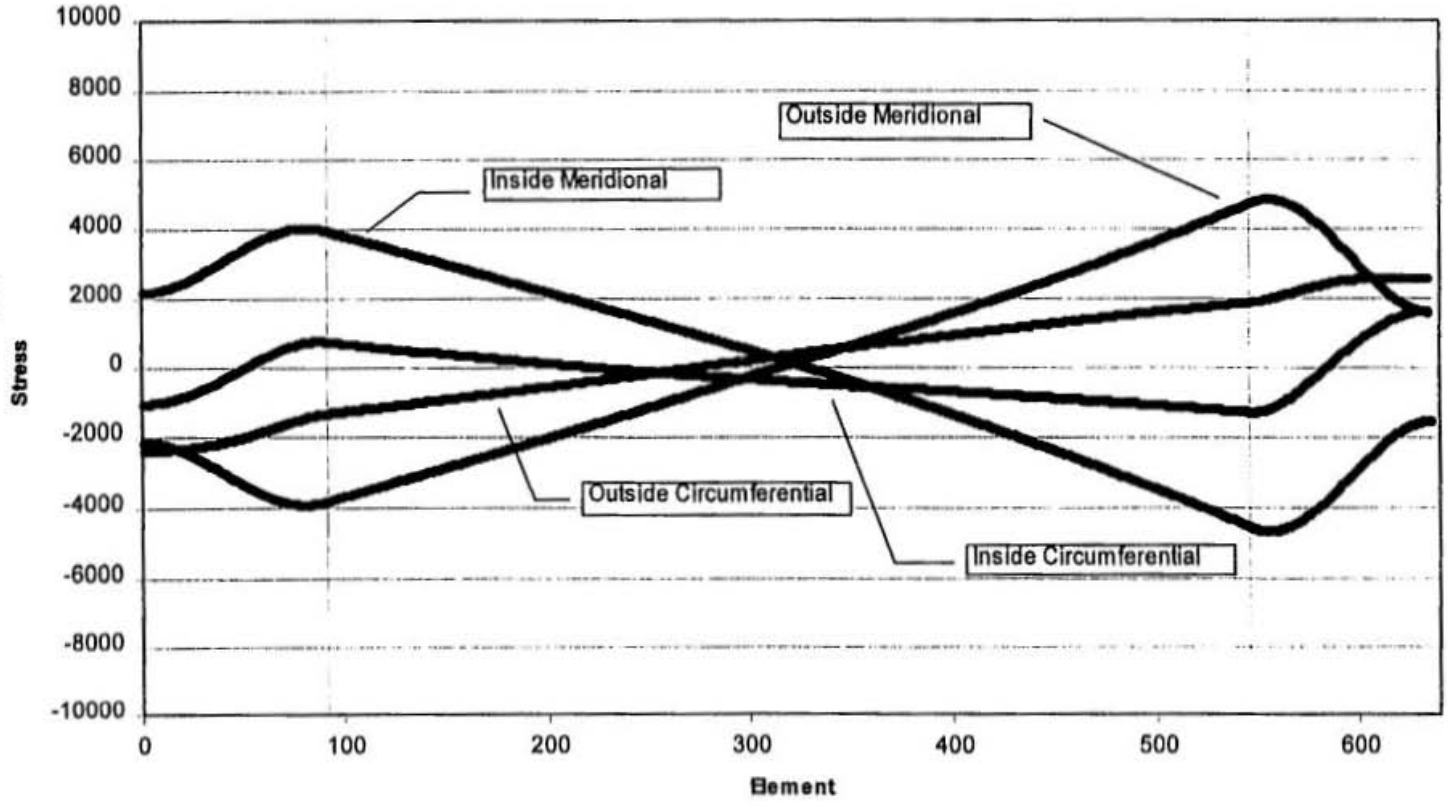

Figure 4.6-9, Surface Stress Due to Extension (QW=0.2, QDT=1.0)

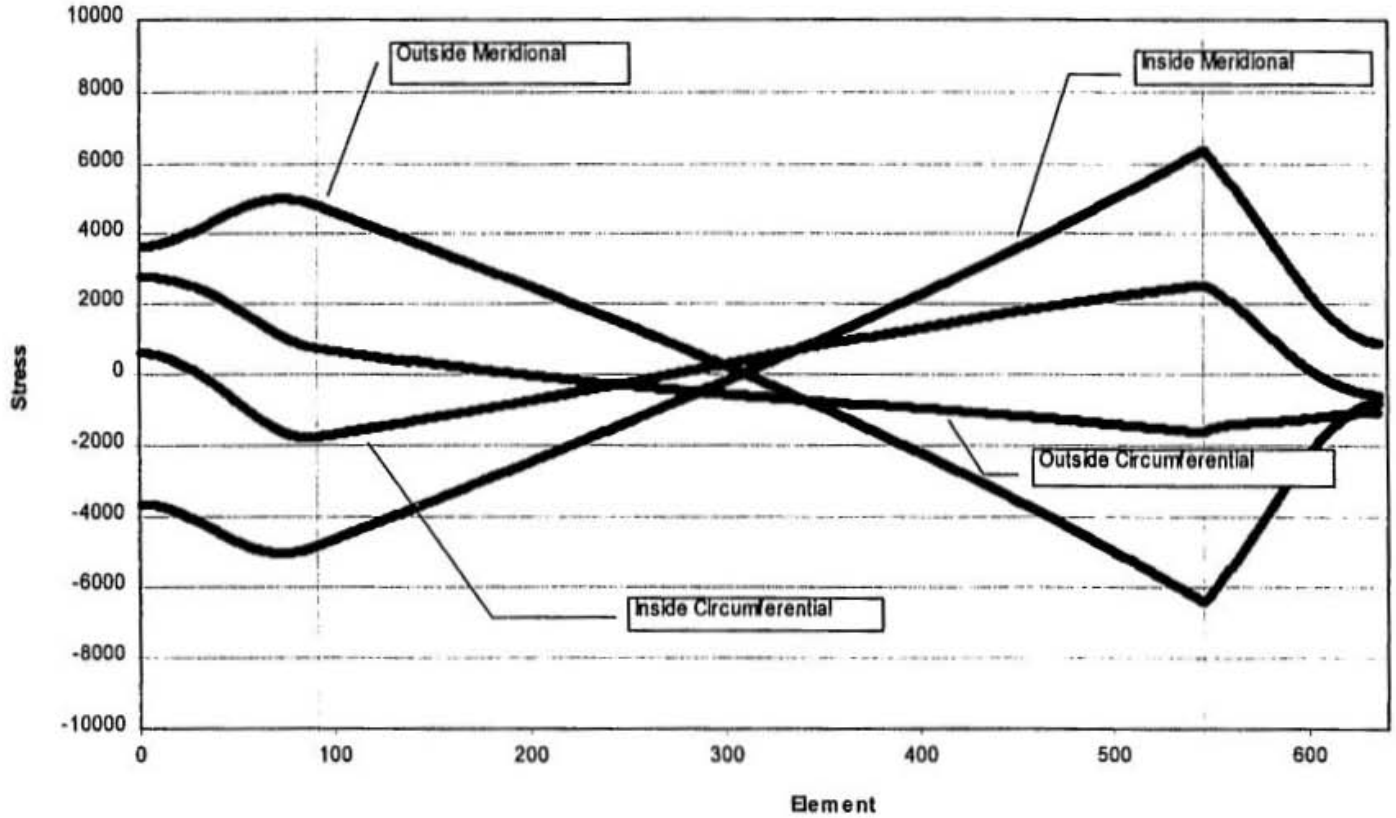

Figure 4.6-10, Surface Stress Due to Compression (QW=0.2, QDT=1.0)

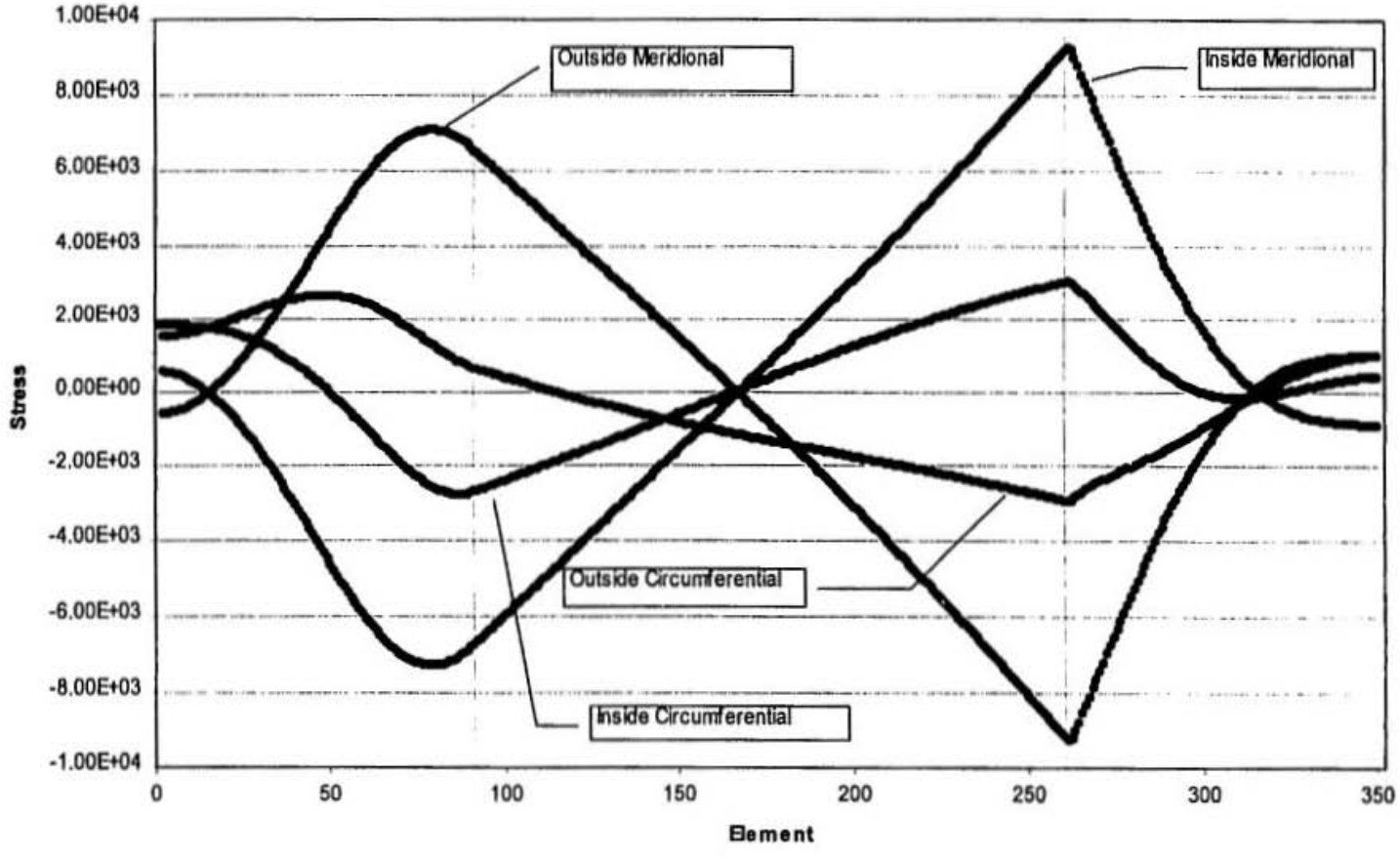

Figure 4.6-11, Surface Stress Due to Compression (QW=0.4, QDT=2.0)

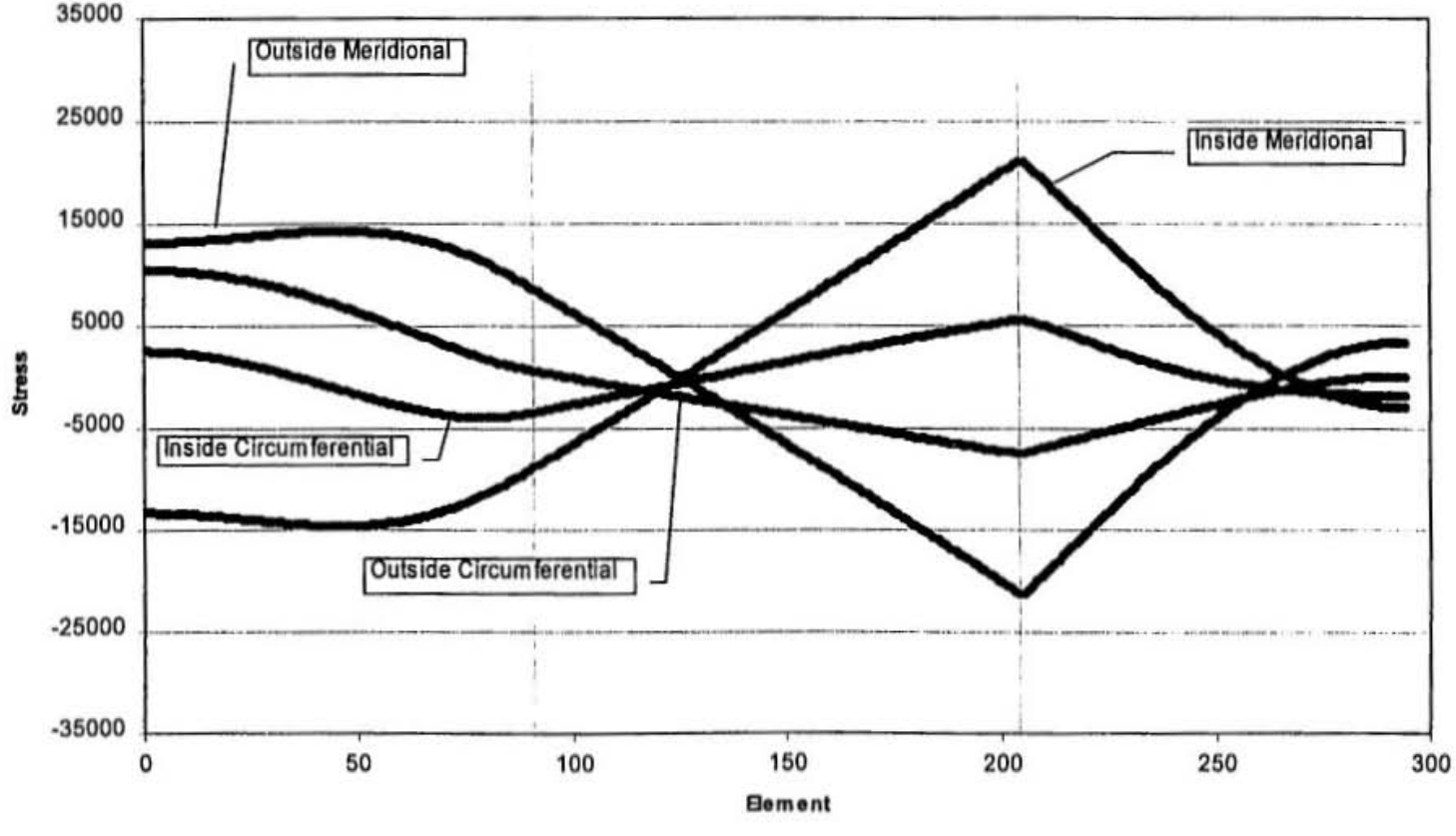

Figure 4.6-12, Surface Stress Due to Compression (QW=0.5, QDT=1.0)

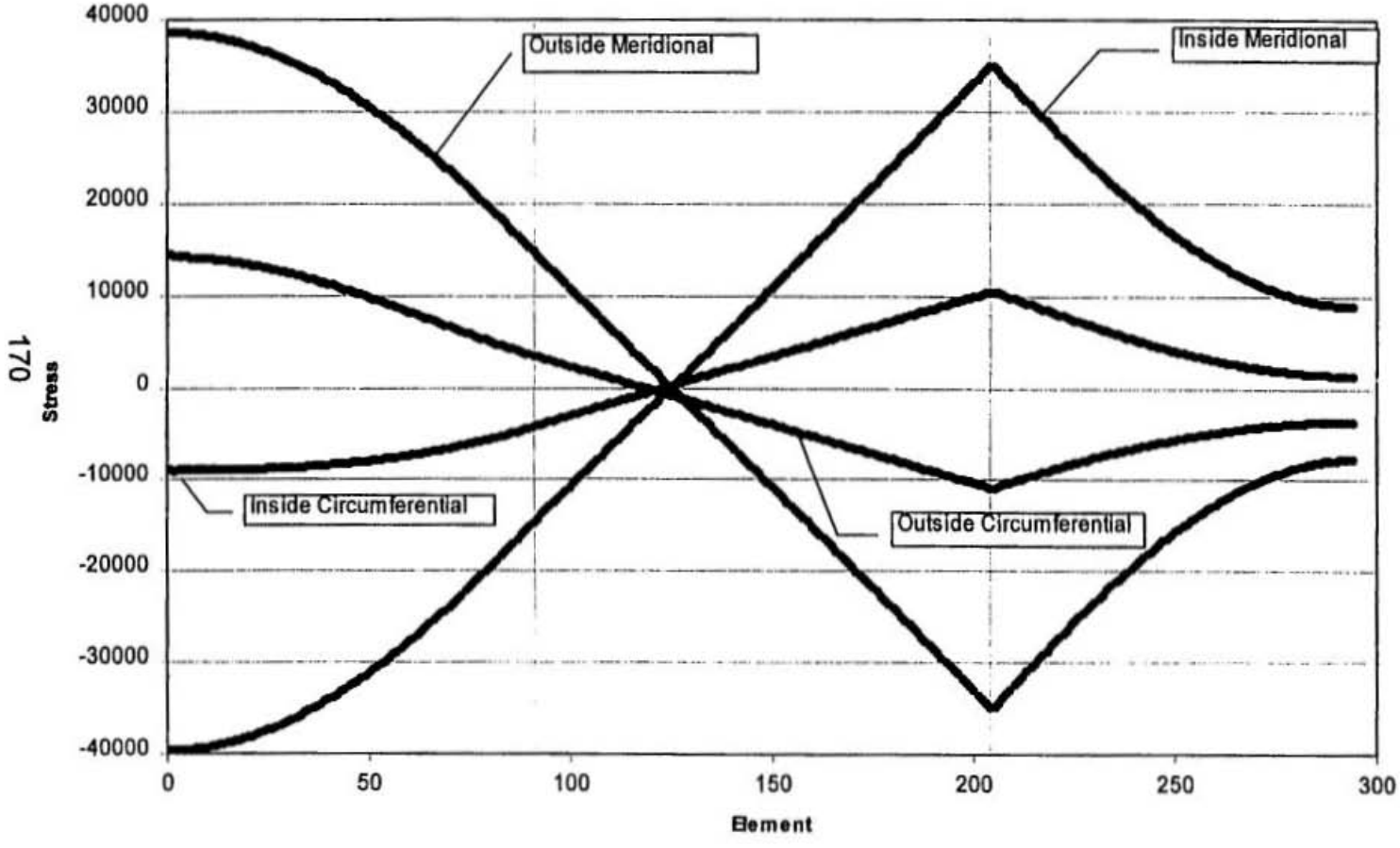

Figure 4.6-13, Surface Stress Due to Compression (QW=0.5, QDT=0.4)

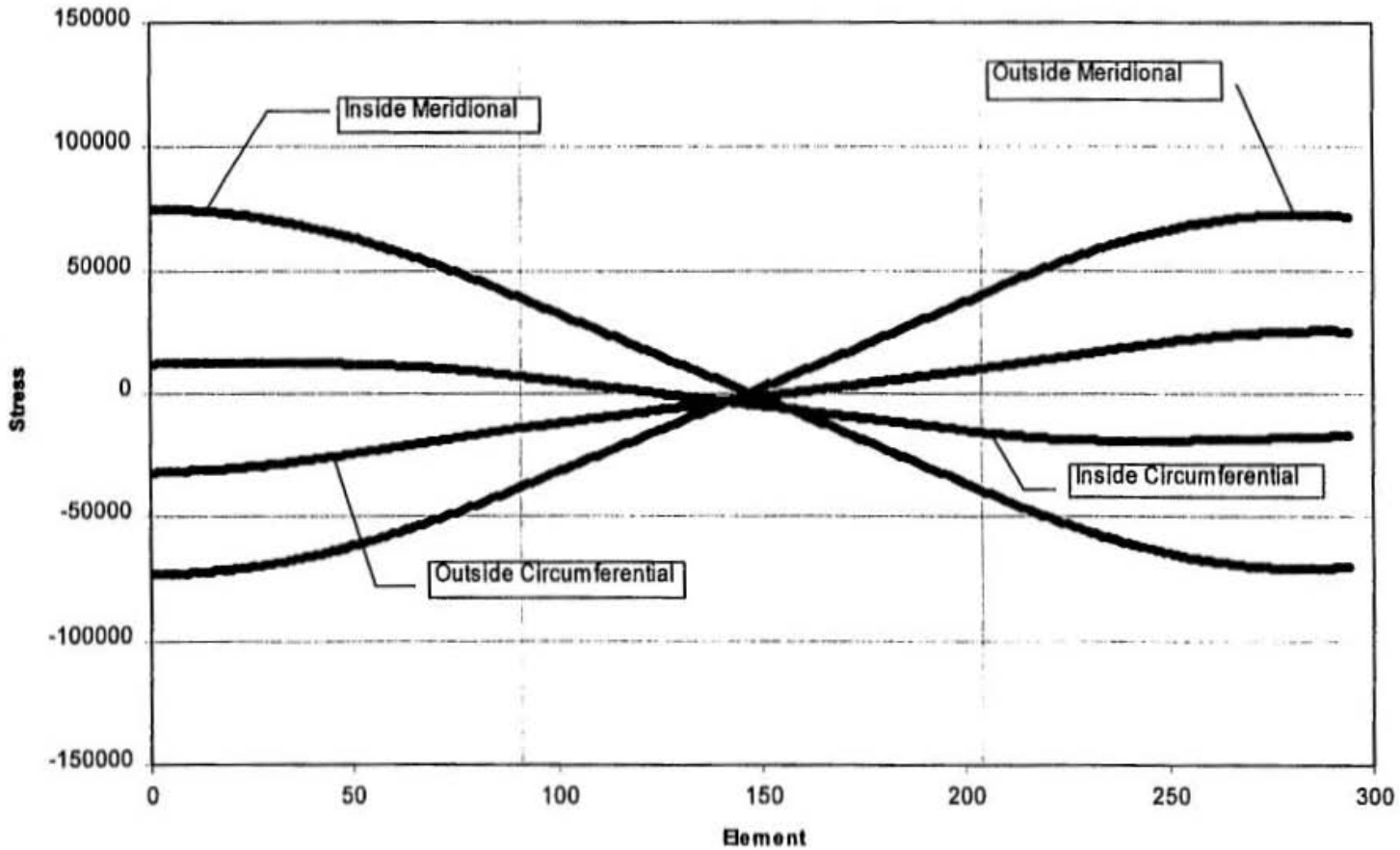

Figure 4.6-14, Surface Stress Due to Extension (QW=0.5, QDT=0.4)

4.7 Inelastic Evaluations of Reinforced Bellows

The elastic-plastic response of reinforced bellows was evaluated. The same material properties as were used in the inelastic analysis of unreinforced bellows, described in Section 4.3, were used.

Considering inelastic behavior, and the fact that bellows are usually cycled well beyond yield, compression would cause permanent deformation, wrapping the convolution around the ring. When the bellows is returned to the original, neutral position, the sidewalls can be pulled off of the reinforcing ring. If this occurs, the strain range due to compressive displacement cycling, after the first cycle, could be more analogous to the tensile displacement loading case. This hypothesis was investigated using elastic-plastic finite element analysis.

The same model as was used with the elastic analysis, but with elastic plastic material properties (207 MPa (30,000 psi) yield strength, 207,000 MPa (30,000,000 psi) elastic modulus, 20,700 MPa (3,000,000 psi) tangent modulus, kinematic hardening) was run through a deflection cycle from zero to 7.6 mm (0.3 inch) compression (for the ½ convolution), back to zero, and again to 7.6 mm (0.3 inch) compression.

Figures 4.7-1 through 4.7-3 show plots of the displacement of the bellows at various steps in the analysis. The deflection scale factor is one, which means that the

deflections are in scale with the geometry of the model. Note that when the bellows is returned to zero displacement, the convolution is pulled away from the ring due to permanent distortion resulting from plasticity.

Figure 4.7-4 plots the meridional bending strain versus displacement for the analysis. The strain range is dramatically reduced after the first cycle due to the permanent distortion of the convolution. Comparison with the elastic opening and closing cases illustrated in Figure 4.6-6 shows that the strain range for the final half cycle was closer to the elastic analysis of opening displacement.

A number of inelastic cases were run to evaluate plastic strain concentration in reinforced bellows. The same as for reinforced bellows, the finite element models were run through 1-1/2 cycles of displacement. The meridional bending strain range for the last ½ cycle was compared to the maximum strain range calculated in an elastic analysis for the same displacement, using the same model, but assuming elastic material properties. Note that in this case, strain concentration can be based on a ratio of strains in two different locations. This is because, due to the nonlinear behavior of reinforced bellows, the maximum elastic-plastic strain for the third half cycle occurs for some geometries at a different location than the maximum elastically calculated strain. This is due to the reshaping of the convolution, discussed above.

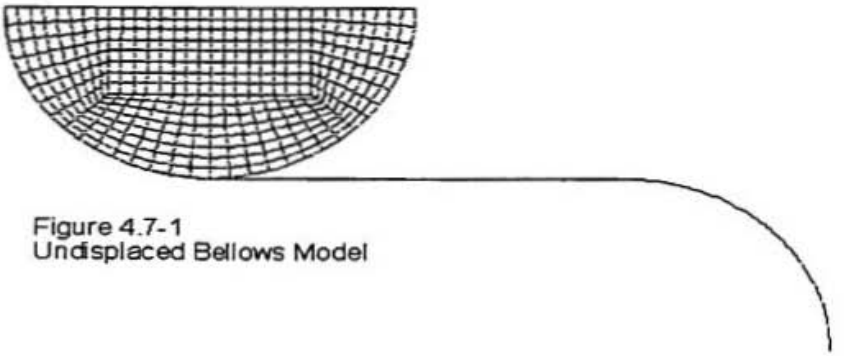

Figure 4.7-1
Undisplaced Bellows Model

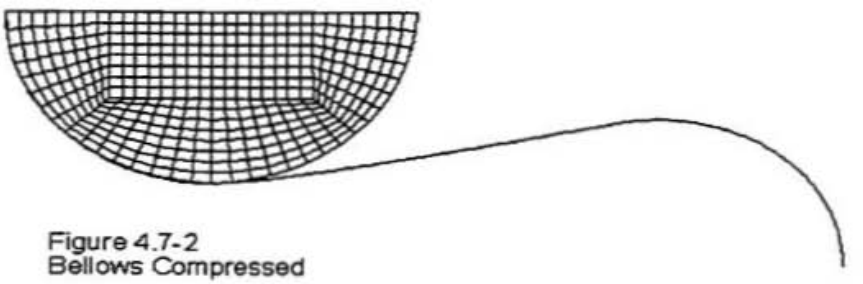

Figure 4.7-2
Bellows Compressed

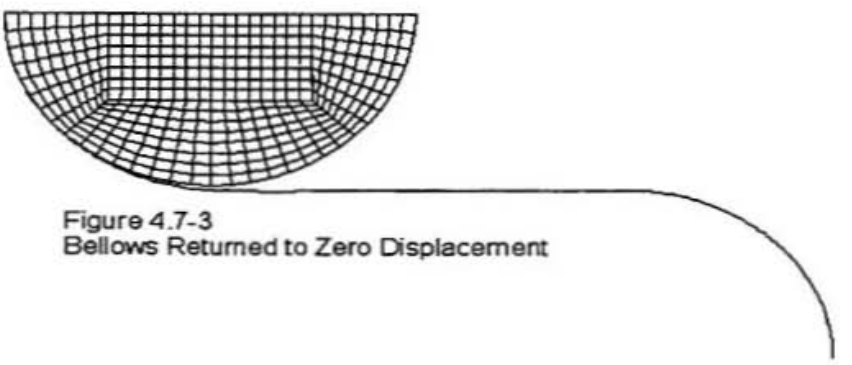

Figure 4.7-3
Bellows Returned to Zero Displacement

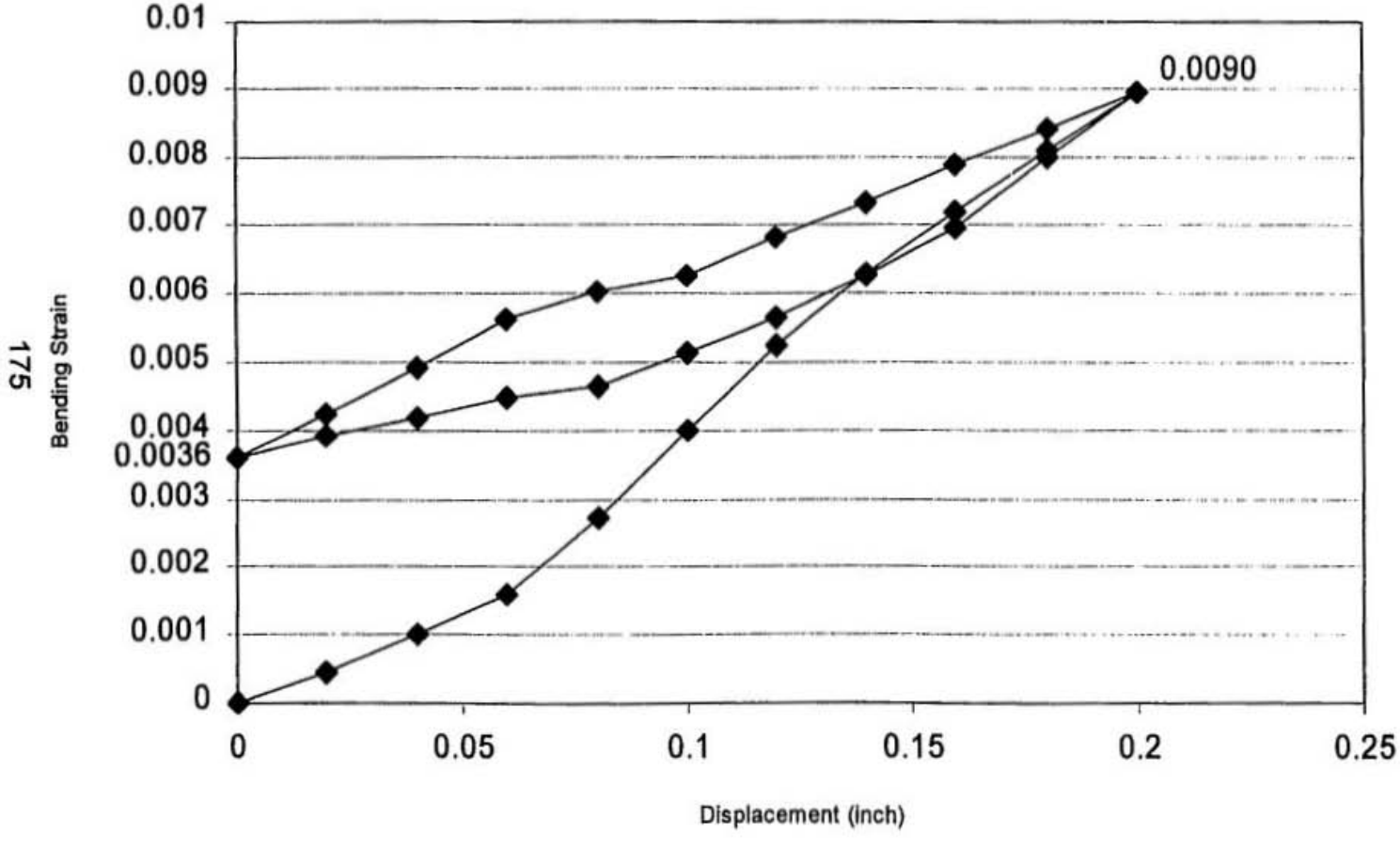

Figure 4.7-4, Strain/Displacement for Compression Displacement

While the distinct peaks in meridional bending stress exhibited in the elastic analyses for closing displacements, shown in the closing Figures in 4.6-9 through 4.6-14, might appear to indicate that the bellows are subject to very severe strain concentration at that location, the calculated strain concentration is not, in fact, severe, based on the way it was calculated. The elastic-plastic strain range from the third half cycle is compared to the elastic strain prediction. The reshaping of the convolution due to permanent deformation greatly reduces the strain range at the elastic peak stress location, thereby reducing the calculated plastic strain concentration.

Calculated plastic strain concentration for various bellows geometries are shown in Figure 4.7-5 for both opening and closing displacement, and at the root and crown. All of the cases are for displacements that would result in an elastic stress that is six times the yield strength. The data is shown in Table V. Note that the strain concentration is not severe for values of QW above about 0.40. The strain concentration at the crown is understated for bellows closing displacement, since the elastic-plastic strain at the crown is generally compared to the elastic strain at the outmost contact point between the convolution and the reinforcing ring.

The key points of Figure 4.7-5 are that plastic strain concentration can occur for deeper convolution reinforced bellows, but is not significant for shallower convolution bellows. This is to be expected, since similar stress peaks occur as for unreinforced bellows. See Figures 4.6-9 through 4.6-14. The primary complicating difference is the reshaping of the convolution that occurs as it plastically deforms around the ring due to closing displacement.

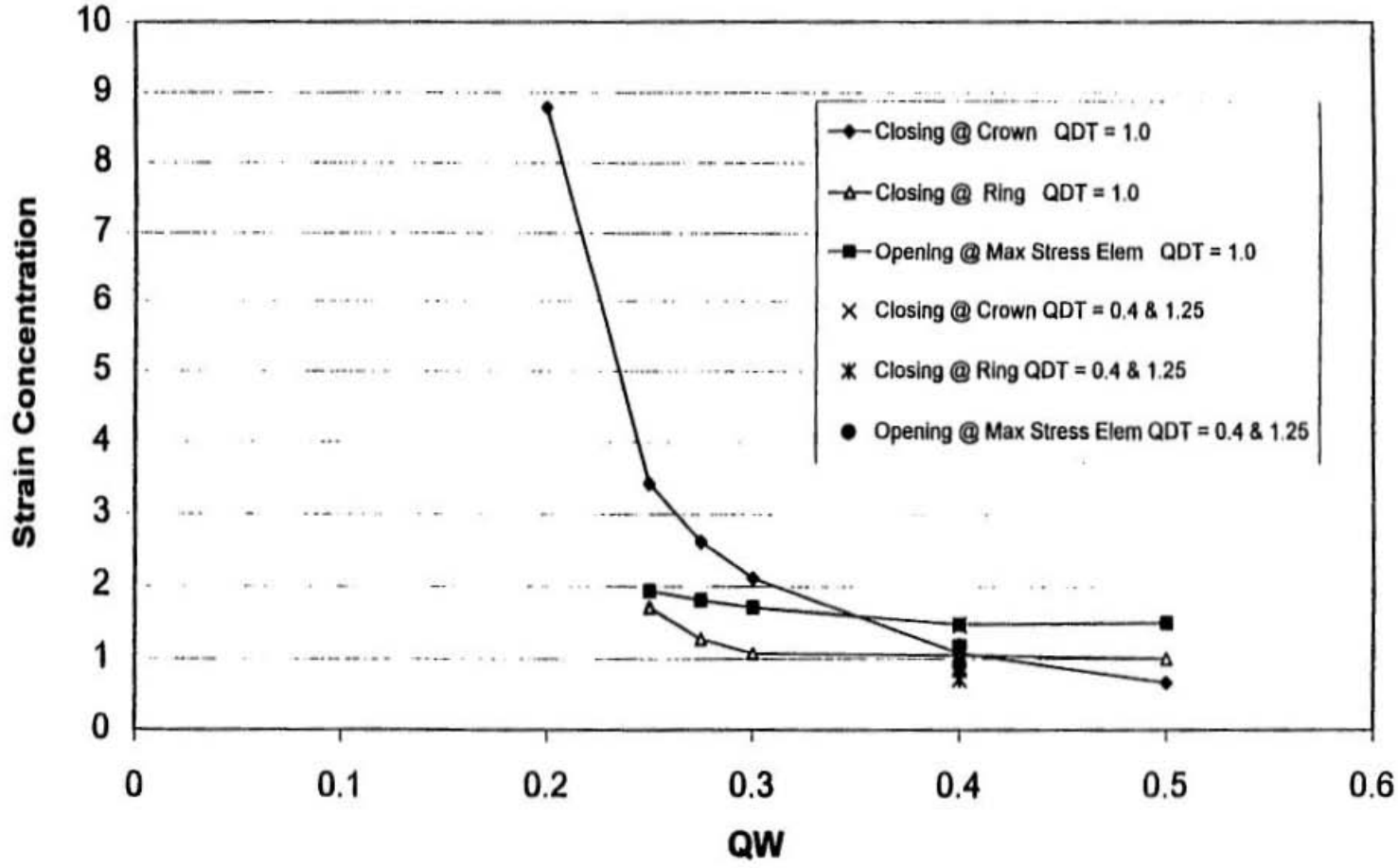

Figure 4.7-5, Strain Concentration for Various Bellows Geometries

TABLE V

Strain Concentration for Reinforced Bellows
Data for 6x Elastic Displacement

D_m = 610 mm (24 in), t_p = 0.51 mm (0.02 in)

			Elastic Analysis			Elastic Plastic Analysis		
Displacement Type & SCF Location	QW	QDT	Disp. (2) inch	S6 (1) psi	6x Max Elastic Disp (3) inch	Low Strain	High Strain	SCF (4)
OPEN	0.5	1	0.025	14502	0.0259	0.00079	0.00887	1.489
OPEN	0.3	1	0.05	12766	0.0587	-0.00071	0.00997	1.973
OPEN	0.275	1	0.05	10847	0.0691	-0.00090	0.01070	2.144
OPEN	0.25	1	0.05	9038	0.0830	-0.00144	0.01164	2.416
OPEN	0.4	0.4	0.01	21161	0.0071	-0.00145	0.00297	0.812
OPEN	0.4	1	0.04	16668	0.0360	0.00091	0.00895	1.483
OPEN	0.4	1.25	0.04	12107	0.0496	-0.00280	0.00939	2.253
OPEN	0.4	1.5	0.05	12086	0.0621	-0.00318	0.01146	2.701
CLOSING @ CROWN	0.5	1	0.025	14502	0.0259	0.00171	0.00529	0.660
CLOSING @ CROWN	0.4	1	0.05	28081	0.0267	0.00143	0.00731	1.082
CLOSING @ CROWN	0.3	1	0.05	12766	0.0587	0.00202	0.01347	2.115
CLOSING @ CROWN	0.275	1	0.05	10847	0.0691	0.00280	0.01700	2.625
CLOSING @ CROWN	0.25	1	0.05	9038	0.0830	0.00398	0.02252	3.422
CLOSING @ CROWN	0.4	0.4	0.01	23301	0.0064	0.00120	0.00929	1.481
CLOSING @ CROWN	0.4	1	0.05	28081	0.0267	0.00143	0.00731	1.082
CLOSING @ CROWN	0.4	1.25	0.05	12107	0.0619	0.00177	0.00777	0.690
CLOSING @ RING	0.5	1	0.025	14502	0.0259	0.00384	0.00924	0.996
CLOSING @ RING	0.3	1	0.05	12766	0.0587	0.00444	0.01031	1.084
CLOSING @ RING	0.275	1	0.05	10847	0.0691	0.00424	0.01116	1.279
CLOSING @ RING	0.25	1	0.05	9038	0.0830	0.00339	0.01264	1.708
CLOSING @ RING	0.4	0.4	0.01	23301	0.0064	0.00430	0.01067	1.166
CLOSING @ RING	0.4	1	0.05	28081	0.0267	0.00379	0.00949	1.049
CLOSING @ RING	0.4	1.25	0.05	12107	0.0619	0.00406	0.00909	0.578

(1) meridional bending stress due to displacement
(2) displacement per convolution
(3) six times elastic displacement per 1/2 convolution = 1/2 Disp(30,000 / S6)
(4) SCF=strain concentration factor

4.8 Evaluation of Reinforced Bellows Fatigue Data

Reinforced bellows fatigue data that was provided by the Expansion Joint Manufacturer's Association for the development of the design rules for bellows in ASME Section VIII, Div 1 and ASME B31.3 were used to evaluate tentative modifications to the EJMA equations for prediction of stress in reinforced bellows. The data is listed in Table VI. Figure 4.8-1 shows the distribution of the data with respect to QW and QDT. Note the cluster of the data with respect to QW. All of the fatigue test data that was considered were for bellows that are not in the regime of significant plastic strain concentration.

The deflection stress ranges were calculated in accordance with the Standards of the Expansion Joint Manufacturer's Association and plotted on Figure 4.8-2. The bellows fatigue data are compared to the raw (no design margin) polished bar fatigue curve for austenitic stainless steel that was used in the development of Section VIII, Div 2, as provided in the Criteria Document (1972). The polished bar fatigue curve is shown as a curve in Figure 4.8-2. Also shown in the Figure are data points based on a modified equation. Note that the data calculated with the modified equation for calculating deflection stress range is quite well characterized by the polished bar fatigue data.

TABLE VI

Reinforced Bellows Fatigue Data

ID #	Inside Diameter inch	Number of Cons, N	Thickness, t inch	Pitch, q inch	Con Height, w inch	Pressure psi	Displacement inch	Cycles to Failure
254	8.625	3	0.053	2.29	2.43	51	0.152	944171
256	8.625	3	0.055	2.25	2.42	12	0.2279	88000
287	8.625	6	0.050	2.29	2.40	282	0.659	1860
292	8.625	7	0.051	2.3	2.40	282	0.711	850
243	8.625	8	0.050	2.27	2.45	207	0.656	1367
244	8.625	8	0.050	2.34	2.49	180	0.655	4349
245	8.625	8	0.053	2.28	2.42	279.5	0.498	3200
324	12.750	3	0.055	2.36	2.78	398	0.250	11251
325	12.750	3	0.059	2.36	2.77	398	0.250	21591
261	20.000	3	0.055	2.29	2.72	250	0.403	16900
265	20.000	3	0.058	2.29	2.74	250	0.403	15245
301	20.000	3	0.057	2.30	2.73	250	1.000	986
302	20.000	3	0.057	2.25	2.71	250	1.000	1033
312	20.000	3	0.056	2.30	2.78	5	1.000	5495
315	20.000	3	0.058	2.36	2.76	6	0.349	358312
316	20.000	3	0.055	2.35	2.77	245	0.672	1857
317	20.000	3	0.054	2.35	2.77	246	0.307	13718
270	20.000	3	0.085	2.29	2.78	400	0.399	3628
190	4.500	3	0.038	1.35	1.45	150.5	0.322	3597
191	4.500	3	0.038	1.35	1.44	150.5	0.501	2248
214	4.500	3	0.037	1.35	1.40	152	0.497	1776
217	4.500	3	0.037	1.33	1.47	275	0.058	529292
223	4.500	6	0.038	1.27	1.42	276	0.502	1070
224	4.500	6	0.038	1.28	1.44	276	0.501	546
277	4.500	7	0.035	1.27	1.42	280	0.255	4170
278	4.500	8	0.036	1.25	1.43	278	0.501	749
279	4.500	8	0.035	1.24	1.43	280	0.254	3353
280	4.500	8	0.037	1.26	1.43	280	0.373	1476
290	4.500	9	0.038	1.28	1.41	205	0.482	1683
220	4.500	10	0.038	1.27	1.43	6	0.240	13881
221	4.500	10	0.037	1.25	1.42	121	0.499	1947
222	4.500	10	0.037	1.27	1.43	121.5	0.499	3425
164	6.625	3	0.035	1.90	1.97	277.5	0.737	1085
165	6.625	3	0.035	1.81	1.99	277.5	0.500	3280
182	6.625	3	0.035	1.85	1.98	276.5	0.337	16453
187	6.625	3	0.035	1.75	2.02	6.3	0.739	4400

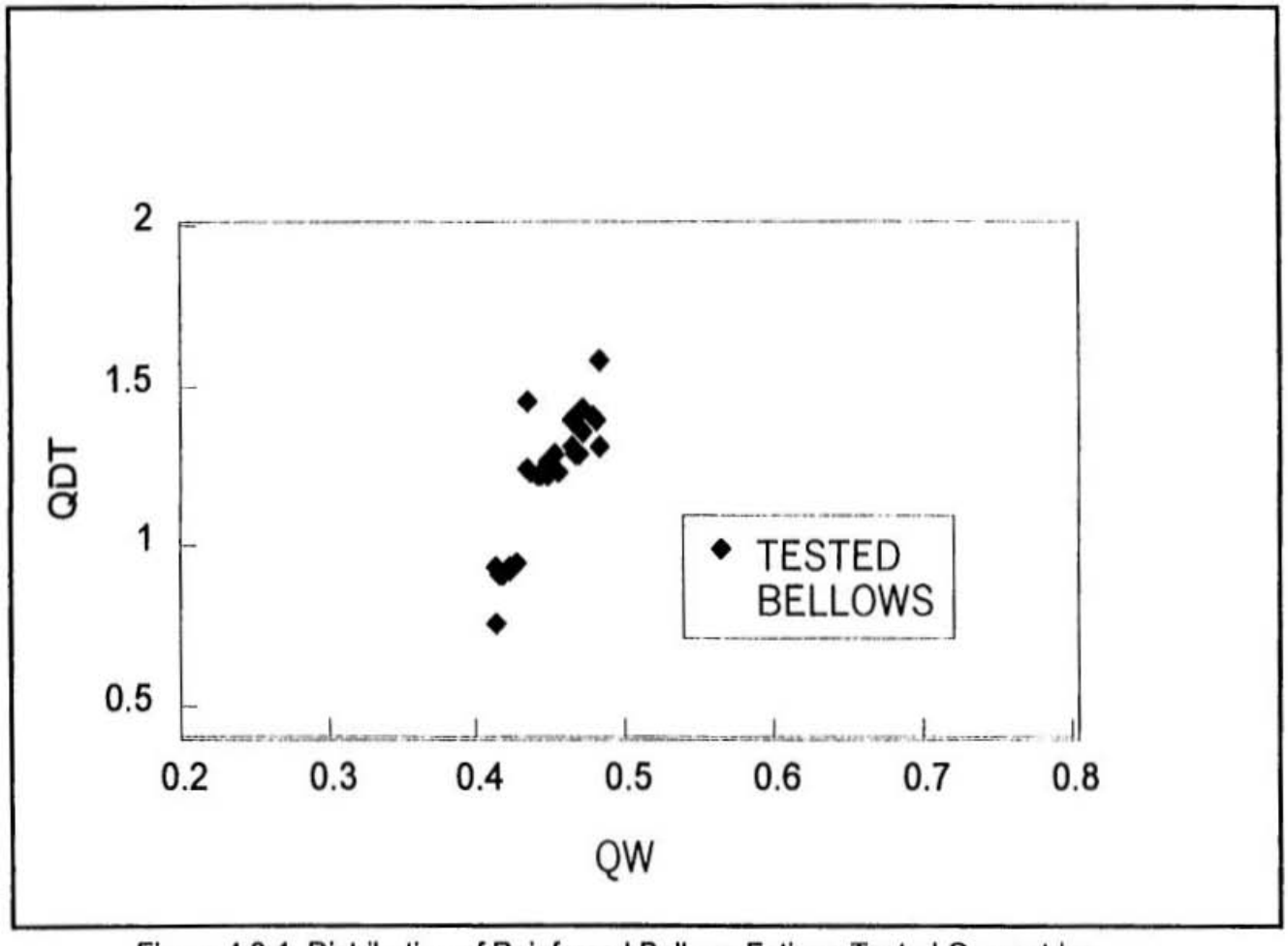

Figure 4.8-1, Distribution of Reinforced Bellows Fatigue Tested Geometries

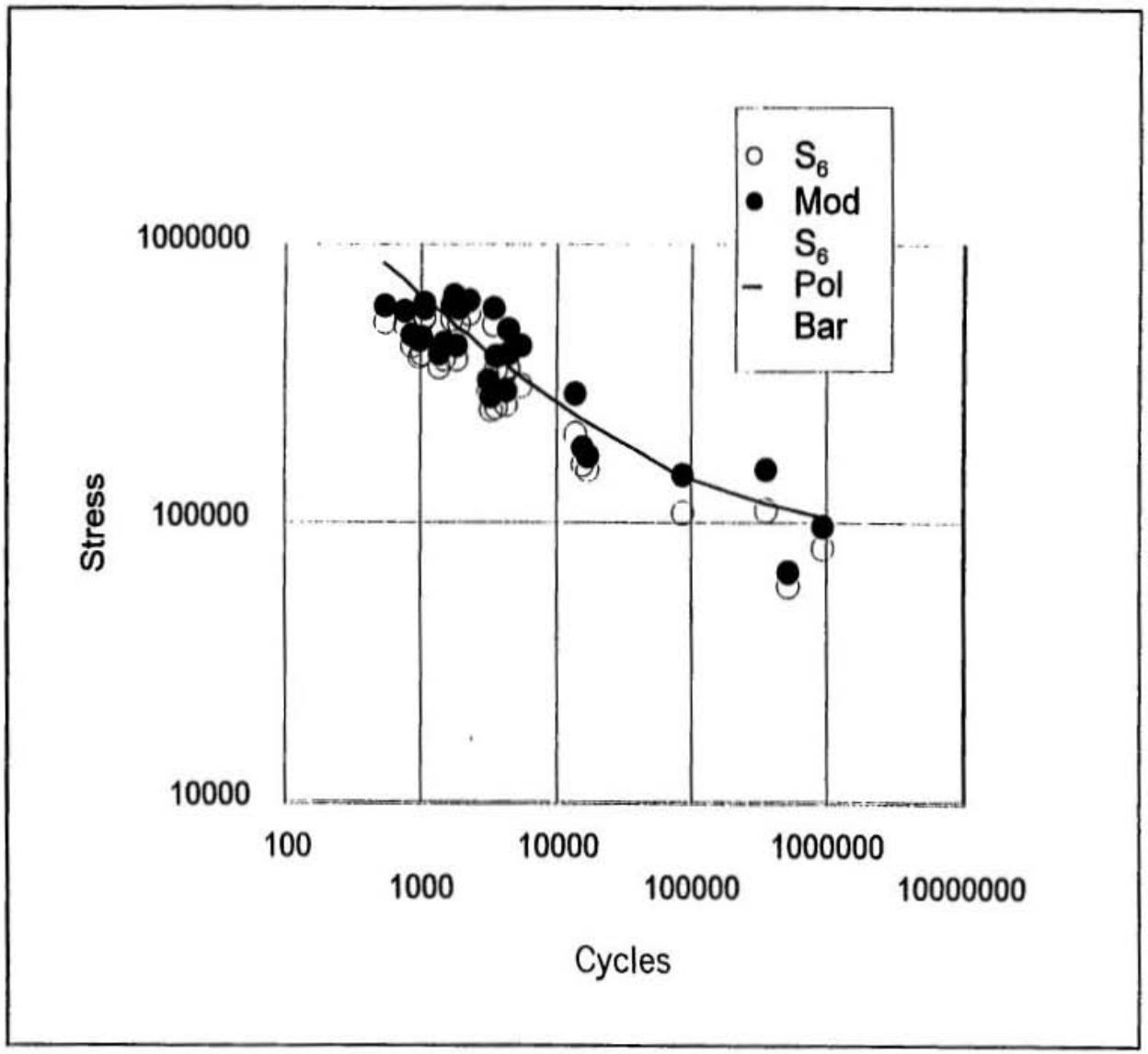

Figure 4.8-2, Reinforced Bellows Fatigue Data

The modifications come from a couple observations based on the evaluations that were performed. First, internal pressure did not appear to significantly affect the elastically calculated stress range. Therefore, the pressure adjustment term was dropped from the S_5 and S_6 equations.

The second modification was to multiply the calculated stress range by a factor of 1.4, the same as was done for unreinforced bellows. This assumes that surface finish and similar effects, and the degree of strain concentration in the reinforced bellows is essentially the same as was present for unreinforced bellows with QW>0.45. In fact, the reinforced bellows that were tested had values of QW between 0.41 and 0.49, so this is not an unreasonable assumption, particularly since the reinforcing ring effectively decreases the convolution height.

The modified equation follows:

$$S_t = 1.4\,S_5 + 1.4\,S_6 \qquad (4.1)$$

Where:

S_5 is per equation 3.12 with P taken as zero in calculation of C_r

S_6 is per equation 3.13 with P taken as zero in calculation of C_r

S_t = Mod S_6 stress range in figure 4.8.2

Both the unreinforced bellows fatigue data for QW>0.45 and the modified reinforced bellows fatigue data fall on the polished bar fatigue curve; so the same fatigue curve applies to both reinforced and unreinforced bellows, as long as strain concentration effects are not significant. The prior observed difference between unreinforced and reinforced bellows behavior was largely due to the difference in bellows geometries that were tested. The unreinforced bellows data base included deep convolution bellows that were subject to significant strain concentration, whereas the reinforced bellows that were tested did not have deep convolutions.

The geometries of the reinforced bellows that were tested are quite significant. The geometries that were tested were limited to those that are not subject to significant plastic strain concentration. If deeper convolution reinforced bellows had been tested, it is quite likely that the fatigue data would have been worse, resulting in a lower fatigue curve.

Reinforced bellows with deeper convolutions than those that were tested can be subject to plastic strain concentration. The present design fatigue curve may be unconservative for reinforced bellows with deeper convolutions.

Chapter 5

Conclusions

The response of bellows to internal pressure and displacement loads was analytically investigated. Existing equations that predict the elastic stresses in unreinforced bellows were evaluated. Meridional bending stresses are well predicted over most of the range of bellows geometries by the existing equations; meridional membrane stresses are not because the location for which they were calculated in the development of the equations was not always the location of highest meridional membrane stress. The maximum membrane stress due to both pressure and deflection deviate significantly from the stress predicted in the EJMA equations for deep convolutions (low QW) and thin walled bellows (high QDT). This is generally not significant in bellows design because the membrane stress is generally one to two orders of magnitude less than the bending stress, and the sum of the two is evaluated in design.

For reinforced bellows, pressure was not found to significantly increase the ply/reinforcing ring interaction, and thus had little effect on the deflection stresses. It is recommended that the pressure term be taken out of the existing equations for deflection bending stress in reinforced bellows.

While the deflection stress in reinforced bellows was found to depend significantly on whether the bellows was being extended or compressed, based on elastic analysis, inelastic analyses showed that after the first cycle the direction of movement was not significant. Permanent inelastic deformation of the convolution that occurs on bellows compression results in the sidewall pulling away from the reinforcing ring when the bellows is returned to zero displacement. Thus, after the first cycle, the stress range in either compression or extension is best represented by the elastic prediction of stresses due to extension. This greatly simplifies the consideration of reinforced bellows response, since the calculation of stress then does not depend on the direction of the deflection (extension versus compression).

It was found that the strain in bellows when they are deflected into the plastic regime is not proportional to the elastic stress for all geometries due to plastic strain concentration. However, it was found that plastic strain concentration effects are relatively stable and low in magnitude for a range of bellows geometries. For bellows in this range of geometries, fatigue data for both reinforced and unreinforced bellows overlay, and are both about a factor of 1.4 on stress below raw polished bar fatigue data. This difference can be attributed to limited plastic strain concentration for these bellows and typical effects found in actual components, such as surface finish effects. The factor of 1.4 is well within typical differences between polished bar fatigue data and component fatigue data.

For the range of bellows geometries without significant strain concentration, it appears that bellows fatigue life can be predicted using elastic stress predictions and raw polished bar fatigue data. This finding may lead to major improvements and simplification in design methods for bellows. For this range of geometries, fatigue behavior between bellows constructed with different materials may be related by basic material properties.

For the range of bellows geometries for which significant strain concentration occurs, the effect of geometry parameters is shown. It was shown that the conclusions of prior work relative to the effect of the parameter QDT were not completely correct. The effects of QW, QDT and displacement stress range (relative to yield stress) are shown, and the difference can be seen to depend on the stress distribution in the bellows.

These findings can lead to the use of the same fatigue curve for reinforced and unreinforced bellows. The use of the same fatigue curve for reinforced and unreinforced bellows can result in significant cost savings in bellows qualification fatigue testing because fewer fatigue tests may be required. Further, it can lead to the development of fatigue design curves without the need for extensive fatigue testing of bellows for each material. These findings should lead to revisions to the EJMA Standards as well as ASME and European (CEN) pressure vessel and piping codes and standards with respect to bellows design.

Key findings and potential consequences of this research include the following.

1) Bellows Fatigue data correlate with polished bar fatigue data for reinforced and unreinforced bellows that are not subject to plastic strain concentration; for these bellows, rather than requiring fatigue testing of bellows to design them with other materials, the existing austenitic stainless steel fatigue curves for bellows may be adjusted by the ratio of polished bar fatigue curves.

2) Unreinforced bellows that are not subject to plastic strain concentration have substantially better fatigue performance than those that are subject to plastic strain concentration; for these bellows, a higher fatigue curve, perhaps the same as the existing reinforced bellows fatigue curve shown in Figure 1-1, may be used.

3) The effect of geometry on plastic strain concentration and fatigue is explained; planning of bellows fatigue testing in the future should consider these findings and data from such tests should be viewed with due consideration of this knowledge.

4) It was found that the data used to develop the fatigue curve for reinforced bellows did not contain any bellows that may be subject to plastic strain concentration; a lower fatigue curve for such bellows may be appropriate. Fatigue testing of reinforced bellows subject to plastic strain concentration should be performed.

curves may be better presented in terms of geometries that are subject to plastic strain concentration and those that are not, rather than reinforced and unreinforced. Further, if qualification testing remains a requirement, data from reinforced and unreinforced bellows may be combined, reducing the required number of bellows fatigue tests.

6) The EJMA equations for meridional membrane stress were shown to be inaccurate; these equations can be corrected by providing new design charts based on parametric analysis, solving for the maximum meridional stress.

References

Abe, H., Shimoyashiki, T., Maeda, O., and Mizuno, S. (1986). "Fatigue Strength of Two-Ply Bellows at Elevated Temperature," *Fatigue and Fracture Assessment by Analysis and Testing,* PVP Vol. 103, ed. S. H. Bhandari et al., The American Society of Mechanical Engineers, pp. 79-86.

Acker, D., Brouard, D., Noudelmann, M., Vrillon, B., and Poette, C. (1989). "A Tentative Approach for the Use of Bellows Expansion Joints on Main Secondary Pipework of LMR *Metallic Bellows and Expansion Joints - 1989*, PVP Vol. 168, ed. C. Becht IV et al., The American Society of Mechanical Engineers, pp. 7-12.

Anderson, W. F. (1964a). "Analysis of Stresses in Bellows, Part I: Design Criteria and Test Results," NAA-SR-4527 (Pt. I), Atomics International Division of North American Aviation.

Anderson, W. F. (1964b). "Analysis of Stresses in Bellows, Part II: Mathematical," NAA-SR-4527 (Pt. II), Atomics International Division of North American Aviation.

ASME B31.3, *Process Piping*, The American Society of Mechanical Engineers.

ASME Section III, Div 1, Subsection NH, "Class 1 Components in Elevated Temperature Service," *ASME Boiler and Pressure Vessel Code*, The American Society of Mechanical Engineers.

ASME Section III, Div 1, Code Case N-290, "Expansion Joints in Class 1, Liquid Metal Piping," , *ASME Boiler and Pressure Vessel Code*, The American Society of Mechanical Engineers.

ASME Section VIII, Div 1, "Pressure Vessels," *ASME Boiler and Pressure Vessel Code*, The American Society of Mechanical Engineers.

ASME Section VIII, Div 2, "Pressure Vessels, Alternative Rules," *ASME Boiler and Pressure Vessel Code*, The American Society of Mechanical Engineers.

Bathe, K. (1982). *Finite Element Procedures in Engineering Analysis*, Prentice-Hall, Englewood Cliffs, N. J.

Becht IV, C. (1980) "Root Bulge of Bellows," DOE Research and Development Report, ESG-DOE-13320, Rockwell International.

Becht, IV, C., and Skopp, G. (1981a). "Root Bulge of Bellows," *Metallic Bellows and Expansion Joints*, PVP-Vol. 51, ed. R. I. Jetter et al., The American Society of Mechanical Engineers.

Becht, IV, C., and Skopp, G. (1981b). "Stress Analysis of Bellows," *Metallic Bellows and Expansion Joints*, PVP-Vol. 51, ed. R. I. Jetter et al., The American Society of Mechanical Engineers.

Becht, IV, C., Horton, P., and Skopp, G. (1981c). "Verification of Theoretical Plastic Ratchet Boundaries for Bellows," Metallic Bellows and Expansion Joints, PVP-Vol. 51, ed. R. I. Jetter et al., The American Society of Mechanical Engineers, pp. 139-154.

Becht, IV, C. (1983). "A Simplified Approach for Evaluating Secondary Stresses in Elevated Temperature Design," ASME Paper No. 83-PVP-51, The American Society of Mechanical Engineers.

Becht, IV, C. (1984). "Design and Analysis of a High Pressure, High Temperature Bellows Expansion Joint," *Expansion Joints in the Process, Power, and Petrochem Industries*, The American Society of Mechanical Engineers.

Becht, IV, C. (1985). "Predicting Bellows Response by Numerical and Theoretical Methods," *A Decade of Progress in Pressure Vessels and Piping Technology - 1985*, ed. C. Sundararajan, The American Society of Mechanical Engineers, pp. 53-65.

Becht, IV, C. (1989a). "Fatigue and Elevated Temperature Design of Bellows," *Metallic Bellows and Expansion Joints - 1989*, PVP Vol. 168, ed. C. Becht IV et al., The American Society of Mechanical Engineers, pp. 27-36.

Becht, IV, C. (1989b). "Considerations in Bellows Thrust Forces and Proof Testing," *Metallic Bellows and Expansion Joints - 1989*, PVP Vol. 168, ed. C. Becht IV et al., The American Society of Mechanical Engineers, pp. 45-50.

Becht, IV, C. (1995). "B31.3 Appendix X Rules for Expansion Joints," *Journal of Pressure Vessel Technology*, Vol. 117, no. 3, pp. 283-287.

Bhavikatti, S. S., Ramakrishnan, C. V., and Mehandru, V. K. (1979). "Optimum Design of Flanged and Flued Expansion Joints," *Engineering Optimization*, Vol. 14.

Bree, J. (1967). "Elastic-Plastic Behavior of Thin Tubes Subjected to Internal Pressure and Intermittent High-Heat Fluxes with Application to Fast-Nuclear-Reactor Fuel Elements," *Journal of Strain Analysis*, Vol. 2, no. 3.

Broyles, R. K. (1989). "Bellows Instability," *Metallic Bellows and Expansion Joints -1989*, PVP Vol. 168, ed. C. Becht IV et al., The American Society of Mechanical Engineers, pp. 37-44.

Broyles, R. K. (1994). "EJMA Design Equations," *Developments in a Progressing Technology - 1994*, PVP Vol. 279, ed. W. J. Bees, The American Society of Mechanical Engineers, pp. 43-50.

Broyles, R. K. (1995). "Bellows High Temperature Cyclic Life," *Developments in Pressure Vessels and Piping 1995*, PVP Vol. 301, ed. J. N. Petrinec, Jr., The American Society of Mechanical Engineers.

Budiansky, B., and Radkowski, P. P. (1963). "Numerical Analysis of Unsymmetrical Bending of Shells of Revolution," *AIAA Journal*.

Bushnell, D. (1973). "Finite Difference Energy Models Versus Finite Element Models: Two Variational Approaches in One Computer Program," *Numerical and Computer Methods in Structural Mechanics*, Academic Press, New York.

Bushnell, D. (1973). "Large Deflection Elastic-Plastic Creep Analysis of Axisymmetric Shells," *Numerical Solution of Nonlinear Structural Problems*, AMD-Vol. 6, The American Society of Mechanical Engineers.

Bushnell, D., and Almroth, B. O. (1971). "Finite Difference Energy Method for Nonlinear Shell Analysis," *Journal of Computers and Structures*, Vol. 1.

Campbell, R. D., Cloud, R. L., and Bushnell, D. (1981a). "Creep Instability in Flexible Piping Joints," *Metallic Bellows and Expansion Joints*, PVP-Vol. 51, ed. R. I. Jetter et al., The American Society of Mechanical Engineers.

Campbell, R. D., and Kipp, T. R. (1981b). "Accelerated Testing of Flexible Piping Joints at Creep Temperature," *Metallic Bellows and Expansion Joints*, PVP-Vol. 51, The American Society of Mechanical Engineers, New York.

Chandler, W. L. (1941). "Bellows in the Refrigeration Industry, Part II Design Theory."

Clark, R. A. (1950). "On Theory of Thin Elastic Toroidal Shells," *Journal of Mathematics Physics*, Vol. 29, pp. 146-178.

Clark, R. A., and Reissner, E. (1953). "A Problem of Finite Bending of Toroidal Shells," *Institute of Mechanical Engineers Proceedings*, Vol. 171.

Clark, R. A. (1958). "Asymptotic Solutions of Toroidal Shell Problems," *Quarterly of Applied Mathematics*, Vol. 16, No. 1.

"Criteria of the ASME Boiler and Pressure Vessel Code for Design by Analysis in Section III and VIII, Division 2," (1972). *Pressure Vessels and Piping: Design and Analysis, A Decade of Progress, Vol 1-Analysis*, The American Society of Mechanical Engineers, pp. 61-82.

Dahl, N. C. (1953). "Toroidal-Shell Expansion Joint," ASME *Journal of Applied Mechanics*, Vol. 20, pp 497-503.

Donnell, L. H. (1932). "The Flexibility of Corrugated Pipes Under Longitudinal Forces and Bending," Trans. ASME, Vol. 54, APM-54-7, The American Society of Mechanical Engineers.

EJMA, see *Standards of Expansion Joint Manufacturers Association*.

Feely, F. J., and Goryl, W. M. (1950). "Stress Studies on Piping Expansion Bellows," ASME *Journal of Applied Mechanics*, Vol. 17, The American Society of Mechanical Engineers, pp. 135-141.

Hamada, M., and Takenzono, S. (1965a). "Strength of U-Shaped Bellows (1st Report, Case of Axial Loading)," *Bulletin of Japanese Society of Mechanical Engineers*, Vol. 8, No. 32, The Japanese Society of Mechanical Engineers.

Hamada, M., and Takenzono, S. (1965b). "Strength of U-Shaped Bellows (2nd Report, Case of Axial Loading-Continued)," *Bulletin of Japanese Society of Mechanical Engineers*, Vol. 9, No. 35, The Japanese Society of Mechanical Engineers.

Hamada, M., and Takenzono, S. (1965c). "Strength of U-Shaped Bellows (3rd Report, Case of Loading of Internal Pressure)," *Bulletin of Japanese Society of Mechanical Engineers*, Vol. 9, No. 35, The Japanese Society of Mechanical Engineers.

Hamada, M., Seguchi, Y., Ito, S., Kaku, E., Yamakawa, K., and Oshima, I. (1968). "Numerical Methods for Nonlinear Axisymmetric Bending of Arbitrary Shells of Revolution and Large Deflection Analysis of Corrugated Diagram and Bellows," *Bulletin of Japanese Society of Mechanical Engineers*, Vol. 11, No. 43, The Japanese Society of Mechanical Engineers.

Hamada, M., et al. (1970). "Analysis of Expansion Joints in Pressure Vessels," *Bulletin of Japanese Society of Mechanical Engineers*, Vol. 13, No. 55, The Japanese Society of Mechanical Engineers.

Hamada, M., Nakagawa, K., Miyata, K., and Nakade, K. (1971). "Bending Deformation of U-Shaped Bellows," *Bulletin of Japanese Society of Mechanical Engineers*, Vol. 14, No. 71, The Japanese Society of Mechanical Engineers.

Hamada, M., and Tanaka, M. (1973). "A Numerical Method for Solving Elastic Plastic Problems of Rotationally Symmetric Shells (2nd Report, Comparison of Analytical Results With Experimental Ones), " *Bulletin of Japanese Society of Mechanical Engineers*, Vol. 16, No. 100, The Japanese Society of Mechanical Engineers.

Hamada, M., and Tanaka, M. (1974). "A Consideration on the Low-Cycle Fatigue Life of Bellows," *Bulletin of Japanese Society of Mechanical Engineers*, Vol. 17, No. 103, The Japanese Society of Mechanical Engineers.

Hamada, M., and Tanaka, M. (1978). "Design of U-Shaped Bellows Considering Low-Cycle Fatigue," ASME Journal of Pressure Vessel Technology, Vol. 100, The American Society of Mechanical Engineers.

Hamada, M., Inque, Y., Nakatani, T., and Moriishi, M. (1976). "Design Diagrams and Formulae for U-Shaped Bellows," *International Journal of Pressure Vessels and Piping*, Vol. 4.

Haringx, J. A. (1952a). "The Instability of Thin-Walled Cylinders Subjected to Internal Pressure," *Phillips Research Report*, Vol. 7, pp. 112-118.

Haringx, J. A. (1952b). "The Instability of Bellows Subjected to Internal Pressure," *Phillips Research Report*, Vol. 7, pp. 189-196.

Hetenyi, M., and Timms, R. J. (1960). "Analysis of Axially Loaded Annular Plates with Application to Welded Bellows," *Journal of Basic Engineering*.

Jacquay, K. and Bigelow, C. (1989). "Summary of the U.S. DOE LMR Flexible Pipe Joint Development Program," *Metallic Bellows and Expansion Joints - 1989*, PVP Vol. 168, ed. C. Becht IV et al., The American Society of Mechanical Engineers, pp. 1-6.

Janzen, P., (1979). "Formulae and Graphs on Elastic Stresses for Design and Analysis of U-Shaped Bellows," International Journal of Pressure Vessels and Piping, Vol. 7, No. 6.

Janzen, P., and Helleur, C. (1978). "Effect of Annealing on Bellows Cyclic Performance," AECL-6080, Chalk River Nuclear Laboratories.

Kalnins, A. (1964). "Analysis of Shells of Revolution Subjected to Symmetrical and Nonsymmetrical Loads," ASME *Journal of Applied Mechanics*, Vol 86, The American Society of Mechanical Engineers.

Kleppe, S. R. (1955). "High Pressure Expansion Joints," ASME Paper No. 55-PET-10, The American Society of Mechanical Engineers.

Kobatake, K., Tsukada, T., Takahashi, S., Akatsu, M., Iikemoto, Y., and Baba, O. (1975). "Elevated Temperature Fatigue Tests and Inelastic Stress Analysis of Bellows," *ASME Journal of Pressure Vessel Technology*, The American Society of Mechanical Engineers.

Kobatake, K., Takahashi, S., Osaki, T., Shimakawa, T., and Baba, O. (1981). "Fatigue Life Prediction of Bellows Joints at Elevated Temperature," *Metallic Bellows and Expansion Joints*, PVP-Vol. 51, ed. R. I. Jetter et al., The American Society of Mechanical Engineers, pp. 75-79.

Kobatake, K., Ooka, Y., Shimakawa, T., and Koe, S. (1986). "Simplified Fatigue Life Evaluation Method of Bellows Expansion Joints at Elevated Temperature," *Fatigue and Fracture Assessment by Analysis and Testing*, PVP Vol. 103, ed. S. K. Bhandari et al., The American Society of Mechanical Engineers, pp. 73-78.

Kopp, S., and Sayre, M. F. (1952). "Expansion Joints for Heat Exchangers," ASME Annual Meeting, New York, The American Society of Mechanical Engineers.

Koves, W. J. (1995). "The Initiation of In-Plane Squirm in Expansion Joint Bellows," *Developments in Pressure Vessels and Piping 1995*, ed. J. N. Petrinec, Jr., The American Society of Mechanical Engineers, pp. 109-119.

Langer, B. F., (1961). "Design of Pressure Vessels for Low Cycle Fatigue," ASME Paper 61-WA-18, The American Society of Mechanical Engineers.

Laupa, A., and Weil, N. A. (1962). "Analysis of U-Shaped Expansion Joints," ASME *Journal of Applied Mechanics*, The American Society of Mechanical Engineers.

Lestingi, J., and Brown, S. Jr. (1973). "Comparison of the Numerical Integration Technique and the Finite Element Method in the Analysis of Thin-Shell Structures," presented at 2nd Structural Mechanics in Reactor Technology Conference, September 10-16.

Lestingi, J. F., and Hulbert, L. E. (1972). "The Application of Linear and Nonlinear Thin Shell Theory in the Analysis of Formed and Welded Metallic Bellows," ASME Paper 72-WA/PVP-3, The American Society of Mechanical Engineers.

Listvinsky, G., Koutouras, N. V., and Wittko, J., "Strength and Fatigue Aspects of the TFTR Vacuum Vessel Bellows Design," *Proceedings Symposium Eng. Probl. Fusion Res. 8th.*, Vol. 1, Institution of Electrical and Electronics Engineers, (Cat No. 79 CH 14441-5 NPS).

Marcal, P. V., and Turner, C. E. (1965). "Limited Life of Shells of Revolution Subjected to Severe Local Bending," Journal of Mechanical Engineering Science, Vol. 7, No. 4.

Miyazaki, N, Munakata, T., Gu W., and Ishikawa, K. (1993). "Strength Analysis of Reinforced Bellows: Effects of Reinforcing Rings," *Design Analysis, Robust Methods, and Stress Classification*, PVP-Vol. 265, ed. W. J. Bees, The American Society of Mechanical Engineers.

Newell, J. F. (1962). "Some Stability and Deflection Problems Associated with Bellows," Masters Thesis, University of California, Los Angeles.

Newland, D. E. (1964). "Buckling of Double Bellows Expansion Joints Under Internal Pressure," *Journal of Mechanical Engineering Science*, Vol. 6, Issue 3.

Newland, D. E. (1976). "Buckling and Rupture of Double Bellows Expansion Joint Assembly at Flixborough," *Proceedings of the Royal Society of London*, Ser. A, Vol. 351, pp. 525-544.

Ooka, Y., Yoshie, S., Morishita, M., and Tsukimori, K. (1989). "Dynamic Buckling Characteristics of Bellows Under Pressure Waves," *Metallic Bellows and Expansion Joints - 1989*, PVP Vol. 168, ed. C. Becht IV et al., The American Society of Mechanical Engineers, pp. 173-178.

Ooka, Y., Ogawa, H., Ohno, K., and Dozaki, K. (1994), "Simulative Analyses of Dynamic Buckling of Bellows," *Developments in a Progressing Technology - 1994*, PVP Vol. 279, ed. W. J. Bees, The American Society of Mechanical Engineers, pp. 51-58.

Osweiller, F. (1989). "Design of an Expansion Joint By a Finite Element Program -Comparison with the EJMA Standards," *Metallic Bellows and Expansion Joints - 1989*, PVP Vol. 168, ed. C. Becht IV et al., The American Society of Mechanical Engineers, pp. 87-94.

Osweiller, F. (1995). "Review of Recent Codes & Standards Devoted to Expansion Bellows," *Developments in Pressure Vessels and Piping 1995*, ed. J. N. Petrinec, Jr., The American Society of Mechanical Engineers, pp. 139-158.

Ota, T., and Hamada, M. (1963). "On the Strength of Toroidal Shells (First Report: A Proposition on the Solutions)," *Bulletin of Japanese Society of Mechanical Engineers*, Vol. 6, No. 24, The Japanese Society of Mechanical Engineers, pp. 4-54.

Ota, T., Hamada, M., and Furukawa, M. (1963). "On the Strength of Toroidal Shells (Second Report: Examples of Applications of the Solutions)," *Bulletin of Japanese Society of Mechanical Engineers*, Vol. 6, No. 24, The Japanese Society of Mechanical Engineers, pp. 655-65.

Palmer, P. J. (1960). "An Approximate Analysis Giving Design Data for Corrugated Pipes," *Proceedings of the Institution of Mechanical Engineer*, Vol. 174, No. 20.

Penny, R. V. (1961). "Symmetric Bending of the General Shells of Revolution by the Finite Difference Method," *Journal of Mechanical Engineering Science*, Vol. 3.

Porowski, J. S. and O'Donnell, W. J. (1977). "Upper Bounds for Creep Ratchetting in Convoluted Bellows," O'Donnell and Assoc. Inc. technical report.

Radkowski, P. P., Davis, R. M., and Bolduc, M. R. (1962). "Numerical Analysis of Thin Shells of Revolution," *American Rocket Society Journal*, Vol. 32.

Salzman, F. (1963). "Compliance of Corrugated Expansion Joints," RSIC-100, U.S. Army Redstone Scientific Information Center, translated from *Schweizerische Bauzeitung*, Vol. 127, No. 11, 1946.

Seide, P. (1960). "The Effect of Pressure on the Bending Characteristics of an Actuator System," ASME *Journal of Applied Mechanics*, The American Society of Mechanical Engineers.

Sepetoski, W. K., Pearson, C. E., and Dingwell, I. W. (1962). "A Digital Computer Program for General Axially Symmetric Thin-Shell Problems," ASME *Journal of Applied Mechanics*, Vol. 84, The American Society of Mechanical Engineers.

Stambaugh, K.A., Leeson, D.H., Lawrence, F.V., Hou, C.Y., and Bana,G. (1995). "Reduction of S-N Curves for Ship Structural Details," WRC Bulletin 398, Welding Research Council.

Standards of the Expansion Joint Manufacturers Association, Inc. - 5th edition (1980). White Plains, N.Y, Expansion Joint Manufacturers Association.

Standards of the Expansion Joint Manufacturers Association, Inc - 6th edition. (1993). White Plains, N.Y Expansion Joint Manufacturers Association.

Standards of the Expansion Joint Manufacturers Association, Inc - 7th edition. (1998). White Plains, N.Y Expansion Joint Manufacturers Association.

Tamura, M., Hashimoto, H., Nakanishi, S., and Taniyama, H. (1989). "Development and Application of Expansion Joints to Main Heat Transport System Piping of LMFBR," *Metallic Bellows and Expansion Joints - 1989*, PVP Vol. 168, ed. C. Becht IV et al., The American Society of Mechanical Engineers, pp. 99-106.

Tanaka, M. (1974). "Fatigue Life Estimation of Bellows Based on Elastic-Plastic Calculations," *International Journal of Pressure Vessels and Piping*, Vol. 2.

Tang-Xi, L., Bang-Lang, G., Tan-Xing, L., and Wang Qing-Chen, W., (1989). "Stresses and Fatigue Failure of U-Shaped Bellows," *Metallic Bellows and Expansion Joints -1989*, PVP - Vol. 168, ed. C Becht IV et al., The American Society of Mechanical Engineers, pp. 13-20.

Trainer, T. M., Hulbert, L. E., Lestingi, J. F., Keith, R. E., et al. (1968). "Final Report on the Development of Analytical Techniques for Bellows and Diaphragm Design," AFRPL-TR-68-22, Battelle Memorial Institute.

Tsukimori, K., Yamashita, T., Kikuchi, M., Iwata, K., and Imazu, A. (1989a). "Fatigue and Creep-Fatigue Life Prediction of Bellows," *Metallic Bellows and Expansion Joints - 1989*, PVP Vol. 168, ed. C Becht IV et al., The American Society of Mechanical Engineers, pp. 113-122.

Tsukimori, K., Iwata, K., Matsunaga, M., Imazu, A. (1989b). "Buckling of Bellows Subjected to Pressure Loadings," *Metallic Bellows and Expansion Joints - 1989*, PVP Vol. 168, ed. C. Becht IV et al., The American Society of Mechanical Engineers, pp. 133-140.

Turner, C. E. (1959). "Stress and Deflection Studies of Flat-Plate and Toroidal Expansion Bellows, Subjected to Axial, Eccentric or Internal Pressure Loading," *Journal of Mechanical Engineering Science*, Vol. 1, No. 2, pp. 130-142.

Turner, C. E., and Ford, H. (1956). "Stress and Deflection Studies of Pipeline Expansion Bellows," *Institution of Mechanical Engineers Proceedings*, Vol. 171, pp. 526-552.

Updike, D. P., and Kalnins, A. (1995). "Plastic Collapse and Bifurcation Buckling Analysis of Bellows," *Developments in Pressure Vessels and Piping 1995*, ed. J. N. Petrinec, Jr., The American Society of Mechanical Engineers, pp. 121-128.

Vrillon B., Jeanpierre, F., Copin, A., and Gregoire, J. P. (1975). "Theoretical and Experimental Studies on Bellows Type Expansion Joints Behavior of Chinon 3

Primary Coolant System," *International Conference on Structural Mechanics in Reactor Technology*, Vol. 2, F6/6, London.

Warner, F., and Newland, D. E. (1975). "Flixborough Explosion, Mechanical Engineering Provides the Key," *Chartered Mechanical Engineer*, Vol. 22.

Winborne, R. A. (1964). "Stress and Elevated Temperature Fatigue Characteristics of Large Bellows," NAA-SR-9762, Atomics International.

Wolf, L. J., and Mains, R. M. (1971). "Analysis of Shells of Revolution Under Axisymmetric Loads Using Ring Finite Elements," ASME Paper No. 71-WA/HT-22, The American Society of Mechanical Engineers.

Wolf, L. J., and Mains, R. M. (1973). "The Stress Analysis of Heat Exchanger Expansion Joints in the Elastic Range," ASME *Journal of Engineering for Industry*, Feb., The American Society of Mechanical Engineers.

Wolf, L. J., and Mains, R. M. (1974). "Heat Exchanger Expansion Joints-Failure Modes, Analysis and Design Criteria," ASME Paper No. 74-PVP-7, The American Society of Mechanical Engineers.

Yamamoto, S., Isobe, K., Ohte, S., Tanaka, N., Ozaki, S., and Kimura, K. (1986). "Fatigue and Creep-Fatigue Testing of Bellows at Elevated Temperature," *Fatigue and Fracture Assessment by Analysis and Testing,* PVP Vol. 103, The American Society of Mechanical Engineers, pp. 87-94.

Yamashita, T., Tsukimori, K., Nakamura, M., Iwata, K., and Imazu, A. (1989). "Ratchetting Mechanism of Bellows and Evaluation Method," *Metallic Bellows and Expansion Joints - 1989*, PVP Vol. 168, ed. C. Becht IV et al., The American Society of Mechanical Engineers, pp. 123-132.

Youn-Sheng, L. (1989). "Study of Fatigue Life For U-Shaped Expansion Joints," *Metallic Bellows and Expansion Joints - 1989*, PVP - Vol. 168, ed. C Becht IV et al., The American Society of Mechanical Engineers.